



# UNIVERSITÀ DEGLI STUDI DI CATANIA

Department of Biomedical and Biotechnological Sciences

Ph.D in Biotechnology

*CURRICULUM IN AGRO-FOOD SCIENCES*

*XXXIV CYCLE*

---

**DANILO FABRIZIO SANTORO**

## **Transcriptional dynamics of *Arundo donax L.* ecotypes to long-term salt and cadmium treatments by unigene-based RNA-Seq**

\_\_\_\_\_  
*PhD thesis*  
\_\_\_\_\_

Supervisor: *Prof. Angela Roberta Lo Piero*  
Coordinator: *Prof. Vito Nicola De Pinto*

---

PhD attended during 2018/2022



## Index

|                                                                                                                                   |    |
|-----------------------------------------------------------------------------------------------------------------------------------|----|
| Abstract.....                                                                                                                     | 6  |
| Sintesi.....                                                                                                                      | 8  |
| Affiliation.....                                                                                                                  | 10 |
| Thesis structure.....                                                                                                             | 11 |
| INTRODUCTION.....                                                                                                                 | 12 |
| 1. Bioenergy as a new alternative renewable energy source.....                                                                    | 12 |
| 1.1 Global warming, energy crisis and new sustainable energy sources.....                                                         | 12 |
| 1.2 The use of bioenergy crops in marginal lands.....                                                                             | 15 |
| 1.3 Giant reed ( <i>Arundo donax</i> L.): a promising suitable bioenergy crop.....                                                | 16 |
| 2. Plant and abiotic stress response.....                                                                                         | 18 |
| 2.1 Salt stress: a huge threat for plant growth and crop productivity.....                                                        | 18 |
| 2.2 Mechanisms of salt stress response in plants.....                                                                             | 19 |
| 2.3 Contaminated soil: traversing the effects of heavy metal stress on plant.....                                                 | 21 |
| 2.4 Physiological and molecular responses to cadmium stress.....                                                                  | 22 |
| 3. High throughput sequencing: the ability to interrogate the genetic and<br>transcriptional landscape in biological systems..... | 25 |
| 3.1 Molecular screening and genetic improvement of <i>Arundo donax</i> L.....                                                     | 25 |
| 3.2 Transcriptomics and RNA Sequencing analysis (RNA-Seq).....                                                                    | 26 |
| 3.2 <i>De novo</i> assembly: a new breakthrough to uncover genetic information.....                                               | 28 |
| Aim of the work.....                                                                                                              | 31 |
| RESULTS.....                                                                                                                      | 33 |
| 4. RNASeq analysis of giant cane reveals the leaf transcriptome dynamics<br>under long-term salt stress.....                      | 33 |
| 4.1 Background.....                                                                                                               | 34 |
| 4.2 Results.....                                                                                                                  | 37 |
| 4.2.1 Effect of salt stress upon <i>A. donax</i> morpho-biophysiological parameters.....                                          | 37 |
| 4.2.2 Transcript assembly and annotation.....                                                                                     | 37 |
| 4.2.3 Identification of differentially expressed genes (DEGs).....                                                                | 42 |
| 4.2.4 Functional classification of DEGs.....                                                                                      | 45 |
| 4.2.5 Identification of functional genes related to salt stress tolerance.....                                                    | 52 |
| 4.2.6 Salt sensory and signaling mechanisms.....                                                                                  | 52 |
| 4.2.7 Transcription factors.....                                                                                                  | 52 |
| 4.2.8 Hormone regulation of salt stress response.....                                                                             | 53 |
| 4.2.9 ROS scavenging regulatory mechanisms.....                                                                                   | 55 |
| 4.2.10 Osmolyte biosynthesis.....                                                                                                 | 55 |
| 4.2.11 Photosynthesis and photorespiration.....                                                                                   | 56 |
| 4.2.12 Biomass digestibility and biofuel production.....                                                                          | 57 |

|                                                                                                                                  |     |
|----------------------------------------------------------------------------------------------------------------------------------|-----|
| 4.2.13 Retrieval and analysis of genes targeted as “salt stress responsive”                                                      | 63  |
| 4.3 Discussion                                                                                                                   | 68  |
| 4.4 Conclusions                                                                                                                  | 76  |
| 4.5 Methods                                                                                                                      | 78  |
| 4.5.1 Plant material and application of salt stress                                                                              | 78  |
| 4.5.2 Sample collection and RNA extraction                                                                                       | 79  |
| 4.5.3 Library preparation for transcriptome sequencing                                                                           | 79  |
| 4.5.4 Clustering and next generation RNA sequencing                                                                              | 80  |
| 4.5.5 <i>De novo</i> transcriptome assembling and gene functional annotation                                                     | 80  |
| 4.5.6 Identification of clusters specifically involved in salt stress response                                                   | 80  |
| 4.5.7 Multiple sequence alignment and phylogenetic analysis                                                                      | 80  |
| 4.5.8 Quantification of gene expression and differential expression analysis                                                     | 81  |
| 4.5.9 Real-time validation of selected DEG candidates using qRT-PCR                                                              | 81  |
| 5. Transcriptional response of giant reed ( <i>Arundo donax</i> L.) low ecotype to long-term salt stress by Unigene-based RNAseq | 82  |
| 5.1 Introduction                                                                                                                 | 83  |
| 5.2 Results                                                                                                                      | 85  |
| 5.2.1 Effect of salt stress upon <i>A. donax</i> morpho-biophysiological parameters                                              | 85  |
| 5.2.2 Transcript assembly and annotation                                                                                         | 85  |
| 5.2.3 Identification of differentially expressed genes (DEG)                                                                     | 88  |
| 5.2.4 Functional classification of DEGs                                                                                          | 89  |
| 5.2.5 Identification of functional genes related to salt stress tolerance                                                        | 92  |
| 5.2.6 Salt sensory and signaling mechanisms                                                                                      | 92  |
| 5.2.7 Hormone regulation of salt stress response                                                                                 | 93  |
| 5.2.8 ROS scavenging regulatory mechanisms                                                                                       | 93  |
| 5.2.9 Osmolyte biosynthesis                                                                                                      | 93  |
| 5.2.10 Photosynthesis and photorespiration                                                                                       | 95  |
| 5.2.11 Transcription factors                                                                                                     | 95  |
| 5.2.12 Comparison between G34 and G2 giant reed ecotypes                                                                         | 96  |
| 5.2.13 Retrieval and analysis of genes targeted as “salt stress responsive”                                                      | 98  |
| 5.2.14 Identification of functional genes related to “carbon metabolism” and “starch and sucrose metabolism”                     | 98  |
| 5.2.15 Identification and distribution of SSR                                                                                    | 101 |
| 5.2.16 Validation of SSR                                                                                                         | 102 |
| 5.3 Discussion                                                                                                                   | 106 |
| 5.4 Conclusions                                                                                                                  | 111 |
| 5.5 Experimental                                                                                                                 | 112 |
| 5.5.1 Plant material and application of salt stress                                                                              | 112 |

|       |                                                                                                                                      |     |
|-------|--------------------------------------------------------------------------------------------------------------------------------------|-----|
| 5.5.2 | Sample collection and RNA extraction.....                                                                                            | 112 |
| 5.5.3 | Library preparation for transcriptome sequencing.....                                                                                | 113 |
| 5.5.4 | Clustering and next generation RNA sequencing.....                                                                                   | 113 |
| 5.5.5 | <i>De novo</i> transcriptome assembling and gene functional annotation.....                                                          | 113 |
| 5.5.6 | Identification of clusters specifically involved in the salt stress response.....                                                    | 113 |
| 5.5.7 | Quantification of gene expression and differential expression analysis.....                                                          | 114 |
| 5.5.8 | Real-time validation of selected DEGs candidates using qRT-PCR.....                                                                  | 114 |
| 5.5.9 | SSR detection and validation.....                                                                                                    | 114 |
| 6     | Global leaf and root transcriptome reprogramming in response to cadmium reveals<br>Tolerance mechanisms in <i>Arundo donax</i> ..... | 116 |
| 6.1   | Introduction.....                                                                                                                    | 117 |
| 6.2   | Material and methods.....                                                                                                            | 119 |
| 6.2.1 | Plant material and application of cadmium nitrate.....                                                                               | 119 |
| 6.2.2 | Sample collection and RNA extraction.....                                                                                            | 120 |
| 6.2.3 | Library preparation for transcriptome sequencing.....                                                                                | 120 |
| 6.2.4 | Clustering and next generation RNA sequencing.....                                                                                   | 121 |
| 6.2.5 | <i>De novo</i> assembly and gene functional annotation.....                                                                          | 121 |
| 6.2.6 | Quantification of gene expression and differential expression analysis.....                                                          | 122 |
| 6.2.7 | Real-Time validation of selected DEG candidates using qRT-PCR.....                                                                   | 122 |
| 6.2.8 | Gene ontology and KEGG enrichment analysis.....                                                                                      | 122 |
| 6.2.9 | KEGG classification of heavy metal and salt common genes.....                                                                        | 123 |
| 6.3   | Results.....                                                                                                                         | 124 |
| 6.3.1 | Effect of cadmium upon <i>A. donax</i> morpho-biometric and physiological<br>parameters.....                                         | 124 |
| 6.3.2 | Transcript assembly and annotation.....                                                                                              | 126 |
| 6.3.3 | Identification of differentially expressed genes (DEGs).....                                                                         | 129 |
| 6.3.4 | Functional classification of DEGs.....                                                                                               | 133 |
| 6.3.5 | Identification of transcription factors families involved in plant response to<br>cadmium.....                                       | 136 |
| 6.3.6 | Main Processes affected by cadmium treatment.....                                                                                    | 137 |
| 6.3.7 | Analysis of the <i>A. donax</i> response to salt and cadmium treatment.....                                                          | 150 |
| 6.4   | Discussion.....                                                                                                                      | 159 |
| 6.5   | Conclusion.....                                                                                                                      | 163 |
| 7     | General conclusion.....                                                                                                              | 164 |
|       | Bibliographic.....                                                                                                                   | 168 |
|       | List of publications.....                                                                                                            | 200 |
|       | List of participations to congress.....                                                                                              | 201 |
|       | Acknowledgments.....                                                                                                                 | 202 |

## Abstract

Global energy demand has been under intense pressure over the last few years, thus many research efforts have been made in many countries in order to evaluate and pose sustainable strategies. Sustainable biomass production by bioenergy crop on non-arable lands can play a crucial role not only in reducing global Greenhouse gas (GHGs) emission responsible for climate change but also providing a significant contribution to satisfy the increasing demand of sustainable energy production without any further risks on food security. The second generation of biofuels, which comes from living organisms, called bioenergy crops, have been considered better biomass producers than food crops, in fact they reach higher ethanol yields per unit of cultivated area. Among them, *Arundo donax* L. is the most promising species for bioenergy production in the Mediterranean basin due to its high yield, low input requirements and its capability to grow on marginal land and in adverse environmental conditions. Although the capability of *A. donax* to withstand a wide range of abiotic stresses condition has been reported worldwide, the investigation at molecular level is just at the beginning. Considering the impact of soil salinization on agricultural areas situated in the Mediterranean basin as well as the lack of information about the molecular mechanism involved in *A. donax* response to salt stress, we *de novo* sequenced, assembled and analysed the leaf transcriptome of two *A. donax* clones (G2 and G34) subjected to two levels of long-term salt stress treatment (namely, S3 severe and S4 extreme). The picture that emerges from the identified genes related to salt stress response in G2 is consistent with a dose-dependent response to salt, it also suggests a deep re-programming of the transcriptomic machinery in the case of S4 extreme salt stress condition, whereby a dramatic switch from C3 to C4 Calvin cycle likely occurred. Although *A. donax* propagates itself vegetatively by rhizomes and stem cutting nodes, variation in gene expression between G2 and G34 ecotypes occurred not only in salt treated but also in untreated samples. Indeed, the severe salt treatment in G34 ecotype resulted in a lower number of DEGs when compared to the same condition in G2 ecotype, indicating a lower re-adjusting of the gene expression. Nevertheless, the comparative analysis between S4 (extreme salt stress) G2 with S3 (severe salt stress) G34 conditions outlines a similar response and suggests that G34 ecotype tries to deal with stress condition as soon as S3 salt dose is applied. Moreover, given the ongoing increase of contaminated soils as well as the remarkable resistance of *A. donax* to heavy metals, we carried out a global *de novo* transcriptomic analysis in leaves and roots of G10 *A. donax* ecotype subjected to cadmium stress condition. By analysing the differential gene expression data, clear organ-specific differences emerged leading to the identification of specifically up-regulated genes in the Cd-treated roots compared to Cd-treated leaves. It is worthwhile to note that the obtained transcriptomic data indicate that after Cd uptake by plant

roots, it is likely that only a small portion reaches the upper aerial plant parts, since a low number of DEGs were retrieved in leaf tissue under cadmium treatment indicating a major role of roots in Cd detoxification. Based on transcriptomic data, the long-term exposure to Cd induced the expression of signaling molecules devoted to induce a downstream signal cascade activated by the phytohormone ethylene. In addition, the results showed a strong regulation of oxidative-responsive genes followed by the induction of transcripts involved in cell wall remodelling and lignification in Cd-treated roots. The identification of candidate genes involved in salt- and cadmium stress response constitute an important database resource towards the characterization of the molecular basis for the high resistance of *A. donax* to unfavourable environmental conditions. Many of the unigenes identified have the potential to be used for improving several important traits and for developing *A. donax* varieties with enhanced productivity and tolerance to different environmental scenarios. In addition, the identified SSRs addressed many challenges to discover molecular markers suitable for marker-assisted selection (MAS) in the breeding programs, to elucidate the interspecific phenotypic variation within *A. donax* ecotypes. Globally, these results support the cultivation of *A. donax* ecotypes in contaminated soils in order to only to avoid the competition with food crops but mainly to fulfil the sustainable energy demand.

**Keywords and abbreviation:**

*Bioenergy crops; Poaceae; Arundo donax L.; RNA-Seq; De novo assembly; Giant reed; leaf and root transcriptome; Salt stress; SSR; Heavy metals; Cadmium.*

## Sintesi

La domanda globale di fonti di energia sostenibili è fortemente aumentata nel corso degli ultimi anni. La produzione di biomassa derivante da colture bioenergetiche in suoli non utilizzabili per le coltivazioni può giocare un ruolo importante non solo nel ridurre le emissioni di gas a effetto serra (GHGs) responsabili del cambiamento climatico, ma anche nel soddisfare l'incremento della domanda di produzione di energia sostenibile, evitando ulteriori rischi sulla sicurezza alimentare. I biocombustibili di seconda generazione, i quali derivano dagli organismi viventi noti come colture bioenergetiche, sono stati considerati migliori produttori di biomassa rispetto alle colture alimentari, in quanto consentono di ottenere elevate rese di etanolo per unità di area coltivata. Tra le diverse colture bioenergetiche, *Arundo donax* L. è la specie vegetale più promettente nel bacino del Mediterraneo grazie al suo elevato rendimento in biomassa, al basso fabbisogno nutritivo e alla sua notevole capacità di crescere in suoli marginali, così come in condizioni ambientali sfavorevoli. Sebbene, la capacità di *Arundo donax* di tollerare un'ampia varietà di stress abiotici sia stata riportata in passato, lo studio a livello molecolare della risposta a condizioni ambientali avverse è in fase iniziale. Considerando l'impatto della salinizzazione dei suoli sulle aree agricole localizzate nel bacino del Mediterraneo, congiuntamente alla mancanza di informazioni sul meccanismo molecolare coinvolto nella risposta di *A. donax* allo stress salino, un'obiettivo di questa tesi è stato il sequenziamento del trascrittoma fogliare e l'assemblaggio *de novo* del trascrittoma di due ecotipi di *A. donax* (G2 e G34) sottoposti a due livelli di stress salino prolungato (S3, severo e S4, estremo). Il risultato che emerge dall'identificazione dei geni coinvolti nella risposta allo stress salino nel clone G2 è consistente con una risposta dipendente dalla concentrazione salina, suggerendo che il trattamento salino estremo (S4) comporta una profonda riprogrammazione del trascrittoma; in particolare si è osservata una modifica dell'espressione genica che testimonia la conversione dal ciclo fotosintetico C3 al C4. Sebbene *A. donax* si moltiplichi per via vegetativa da rizomi o segmenti di culmi, è stata osservata una differente espressione genica tra i cloni G2 e G34 non solo in campioni trattati con lo stress salino, ma anche nei campioni controllo. Difatti, il trattamento salino severo (S3) applicato sull'ecotipo G34 ha indotto un numero minore di geni differenzialmente espressi rispetto a quelli ottenuti nell'ecotipo G2 a parità di concentrazione salina. Inoltre, l'analisi comparativa condotta tra l'ecotipo G2 sottoposto al trattamento S4 (stress salino estremo) e l'ecotipo G34 sottoposto al trattamento S3 (stress salino severo) evidenzia una risposta simile, suggerendo che l'ecotipo G34 risponde a concentrazioni più basse di stress salino. Inoltre, visto l'incremento crescente di suoli contaminati da metalli pesanti, è stata effettuata un'analisi trascrittomica globale con assemblaggio *de novo* sia in foglia che radice dell'ecotipo G10 sottoposto a trattamento con cadmio. L'analisi dei dati di



espressione genica ha condotto all'identificazione di geni specificatamente sovra-regolati nelle radici sottoposte al trattamento con il cadmio rispetto alle foglie. I dati di trascrittoma indicano che le radici svolgono un ruolo primario nell'interazione con il cadmio anche in funzione del fatto che solo un ridotto numero di geni differenzialmente espressi è stato riscontrato nel tessuto fogliare sottoposto al trattamento del cadmio. Inoltre, l'esposizione prolungata al metallo pesante ha indotto nelle radici l'espressione di molecole segnale indirizzate ad attivare la via di segnalazione a cascata dell'etilene, di geni coinvolti nello stress ossidativo e nel rimodellamento e lignificazione della parte cellulare. L'identificazione di geni candidati coinvolti nella risposta allo stress salino e da cadmio costituisce un'importante risorsa per la caratterizzazione delle basi molecolari della risposta di *A. donax* a condizioni ambientali sfavorevoli. Molti dei geni identificati potranno essere utilizzati per lo sviluppo di varietà di *A. donax* caratterizzate da una maggiore produttività e tolleranza agli stress. Infine, i marcatori microsatelliti SSR identificati in questo lavoro di tesi sono ideali per la selezione assistita da marcatori (MAS) in programmi di breeding e possono fare luce sulla variabilità fenotipica intraspecifica all'interno degli ecotipi della specie *A. donax*.

### **Parole chiave e abbreviazioni:**

Colture bioenergetiche; *Poaceae*; *Arundo donax* L.; *RNA-Seq*; assemblaggio *De novo*; *Giant reed*; trascrittoma fogliare e radicale; stress salino; *SSR*; metalli pesanti; cadmio.

**Affiliation:**

- Department of Agriculture, Food and Environment, University of Catania, via Santa Sofia 98, 95123 Catania (Italy).
- Institute for Plant Molecular and Cell Biology (IBMCP), Consejo Superior de Investigaciones Científicas (CSIC), Universidad Politécnica de Valencia (UPV), Camino de Vera s/n, 46022 Valencia (Spain).

A period of 7 months was conducted in IBMCP, Valencia, under the supervision of Doctor Diego Vicente Orzáez Calatayud.

## Thesis structure

The thesis was organized as follows:

- Firstly, a comprehensive scientific literature was thoroughly analysed and designed so as to provide an appropriate background information (**Introduction**). In particular, we focused on different topics related to the use of perennial grasses as biomass source for bioenergy production, especially in salty and contaminated soil. Notably, a pertinent knowledge of the molecular basis of the response to salinity and cadmium stress was discussed, aimed at ensuring sustainable biomass production on marginal lands. Afterwards, we covered the use of transcriptomic approaches, focusing mainly on RNA Sequencing (RNA-Seq) tool, in order to enlance and characterize the mechanisms by which plants growth and respond to environmental stresses.
- Secondly, the thesis was organised in three **manuscripts** (two already published and one submitted to BMC Genomics): the first manuscript concerns the transcriptional dynamics of G2 *Arundo donax* L. ecotype subjected to severe and extreme, long-term salt treatments by unigene-based RNA- The second one reports the results of an experiment conducted by using a dwarf G34 *A. donax* ecotype under severe salt stress condition. The third manuscript relies on the global leaf and root transcriptomic response to cadmium exposure.
  - Finally, the main findings are reported in the “**General conclusions**” section, pointing out how the identification of several genes differentially regulated in both salt and cadmium conditions might be usefull markes for obtaining *A. donax* ecotypes with improved lignocellulosic biomass production and both salt and cadmium tolerance.

## INTRODUCTION

### ***1. Bioenergy as a new alternative renewable energy source***

#### ***1.1 Global warming, energy crisis and new sustainable energy sources***

During the past few centuries, climate change has become one of the most important environmental problem, due to the ongoing Greenhouse Gas Emission (GHGs) into the atmosphere. The use of fossil fuels and the rise of deforestation have increased the GHG concentrations and all of these events are leading to a worldwide climate crisis (IPCC, 2020). Moreover, both industrialization and demographic growth are intensifying the land use demand, which in turn increases the GHG emissions. Recently, it was reported that human population may grow to reach 9.7 billion of people by 2050 (ONU, 2019). Hence, a considerable increase in global crop production is required to satisfy the human requirements along with the reduction of its environmental impact (Hunter et al., 2017). Mitigation strategies are needed to reduce the negative effects on environment as well as to ensure food security and energy demands. The energy demand was partially met in the 20<sup>th</sup> century by using fossil fuels from organic origin, such as coal and a natural gas, which represents a non-renewable energy source. Nevertheless, the large use of fossil fuels has caused the major environmental threats, including air and water pollutions, acidification of rainfalls and global warming. Global warming caused by GHG accumulation, is leading to the melting of glaciers, desertification or flooding in many regions all over the world. Therefore, many challenges must be planned to deal with the aforementioned issues in the next years (Brennan and Owende, 2010; Castelli, 2011; Yusuf et al., 2011; Aguirre et al., 2013; Gupta and Verma, 2015). Because of the depletion of non-renewable sources, an increasing on the prices of the raw materials is expected, posing a much more concerns on the security of raw material supplies. Since the use of fossil fuels is becoming unsustainable from an environmental, economic, and political point of view, new breakthroughs are focusing on the use of alternative energy sources. Over the past few years, conferences on climate change have taken place to investigate the upcoming threats in order to choose the best solutions to face these issues. Besides, the main subject covered during these conferences relied on new ways for balancing the greenhouse gas concentrations into the atmosphere, in order to forestall its negative consequences with the implementation of natural tasks, addressed to enhance of the greenhouse gas sinks (Fawzy et al., 2020). At the beginning, the Kyoto protocol was launched to encourage the developed countries to reduce the GHG emissions, in a period between 2008 and to 2012, using clean development mechanisms (Ki-moon, 2008). Unfortunately, the protocol did not achieve the undertaken commitments. Subsequently in 2016, during the 21<sup>st</sup> conference of the parties (COP21), the Paris agreement has been accepted and

ratified in the same year by all parties (United Nations, 2015), aimed on the restriction of the global average temperature to 1.5°C. The Paris agreement has posed such obligations for the participating country to enhance the investment on sustainable resources as well as to bring up suitable measurements for vulnerable countries. Since then, many countries have begun to address new energetic policies based on the use of alternative energetic sources which are sustainable from an environmental and economic point of view. In particular, a wide range of different breakthroughs has emerged, ranging from decarbonization techniques to renewable fuels (Ricke et al., 2017; Victor et al., 2018; Bataille et al., 2018; Mathy et al., 2018; Bustreo et al., 2019). The most prominent technologies are based on photovoltaic solar power, solar thermal power, onshore and offshore wind power, hydropower, marine power, geothermal power, biomass power and biofuels (Mathy et al., 2018; REN21, 2019; Hussain et al., 2017; Østergaard et al., 2020; Shivakumar et al., 2019; Gude and Martinez-Guerra, 2018; Akalın et al., 2017; Srivastava et al., 2017). According to the last recorded data the renewable resources account for 26.2 % of the global energy production, of which the hydropower energy represents 15.8 %, wind power 5.5 %, photovoltaic solar power 2.4 %, biopower 2.2 %, whereas geothermal, concentrate solar power and marine power represent about 0.4 % (REN21, 2019). Decarbonization based on the use of renewable resources plays a fundamental role in overcoming the global climate change crisis and meet the energy demand, as well. In this framework, the policy choice assumes an important aspect in promote renewable energy technology innovation. Pitelis et al. (2020) evaluated the effect of each policy instruments on technology innovation of the different renewable energy technologies (solar, wind, biomass, geothermal and hydrothermal) for a period between 1994 - 2014. The study reported that the policymaker's programmes are more effective in promoting renewable energy technologies compared to alternative policy types. European (EU) countries have just enhanced the use of renewable energy in order to increase the bioenergy production (Marques et al., 2018). Therefore, the Directive 2009/28/EC allowed the EU countries to coordinate the actions for ensuring a self-sufficiency energy supply by enhancing the use of renewable energy resources (European Commission, 2015; Scarlat et al., 2015). In addition, the Life Cycle Assessment (LCA) has been launched as reference platform to assess the environmental contribution of several renewable energy sources (Fazio and Monti, 2011; Buonocore et al., 2015; Röder and Thornley, 2018). According to LCA studies, many environmental benefits are based on the use of biomass as bioenergy sources to reduce the GHG emissions and achieve a suitable energy balance (Muench and Guenther, 2013; Roos and Ahlgren, 2018). Biomass is defined as any substance of organic origin, derived from living organisms, plants or animals, which has not undergone any fossilization process. Biomass has a ubiquitous applications (Castelli, 2011; Brennan and Owende, 2010; Ho

et al., 2014; Guo et al., 2015; Gupta and Verma, 2015; Sarsekeyeva et al., 2015), since it can be used to produce thermal and electrical energy by its direct combustion; other ways of energy production concern the use of biomass to produce various kind of fuels, liquids, solids, and gases, which in turn might be used to obtain heat, electricity, chemical substances, and biofuels in transport sector. Furthermore, biomass and waste may be accounting for over 70 % of all renewable energy which pull a significant contribution to the final energy production than coal (IEA, 2017). The use of biomass as feedstock for energy production has been seen as an opportunity to reach out the energy demand and promoting the rural development (Fernando A. L. et al., 2015). According to European commission (European Commission, 2014), the raising use of biomass as energy source enhances Europe's energy supply as well as the development of new jobs. The main biofuel producing country is the United States (46 % of global production) followed by Brazil 46% and EU 26 % of global production. The bioenergy sources are mainly used on the heat sector (27 % of global production), though the production of electricity and biofuels comes from by biomass that are growing faster and faster (REN21, 2018). Biomass is a suitable energy source dedicated to bioenergy production, because it does not rise the CO<sub>2</sub> concentration in the atmosphere (Pires, 2019; Dowling and Venki, 2018). The amount of CO<sub>2</sub> emitted upon its combustion corresponds to that absorbed by photosynthetic activity during plant growth, which is returned to the atmosphere, rendering it available again for photosynthesis processes. The sustainability of bioenergy production and its widespread use are threatened because of the environmental, economic and social issues (Jin and Sutherland 2018). As regards the nature of biomass used for energy production, we can classify biofuels as first, second, third and fourth generation of biofuels which are based on the synthetic biology (Gressel, 2008; Baeyens et al. 2015; Aro, 2016). The first generation of biofuels is based on the use of crop species characterized by high content of sugar and starch for bioethanol production, such as sugar cane, sugar beet, sweet sorghum, or cereals, tubers and roots, and oilseeds like rapeseed and soybean for biodiesel production (Ho et al., 2014). Taha (2016) reported that the production of first-generation of biofuels does not satisfy the total energy demand required by the transport sector. Thereby, many doubts have been arisen about their sustainability to substitute the use of fossil fuels, considering also their impact in food supply and prices (Hill et al., 2006; Gressel, 2008; Deenanath et al., 2012; Ho et al., 2014; Aro, 2016), Hence, a considerable amount of cereal and vegetable oils should be used for biofuels production by sequestering lands for bioenergy scope. Thus, energy and food production coming from first-generation of biofuels are in constant competition for soil destination and resources, opening new questions about their effective sustainability usage (Hasegawa et al., 2020). To avoid these competitions and guarantee an adequate food and energy security, second

generation of biofuels derived from lignocellulosic crops has become a promising strategy in sustainable energy production (Souza et al., 2017). Second generation of biofuels comes from organic compounds, has not to be intended for food supply, in fact their use does not have any effect on the agri-food field.

## **1.2 The use of bioenergy crops in marginal lands**

Since cellulosic feedstocks cannot be produced on arable lands because of both environmental and economic issues, a suitable strategy is to grow them on marginal lands, overcoming competition with the cultivation of food crops. According to Tang et al. (2010), various kinds of lands are unproductive or inadequate for food crop cultivation due to poor soil properties, bad quality of underground water, drought undesired topology and unfavourable pedo-climatic conditions. Marginal lands include brownfields (Smith et al., 2013), previously contaminated lands, and/or affected by diffused contamination, fallow agricultural land because of unfavourable crop cultivation conditions, degraded lands (Tilman et al., 2006), or landfills previously used to dispose-off city waste (Nixon et al., 2001). The application of marginal lands for cellulosic crops might potentially avoid many drawbacks associated with biofuel production using cropland (Skevas et al., 2014). Moreover, benefits of using cellulosic biomass on marginal lands rely on the less need of fertilizers and pesticides coupled with mitigation of water pollution and GHG emissions (Hill et al., 2006; Robertson et al., 2008). The use of marginal lands can shed new light on the cultivation of crop species, to produce biomass feedstock in order to reduce the impacts on agri-food chain (Cai et al., 2011; Campbell et al., 2008; Liu et al., 2011; Skevas et al., 2014). Therefore, the selection of suitable cellulosic crops produced on marginal lands (Lord, 2015) could be a viable choice, reducing negative competition between fuel and food as well as environmental threats (Qin et al., 2011). Lignocellulosic crops have the peculiarity to grow and produce high biomass yield on marginal land, owing their high capability to withstand in case of low water and nutrients as well as their better water use efficiency (Hill et al., 2006; Heaton et al., 2008; Fargione et al., 2010). Biogas is produced from dedicated lignocellulosic crops, manure, or waste by the anaerobic digestion process (Weiland, 2010). Many studies outlined as the production and combustion of biogas for heat and electricity production has a significant carbon mitigation potential and can replace the use of fossil fuels (Lansche and Müller, 2012; Rehl et al., 2012; Wagner et al., 2019). In Germany, over 18 million tonnes of GHG emissions have not been emitted due to the use of biogas derived from dedicate bioenergy crops (FNR, 2017). Perennial grasses are lignocellulosic rhizomatous crops, which are suitable substitute of fossil fuels to produce paper pulp, fibreboards, and composites as well (Alexopoulou et al., 2018). The Switchgrass (*Panicum*

*virgatum*), *Miscanthus* (*Miscanthus sinensis x giganteus*) and giant reed (*Arundo donax L.*) are the most promising candidate bioenergy crops in the United States and European Union (Ho et al., 2014). For this purpose, the Optimization of Perennial Grasses for Biomass Production (OPTIMA) project has been launched to assess the potential use of perennial grasses on marginal land in Mediterranean basin (Monti and Cosentino, 2015). Growing perennial grasses on marginal lands in Mediterranean basin has allowed to reduce the leaching of heavy metals into the groundwater, enhancing carbon sequestration from soils and slow down the GHG concentration, providing a potential benefits for climate change related-issues (Lal, 2006; Curley et al., 2009; Dabney et al., 2009; Blanco-Canqui et al., 2010; Feng et al., 2015; Gessesse et al., 2015; Monti and Cosentino, 2015). The global energy analysis estimated that in year 2030 global energy demand will be provided by the cultivation of bioenergy crops on non-arable lands (Metzger and Hüttermann, 2009; Skevas et al., 2014). It has been estimated that the bioenergy potentials by using marginal lands ranging from ~30 to 1000 Extra-joule (EJ; 1 EJ = 1018 J) per year of primary energy (Haberl et al., 2011; Hoogwijk et al., 2005; Smeets et al., 2007).

### **1.3 Giant reed (*Arundo donax L.*): a promising suitable bioenergy crop**

Among the different crop species dedicated to energy production, *Arundo donax L.* also known as giant reed or giant cane, is one of the most promising bioenergy crops along with *Phalaris arundinacea*, *Miscanthus* and *Switchgrass* (Lewandowski et al., 2003; Soldatos, 2015). *Arundo donax L.* is a plant that grows spontaneously in different kinds of environments and that it is widespread in temperate and hot zones all over the world (Corno et al., 2014). *A. donax* belongs to the *Poaceae* family, tribe of *Arundinaceae* as many other species, including *Arundo plinii* Turra, *Arundo collina* Tenore, *Arundo mediterranea* Danin and other ornamental species (Mariani et al. 2010). *A. donax* is a hydrophyte plant able to grow in soil rich water, especially near channels, rivers, lakes, ponds, and marshes, where it shows the maximum biomass yield. *Arundo donax* is an octadecaploid perennial grass ( $2n = 18x = 108 - 110$ ), with a C3 photosynthetic cycle, complete sterility due to early failure of both male and female gametophytes during germination (Balogh et al., 2012; Hardion et al., 2015). Despite to owing a C3 photosynthetic Calvin Cycle, its photosynthetic efficiency is comparable to a C4 photosynthetic cycle (Castiglia et al., 2016; Webster et al., 2016). Although, giant reed propagates itself vegetatively by rhizomes or stem cutting nodes, such a genetic plasticity can occur to increase the likelihood of build-up chromosomal mutations. A simple hypothesis to explain the formation of the  $2n = 108 - 110$  is based on the fusion of reduced ( $n = 36$ ) and unreduced ( $n = 72$ ) gametes from fertile progenitors ( $2n = 72$ ), such as *A. donax plinii* (Bucci et al. 2013; Hardion et al. 2012). Several varieties of *A.*



*donax* has been well characterized, sometimes with putatively lower chromosome numbers, like *A. donax* var. *macrophylla* ( $2n = 40$ ), which having large glaucous leaves and shorter culms (Lewandowski et al., 2003). The extraordinary vigour of *A. donax* does not seem to be explained along by its polyploid level, since several traits like plant height and rhizome size are only partially correlated with chromosome numbers within the genus (Hardion et al., 2012). Even though there was a debated about the origin of the giant reed species, and the latest evidences from genetic studies indicates that *A. donax* geographically originated in easter Asia, from where it spread all around the world by human activities (Hardion et al., 2014). *A. donax* propagates itself vegetatively, and thus a low genetic diversity is expected. Nonetheless, heritable phenotypic differences among clones have been reported, which may be explored to improve several plant traits, such as number of culms, culm diameter and height (Cosentino et al. 2006; Pilu et al. 2014). Considering the aboveground part of plant, average biomass production is roughly 15.5 kg dry matter (DM)  $m^{-2}$  (Giessow et al., 2011). The adaptability of *A. donax* to grow in different kind of environmental, soils and growing conditions confers to *A. donax* many advantages compared to other energy crops, making this plant suitable for marginal and abandoned lands (Lewandowski et al., 2003). Initially, it was observed that *A. donax* could withstand either soils characterized by the lack of water or water-saturated soils (Lewandowski et al., 2003). Nevertheless, it was recently demonstrated that *A. donax* is very sensitive to water deficiency (Haworth et al. 2017a; Pompeiano et al. 2017; Zegada et al., 2020) because of the physiological parameter reduction (Mann et al. 2013; Haworth et al. 2017b) and biomass yield under water stress. By contrast, a huge body of evidences showed the ability of *A. donax* to tolerate high salt concentrations and to maintain high yield in terms of biomass production (Williams et al., 2008; Sánchez et al., 2015; De Stefano et al., 2017). The physiological responses to salinity (NaCl) has been evaluated across a range of salinities (0-42 dS  $m^{-1}$ ) (Nackley and Kim 2015) showing a 50 % reduction at 11 dS  $m^{-1}$  salinity concentration. A classic growth analysis showed > 80% reduction in overall growth at the highest salt concentration, and the plants at 40 dS  $m^{-1}$  grew without chlorosis, maintaining net assimilation rates of 7-12  $\mu mol m^{-2} s^{-1}$ , confirming that *A. donax* is a halophyte plant (Williams et al. 2009; Quinn et al. 2015). The capability of *A. donax* to grow in different environments has also been verified in urban wastewater (Mandi and Abissy, 2000), aqueous solutions from industrial processes (Zhang et al., 2008), and in wastewater containing organic wastes (Sudha and Vasudeva, 2009). Lately, *A. donax* has been proposed as species to be employed for phytoremediation (Fernando et al. 2016) owing its ability to accumulate and tolerate high doses of heavy metals, such as Ni, Cd and As (Papazoglou et al. 2005, 2007; Mirza et al. 2011; Sabeen et al. 2013). Given that energy crops could be cultivated in marginal or degraded soils, so as not to compete with food

crops, the high yield in dry matter per hectare, low input requirements and its tolerance, render *A. donax* a promising bioenergy crop on soil not suitable for conventional crop cultivation.

## **2 Plant and abiotic stress response**

### **2.1 Salt stress: a huge threat for plant growth and crop productivity**

Abiotic stress represents the main cause of losses in agricultural crop production, dipping average yields for most major crops by more than 50 % (Bray et al., 2000; Wang et al., 2003; Wani et al., 2016). In Mediterranean basin, the major abiotic stresses that affect crop production include water scarcity, salt-contaminated soils, and polluted area. Salinity is one of the most important global threat which negatively affects crop productivity worldwide (Flowers 2004; Munns and Tester 2008; B. Gupta and Huang 2014). Salt affected soil depend mainly on the balance between the evaporation and precipitation, leading to increase or decrease in salt content, respectively. Arid and semi-arid areas are marked by high salinity because the rate of evaporation far exceeds the rate of precipitation; in addition, these soils have been heavily irrigated by brackish water. Therefore, a huge loss in terms of arable land and productivity occurred because most of the crop species are very sensitive to soil salinity. The standard method used to established the salinity of soil relies on the measurements of the electrical conductivity of saturated paste extracts ( $EC_e$ ) (McGeorge 1954). The  $EC_e$  indicator stimulates a naturally occurring state of the soil solution in terms of the osmotic component of the water potential. According to the U.S. Salinity Lab. Riverside guidelines, saline soils are those whose  $EC_e$  value in the root zone is greater than 4  $dS\ m^{-1}$  at 25°C and having an exchangeable  $Na^+$  level of 15% (Shrivastava & Kumar, 2014). Crops like wheat and maize showed a 10% yield decrease at soil  $EC_e$  of 2.5 or 7.2  $dS\ m^{-1}$ , whereas a yield decrease of 50% occurs at  $EC_e$  levels of 5.5 or 13  $dS\ m^{-1}$  (Panta et al., 2014). This reference value was widely adopted because most often vegetable crops have a very low salinity threshold equal to 2.5  $dS\ m^{-1}$  (Snapp et al., 1991). Salinity impairs plant growth and development *via* the following mechanisms: firstly, excessive salinity reduces soil water potential, thus impacting on plant water uptake and resulting in water deficiency and osmotic stress; subsequently,  $Na^+$  and  $Cl^-$  ions are toxic to plant cells, causing reduced photosynthesis, oxidative damage due to the generation of reactive oxygen species, nutritional imbalance and metabolic changes (Tsugane et al 1999; Hasegawa et al. 2000; Isayenkov, 2012; Negrão et al. 2017; Isayenkov and Maathius, 2019). Salinity affects plants by two main process: an ion-independent growth reduction, which takes place within minutes to days, causes stomatal closure and inhibition of cell expansion (Munns and Termaat, 1986; Rajendran et al., 2009); the second one takes place over days or weeks, and pertains to the accumulation of cytotoxic ion levels, which in turn slow-down metabolic

processes, causing a premature senescence, and finally cell death (Munns and Tester, 2008; Roy et al., 2014).

## **2.2 Mechanisms of salt stress response in plants**

Plants develop several physiological, biochemical, and molecular responses to overcome and survive in salt-affected lands, including ion homeostasis and compartmentalization, ion transport and uptake, biosynthesis of osmoprotectants and compatible solutes, activation of antioxidant enzymes and synthesis of antioxidant compounds, synthesis of polyamines, generation of nitric oxide (NO) and hormone modulation (B. Gupta and Huang 2014). Salinity tolerance is a complex feature orchestrated by several genes involved in osmoregulation, exclusion of toxic ions and tissue tolerance which are controlled by different pathways (DeRose-Wilson and Gaut, 2011). Moreover, in leaf of sensitive plants, photosynthesis efficiency is inhibited which in turn the photosynthetic electron transport turns over-reduced in the light and reactive oxygen species (ROS) are accumulated (Miller et al., 2010). In addition, mitochondrial respiration is perturbed thus further enhancing the ROS production in respiratory electron transport (Jacoby et al., 2010). Moreover, rates of photorespiration increase due to stomatal closure and CO<sub>2</sub> concentration drops which in turn increases ROS levels (Voss et al., 2013). Both salt tolerance and sensitivity of a specific crop is based on its capability to extract water and nutrients from saline lands and to avoid excessive tissue accumulation of salt ions (Ahmad et al., 2017; Kaleem et al., 2018). Osmotic tolerance begins immediately and pertains a quickly decrease in stomatal conductance to regulate the water status by long-distance root-to-shoot signalling transduction mechanisms (Ismail et al. 2007; Maischak et al. 2010; Roy et al. 2014). Early components of salt sensing could be related to membrane depolarization and Ca<sup>2+</sup> signals as immediate responses. Ca<sup>2+</sup> signals play a key role in root-to-shoot signalling transduction processes in case of salt stress condition (Choi et al. 2014). It has been demonstrated that the increasing of NaCl causes a rapid rise of Ca<sup>2+</sup> content in the cytosol (Knight et al., 1997), which subsequently regulates the upstream component of the Reactive Oxygen Species (ROS). A key component of osmotic homeostasis and salinity tolerance is the Salt Overly Sensitive (SOS) signaling pathway (Liu and Zhu 1998; Hasegawa et al. 2000; Ishitani et al. 2000; Qiu et al., 2002; Yang et al., 2009; Gupta and Huang 2014). Under salt stress, the protein kinases SOS2 and SOS3 activate a Ca<sup>2+</sup>-dependent signalling cascade, which promotes Na<sup>+</sup> efflux from the cells by SOS1 (Na<sup>+</sup>/H<sup>+</sup> antiporter) as well as abscisic acid (ABA) signalling involved in root to shoot communication of salinity stress (Munns and Tester 2008; Zhu, 2016). Additionally, salt tolerance mechanism is mediated by high-affinity plasma membrane K<sup>+</sup> channel (HKT), which alleviates Na<sup>+</sup> toxicity by promoting Na<sup>+</sup> efflux and K<sup>+</sup> uptake in the cytoplasm

(Davenport et al. 2007; Kobayashi et al. 2017). Excessive  $\text{Na}^+$  levels disturb the uptake of cationic nutrients such as  $\text{K}^+$  (Wakeel et al., 2011; Zörb et al., 2014) or  $\text{Ca}^{2+}$  (Ehret et al., 1990; Gardner, 2016), leading to nutrient imbalance. So as to avoid the negative consequences triggered by  $\text{Na}^+$  ions on cell metabolism, they are also directed to the cell vacuole by the tonoplast  $\text{Na}^+/\text{H}^+$  antiporter (NHX), whose activity is positively regulated by SOS2 protein. Indeed, several members of NHX family show specific role as  $\text{H}^+/\text{K}^+$  exchangers, thus contributing to equilibrate higher level of cytosolic  $\text{K}^+$  ions and to preserve K-dependent metabolic processes, including protein synthesis (Moller et al, 2009). To ameliorate the detrimental effects of salinity, osmotic adjustment *via* the accumulation of compatible solutes permits the maintenance of turgor, because it can counteract the effects of a rapid decline in leaf water potential (Hussain Wani et al. 2013). Many plant species accumulate significant amounts of proline (Poustini et al., 2017; Gharsallah et al., 2016), glycine betaine (Khan and Stone 2007; Wang and Nii 2000), sugars (Kerepesi and Galiba 2000), and polyols (Dopp et al., 1985; Saxena et al., 2013). To reinforce this state, it has been reported a positively correlations between the accumulation of glycine betaine and proline with salinity tolerance (Hare and Cress, 1997; Meloni et al., 2001). Proline accumulation is a well know strategy adopted by plants to overcome salinity stress (Matysik et al. 2002; Saxena et al., 2013). Intracellular proline accumulation during salinity stress exposure not only provides tolerance towards stress but also serves as an organic nitrogen reserve during stress recovery. Accumulation of soluble carbohydrates play an important role in maintaining an adequate osmotic regulation, such as sugars (e.g., glucose, fructose and trehalose) and starch in case of salt stress condition (Parida et al., 2004). Besides, stress signals activate ABA-dependent and ABA-independent transcription factors (TFs), such as bZIP, WRKY, AP2, NAC, C2H2 zinc finger gene, and Dehydration-Responsive Element Binding (DREB) families, which are well known to control the expression of a broad range of target genes by binding to the specific *cis*-acting element in their promoter regions (Golldack et al. 2014). These TFs assist the above-reported pathways and orchestrate a signalling transduction cascade tightly linked to cell metabolism and strengthen the tolerance to salinity because of the accumulation of antioxidant enzymes (Sairam and Tyagi, 2004; Gill and Tuteja, 2010). Furthermore, salt stress leads to the accumulation of Reactive Oxygen Species (ROS), such as  $\text{O}_2^-$ ,  $\bullet\text{OH}$ ,  $\bullet\text{O}_2^-$  and  $\text{H}_2\text{O}_2$  (Mittler, 2002), which cause cell integrity damage and lipid peroxidation. To cope with these toxic compounds, plants have developed both a robust antioxidant defences though enzymatic reactions, including superoxide dismutase (SOD), catalase (CAT), glutathione peroxidase (GPX), ascorbate peroxidase (APX) and glutathione reductase (GR), and the accumulation of non-enzymatic compounds, such as ascorbic acid, glutathione regenerated by glutathione reductase, and polyphenolic compounds (Gupta et al., 2005). Several

results suggested the participation of polyamines in providing tolerance against several abiotic stress conditions, including salinity through different mechanisms (Gupta et al., 2013; Groppa and Benavides 2008). Intracellular polyamine level is regulated by polyamine catabolism by amine oxidases which include copper binding diamine oxidases and FAD binding polyamine oxidases, whose gene expression levels were associated to salinity tolerance (Cona et al. 2006; Takahashi and Kakehi 2010) probably by stabilizing the photosynthetic apparatus (Shu et al., 2012). Because salinity stress leads to water deprivation in soils, the osmotic stress increases the abscisic acid (ABA) content to ameliorate the negative effect of salinity condition. The positive correlation between high ABA levels and salinity tolerance has been partially assigned to the rises of  $K^+$ ,  $Ca^{2+}$  and compatible solutes, such as proline and sugars in vacuole of roots, which compete with  $Na^+$  and  $Cl^-$  uptake (Chen et al. 2001a; Gurmani et al. 2011). Indeed, the participation of brassinosteroids (Cui et al., 2012), salicylic acid and ethylene in tuning ion uptake, antioxidant defence and concomitant gene expression (Jayakannan et al., 2015; Zhang et al., 2015) has been associated to the reshaping of the plant response to salt condition. Moreover, salicylic acid promotes plant resilience by improving photosynthesis, osmotic homeostasis, induction of compatible osmolytes metabolism, and alleviating membrane damage (Mimouni et al. 2016). Notably, brassinosteroids enhanced the activity of antioxidant enzymes (SOD, POX, APX and GPX) and non-enzymatic antioxidant compounds (tocopherol, ascorbate, and reduced glutathione) to mitigate the harmful effects of salt stress (El-Mashad and Mohamed 2012).

### **2.3 Contaminated soil: traversing the effects of heavy metal stress on plant**

Although heavy metals occur naturally as trace components of the earth's crust at various level (Fraústo da Silva and Williams 2001), the problems arise when they are released in excess into the environment due to natural and/or anthropogenic activities (Singh et al. 2016). Soil contaminated by heavy metals (HMs) are growing worldwide due to the anthropic activities, such as mining, motorized transport and industry (Nagajyoti et al, 2010; Tchounwou et al., 2012). Many areas of lands have been contaminated with heavy metals because of the use of pesticides, fertilizers, municipal and compost wastes coupled with the release from smelting industries and metalliferous mines (Yang et al., 2015). Elements belonging to the d-block have been categorized as "heavy metals" based on their density ( $>5 \text{ g/cm}^3$ ) (Järup, 2003). Some of these elements (e.g., Cu, Mn, Ni, Zn, Fe) are essential nutrients for the majority of organism, while others, such as Cd, Hg, Pb and As, lack of any biological function and are toxic even at low concentrations (Tchounwou et al., 2012). HMs at elevated concentration produce severe toxicity symptoms in plants, including low biomass accumulation, chlorosis, inhibition of growth and photosynthesis,

both altered water balance and nutrient assimilation, and senescence (Janicka-Russak et al., 2008; 2010; DalCorso et al., 2013; Farias et al., 2013; Fidalgo et al., 2013). The roots of plants represent the first organ that encounter with heavy metals, and thus they have been widely studied to evaluate the impact of these stressors. Firstly, a decrease in mitotic activity has been observed in several plant species as soon as they were subjected to heavy metal exposure which resulted in an inhibited root growth (Doncheva et al., 2005; Sundaramoorthy et al., 2010; Hossain et al., 2012). Subsequently, HM stress alters water and nutrient absorption by roots thus affecting their transport to the aboveground parts, affecting shoot growth and ultimately decreasing biomass accumulation (Singh et al. 2016). At cellular and molecular levels, heavy metal toxicity affects plant in several ways. For instance, it alters key physiological and biochemical processes, such as seed germination, pigment synthesis, photosynthesis, gas exchanges, respiration, it causes inactivation and denaturation of enzymes, it blocks functional groups of metabolically fundamental molecules, hormonal balance, nutrient assimilation, protein synthesis, and DNA replication (Nagajyoti et a., 2010; Yadav, 2010; Keunen et al., 2011; Hossain et al., 2012; Wani et al., 2012).

#### **2.4 *Physiological and molecular responses to cadmium stress***

Due to the rapid industrialization and urbanization along with the extensive use of fertilizers and pesticides in agriculture, the concentration of  $Cd^{2+}$ , one of the most toxic non-essential heavy metals, increased in the soil (Huang et al. 2018). Cd represents one of the most studied HMs because of the lack of any biological function, high toxicity even at low concentration and its widespread in soils worldwide (Tchounwou et al. 2012; Mahar et al., 2020). Uptake of  $Cd^{2+}$  from the rhizosphere into the cells is derived by the activity of plasma membrane transporters necessary for the transport of essential metal ions, especially Mn and Fe (Redjala et al., 2009; Sasaki et al. 2012; Uraguchi and Fujiwara 2013).  $Cd^{2+}$  exerts toxicity by at least three mechanisms: (i) displacing of fundamental bivalent cations (e.g.  $Zn^{2+}$ , and  $Fe^{2+}$ ) from their binding sites or blocking functional groups which leads to inactivation of biomolecules (Stohs and Bagchi 1995); (ii) inducing a cascade of aberrant reactions triggered by the oxidative stress because of the production of reactive oxygen species (ROS) (Vanhoudt et al. 2010); (iii) binding to protein with thiol group which disrupts enzyme activity (Yadav 2010). Plants respond to Cd exposure *via* a different range of mechanisms, including sensing of external stress stimuli, signal transduction and transmission of a signal into the cell. They activate an appropriate measure to counterbalance the negative consequences of stress stimuli by modulating the physiological, biochemical, and molecular status of the cell as well as Cd accumulation. Considering metallophytes or hyperaccumulator plants, roots allow the transportation of HMs to the aboveground part of the plant for sequestration into

the vacuoles, rendering them inactive and thus non-reactive (Singh et al. 2016). Generally, different genes are induced in response to stress, which can be broadly divided in early and late induced genes. The early responsive genes are activated as soon as the stress signals are perceived by plants, whilst late induced genes are activated more slowly, i.e., after hours of stress perception showing a stable long-term expression level. Early genes encode for the transcription factors which activate the delayed stress responsive genes (Mahajan and Tuteja 2005). In many crops, the early signal of metal toxicity is known to be similar to other environmental stresses, like osmotic or dehydration stress, oxidative stress and nutrient imbalance (Yadav, 2010; Rucinska-Sobkowiak, 2016). The genes that generally get regulated in the context of heavy metal stress include those genes for metal chelators and transporters (Singh et al., 2015). Several signal transduction units operate in response to Cd through different signaling pathways, acting in response to different species and concentrations of metals. Mitogen-activated protein kinases (MAPKs) are well known to be activated by perception of specific metal ligand, and by ROS molecules produced in response to metal stress (Jonak et al., 2004; Smeets et al., 2013; Jalmi and Sinha, 2015). Since the physiochemical properties of Cd ions are very similar to that of calcium (Choong et al., 2014), an exchangeability of the two ions in  $\text{Ca}^{2+}$  binding proteins might occur, indicating the possibility of Cd uptake through receptor or voltage-gated  $\text{Ca}^{2+}$  channels. Plants exposed to cadmium show a higher level of intracellular  $\text{Ca}^{2+}$ , triggering adaptive mechanisms in order to mitigate the toxic effects of the heavy metal (Yang and Poovaiah, 2003) by maintaining auxin homeostasis, indicating a cross-talk between signaling pathways so as to cope with its exposure (Zhao et al., 2015). Cd sensing occurs through several signals, such as plant hormone, ROS, nitric oxide and hydrogen sulfide that are immediately transmitted to target TFs via signaling pathways (Chmielowska-Bąk et al. 2014; Islam et al., 2015). Various TF families, including WRKY, HSF, AP2/ERF, C2H2, MYB, bZIP, DREB/CBF, NAC, bHLH and bZIP resulted regulated by Cd treatment (Shim et al., 2009; Wu et al., 2012; Gao et al., 2013; Zhang et al., 2019), which in turn can regulated stress-responsive genes networks, eliciting the response to heavy metal. Several studies have showed that HMs enhance ROS accumulation, and hence, a considerable increase in the activities of SOD, CAT, and APX was observed (Bharwana et al., 2013; Bashri and Prasad, 2015). Additionally, Cd accumulation-related molecules, including many transporters (e.g., IRT, ZIP, HMA, ABCC, YSL and NRAMP), chelators (e.g., GSH, PCs, MTs amino acids and organic acids), and genes related to the biosynthesis of these molecules were putatively characterized in *Arabidopsis thaliana*, *Oryza sativa* and other species (Luo et al. 2016; Fan et al. 2018). Pena et al. (2012) have reported that Cd toxicity affects the cell cycle G1/S transition and progression through S phase *via* decreased expression of a cyclin-dependent kinase (CDK). Furthermore, Cd stress

decreases CO<sub>2</sub> assimilation by either diminishing the RUBP carboxylase activity as Cd ions affects the reductant pool for reduction reactions, or by reacting with thiol group of Rubisco (Ferretti et al., 1993; Siborova, 1988). Furthermore, Cd affects the permeability of plasma membrane, and hence interferes with the nitrogen metabolism by inhibiting nitrate uptake and transport, nitrate reductase, and glutamine synthase activity (Hernández et al., 1997). Amino acids, particularly proline and histidine, and their derivatives have been reported to chelate metal ions in cells as well as in the xylem sap to enhance metal tolerance (Rai, 2002; Sharma and Dietz, 2006). Increased activity of enzymes involved in the biosynthesis of phenolic compounds under Cd stress has been correlated with the high tendency to chelate metals due to the presence of hydroxyl and carboxyl groups which bind to metal ions (Jun et al., 2003). The stimulation of CHS (chalcone synthase) and PAL (phenylalanine ammonia-lyase) activities has been reported in several plants exposed to Cd ions (Sobkowiak and Deckert, 2006; Kováčik and Klejdus, 2008; Pawlak-Sprada et al., 2011). Generally, plants respond to Cd stress by chelating and sequestering them in the vacuoles, serving as temporary storage of essential as well as toxic metabolites (Verbruggen et al., 2009; Mendoza-Cózatl et al., 2011). The transport of heavy metals inside the vacuole is performed by transporters localized in the parenchyma cells of xylem and companion cells of phloem. Cys-rich metal binding peptides like phytochelatins (PCs) and metallothionines, nicotinamide and glutathione are also important players in HM tolerance by adsorbing, transporting and sequestering them into the vacuoles (Jalmi et al. 2018). Prominent groups of transporters that maintain physiological concentration of HMs are the following: zinc-iron permease (ZIP), heavy metal transport ATPase (CPx- and PqB-ATPase), natural resistant associated macrophage protein (NRAMP), cation diffusion facilitator (CDF), and ATP-binding cassette (ABC), which are localized at the plasma membrane and on tonoplast membrane of cells (Park et al., 2012; Singh et al., 2015). The reshape of root architecture in response to Cd ions is a further mechanism employed in order to escape from polluted site by heavy metals. Roots activate several mechanisms to cope with Cd toxicity, such as synthesis and deposition of callose to create a barrier for the entry of heavy metal, enhancing plasticity of roots. Many studies report the involvement of phytohormones, such as auxin, ethylene and cytokinin to modulate patterning (Vanstraelen and Benková, 2012) and lateral root formation (De Smet et al., 2015) in case of HM stress. Research in literature showed that Cd interferes with the maintenance of auxin homeostasis either by increasing indole-3-acetic acid (IAA) oxidase activity or altering the expression of several auxin biosynthetic and catabolic genes (Hu et al., 2013). However, most key genes of auxin signalling, including YUCCA, PIN, ARG, IAA, and cell cycle related genes resulted negatively regulated by Cd exposure (Zhao et al., 2015). Cd ions may also participate in the regulation of ethylene synthetic genes, MAPK cascades, NO



accumulation, and polyamine metabolism (Chmielowska-Bak et al., 2014; Schellingen et al., 2015).

Therefore, salt and heavy metal stresses regulate a wide range of genes inducing the generation of signalling molecules, including hormones,  $\text{Ca}^{2+}$ , ROS generation and so on. These molecules interplay with others at different levels either synergistically or antagonistically to activate or inhibit downstream effectors, such as TFs to regulate gene expression levels and protein/enzyme activities in a specific way.

### ***3 High throughput sequencing: the ability to interrogate the genetic and transcriptional landscape in biological systems***

#### ***3.1 Molecular screening and genetic improvement of *Arundo donax* L.***

Marginal lands are growing worldwide, where salinization is going to affect 20% of irrigated (Mayak et al., 2004), whereas in Europe the soil contaminated with heavy metals represent 6.24% (137,000 km<sup>2</sup>) of the total agricultural land (Tóth et al. 2016). During the last 20 years, many studies have analysed the genetic variability among *A. donax* populations not only for taxonomic scope, but also for genetic improvement purposes. Fingerprinting of *A. donax* by molecular markers showed low genetic differences even in populations with large area of spread. The “European Giant Reed (*Arundo donax* L.) Network” showed a low percentage of polymorphism among populations from Greece, Italy and southern France, clustered by their respective origin by using RAPD (Random Amplification of Polymorphic DNA) markers (Lewandowski et al. 2003). Subsequently, analysis by 10 SRAP (Sequence Related Amplified Polymorphism) and 12 TE-based (Transposable element) primer combinations on 185 accessions from a wider area in the United States clearly indicated the occurrence of low genetic diversity because the G/N index was 0.011 (Ahmad et al. 2008). Furthermore, AFLP (Amplified Fragment Length Polymorphism) fingerprinting scored the lowest genetic diversity among 16 accessions in the Mediterranean basin, with Nei’s diversity index of 0.008 (Hardion et al. 2012). By contrast, higher diversity has been reported in an Australian study, where the investigation on three river system led to 31 unique genotypes among 58 plant samples, with a G/N ratio equal to 0.815 (Haddadchi, Gross, and Fatemi 2013). Limited genetic variability is unlikely to explain the physiological variations among accessions, and thus epigenetic variations need to be considered (Danelli et al. 2020). Recently, phenotypical differences among ecotypes due to genetic and epigenetic differences were studied by analysing 96 accessions of *A. donax* collected from 14 different populations in Italy by a combination of AFLP and MSAP markers (Guarino et al. 2019). Besides, pedo-climatic conditions may generate variations in DNA methylation status, which lead to a different convergence and/or divergence of populations in response to stress; these contrasting

behaviours may vary among each ecotype. Observing the rise of epigenetic variants as consequence of environmental conditions, increment of genetic variability can be caused by somaclonal variation and mutagenesis. Somaclonal variation can occur in such cytological abnormalities and in frequent qualitative and quantitative phenotypic mutations, sequence changes, and gene activation and silencing. Somatic variation could be the source of this variability, though the frequency of mutations for *A. donax* has not yet been reported (Malone et al. 2017). Being *A. donax* a polyploid species, it is very difficult to genetically modify it and overcome the redundancy of genetic information. Physical/chemical mutagenesis by gamma radiation can drive modifications in biomass composition of *A. donax* as the increase of cellulose levels, to generate promising clones for second-generation bio-ethanol production, but also with reduced Si/K ratio of biomass and so the ash melting point, which represent a detrimental trait for thermochemical conversion (Zegada-Lizarazu et al., 2020). Clonal selection was already used at the end of 1970s to improve the cane number trait (Janin et al., 1977). Literature data reported that clonal selection is the best effective method up to now for selection towards yield (Pilu et al., 2013; Cosentino et al., 2006), *in vitro* propagation efficiency (Danelli et al., 2019), salt tolerance (De Stefano et al., 2014; Sánchez et al., 2015) and phytoremediation (Domokos-Szabolcsy et al., 2014; Elhawat et al., 2014; Liu et al., 2019). So far, the data used for genetic improvement have been obtained by agronomic studies with the aim of enhancing biomass production. As to render second generation of biofuel a valid alternative to fossil fuels, genetic improvement coupled with breeding programs would allow to enhance oil levels and biomass yields for biodiesel and ethanol production, respectively. Furthermore, these outcomes will be conducted on marginal lands, using little agronomical input and with less interventions by farmer. In order to reach out these goals, the genetic improvements should implicate the increase of total leaf number or its leaf surface, improvement of photosynthetic efficiency, better allocation and efficiency use of resources and the resistance towards biotic and abiotic stresses.

### **3.2 Transcriptomics and RNA Sequencing analysis (RNA-Seq)**

Over the last few years, thanks to the knowledges of molecular biology techniques along with the traditional genetic improvement, it was possible to analyse each phenotypic trait derived by a modified gene (Estrela and Cate, 2016). It has been established that this approach is pivotal for either plants characterized by long life cycle (Allwright and Taylor, 2016) or lignocellulosic species. For instance, the use of SNPs as molecular markers in *Miscanthus* genome allowed to identify associated with cell wall composition and biomass yield markers (Slavov et al., 2014). Another study conducted in *Panicum virgatum* analysed thousands of SNPs by the transcriptome

sequencing (Serba et al. 2016). Therefore, it emerged that the use of new methods developed by the synthetic biology (Lu and Kang, 2008) together with the availability of both transcriptome and genomic data (Nguyen et al., 2013; Abdullah et al., 2016) allow to improve either agronomic yields or the quality of the obtained oils. To achieve these goals, initially preliminary genetic, transcriptome and epigenetic studies are requested in order to enlarge and characterize the mechanisms by which plants growth and respond to environmental stresses, also coupled with the detection of molecular markers associated with the desirable phenotype of crops. Regulation of gene expression in case of abiotic stress conditions includes a wide range of mechanisms to upregulate or downregulated the production of specific gene products (protein or RNA). Transcriptional approach provides deep details about the gene expression levels to identify candidate genes involved in stress response mechanisms. The transcription of a subset of genes into RNA molecules specifies a cell's identity and regulates the biological activities within the cell in order to decode the functional elements of the genome and understanding the process of development and disease (Kukurba et al., 2015). According to the central dogma of molecular biology, RNA molecules act mainly as intermediate between genes and proteins; thus, RNA molecules were the most frequently studied RNA species since they encoded proteins *via* genetic code. In the first approaches, gene expression studies were based on low-throughput methods, such as Northern blots and quantitative polymerase reaction (qRT-PCR), which are useful to measure single transcripts. Over the last decades, methods have evolved to enable genome-wide quantification of gene expression, leading to a new branch of molecular biology known as transcriptomics. The first transcriptomic studies were carried out by using hybridization-based microarray technologies, which provide a high-throughput system at relatively low cost (Schena et al., 1995). Nevertheless, these methods have reported some drawbacks: the requirement for a priori knowledge of the sequences being interrogated, problematic cross-hybridization artefacts in the analysis of highly similar sequences and limited ability to accurately determine the levels of lowly expressed and very highly expressed genes (Casneuf et al., 2007; Shendure, 2008). Instead of hybridization-based methods, sequence-based approaches have been developed to clarify the transcriptome by directly determining the transcript's sequences. The development of high-throughput Next-Generation Sequencing (NGS) revolutionized transcriptomics by allowing RNA analysis through the direct sequencing of complementary DNA (cDNA) (Wang et al., 2009). The benchmark method, known as RNA-Sequencing (RNA-Seq) shows specific advantages over the previous approaches, which has revolutionized our understanding of the complex and dynamic nature of the transcriptome. RNA-Seq provides a more detailed and quantitative view of gene expression, alternative splicing, and allele-specific expression. Advances in the RNA-Seq

workflow, from sample preparation to bioinformatic data analysis enabled deep profiling of the transcriptome as well as the opportunity to investigate the different physiological and pathological conditions. Given that RNA-Seq experiments rely on the use of sequencing platforms to process the sample data, several NGS platforms are commercially available, whilst others are under active technological development (Metzker, 2010). The majority of high-throughput sequencing platforms uses a sequencing-by-synthesis method to sequence tens of millions of sequence clusters in parallel. In recent years, the sequencing industry has been dominated by Illumina, which applies an ensemble-based sequencing-by-synthesis approach (Bentley et al., 2008). Using fluorescently labelled reversible-terminator nucleotides, DNA molecules are clonally amplified while immobilized on the surface of a glass flow-cell. Since, molecules are clonally amplified, this approach provides the relative RNA expression levels of genes. One of the most benefit of ensemble-based platforms is low sequencing error rates (<1%) dominated by a single mismatch. The Illumina HiSeq platform is the most applied next-generation sequencing technology for RNA-Seq and has set the reference for NGS approach. Additionally, an important consideration to take into account for choosing a suitable sequencing platform is based on the transcriptome assembly as to convert a collection of short sequencing reads into a set of full-length transcripts. Gene expression profiling performed by RNA-Seq provides an unprecedented high-resolution view of the global transcriptomic landscape. The conventional pipeline for RNA-Seq data include the following three steps: (i) generation of FASTQ-format files contains sequenced from a NGS platform reads; (ii) reads are assembled into transcripts by mapping each reads onto annotated reference genome or *de novo* assembly of the transcriptome; (iii) quantification of gene expression of each gene by counting the number of reads that aligns to each exon or full-length transcript.

### **3.3 *De novo assembly: a new breakthrough to uncover genetic information***

*De novo* assembly is an alternative approach for reconstructing a reference transcriptome, in which contiguous transcript sequences are assembled with the use of a reference genome or annotations (Robertson G., et al. 2010; Grabherr et al. 2011; Schulz et al. 2012). To accurately estimate gene expression, read counts must be normalized in order to correct the systematic variability, including library fragment size, sequence composition bias, and read depth (Oshlack and Wakefield 2009; Roberts et al. 2011). To cancel these sources of variability, the reads per kilobase of transcripts per million mapped reads (RPKM) metric is used to normalize transcript's read count by using both the gene length and the total number of mapped reads in the sample. For paired end-reads, a metric that normalizes the source of variances in transcript quantification is the paired fragments per kilobase of transcript per million mapped reads (FPKM), which accounts for

the dependency between paired-end reads in the RPKM estimation (Trapnell et al. 2011). A principal aim of many gene expression trials is to assess whether transcripts show a differential expression across various conditions. Next-generation high-throughput sequencing techniques have become an increasingly useful tool for analysing the whole plant genome, proving a mean to decipher the plant molecular regulatory mechanisms in case of specific stressful environments, including heavy metal, herbicide and salt toxicity (Zhang et al. 2016c; Gu et al. 2017). *De novo* assembly might be used to study the transcriptomes for those species for which the genome sequencing is not available, like *Arundo donax* L. This approach would enable an almost exhaustive survey of virtually all expressed genes in a plant tissue subjected to abiotic stress condition. At the beginning, *A. donax* genomic resources were provided by Sablok et al. (2014) by using tissue-specific NGS for four different organs (leaf, culm, bud and root) of one *A. donax* ecotype constituting a comprehensive reference catalogue of transcripts aimed at characterizing and improving the spatial and temporal patterns of expression underlying the high productivity of biomass. The transcriptional analysis revealed differences among each organ in terms of Gene Ontology (GO) categories as well as different relative expression. About of 40-45% of transcripts showed homologies with known sequences and functional annotations of *Oryza sativa* L., *Triticum aestivum* L., and mostly with *Setaria italica* L. and *Zea mays* L., in particular for gene categories related to flowering time, plant height and structure, carbohydrates composition and vernalization response. Afterwards, another transcriptional approach was carried out by using shoot tissue of *A. donax* ecotype to establish a molecular dataset launched following studies on *A. donax* subjected to abiotic stresses condition (Barrero et al. 2015). Furthermore, *de novo* transcriptome assembly of leaf tissue was provided by Evangelistella et al. (2017) to have a more comprehensive gene expression catalogues. In this study three different ecotypes of *A. donax* coming from distant geographical locations, respectively Greece, Croatia and Portugal were grown under natural condition to identify putative genes controlling important agronomic traits, such as stress-associated genes (SAPs), lignin and stomatal development. Additionally, the analysis showed that purine and thiamine metabolism, phenylpropanoid biosynthesis, starch and sucrose metabolism, cellulose biosynthesis, carbon fixation and stomatal development and distribution pathways were the most enriched pathways. Furthermore, simple sequence repeats (SSRs) were identified in the leaf transcriptome to achieve the first genetic market catalogue for *A. donax*, which could be used for population genetics studies. Recently, the first characterization of *A. donax* shoot and root transcriptome in response to water stress induced by 10 and 20 % of polyethylene has been reported by Fu et al. (2016). The data showed a total of 3034 differentially expressed genes (DEGs) between stressed and control conditions in each organ. Notably, a great common genes resulted

differentially expressed between control and severe water stress compared to the control and mild water stress. Interestingly, most stress-related genes belong to “salt”, “osmotic”, “oxidative” and “dehydration” categories. They further identified organ-specific differences in terms of drought-related TFs, such as AP2-EREBP, AUX/IAA, MYB, bZIP, C2H2 and GRAS families. The higher responsivity was found in roots, compared to shoots at the early stage of water stress condition. This work led the fundamental discover and characterization of early responsive genes to water stress which may constitute a basin of information for the improvement of giant reed productivity, under water limitation. Recently, giant reed’s plasticity to salt stress has been investigated at the transcriptional, metabolic and epigenetic level by using three *A. donax* ecotypes characterized by a different sensitivity to saline conditions (Docimo et al., 2019). The transcriptional analysis of key genes related to salt tolerance showed an ecotype- and tissue-dependent response not only in samples treated but also in control conditions, hence suggesting a distinct manner of acclimatization to environmental conditions. Additionally, it was highlighted that each ecotypes respond differently to environmental cues in function of their own genetic constitutive differences and methylome plasticity, since each ecotype displayed differential methylome patterns upon stress imposition, underpinning an inter-link between the salt resistance and epigenetic patterns. Up to now, genomic resources of *Arundo donax* subjected to both salty and contaminated soil, are still poorly understood, which might be useful to outline the whole response mechanisms to these abiotic stresses, in order to establish its cultivation on marginal lands for bioenergy scope.

## *Aim of the work*

Global energy demand is growing rapidly due to the demographic explosion and to strong worldwide urbanization. Additionally, the dwindling fossil energy reserves have posed many challenges to scientific communities to find sustainable alternative resources of renewable energy. The urge necessity of the increasing global energy demand and at the same time the struggle against the climate change, lead the polices of many countries to invest in renewable energy as alternative sources, instead of fossil resources. Among the different resource of renewable energy, biomass gathered by plant species, dedicated to energy production, also known as bioenergy crops, represent a promising alternative to fulfil the energy demand. Bioenergy crops can provide a fundamental contribution for satisfying the demand of energy resources of our planet, due to its high biomass yield, to low irrigation and nitrogen input requirements and biotic and abiotic stress tolerance. Considering that cellulosic feedstock can grow in fields irrigated with waste or salty water, a recommended strategy relies on their cultivation on marginal lands. The Mediterranean basin is characterised by the frequent occurrence of soil salinity linked with the upcoming rapid industrialization and urbanization which are leading to an increase in trace metal contamination in soils. Therefore, a deep knowledge of the global physiological and transcriptomic response of bioenergy crops in case of unfavourable environmental conditions is needed. Within the bioenergy crops, *Arundo donax* L. has been assigned as one of the most promising lignocellulosic crops for the Mediterranean area, in which its biomass feedstock can be readily converted to produce heat, electricity, biofuels and biomaterials. Furthermore, transcriptomic information is still not available about the *A. donax* response to salt and cadmium stress. Our aim is to analyse the effect of long-term period of two levels (severe and extreme) of salt stress upon the *A. donax* whole leaf transcriptome. In fact, as well as the global transcriptome network, in both leaves and roots with the cadmium treatment, using RNA-Seq approach in order to elucidate and characterize the molecular and biological processes, emerge both the salt and cadmium tolerance. Although, *A. donax* represents one of the most promising resources for bioenergy production, we do not know on the molecular characterization of the genes involved in salt stress response and HM detoxification in this bioenergy crop. Thus, the research activity is based on the following aims:

- Analysis the effect of two level of long-term salt and cadmium stress in different *A. donax* ecotypes in terms of their morpho-biometric and physiological parameters;
- *De novo* transcriptome assembly, functional annotation, and analysis of the giant cane transcriptome by RNA-Seq approach;

- Dissect the molecular and physiological bases of *A. donax* resistance to both salt and cadmium treatment;
- Identification of differentially expressed genes (DEGs) and molecular pathways specifically regulated by salt and cadmium exposure;
- Co-expression network analysis and their different regulation in each clone;
- Look for molecular markers capable to genetically discriminates the different clones or associated to specific phenotypes.

This study supplies the first reference transcriptome of *A. donax* bioenergy crop in the prolonged period of salt and cadmium stress condition, for mining and exploring the genetic potential of this crop species. The dissect of the transcriptome reveals strong differences in the enrichment of the Gene Ontology categories and in the relative expression among different environmental conditions, which can drive future attempts for functional genomics or genetic improvement. The functional annotation and characterization of the transcriptome explain into the molecular mechanisms the extreme adaptability to grown in soil affected by salt and heavy metal stress, especially in Mediterranean area. The identification of putative unigenes involved in metabolic pathways offers a pipeline for undertake future efforts in genetic improvement of this species. Furthermore, the identified SSR molecular marker will allow to decipher the interspecific phenotypic diversity to abiotic stress condition among each *A. donax* clones. Therefore, these genetic resources together with the recent knowledges of early transcriptional response to water stress will be available to support future functional genomic and genetic studies to characterize metabolic traits and to underline the high productivity of biofuel feedstock in this crop of paramount economic importance.



## RESULTS

### 4 RNASeq analysis of giant cane reveals the leaf transcriptome dynamics under long-term salt stress

Sicilia et al. BMC Plant Biology (2019) 19:355  
https://doi.org/10.1186/s12870-019-1964-y


BMC Plant Biology

RESEARCH ARTICLE

Open Access

## RNASeq analysis of giant cane reveals the leaf transcriptome dynamics under long-term salt stress



Angelo Sicilia, Giorgio Testa, Danilo Fabrizio Santoro, Salvatore Luciano Cosentino and Angela Roberta Lo Piero\* 

### Abstract

**Background:** To compensate for the lack of information about the molecular mechanism involved in *Arundo donax* L. response to salt stress, we *de novo* sequenced, assembled and analyzed the *A. donax* leaf transcriptome subjected to two levels of long-term salt stress (namely, S3 severe and S4 extreme).

**Results:** The picture that emerges from the identification of differentially expressed genes is consistent with a salt dose-dependent response. Hence, a deeper re-programming of the gene expression occurs in those plants grew at extreme salt level than in those subjected to severe salt stress, probably representing for them an “emergency” state. In particular, we analyzed clusters related to salt sensory and signaling, transcription factors, hormone regulation, Reactive Oxygen Species (ROS) scavenging, osmolyte biosynthesis and biomass production, all of them showing different regulation either versus untreated plants or between the two treatments. Importantly, the photosynthesis is strongly impaired in samples treated with both levels of salinity stress. However, in extreme salt conditions, a dramatic switch from C3 Calvin cycle to C4 photosynthesis is likely to occur, this probably being the more impressive finding of our work.

**Conclusions:** Considered the distinct response to salt doses, genes either involved in severe or in extreme salt response could constitute useful markers of the physiological status of *A. donax* to deepen our understanding of its biology and productivity in salinized soil. Finally, many of the unigenes identified in the present study have the potential to be used for the development of *A. donax* varieties with improved productivity and stress tolerance, in particular the knock out of the GTL1 gene acting as negative regulator of water use efficiency has been proposed as good target for genome editing.

**Keywords:** Bioenergy crops, De novo assembly, Giant reed, Leaf transcriptome, RNA-seq, Salt stress

## 4.1 Background

By 2050, human population may grow to 9.6 billion or about 2.0 people ha<sup>-1</sup> of cultivated land, which calls for considerable increases in agricultural production (Bruinsma, 2009). To meet growing world population and improvements in nutrition and food quality, the demand for energy, particularly with respect to terrestrial and air transports, will also increase. Since petro-chemical resources will become less available, an increase demand for alternative energy that substitutes for fossil fuel transport energy will be met in significant measure by biofuels (Harvey and Pilgrim, 2011; Harvey, 2014). Therefore, the end use of land as a global resource is likely to become the focus of intensified competition between food or feed function and biofuel cultivation. At present, the main feedstock of biofuels all over the world is agricultural product such as sugarcane, cassava, wheat, potato and other crops called *first generation biofuels* (Koizumi, 2015). Cellulosic crops (traditionally called energy crops), referred to as *second generation biofuels*, cultivated with the specific purpose of producing alternative fuels might represent a promising alternative considering that they may satisfy at least part of the energy demand and at the same time mitigate greenhouse gases emission (GHGs), in particular the carbon dioxide emission, by sequestering them into biomass (Mehmood et al., 2017). As cellulosic feedstocks cannot be produced on arable lands due to the aforementioned environmental and economic concerns, a recommended strategy is to grow them on “marginal lands”, usually described as unproductive lands, due to poor soil properties, bad quality of underground water, drought or unfavorable climatic conditions, subsequently with no or little potential of profitability for conventional food crops (Tang et al., 2010). Salt affected soils are also considered marginal due to high salinity and sodicity (Shahid and Al-Shankiti, 2013). They may be practically suitable to grow perennial rhizomatous grasses, which are better adapted to poor soils providing high cellulosic biomass without competition with food crops and overcoming risks for food security. Perennial rhizomatous grasses also display several positive attributes because of their low demand for nutrient inputs consequent to the recycling of nutrients by their rhizomes, and resistance to biotic and abiotic stresses (Mariani et al., 2010). Several studies have been conducted all over the world to evaluate the potential of marginal lands for selected plant species for biomass–bioenergy production. The European project, Optimization of Perennial Grasses for Biomass Production in the Mediterranean Area (OPTIMA) was launched with the aim to establish new strategies for the sustainable use of the marginal land in Mediterranean areas (Monti and Cosentino, 2015). In that project, *Arundo donax* L. (giant reed), among others perennial grasses, was studied in sufficient depth, in terms of biomass production potential in warm-temperate and semi-arid areas (Monti and Cosentino, 2015; Fernando et al., 2015). The adaptability of the plants to different kinds of environments, soils and growing

conditions, in combination with the high biomass production confers on *A. donax* many advantages when compared to other energy crops. *A. donax* requires low irrigation and nitrogen inputs and salinity does not seem to affect plant growth, as it is possible to achieve acceptable biomass yields under high salinity conditions due to its halophyte behavior (Sánchez et al., 2015). *Arundo donax* L., common name “giant cane” or “giant reed”, is a polyploid perennial grass plant belonging to the *Poaceae* family. The phylogenetic origin is unclear, although recent evidences obtained by chloroplastic DNA sequencing suggest a middle-east origin (Hardion et al., 2014). *A. donax* is a sterile plant because of the defective development of male and female gametophytes (Balogh et al., 2012). The reproduction only occurs by the vegetative growth of rhizomes and of stem nodes of broken canes. Consequently, the genotypic diversity among clonal populations is expected to be very low and the genetic improvement of this plant to ameliorate its performance as energy crop in adverse environmental conditions is mainly based on clonal selection (Cosentino et al., 2006; Pilu et al., 2014). As transformation and regeneration protocols are available (Dhir et al., 2010; Takahashi et al., 2010), the genetic engineering could represent a feasible option for the improvement of *A. donax* and these approaches might greatly take advantage from the availability of transcriptomic data sets. Next-generation high-throughput sequencing techniques have become an increasingly useful tool for exploring whole plant genomes, providing a means for analyzing plant molecular regulatory mechanisms in specific environments such as various abiotic stress conditions, including heavy metal toxicity, herbicide toxicity and salt toxicity (Bahieldin et al., 2009; Zhang et al., 2016b; Gu et al., 2017). Soil salinization is referred as the accumulation of soluble salts in the soils (Bockheim and Gennadiyev, 2000). This takes place particularly in arid and semi-arid areas characterized by both great amount of evaporation and minimal precipitation volumes. Salinity affects all plant physiological responses and production by reducing the uptake of water and nutrients and creating an ion imbalance and toxicity (Munns and Tester, 2008; Deinlein et al., 2014; Hanin et al., 2016). Salt may affect plant growth indirectly by decreasing the rate of photosynthesis and stomatal conductance. Stomatal closure is considered as the most dramatic response that occurs in plants after exposure to salinity owing to the osmotic effect of salt outside the roots. Moreover, the reduced rate of photosynthesis increases the formation of reactive oxygen species (ROS) leading to oxidative stress (Munns and Tester, 2008; Deinlein et al., 2014; Hanin et al., 2016; Hossain and Dietz, 2016). The hormone-mediated regulatory network is a key molecular mechanism of salt tolerance in various plants, and transcriptome analysis has indicated that abscisic acid (ABA) signaling plays an important role (Tsukagoshi et al., 2015). After signal perception and transmission, plants respond to salinity by coordinating the regulation of gene expression and triggering a series of physiological and biochemical changes to adapt to

high-salt environments including the activation of specific transcription factors (TFs), and the control of downstream structural genes (Deinlein et al., 2014; Liu et al., 2018). In addition, the synthesis of osmolytes such as proline, betaine, mannitol, flavonoids, and organic acids in plants increases, and related synthetic genes are up-regulated (Chakraborty et al., 2012; Zhang et al., 2016a). Nevertheless, salt stress response mechanisms in plants remain poorly understood due to the complexity of the response process and the genetic variability among plant species. Moreover, our knowledge of the genetic bases of salt tolerance is largely based on genetic studies in model or crop species (Hanin et al., 2016). *De novo* RNA sequencing (RNA-Seq) assembly might facilitate the study of transcriptomes for non-model plant species for which the genome sequence is not available by enabling an almost exhaustive survey of their transcriptomes and allowing the discovery of virtually all expressed genes in a plant tissue under abiotic stress. Useful *A. donax* genomic resources were provided by the work of Sablok et al. (2014), which used tissue-specific NGS of four different organs (leaf, culm, bud and root) of one *A. donax* ecotype constituting a comprehensive reference catalog of transcripts aimed at characterizing and improving the spatial and temporal patterns of expression underlying the high productivity of biomass. Moreover, a shoot transcriptome was obtained from an *A. donax* invasive ecotype (Barrero et al., 2015). To provide a more complete gene expression catalogue and allow a comprehensive comparison among various assemblies, a genomic resource was generated using three ecotypes originating from distant geographical locations that, for this reason, could have accumulated heritable phenotypic differences (Evangelistella et al., 2017). Recently, the characterization of *A. donax* transcriptome in response to drought has been reported leading to the identification of early-responsive genes to water stress which might constitute a basin of information for the improvement of giant reed productivity under water limitation (Fu et al., 2016). Considering the frequent occurrence of soil salinity in the Mediterranean area and the potential use of marginal soil for energy crop cultivation aimed to overcome the incoming food security risks, a deep knowledge of the global transcriptomic response of giant reed to salt is needed seeing as it is not yet available. In this study, we analyzed the effect of two levels of prolonged period of salt stress upon the *A. donax* whole leaf transcriptome by using an RNA-seq approach in order to elucidating the biological processes underlying the salt tolerance in a non- model plant. This study lays the foundation to select candidate genes for cis- but also trans-genesis with the aim to develop plants with improved salt stress tolerance.

## 4.2 Results

### 4.2.1 Effect of salt stress upon *A. donax* morpho-biophysiological parameters

As described in the Methods section, *A. donax* G2, G18 and G20 morpho-biometric and physiological parameters were measured at sampling date after being subjected to two levels of prolonged salt stress imposition (S3, severe and S4, extreme), being both doses much higher than that used to define a soil area as “salinized” (EC 4 dS m<sup>-1</sup>). Considering the average values of the three clones, we observed that both the leaf number per pot, the stem number and the main stem height per pot, were significantly reduced by salt stress, and this effect was more pronounced in correspondence of the S4 treated samples (Figure 1a, 1b and 1c). Similarly, physiological parameters such as SPAD, leaf chlorophyll content, net photosynthesis and biomass yield per pot decreased especially under extreme salt stress conditions (S4) compared with untreated S0 samples (Figure 1d, 1e and 1f). The ecotypes under investigation exhibited different phenotypes in response to salt treatments, although they reproduce asexually and, for this reason, they should have low levels of genetic diversity. In particular, the whole data analysis revealed that G20 clone did not grow under extreme salt stress conditions, suggesting that it is highly sensitive to high salt concentration (Figure 1). Although both G2 and G18 clone grew under severe (S3) and extreme (S4) salt stress conditions, G2 clone showed higher stem and leaf number per pot, and higher physiological parameters than those recorded in G18 clone in S4 conditions. Indeed, G2 clone produced considerable higher biomass yield than that reported in G18 clone in extreme salt stress conditions, in an environment in which likely none crops could have survived (Zörb et al., 2018) (Figure 1f). Therefore, further transcriptomic analysis was conducted upon G2 clone subjected to severe and extreme salt stress. The picture of giant reed phenotype under salt stress is shown in Figure 2.

### 4.2.2 Transcript assembly and annotation

In this study, we carried out a comprehensive identification of transcriptional responses of *A. donax* G2 clone to two different levels of prolonged salt stress by RNA-Seq (see experimental design in Methods section). In Figure 3, a flow chart for *de novo* transcriptome assembly is reported (see details in Figure 3 caption). Raw reads were filtered to remove reads containing adapters or reads of low quality, so that the downstream analyses are based on a total of 643 million clean reads with an average of ~ 71.5 million reads (~10.7 G) per sample, the average percentage of Q30 and GC being 94.7 % and 53.3 %, respectively (Table 1). *De novo* assembly of clean reads resulted in 255,809 transcripts and 186,740 unigenes with N50 length of 1,857 and 1,845,

respectively (Table 1), in line with previous N50 reports (Sablock et al., 2014; Fu et al., 2016), indicating that a good coverage of the transcriptome has been achieved.

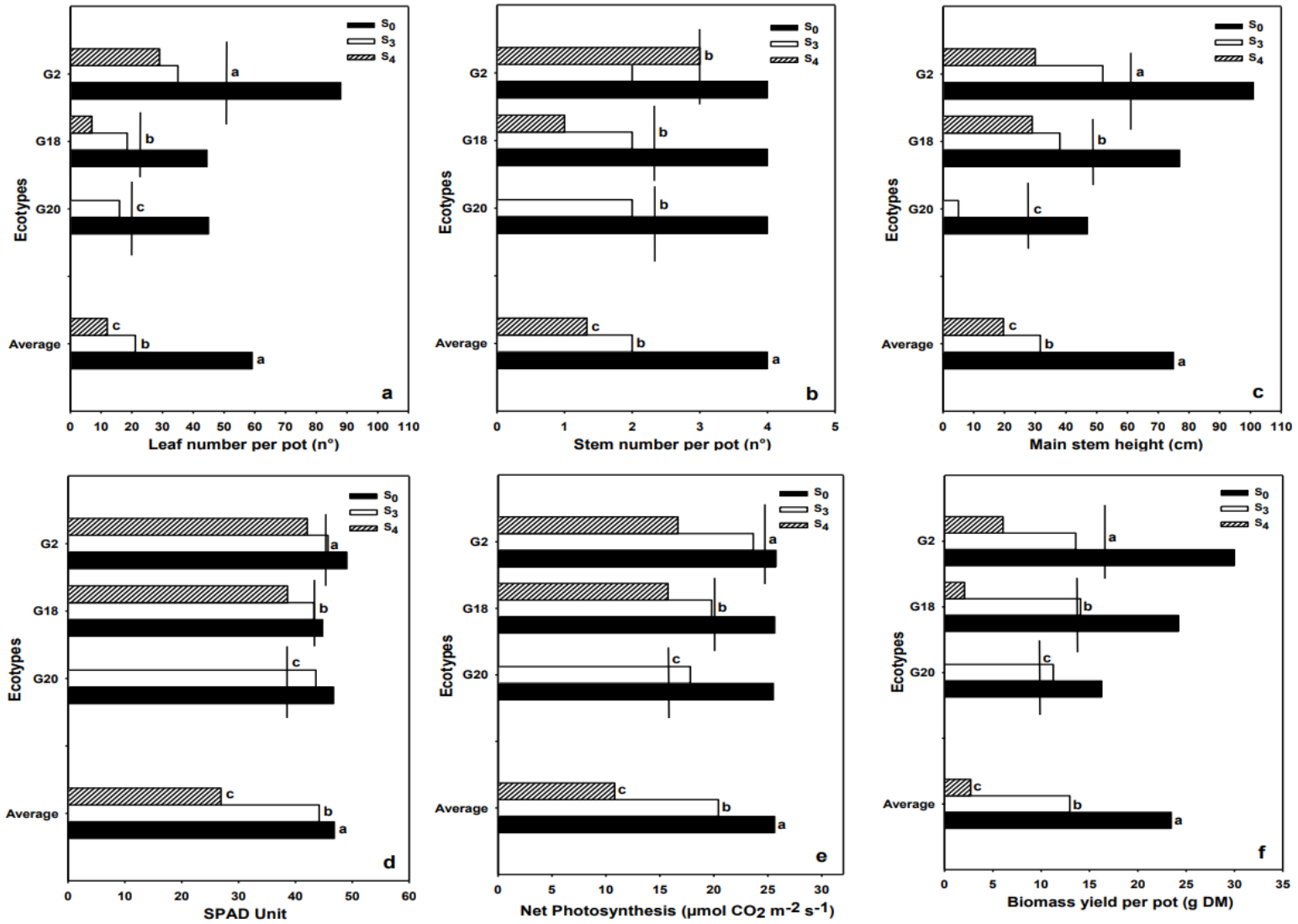


**Figure 1.** Effect of salt stress upon G2, G18 and G20 ecotype morpho-biometric and physiological parameters. A Leaf number per pot. B Stem number per pot. C Main stem height. D SPAD. e Net photosynthesis. F Dry biomass.



**Figure 2.** Picture of giant reed phenotype under salt stress.

To evaluate the assembly consistency, the filtered unique reads were mapped back to the final assembled leaf transcriptome and the average read mapping rate using the alignment software Bowtie2 was 71.85 %. (Table 1). Both transcript and Unigene length distribution is reported in Figure 4. These data showed that the throughput and sequencing quality were high enough to warrant further analysis.

**Table 1.** Summary statistics of the RNA quality and sequencing results

|                             |             |
|-----------------------------|-------------|
| Average RIN                 | 8           |
| Clean reads                 | 634 million |
| N° of transcripts           | 255,809     |
| N° of Unigenes              | 186,740     |
| Average of read mapped rate | 71.85%      |
| Transcripts N50 (bp)        | 1857        |
| Unigenes N50 (bp)           | 1845        |
| Q30 (%)                     | 94.7        |
| GC content (%)              | 53.3        |

To achieve comprehensive gene functional annotation, all assembled unigenes were blasted against public databases, including National Center for Biotechnology Information (NCBI), Protein family (Pfam), Clusters of Orthologous Groups of proteins (KOG/COG), Swiss-Prot, Ortholog database (KO) and Gene Ontology (GO) (Table 2). A total of 116,488 unigenes were annotated in at least one searched database, accounting for 62.38 % of the obtained total unigenes. Among them, 35,630 (19.08%) and 41,101 (22.01%) assembled unigenes showed identity with sequences in the Nr and Nt databases, respectively. The percentage of assembled unigenes homologous to sequences in KO, Swiss-Prot, Pfam, GO and KOG databases were 20.63, 32.41, 26.96, 42.28 and 16.72%, respectively (Table 2).



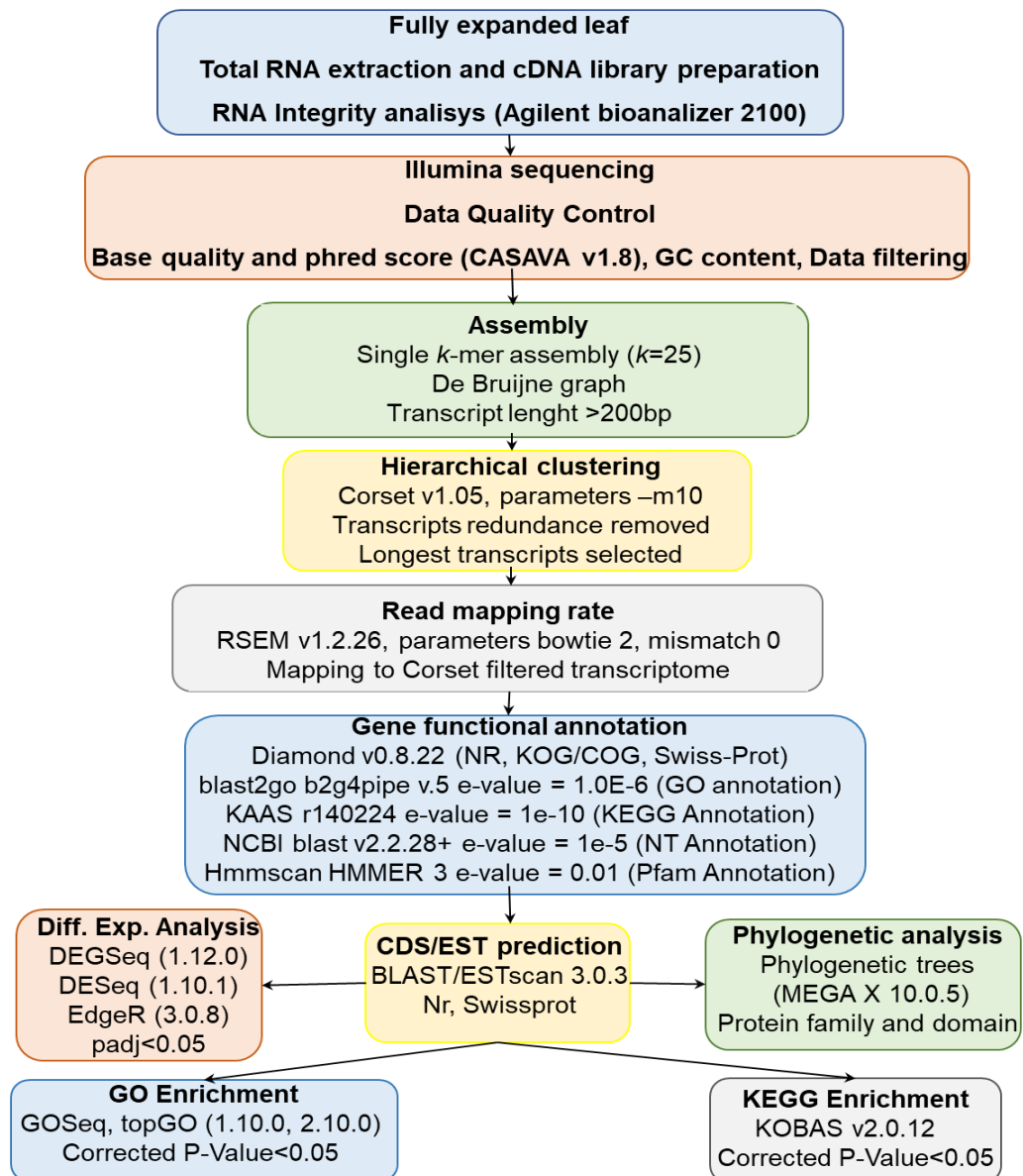


**Figure 3.** Flowchart of de novo assembly and analysis of *Arundo donax* leaf transcriptome. After the fully expanded leaf sampling, total RNA extraction and cDNA library preparation was carried out. The RNA integrity and quality analysis were performed (blue) before the Illumina sequencing. The sequencing output data were subjected to quality control of both reads and bases and data filtering (orange) in order to remove containing adapter reads or reads of low quality. Clean data were used for the de novo assembly of transcripts choosing the single k-mer approach ( $k = 25$ ) (green), and the pre-assembled transcriptome obtained was further processed with Corset for hierarchical clustering by removing transcripts redundancy and by selecting the longest transcripts as unigenes (yellow). The quality of the assembly was assessed by mapping back the reads onto the filtered transcriptome (grey). Finally, gene functional annotation, CDS/EST prediction, differential expression analysis, phylogenetic analysis and GO and KEGG enrichment were carried out.

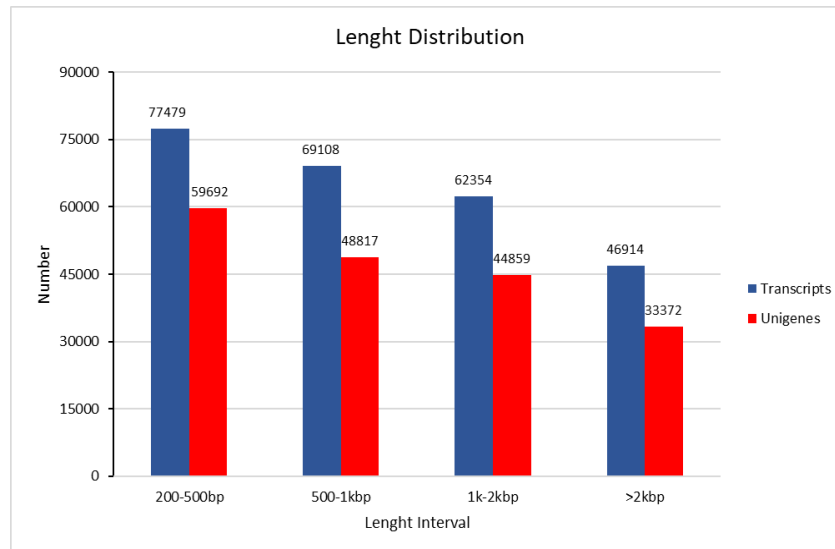


**Figure 4.** Length distribution of transcripts and Unigenes

**Table 2.** The number and percentage of successful annotated genes

| Database                           | N° of Unigenes | %     |
|------------------------------------|----------------|-------|
| Annotated in Nr                    | 128,536        | 56.31 |
| Annotated in Nt                    | 116,575        | 51.07 |
| Annotated in KO                    | 45,516         | 19.94 |
| Annotated in SwissProt             | 86,398         | 37.85 |
| Annotated in Pfam                  | 91,534         | 40.1  |
| Annotated in GO                    | 96,260         | 42.17 |
| Annotated in KOG                   | 36,454         | 15.97 |
| Annotated in at least one database | 148,190        | 64.92 |

### 4.2.3 Identification of differentially expressed genes (DEGs)

The characterization of *A. donax* transcriptional response to salt stress was carried out by the identification of the unigenes whose expression level changed upon NaCl treatments (Table 3). According to the experimental design, a total of 38,559 differentially expressed genes (DEGs) were identified from all the comparisons. In details, 2,086 up-regulated genes and 1,766 down-regulated genes were detected in the G2-S3 vs G2-CK (severe salt stress samples versus control samples), whereas in the G2-S4 vs G2-CK set (extreme salt samples versus control samples) 13,835 up-regulated genes and 11,205 down-regulated genes were found, thus suggesting that G2 clone re-adjusts the network of transcriptional machinery in order to deeply modify gene expression under salt extreme stress conditions (S4) with respect to severe salt conditions (S3) (Table 3).

| Comparison       | Up-regulated | Down-regulated | Total DEGs |
|------------------|--------------|----------------|------------|
| G2-S3 vs G2-CK   | 2,086        | 1,766          | 3,852      |
| G2-S4 vs G2-CK   | 13,835       | 11,205         | 25,040     |
| G2-S4 vs G2-S3   | 5,765        | 3,902          | 9,667      |
| G34-S3 vs G34-CK | 977          | 801            | 1,778      |
| G34-S3 vs G2-S3  | 836          | 1311           | 2,147      |
| Total DEGs       | 23,499       | 18,985         | 42,484     |

**Table 3.** DEG number of different comparisons under salt treatments

Venn diagram analysis showed that 2,702 common DEGs are in both G2-S3 vs G2-CK and in G2-S4 vs G2-CK comparisons thus suggesting that their specific involvement in the response to salt stress is not dependent by salt doses (Figure 5). A total of 1,150 genes are exclusively regulated under severe salt stress condition (G2-S3 vs G2-CK data set), whereas a total of 22,338 genes are specifically regulated during extreme salt stress condition (G2-S4 vs G2-CK data set). Among a total of 9,667 observed DEGs, 1,554 genes were identified as specifically regulated in the G2-S4 vs G2-S3 (extreme salt samples versus severe salt samples) comparison (Figure 5).

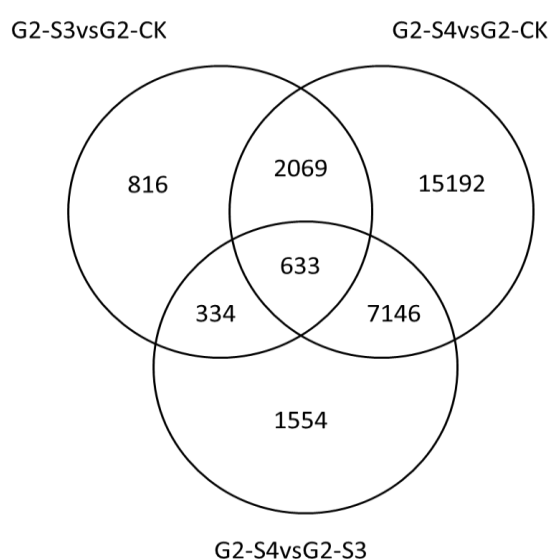


**Figure 5.** Venn diagram of differently regulated genes. Comparison among G2-S3 vs G2-CK, G2-S4 vs G2-CK, G2-S4 vs G2-S3 sample set

Validation of expression levels for ten selected DEG candidates was carried out by quantitative real-time PCR (qRT-PCR) (Table 4). The results show high congruence between RNA-Seq results and qRT-PCR (coefficient of determination  $R^2 = 0.91$ ) indicating the reliability of RNA-Seq quantification of gene expression (Figure 6). Therefore, the selected genes could also constitute useful markers of salt stress in *A. donax*.

**Table 4.** List of DEGs and sequences primers used for Real Time qRT-PCR validation.

| Pattern             | Cluster ID   | Annotation                                       | log <sub>2</sub> FC Illumina | log <sub>2</sub> FC rt-PCR |
|---------------------|--------------|--------------------------------------------------|------------------------------|----------------------------|
| G2_S4vsG2_CK / Up   | 14027.257437 | methyltransferase PMT26                          | 47,70                        | 2,75                       |
| G2_S3vsG2_CK / Up   | 14027.6881   | anthocyanidin 3-O-glucosyltransferase            | 26,35                        | 2,93                       |
| G2_S4vsG2_CK / Up   | 14027.62961  | senescence-associated protein DH                 | 14,488                       | 2,59                       |
| G2_S4vsG2_CK / Up   | 14027.99727  | ACC oxidase                                      | 2,28                         | 0,87                       |
| G2_S4vsG2_CK / Up   | 14027.51601  | uncharacterized protein                          | 65,81                        | 6,82                       |
| G2_S4vsG2_CK / Down | 14027.163842 | proline dehydrogenase 2                          | -16,64                       | -0,23                      |
| G2_S4vsG2_S3 / Down | 14027.231635 | palmitoyltransferase                             | -13,73                       | -0,56                      |
| G2_S4vsG2_S3 / Down | 14027.159114 | Ribulose biphosphate carboxylase                 | -27,5                        | -0,98                      |
| G2_S3vsG2_CK / Down | 14027.226133 | probable WRKY transcription factor 4             | -54,44                       | -2                         |
| G2_S3vsG2_CK / Down | 14027.24929  | NAC domain-containing protein 77                 | -21,56                       | -0,47                      |
| All                 | 14027.113435 | 26 S proteasome non-ATPase regulatory subunit 11 |                              |                            |

| Cluster ID   | Primer F 5'→3'         | Primer R 5'→3'        |
|--------------|------------------------|-----------------------|
| 14027.257437 | GCCTCGACAATGAGAAGGCT   | GCTTGGTGTGAGGCACATTG  |
| 14027.6881   | GTGAAGGGCGACCAGTACCT   | CCGCGAATATCCTCTGCACG  |
| 14027.62961  | CGATCACCACCAACTCGACG   | GCAGCCGATGGAGTAGACGA  |
| 14027.99727  | CAACGGCAGGTACAAGAGCG   | TCCTCGAACACGAACCTGGG  |
| 14027.51601  | CCTCTCAGATCCAAGCTCCTCA | TCGGAATCACCTTGTGCCG   |
| 14027.163842 | GCGTGTTTCGTCTCTTGTGTCC | AACTCGAGCACCTTCCTCTCG |
| 14027.231635 | AGGTTCGTTTCTGCACAGGC   | GGGTCACTGGGAACGAACAC  |
| 14027.159114 | CAGCAACGGTGGAAGGATCA   | TTCTCACGGAAGACGAAGCC  |
| 14027.226133 | CCAGTGTCAGTCTCCTCCTG   | GTCGTCAGATAGCCCGTAGG  |
| 14027.24929  | CATGCACGAGTATCGCCTCG   | GAAGTTTGGCGTTTCGGCAG  |
| 14027.113435 | CACACGACTAGCAGCTTCAAG  | TTCAAACGTCGGGAAGGTTG  |

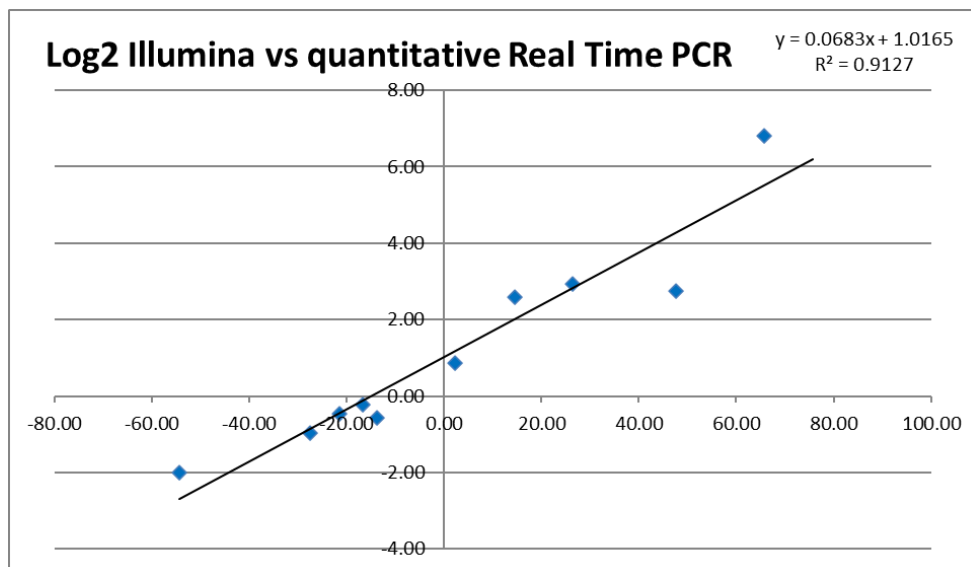


**Figure 6.** Validation of *A. donax* DEGs by Real Time qRT-PCR

#### 4.2.4 Functional classification of DEGs

Gene Ontology (GO) terms, Clusters of Orthologous Groups of proteins (KOG) classification and Kyoto Encyclopedia of Genes and Genomes (KEGG) pathway functional enrichment were performed to identify possible biological processes or pathways involved in salt stress response. Considering the G2-S3 vs G2-CK sample set (Figure 7a), “oxidation-reduction process” (222 up- and 119 down-regulated genes), “transmembrane transport” (125 up- and 97 down-regulated genes) and “carbohydrate metabolic process” (152 up- and 54 down-regulated genes) are the three most enriched GO terms in the Biological Process (BP) ontology. “Oxidoreductase activity” (216 up- and 122 down-regulated genes) is the most enriched GO terms in the Molecular Function (MF) category ontology indicating that genes acting in this process may play crucial roles in the response to salt treatment. Among the DEGs belonging to G2-S4 vs G2-CK data set, “metabolic process” (5,934 up- and 4,493 down-regulated genes), “single organism process” (4,834 up- and 3,404 down-regulated genes), “single organism metabolic process” (2,988 up- and 2,090 down-regulated genes) and “oxidation-reduction process” (1,355 up- and 831 down-regulated genes) are the most represented in the category of BP. “Catalytic activity” is the main category in the MF group (5,380 up- and 3,836 down-regulated genes) but also “oxidoreductase activity” and “transporter activity” are highly represented in this group (Figure 7b). Interestingly, the same categories are represented in the G2-S4 vs G2-S3 sample set (Fig. 7c), although in this last comparison a lower number of genes are involved (Figure 7c).

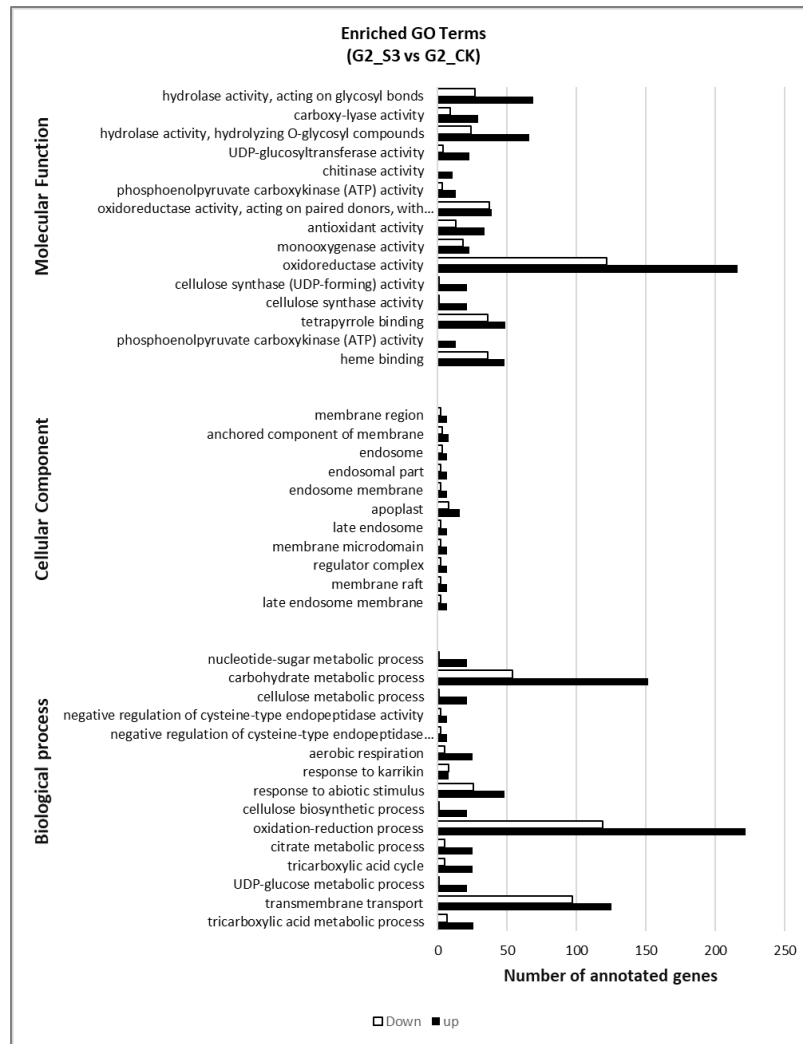


**Figure 7a.** GO enrichment analysis for the DEGs in *A. donax*. G2-S3 vs G2-CK. The Y-axis indicates the subcategories, and the X-axis indicates the numbers related to the total number of GO terms. BP, biological processes; CC, cellular components; MF, molecular functions.

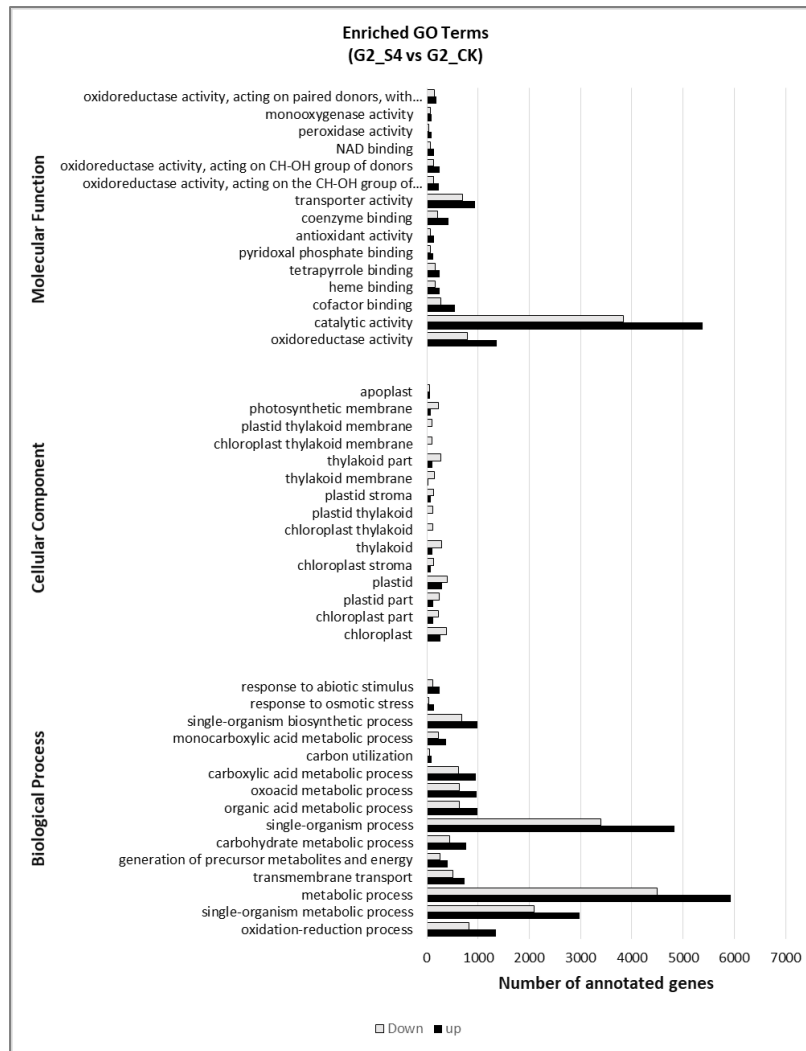


**Figure 7b.** GO enrichment analysis for the DEGs in *A. donax*. G2-S4 vs G2-CK. The Y-axis indicates the subcategories, and the X-axis indicates the numbers related to the total number of GO terms. BP, biological processes; CC, cellular components; MF, molecular functions

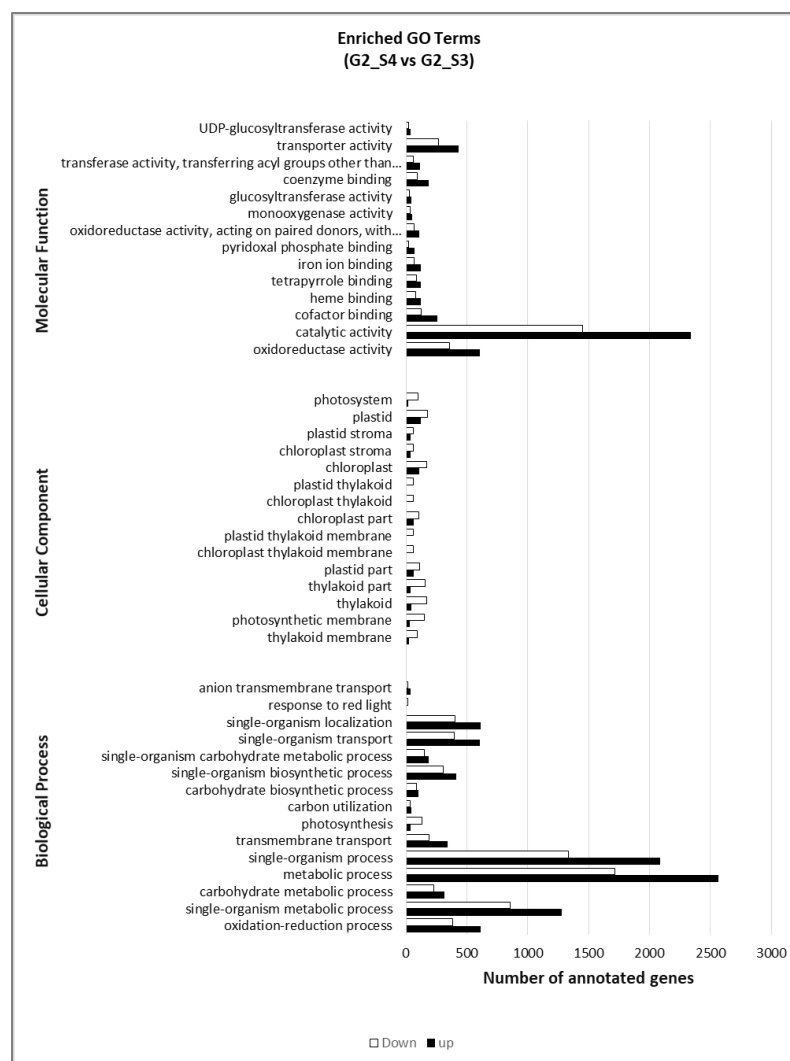


**Figure 7c.** GO enrichment analysis for the DEGs in *A. donax*. G2-S4 vs G2-S3. The Y-axis indicates the subcategories, and the X-axis indicates the numbers related to the total number of GO terms. BP, biological processes; CC, cellular components; MF, molecular functions.

To predict and classify possible functions, all unigenes (255,809) were aligned to the KOG database and were assigned to the KOG categories (Figure 8). Among the KOG categories, the cluster for “general function” (16%) represented the largest group, followed by “posttranslational modification, protein turnover, chaperones” (13.4%) and “signal transduction mechanisms” (9.3%). “Translation, ribosomal structure and biogenesis” (8%), “RNA processing and modification” (6.4%) and “transcription” (5.6%) were the largest next categories, whereas, only a few unigenes were assigned to “nuclear structure” and “extracellular structure”. In addition, a discrete number of unigenes were assigned to “intracellular trafficking, secretion, and vesicular transport” (Figure 8). The sets of DEGs originated from the above-described three comparisons were also mapped onto KEGG pathways. Table 5 shows the main fifty KEGG pathway terms sorted by a decreasing order of the gene number involved in the pathways in relation to all the comparison under investigation (G2-



S3 vs G2-CK, G2-S4 vs G2-CK, G2-S4 vs G2-S3). Overall, the results show that the maximum number of DEGs were observed in the “carbon metabolism” pathway, followed by the “biosynthesis of amino acids” and “carbon fixation in photosynthetic organisms” indicating that a deep reprogramming of these metabolisms under salt treatments occurred. The reprogramming activity of the metabolic pathways is supported by the involvement of other important pathways such as “ribosome”, “RNA transport”, “mRNA surveillance pathway” and “aminoacyl-tRNA biosynthesis” that gives support to an increased re-modulation of protein biosynthesis. “Plant hormone signal transduction”, which comprises the transcripts of several hormone-responsive proteins involved in regulation and signal transduction and two other important pathways, including ‘phenylalanine metabolism’ and ‘plant-pathogen interaction’ were also found to be regulated by salt in our study (Table 5). Other examples of relevant pathways, which are known to be involved in responses to abiotic stresses, in general are ‘starch and sucrose metabolism’, ‘arginine and proline metabolism’ and “AMPK signaling pathway” (Table 5) (Fu et al., 2016).

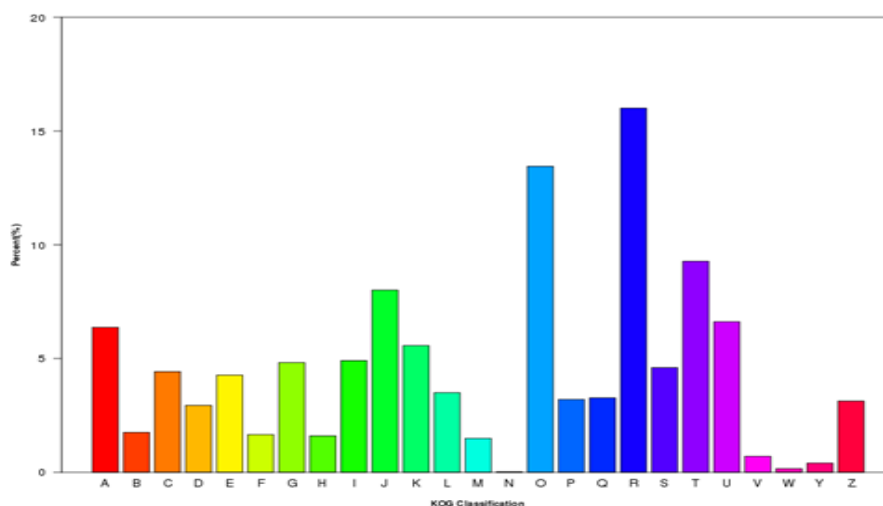


**Figure 8. Clusters of orthologous groups (KOG) classification.** All unigenes were aligned to KOG database to predict and classify possible functions. Out of 255809 unigenes, 49848 sequences were assigned to 25 KOG classifications. (A) RNA processing and modification; (B) chromatin structure and dynamics; (C) energy production and conversion; (D) cell cycle control, cell division, chromosome partitioning; (E) amino acid transport and metabolism; (F) nucleotide transport and metabolism; (G) carbohydrate transport and metabolism; (H) coenzyme transport and metabolism; (I) lipid transport and metabolism; (J) transition, ribosomal structure and biogenesis; (K) transcription; (L) replication, recombination and repair; (M) cell wall/membrane/envelope biogenesis; (N) cell motility; (O) posttranslational modification, protein turnover, chaperones; (P) inorganic ion transport and metabolism; (Q) secondary metabolites biosynthesis, transport and catabolism; (R) general function prediction only; (S) function unknown; (T) signal transduction mechanisms; (U) intracellular trafficking, secretion, and vesicular transport; (V) defense mechanisms; (W) extracellular structures; (X) unnamed protein; (Y) nuclear structure; (Z) cytoskeleton.

**Table 5.** Distribution of KEGG pathways for DEGs in the three sample sets. Data are sorted by number of G2-S4 vs G2-CK DEGs mapping to KEGG pathways.

| <b>Enriched Pathway terms</b>               | <b>G2-S3<br/>vs<br/>G2-CK</b> | <b>G2-S4<br/>vs<br/>G2-CK</b> | <b>G2-S4<br/>vs<br/>G2-S3</b> | <b>Total</b> |
|---------------------------------------------|-------------------------------|-------------------------------|-------------------------------|--------------|
| Carbon metabolism                           | 55                            | 548                           | 273                           | 876          |
| Biosynthesis of amino acids                 | 44                            | 463                           | 203                           | 710          |
| Carbon fixation in photosynthetic organisms | 37                            | 259                           | 149                           | 445          |
| Ribosome                                    | 7                             | 252                           | 148                           | 407          |
| Plant hormone signal transduction           | 52                            | 252                           | 89                            | 393          |
| Starch and sucrose metabolism               | 41                            | 249                           | 102                           | 392          |
| Phenylpropanoid biosynthesis                | 61                            | 208                           | 103                           | 372          |
| Oxidative phosphorylation                   | 20                            | 257                           | 85                            | 362          |
| Glycolysis / Gluconeogenesis                | 26                            | 237                           | 83                            | 346          |
| Glyoxylate and dicarboxylate metabolism     | 18                            | 189                           | 129                           | 336          |
| Pyruvate metabolism                         | 30                            | 204                           | 101                           | 335          |
| Arginine and proline metabolism             | 31                            | 186                           | 99                            | 316          |
| Cysteine and methionine metabolism          | 15                            | 182                           | 86                            | 283          |
| Phenylalanine metabolism                    | 41                            | 161                           | 77                            | 279          |
| Pantothenate and CoA biosynthesis           | 7                             | 249                           | 19                            | 275          |
| Glycerophospholipid metabolism              | 22                            | 154                           | 78                            | 254          |
| Peroxisome                                  | 16                            | 158                           | 79                            | 253          |
| Protein processing in endoplasmic reticulum | 19                            | 178                           | 46                            | 243          |
| Alanine, aspartate and glutamate metabolism | 19                            | 143                           | 77                            | 239          |
| Citrate cycle (TCA cycle)                   | 23                            | 137                           | 67                            | 227          |
| Glutathione metabolism                      | 11                            | 155                           | 59                            | 225          |
| Purine metabolism                           | 20                            | 156                           | 49                            | 225          |
| Glycine, serine and threonine metabolism    | 17                            | 132                           | 70                            | 219          |
| Cyanoamino acid metabolism                  | 19                            | 115                           | 75                            | 209          |
| Amino sugar and nucleotide sugar metabolism | 20                            | 135                           | 48                            | 203          |
| AMPK signaling pathway                      | 20                            | 119                           | 54                            | 193          |

|                                                     |    |     |    |     |
|-----------------------------------------------------|----|-----|----|-----|
| Plant-pathogen interaction                          | 14 | 135 | 43 | 192 |
| 2-Oxocarboxylic acid metabolism                     | 12 | 128 | 52 | 192 |
| Lysosome                                            | 23 | 112 | 54 | 189 |
| Tyrosine metabolism                                 | 7  | 114 | 59 | 180 |
| Methane metabolism                                  | 9  | 120 | 48 | 177 |
| Pentose phosphate pathway                           | 5  | 114 | 53 | 172 |
| RNA degradation                                     | 10 | 105 | 30 | 164 |
| Endocytosis                                         | 12 | 111 | 38 | 161 |
| Fatty acid metabolism                               | 7  | 105 | 49 | 161 |
| Phagosome                                           | 21 | 107 | 33 | 161 |
| RNA transport                                       | 9  | 109 | 40 | 158 |
| Photosynthesis                                      | -  | 113 | 93 | 156 |
| Fructose and mannose metabolism                     | 5  | 102 | 48 | 155 |
| Phenylalanine, tyrosine and tryptophan biosynthesis | 9  | 98  | 44 | 151 |
| Ubiquinone and other terpenoid-quinone biosynthesis | 9  | 97  | 43 | 149 |
| Fatty acid degradation                              | 3  | 88  | 49 | 140 |
| Galactose metabolism                                | 13 | 92  | 28 | 133 |
| Spliceosome                                         | 11 | 79  | 22 | 112 |
| alpha-Linolenic acid metabolism                     | 3  | 63  | 43 | 109 |
| Carotenoid biosynthesis                             | 14 | 58  | 31 | 103 |
| mRNA surveillance pathway                           | 5  | 70  | 26 | 101 |
| Drug metabolism - cytochrome P450                   | 8  | 62  | 29 | 99  |
| Aminoacyl-tRNA biosynthesis                         | 3  | 78  | 14 | 95  |
| Porphyrin and chlorophyll metabolism                | 2  | 61  | 22 | 85  |

#### 4.2.5 Identification of functional genes related to salt stress tolerance

To unravel the *A. donax* G2 salt stress response and to investigate the effect of salt dose, we analyzed the RNA-Seq datasets from each of the aforementioned comparisons, focusing on genes and pathways known to be related to soil salinity. In this further analysis, those clusters showing a threshold of +/- 10.000 log<sub>2</sub>fold change have been considered as DEGs (up- or down-regulated) in the *A. donax* transcriptome (Table 6-8). For each cluster, the alignment of *A. donax* sequence has been performed and the score of these alignments was reported (% identity and *e* value) thus providing valuable indications of the cluster similarity with the reported genes (Table 6-8). Congruously, tables report clusters whose % of identity was higher than 50 and the *e* value < 0.05.

#### 4.2.6 Salt sensory and signaling mechanisms

The analysis of different expressed genes between G2-S3 and G2-CK revealed that homologous to *Oryza sativa* (CBL-interacting protein kinases 1) CIPK1-SOS2-like protein and homologous to *Setaria italica* HKT9 gene are up-regulated in the salt treated samples, whereas genes homologous to the *Arabidopsis* NHX1 and NHX2 (Na<sup>+</sup>/H<sup>+</sup> antiporters) are down regulated in response to severe S3 salt stress (Table 6). CIPK1-SOS2-like protein is a serine/threonine protein kinase involved in the activation of plasma membrane Na<sup>+</sup>/H<sup>+</sup> antiporter (SOS1) which mediates the exclusion of Na<sup>+</sup> excess out of the cells, whereas HKT9 gene encodes a probable cation transporter. Consequently, the data suggest that the plant response to the S3 salt dose is likely either to increase the activation upon the existing Na<sup>+</sup>/H<sup>+</sup> antiporter (SOS1) by the CIPK1-SOS2 like activity, or to adjust the K<sup>+</sup> homeostasis by inducing the expression of HKT9. The down regulation of NHXs indicates that the vacuolar sequestration of Na<sup>+</sup> excess seems to be impaired in the *A. donax* subjected to severe salt stress condition. Considering the G2-S4 vs G2-CK data set, a distinct response to extreme salt stress has been detected (Table 7). Along with the up regulation of CIPK1-SOS2 like and HKT9, the induction of CBL-interacting protein kinase 24 SOS2 (homologs of *Oryza sativa* subsp. Japonica protein) is also specifically up regulated under extreme salt stress conditions (S4). Moreover, the up regulation of NHX1 expression (*Arabidopsis thaliana* sodium/hydrogen exchanger 1) encoding the vacuolar Na<sup>+</sup>/H<sup>+</sup> antiporter is observed (Table 7).

#### 4.2.7 Transcription factors

In our study, DEGs encoding TFs were identified and divided in 16 subfamilies, as showed in Figure 9, which reports the transcription factor subfamilies sorted by the G2-S4 vs G2-CK DEG number. The results showed that under S3 severe stress condition, an average of 12 TFs for each family are differently regulated. In particular, 23 DEGs belong to auxin/indole acetic acid (AUX/IAA), 21 to bHLH and 19 to NAC families, respectively, indicating that these are the most

represented subfamilies and they probably play a key role in regulating the changes of transcriptional regulation in response to salt (Figure 9). It worthwhile to mention that among the downregulated genes belonging to G2-S3 vs G2-CK DEGs, a homolog of *Setaria italica* protein TIFY 10B-like (LOC101761171) known to be a repressor of jasmonate (JA) responses, has been found (Table 6). Moreover, a homolog of *Setaria italica* trihelix transcription factor GTL1 (LOC101762434), that acts as negative regulator of water use efficiency (Yoo et al., 2010; Weng et al., 2012) has been found up-regulated in G2-S3 vs G2-CK DEGs (Table 6). Finally, homologs of *Setaria italica* bZIP ABSCISIC ACID-INSENSITIVE 5-like protein 7 functioning as transcriptional activator in the ABA-inducible expression of rd29B have been also found among the up-regulated clusters. The role of these differently regulated clusters will be discussed below.

In the G2-S4 vs G2-CK comparison, a deeper modification of the transcription regulation is detected since an average of 53 TFs for each family resulted differently regulated in comparison with untreated samples, being the bHLH (94 DEGs), AUX/IAA (109 DEGs), MYB (88 DEGs) and NAC (91 DEGs) subfamilies the most represented (Figure 9). A comparative analysis performed using the available database of rice transcription factors under salt stress led to the identification of 449 *A. donax* unigenes, corresponding to high confidence rice TF homologs previously identified as salt or salt/drought genes (Table 9) (Priya and Jain, 2013). Probably because of the altered water potential under salt stress, the majority of these genes (434) are also responsive to drought. A total of 15 genes are specifically responding to salt (Table 9), and among them, 9 (six up regulated and three downregulated) belong to the AP2-EREBP family (Chen et al., 2016). Interestingly, 14 out of the 15 specific salt-related transcription factors are differently regulated exclusively in extreme salt stress condition (G2-S4 vs G2-CK) (Table 9).

#### 4.2.8 Hormone regulation of salt stress response

We focused our attention on the main plant hormones involved in salt stress response, such as abscisic acid, brassinosteroid, ethylene, auxin/IAA and jasmonic acid (Golldack et al., 2014; Gupta and Huang, 2014). The analysis of G2-S3 vs G2-CK data set revealed that the genes involved in abscisic acid biosynthesis (NCED, zeathaxin oxidase and aldehyde oxidase) are not differently regulated by the long term salt stress, otherwise homolog of *Triticum urartu* (Nr ID: EMS68885.1) abscisic acid 8'-hydroxylase 1 (LOC101782596), involved in ABA catabolism, has been found among the up-regulated genes (Table 6). Based on these differential expressions, it seems that circulating ABA is channeled in a degradation pathway and the plant responds to prolonged severe stress by lowering ABA levels. Among the up-regulated genes, homologs of *Setaria italica* abscisic acid receptor PYL8 (LOC101768693), of *Setaria italica* ABSCISIC ACID-INSENSITIVE 5-like protein

7 (LOC101778442), *Setaria italica* abscisic acid receptor PYR1-like (LOC101776342), *Oryza sativa* serine/threonine-protein kinase SnRK (SnRK) and to *Setaria italica* probable protein phosphatase 2C 30 (LOC101766228) were discovered. According to these results, although ABA levels seems to be lowered, as the up regulation of abscisic acid 8'-hydroxylase homolog suggests, ABA signal is probably persisting since ABA nucleoplasmatic receptors are up-regulated as well as the SnRK2 which active many downstream ABA-responsive processes (Golldack et al., 2014). As regards G2-S4 vs G2-CK and G2-S4 vs G2-S3 sample data, *Setaria italica* abscisic acid 8'-hydroxylase 3 (LOC101760218) and *Setaria italica* abscisic acid receptor PYL8 (LOC101768693) are up-regulated (Table 7 and 8). Moreover, the downregulation of homolog to *Oryza sativa* 9-cis-epoxycarotenoid dioxygenase (NCED) in the G2-S4 vs G2-S3 comparison, which is not detected in the G2-S3 vs G2-CK, is observed and it might more clearly indicate that ABA synthesis is not induced in samples subjected to long-term extreme salt stress. As regards brassinosteroid, in the G2-S3 vs G2-CK data set, homolog of *Setaria italica* cytochrome P450 734A6-like BAS1 (LOC101760518), a brassinosteroid inactivator, is up-regulated indicating that brassinosteroid signaling is likely interrupted in response to S3 severe salt treatment (Table 6). Conversely, by the analysis of the G2-S4 vs G2-CK data set (Table 7), confirmed by the G2-S4 vs G2-S3 comparison (Table 8), we discovered that homolog of *Setaria italica* cytochrome P450 85A1 (LOC101770408) encoding brassinosteroid-6-oxidase 2, that is implicated in brassinosteroid biosynthesis, is up-regulated under extreme salt stress (Table 7). Transcripts encoding ACC oxidase, namely the ethylene-forming enzyme, have been found up-regulated both under severe (homolog of *Saccharum arundinaceum* 1-aminocyclopropane-1-carboxylate oxidase) and extreme salt stress (homolog of *Oryza brachyantha* 1-aminocyclopropane-1-carboxylate oxidase (LOC102702913). However, in G2-S3 vs G2-CK sample data, none of the ethylene downstream acting genes have been found, neither among the up-regulated nor among the down-regulated clusters (Table 6). Conversely, the analysis of the G2-S4 vs G2-CK revealed that homolog of *Arabidopsis thaliana* receptor ethylene response 1 (ETR 1) is downregulated, whereas clusters related to CTR1 (*Zea mays* serine/threonine-protein kinase CTR1-like) and EIN3 (*Setaria italica* ETHYLENE INSENSITIVE 3-like 3 protein), both implicated in quenching the ethylene signal, are up-regulated (Table 7). Sharp differences between the response of *A. donax* to salt dose have been detected once we considered the role of auxin/IAA as signal molecule. In this respect, the genes encoding the main biosynthetic enzyme, such as indole-3-pyruvate monooxygenase YUCCA2-like (LOC101757189) (Woodward and Bartel, 2005), is downregulated in G2-S3 vs G2-CK comparison indicating that severe salt stress seems not to implicate an increase in IAA levels. Analyzing the response to extreme salt stress upon *A. donax* leaves, we found a strong induction of different clusters relative to YUCCA-like indole-3-pyruvate monooxygenases, which

have been described as a high redundant gene family (Woodward, 2005). Unfortunately, several clusters are also found among the downregulated genes thus rendering difficult to make general conclusions (data not shown). However, a homolog of *Zea mays* indole-3-acetaldehyde oxidase (AAO), involved in the biosynthesis of auxin, is upregulated in S4 samples and also in the G2-S4 vs G2-S3 comparison suggesting that IAA might be synthesized in S4 extreme conditions (Table 8). Moreover, exclusively under extreme stress condition a homolog of auxin responsive GH3 gene family, regulating levels of biologically active auxin, is also up-regulated (Table 7). Finally, homolog of *Oryza sativa* subsp. *japonica* jasmonic acid-amido synthetase JAR1 is down regulated in G2-S4 vs G2-CK comparison (Table 7) but not in the G2-S3 vs G2-CK samples indicating that under extreme salt stress conditions jasmonic acid biosynthesis might be impaired.

#### 4.2.9 ROS scavenging regulatory mechanisms

The analysis of G2-S3 vs G2-CK revealed that, among the antioxidant enzymes, ascorbate peroxidase (APX) expression is up-regulated suggesting that H<sub>2</sub>O<sub>2</sub> could be the main ROS the *A. donax* cells have to cope with under severe salt stress (Table 6). Many GSTs are also up-regulated concordantly with their role in salt stress relief (Puglisi et al., 2013; Lo Cicero et al., 2015). Also the plastid NADP-malic dehydrogenase, reducing oxalacetate to malate, thus regenerating the NADP<sup>+</sup>, is among the up-regulated genes of the G2-S3 vs G2-CK data set, this result being consistent with the electron drainage from an over-reduced photosynthetic chain to other cellular compartments, in particular towards the mitochondria. Indeed, homolog of the mitochondrial malate dehydrogenase (MHD) are also induced by salinity (Table 6). As concerns either the G2-S4 vs G2-CK or G2-S4 vs G2-S3 comparisons (Table 7 and 8), the plastid NADP-malic dehydrogenase and alternative oxidase (AOX), that transfers electrons towards the respiratory electron chain for energy dissipation, are unequivocally up regulated under extreme salt stress conditions.

#### 4.2.10 Osmolyte biosynthesis

The accumulation of compatible osmolytes, such as proline, glycine betaine, polyamines and sugar alcohols plays a key role in maintaining the low intracellular osmotic potential of plants and in preventing the harmful effects of salinity stress (Deinlein et al., 2014; Gupta and Huang, 2014; Hoque et al., 2008). In our study, 1-delta-pyrroline-5-carboxylate synthase (P5CS), the key enzyme of proline biosynthesis, was found up regulated in all comparisons (G2-S3 vs G2-CK, G2-S4 vs G2-CK and G2-S4 vs G2-S3) (Table 6-8) suggesting that proline accumulation might represent a pivotal mechanism to overcome the hypersaline conditions and adjust the osmotic status in *A. donax*. Consistent with its catabolic role, proline dehydrogenase (PDH) expression is down regulated in G2-S3 vs G2-CK data set suggesting that the mitochondrial degradation of proline is prevented (Table

6). Conversely, PDH and 1-delta-pyrroline-5-carboxylate dehydrogenase (P5CSDH), both involved in proline catabolism, resulted up regulated in both G2-S4 vs G2-CK and G2-S4 vs G2-S3 data sets (Table 7 and 8). Biosynthesis pathway of betaine comprises a two steps oxidation of choline in which betaine aldehyde dehydrogenase (BADH) synthesizes betaine from betaine aldehyde. BADH expression is up regulated in G2-S4 vs G2-CK and G2-S4 vs G2-S3 comparisons indicating that betaine might play a crucial role under S4 extreme stress conditions (Table 7 and 8). Due to their cationic nature, polyamines can interact with proteins, nucleic acids, membrane phospholipids and cell wall constituents, either activating or stabilizing these molecules. Considering all the comparison data set, clusters encoding arginine decarboxylase (ADC, polyamine biosynthetic enzyme) are up-regulated suggesting that polyamines biosynthesis is induced during long term salt stress in *A. donax*, having most likely a role in the salt tolerance mechanism, both under severe and extreme stress condition (Table 6-8). In addition, clusters homolog to ornithine decarboxylase (ODC) and to spermine synthase (SPMS) are exclusively up-regulated in G2-S4 vs G2-CK comparison, indicating that a stronger activation of the polyamine biosynthesis occurs under extreme salt stress, also involving the polyamine biosynthetic pathway starting from ornithine by the action of ODC (Table 7). Sugar alcohols are compatible solutes classified into two major types cyclic (e.g., pinitol) and acyclic (e.g., mannitol) (Gupta and Huang, 2014). In our study, neither mannitol-1-phosphate dehydrogenase (*mldh*) nor inositol methyl transferase (*imt*) transcripts, respectively involved in mannitol and pinitol biosynthesis, were in the all the comparisons under investigation, indicating that the synthesis of these compounds might be not crucial for salt stress overcoming in *A. donax*.

#### 4.2.11 Photosynthesis and photorespiration

The analysis of G2-S3 vs G2-CK DEGs reveals that homologs of both small and large subunits of ribulose-1,5-bisphosphate carboxylase/oxygenase (Rubisco) are not represented neither in the up-regulated or in the down regulated clusters (Table 6). However, homologs of *Pisum sativum* Rubisco large subunit-binding protein subunit alpha, required for the correct assembly of Rubisco, have been discovered among the down-regulated genes, indicating that the process of Rubisco assembly could be strongly affected under S3 salt stress (Table 6). Moreover, clusters encoding glycolate oxidase (*Setaria italica* peroxisomal (S)-2-hydroxy-acid oxidase, LOC101764130), which is a key enzyme of the glycolate recovery pathway induced by photorespiration, is up-regulated in G2-S3 vs G2-CK comparison suggesting that CO<sub>2</sub> assimilation via the C<sub>3</sub> Calvin cycle might be impaired in favor of oxygen fixation through the photorespiration pathway (Table 6). This result is consistent with the decrease of net photosynthesis showed in Figure 1. Conversely, a surprising scenario takes place in the case of *A. donax* samples subjected to extreme salt stress conditions (Table 7). Mainly, clusters



encoding both the small and the large Rubisco subunits (homologs of *Oryza sativa* ribulose biphosphate carboxylase small chain), clusters encoding *Arundo donax* Rubisco large subunit-binding proteins (involved in Rubisco assembly) and *Setaria italica* ribulose biphosphate carboxylase/oxygenase activase, are among the down-regulated genes. Rubisco activase plays an important role adjusting the conformation of the active center of Rubisco by removing tightly bound inhibitors thus contributing to the enzyme rapid carboxylation (Carmo-Silva and Salvucci, 2013). These findings indicate that extreme salt treatment induce a strong slowdown if not even a dramatic stop of the C3 Calvin cycle (Table 7 and 8). However, specifically under S4 extreme salt stress, among the up-regulated DEGs, homologs of *Flaveria trinervia* phosphoenolpyruvate carboxylase (PEPC) and of *Oryza sativa* chloroplastic pyruvate phosphate dikinase 1 (PPDK1) have been identified, both involved in C4 photosynthesis, in which the spatial separation of the initial fixation of atmospheric CO<sub>2</sub> from the Calvin cycle occurs. Concordantly, homologs of *Setaria italica* phosphoenolpyruvate carboxylase kinase 2-like (LOC101779241), the PEPC inactivating enzyme by decreasing of maximal reaction rate, were found down-regulated, suggesting that giant reed response to extreme salt stress tends to maximize the catalytic efficiency of PEPC (Table 7 and 8).

#### 4.2.12 Biomass digestibility and biofuel production

Considering the economical relevance that bioenergy crops assume as source of bioethanol, we analyzed the regulation of several genes involved in the improvement of lignocellulosic biomass. In the *A. donax* transcriptome subjected to both severe and extreme salt stress, several homologs of phenylpropanoid biosynthetic genes were highly expressed (Table 6-8). In particular, homologs of *Setaria italica* cinnamoyl-CoA reductase 2-like and *Zea mays* caffeoyl CoA 3-O-methyltransferase are among the up-regulated clusters in G2-S3 vs G2-CK samples, being both specifically involved in lignin biosynthesis (Table 7 and 8) (Xie et al., 2018). Similarly, homolog of *Setaria italica* cinnamyl alcohol dehydrogenase was observed among the up-regulated clusters in the G2-S4 vs G2-CK but also in G2-S4 vs G2-S3 sample indicating that lignin biosynthesis is induced under extreme salt stress condition. Besides the homologs of the phenylpropanoid pathway discussed above, we identified transcripts homologous to sucrose synthase (*Setaria italica* sucrose synthase) in the G2-S3 vs G2-CK comparison, a key enzyme in cellulose biosynthesis. Considered that also lipids can participate to biomass yield, we focused our attention on genes encoding key enzymes such as triacylglycerol lipase and diacylglycerol kinase that were found to be up regulated under severe salt stress (Table 6).

**Table 6** – List of DEGs related to salt stress response identified in G2-S3 vs G2-CK comparison

| Cluster ID                                        | Database description                                                                                                        | Percent identity | Evalue | log <sub>2</sub> fold change |
|---------------------------------------------------|-----------------------------------------------------------------------------------------------------------------------------|------------------|--------|------------------------------|
| <i>Salt sensory and signaling mechanisms</i>      |                                                                                                                             |                  |        |                              |
| 14027.182899                                      | <i>Oryza sativa</i> subsp. <i>japonica</i> Group CBL-interacting protein kinase 1 (CIPK1-SOS2 like), (XM_015766590.1)       | 93.33%           | 4e-23  | + 39.581                     |
| 14027.54233                                       | <i>Setaria italica</i> probable cation transporter HKT9 (XM_004967183.2)                                                    | 86.32%           | 1e-132 | + 18.352                     |
| 14027.155903                                      | <i>Phragmites australis</i> penhx1 mRNA for putative Na <sup>+</sup> /H <sup>+</sup> antiporter (NHX1), (Nt ID: AB211145.1) | 93.40%           | 3e-54  | - 21.136                     |
| 14027.181583                                      | <i>Arabidopsis thaliana</i> Sodium/hydrogen exchanger 2 (NHX2), (Swissprot ID: Q56XP4)                                      | 77.78%           | 8e-79  | - 19.411                     |
| <i>Transcription factors</i>                      |                                                                                                                             |                  |        |                              |
| 14027.152638                                      | <i>Setaria italica</i> protein TIFY 10B-like (Nr ID: XP_004958300.1)                                                        | 84.77%           | 2e-131 | - 25.354                     |
| 14027.159286                                      | <i>Setaria italica</i> trihelix transcription factor GTL1 (Nt ID: XM_012842882.1)                                           | 88.89%           | 2e-101 | + 14.963                     |
| 14027.107730                                      | <i>Setaria italica</i> bZIP ABSCISIC ACID-INSENSITIVE 5-like protein 7 (Nr ID: XP_004954029.1)                              | 45.04%           | 2e-18  | + 15.107                     |
| <i>Hormone regulation of salt stress response</i> |                                                                                                                             |                  |        |                              |
| 14027.74861                                       | <i>Triticum urartu</i> Abscisic acid 8'-hydroxylase 1 (Nr ID: EMS68885.1)                                                   | 85.54%           | 4e-112 | + 47.347                     |
| 14027.144393                                      | <i>Setaria italica</i> abscisic acid receptor PYL8 (Nt ID: XM_004951229.2).                                                 | 77.85%           | 4e-80  | + 11.825                     |
| 14027.137264                                      | <i>Setaria italica</i> abscisic acid receptor PYR1-like (Nr ID: XP_004983564.1)                                             | 85.34%           | 1e-104 | + 12.624                     |
| 14027.173535                                      | <i>Oryza sativa</i> serine/threonine-protein kinase SnRK (SnRK), (Swissprot ID: Q75H77)                                     | 79.69%           | 8e-32  | + 14.238                     |
| 14027.235757                                      | <i>Setaria italica</i> probable protein phosphatase 2C 30 (Nt ID: XM_004984868.2)                                           | 87.80%           | 6e-170 | + 27.333                     |
| 14027.228612                                      | <i>Setaria italica</i> cytochrome P450 734A1 (Nr ID: XP_004962129.1)                                                        | 89.90%           | 2e-58  | + 16.547                     |
| 14027.99729                                       | <i>Saccharum arundinaceum</i> 1-aminocyclopropane-1-carboxylate oxidase (ACC oxidase) (Nr ID: ABM74187.1)                   | 91.46%           | 1e-122 | + 15.804                     |
| 14027.265476                                      | <i>Setaria italica</i> indole-3-pyruvate monooxygenase YUCCA2-like (Nr ID: XP_004967465.1)                                  | 75.33%           | 1e-107 | - 40.837                     |
| <i>ROS scavenging regulatory mechanisms</i>       |                                                                                                                             |                  |        |                              |
| 14027.179813                                      | <i>Setaria italica</i> L-ascorbate peroxidase (Nt ID: XM_004984762.3)                                                       | 92.70%           | 2e-67  | + 17.074                     |
| 14027.36507                                       | <i>Zea mays</i> glutathione transferase 23 (GST) (Swissprot ID: Q9FQA3)                                                     | 86.94%           | 1e-142 | + 14.004                     |
| 14027.206288                                      | <i>Setaria italica</i> NADP-dependent malic enzyme, chloroplastic (Nr ID: XP_004960887.1)                                   | 99.50%           | 4e-152 | + 15.008                     |
| 14027.147540                                      | <i>Setaria italica</i> malate dehydrogenase, mitochondrial (MDH), (Nt ID: XM_004961089.3)                                   | 84.14%           | 2e-167 | + 12.416                     |
| <i>Osmolyte biosynthesis</i>                      |                                                                                                                             |                  |        |                              |
| 14027.146844                                      | <i>Setaria italica</i> delta-1-pyrroline-5-carboxylate synthase (P5CS), (Nt ID: XM_004961829.3)                             | 91.92%           | 6e-168 | + 40.924                     |
| 14027.163839                                      | <i>Setaria italica</i> proline dehydrogenase (PDH) (Nt ID: XM_004983669.2)                                                  | 89.55%           | 3e-114 | - 28.271                     |
| 14027.196396                                      | <i>Setaria italica</i> arginine decarboxylase (ADC) (Nt ID: XM_004964376.3)                                                 | 47.70%           | 3e-179 | + 46.553                     |
| <i>Photosynthesis and photorespiration</i>        |                                                                                                                             |                  |        |                              |
| 14027.153819                                      | <i>Pisum sativum</i> RuBisCO large subunit-binding protein subunit alpha, chloroplastic (Swissprot ID: P08926)              | 74.89%           | 4e-110 | - 35.119                     |

|                                                     |                                                                                          |        |        |          |
|-----------------------------------------------------|------------------------------------------------------------------------------------------|--------|--------|----------|
| 14027.193818                                        | <i>Setaria italica</i> peroxisomal (S)-2-hydroxy-acid oxidase<br>(Nt ID: XM_004958250.2) | 92.51% | 5e-156 | + 22.634 |
| <i>Biomass digestibility and biofuel production</i> |                                                                                          |        |        |          |
| 14027.274380                                        | <i>Setaria italica</i> cinnamoyl-CoA reductase 2-like<br>(Nt ID: XP_004956337.1)         | 67.31% | 3e-149 | +39.522  |
| 14027.178971                                        | <i>Zea mays</i> caffeoyl CoA 3-O-methyltransferase<br>(Nr ID: AAP33129.1)                | 91.10% | 6e-163 | + 13.644 |
| 14027.116333                                        | <i>Setaria italica</i> sucrose synthase<br>(Nr ID: XP_004984440.1)                       | 70.19% | 2e-136 | + 11.104 |
| 14027.238308                                        | <i>Setaria italica</i> triacylglycerol lipase SDP1-like<br>(Nr ID: XP_004970049.1)       | 78.83% | 6e-112 | + 10.393 |
| 14027.166055                                        | <i>Setaria italica</i> diacylglycerol kinase 1-like<br>(Nt ID: XM_004983930.1)           | 45.50% | 6e-94  | - 15.699 |

**Table 7** – List of DEGs related to salt stress response identified in G2-S4 vs G2-CK comparison

| <i>Cluster ID</i>                                 | <i>Database description</i>                                                                                  | <i>Identity score</i> | <i>Identity value</i> | <i>E</i> | <i>log<sub>2</sub> fold change</i> |
|---------------------------------------------------|--------------------------------------------------------------------------------------------------------------|-----------------------|-----------------------|----------|------------------------------------|
| <i>Salt sensory and signaling mechanisms</i>      |                                                                                                              |                       |                       |          |                                    |
| 14027.85357                                       | <i>Setaria italica</i> CBL-interacting protein kinase 1 (CIPK1-SOS2-like)<br>(Nt ID: XM_004967556.3)         | 92.31%                | 8e-73                 |          | Inf*                               |
| 14027.198243                                      | <i>Oryza sativa subsp. japonica</i> CBL-interacting protein kinase 24 (SOS2)<br>(Swissprot ID: Q69Q47)       | 87.88%                | 8e-126                |          | + 11.098                           |
| 14027.54233                                       | <i>Setaria italica</i> probable cation transporter HKT9<br>(Nr ID: XP_004967240.1)                           | 86.32%                | 1e-132                |          | + 35.667                           |
| 14027.155893                                      | <i>Arabidopsis thaliana</i> Sodium/hydrogen exchanger 1 (NHX1)<br>(Swissprot ID: Q68KI4)                     | 68.46%                | 6e-177                |          | + 14.324                           |
| <i>Transcription factors</i>                      |                                                                                                              |                       |                       |          |                                    |
| 14027.159287                                      | <i>Setaria italica</i> trihelix transcription factor GTL1,<br>(Nt ID: XM_012842882.1)                        | 81.72%                | 6e-45                 |          | + 29.044                           |
| 14027.82197                                       | <i>Setaria italica</i> bZIP ABSCISIC ACID-INSENSITIVE 5-like protein 7<br>(Swissprot ID: Q9M7Q2)             | 79.96%                | 9e-82                 |          | + 17.106                           |
| <i>Hormone regulation of salt stress response</i> |                                                                                                              |                       |                       |          |                                    |
| 14027.234361                                      | <i>Setaria italica</i> abscisic acid 8'-hydroxylase 3<br>(Nr ID: XP_004957014.1)                             | 83.43%                | 0.0                   |          | + 41.107                           |
| 14027.144393                                      | <i>Setaria italica</i> abscisic acid receptor PYL8<br>(Nt ID: XM_004951229.2)                                | 77.85%                | 4e-80                 |          | + 12.599                           |
| 14027.36786                                       | <i>Setaria italica</i> brassinosteroid-6-oxidase 2 cytochrome P450 85A1<br>(KO ID: K12640)                   | 93.36%                | 4e-141                |          | + 19.415                           |
| 14027.99735                                       | <i>Oryza brachyantha</i> 1-amino cyclopropane-1-carboxylate oxidase (ACC oxidase)<br>(Nt ID: XM_006647913.2) | 72.38%                | 2e-149                |          | + 22.325                           |
| 14027.89434                                       | <i>Arabidopsis thaliana</i> ethylene receptor 1 (ETR1),<br>(KO: K14509)                                      | 31.67%                | 1e-15                 |          | - 18.141                           |
| 14027.182197                                      | <i>Arabidopsis thaliana</i> serine/threonine-protein kinase CTR1, (Swissprot ID: Q05609)                     | 87.50%                | 3e-145                |          | + 11.918                           |
| 14027.226694                                      | <i>Setaria italica</i> ETHYLENE INSENSITIVE 3-like 3 protein (EIN3)<br>(Nr ID: XP_004973869.1)               | 61.43%                | 1e-113                |          | + 14.849                           |
| 14027.190058                                      | <i>Zea mays</i> Indole-3-acetaldehyde oxidase (AAO)<br>(Swissprot ID: O23887)                                | 67.55%                | 4e-175                |          | + 13.436                           |
| 14027.58358                                       | <i>Setaria italica</i> probable indole-3-acetic acid-amido synthetase GH3.8<br>(Nr ID: XP_004958192.1)       | 69.87%                | 2e-133                |          | Inf*                               |

|                                                     |                                                    |                                                                                                       |         |        |          |
|-----------------------------------------------------|----------------------------------------------------|-------------------------------------------------------------------------------------------------------|---------|--------|----------|
| 14027.189947                                        | <i>Oryza sativa</i> subsp. <i>japonica</i>         | Jasmonic acid-amido synthetase JAR1<br>(Swissprot ID: Q6I581)                                         | 60.65%  | 2e-167 | - 28.213 |
| <i>ROS scavenging regulatory mechanisms</i>         |                                                    |                                                                                                       |         |        |          |
| 14027.42850                                         | <i>Flaveria pringlei</i>                           | NADP-dependent malic enzyme, chloroplastic<br>(Swissprot ID: P36444)                                  | 55.29%  | 6e-111 | Inf*     |
| 14027.184286                                        | <i>Setaria italica</i>                             | ubiquinol oxidase 2, mitochondrial-like (AOX)<br>(Nr ID: XP_004976683.1)                              | 93.02%  | 1e-64  | + 20.525 |
| 14027.154629                                        | <i>Setaria italica</i>                             | superoxide dismutase [Cu-Zn]<br>(Nt ID: XM_004958551.3)                                               | 89.43%  | 2e-74  | + 36.275 |
| 14027.237926                                        | <i>Setaria italica</i>                             | superoxide dismutase [Fe] 2, chloroplastic-like<br>(Nt ID: XM_004964461.2)                            | 98.26%  | 2e-68  | - 11.661 |
| <i>Osmolyte biosynthesis</i>                        |                                                    |                                                                                                       |         |        |          |
| 14027.146844                                        | <i>Setaria italica</i>                             | delta-1-pyrroline-5-carboxylate synthase (P5CS)<br>(Nt ID: XM_004961829.3)                            | 91.92%  | 6e-168 | + 68.438 |
| 14027.197137                                        | <i>Brachypodium distachyon</i>                     | delta-1-pyrroline-5-carboxylate dehydrogenase 12A1, mitochondrial (P5CSDH)<br>(Nr ID: XP_010231104.1) | 92.46%  | 5e-138 | + 17.285 |
| 14027.163909                                        | <i>Oryza sativa</i> subsp. <i>indica</i>           | Betaine aldehyde dehydrogenase (BADH)<br>(Swissprot ID: B3VMC0)                                       | 92.96%  | 1e-41  | + 15.021 |
| 5159.0                                              | <i>Zea mays</i>                                    | ornithine decarboxylase-like (ODC)<br>(Nr ID: XP_008653000.1)                                         | 52.96%  | 1e-112 | + 51.866 |
| 14027.196396                                        | <i>Oryza sativa</i> subsp. <i>japonica</i> Group   | arginine decarboxylase 1 (ADC)<br>(Swissprot ID: Q9SNN0)                                              | 47.70%  | 3e-179 | + 65.072 |
| 14027.211822                                        | <i>Setaria italica</i>                             | spermine synthase-like (SPMS)<br>(Nr ID: XP_004951294.1)                                              | 89.78%  | 2e-175 | + 10.003 |
| <i>Photosynthesis and photorespiration</i>          |                                                    |                                                                                                       |         |        |          |
| 14027.158740                                        | <i>Oryza sativa</i> , subsp. <i>japonica</i> Group | Ribulose biphosphate carboxylase small chain A<br>(Swissprot ID: P18566)                              | 88.96%  | 3e-100 | - 24.091 |
| 14027.70509                                         | <i>Arundo donax</i>                                | ribulose-biphosphate carboxylase large subunit (rbcL)<br>(Nt ID: KJ880079.1)                          | 100.00% | 1e-104 | - 17.789 |
| 14027.158959                                        | <i>Setaria italica</i>                             | ruBisCO large subunit-binding protein subunit beta<br>(Nr ID: XP_004975721.1)                         | 95.45%  | 2e-19  | - 14.938 |
| 14027.168331                                        | <i>Setaria italica</i>                             | ribulose biphosphate carboxylase/oxygenase activase<br>(Nt ID: XM_004960085.2)                        | 84.71%  | 1e-46  | - 15.647 |
| 14027.198015                                        | <i>Oryza brachyantha</i>                           | phosphoenolpyruvate carboxylase (PEPC)<br>(Nr ID: XP_006644735)                                       | 93.85%  | 1e-174 | + 11.496 |
| 14027.153211                                        | <i>Oryza sativa</i>                                | chloroplastic pyruvate phosphate dikinase 1 (PPDK1)<br>(Swissprot ID: Q6AVA8)                         | 88.41%  | 1e-163 | + 29.711 |
| 14027.158029                                        | <i>Setaria italica</i>                             | phosphoenolpyruvate carboxylase kinase (PEPC kinase)<br>(Nr ID: XP_004976235.1)                       | 84.05%  | 2e-127 | - 40.627 |
| <i>Biomass digestibility and biofuel production</i> |                                                    |                                                                                                       |         |        |          |
| 14027.150588                                        | <i>Setaria italica</i>                             | putative cinnamyl alcohol dehydrogenase<br>(Nt ID: XM_004972526.2)                                    | 79.53%  | 6e-116 | + 14.463 |

**Table 8** – List of DEG related to salt stress response identified in G2-S4 vs G2-S3 comparison

| Cluster                                           | Database description                                                                                                              | Identity score | Identity Evaluate | log <sub>2</sub> fold change |
|---------------------------------------------------|-----------------------------------------------------------------------------------------------------------------------------------|----------------|-------------------|------------------------------|
| <i>Salt sensory and signaling mechanisms</i>      |                                                                                                                                   |                |                   |                              |
| 14027.81324                                       | <i>Setaria italica</i> probable cation transporter HKT9 (Nr ID: XP_004967240.1)                                                   | 65.10%         | 5e-142            | + 25.926                     |
| <i>Transcription factors</i>                      |                                                                                                                                   |                |                   |                              |
| 14027.184776                                      | <i>Setaria italica</i> trihelix transcription factor GTL1 (Nt ID: XM_012842882.1)                                                 | 80.41%         | 2e-69             | + 29.515                     |
| <i>Hormone regulation of salt stress response</i> |                                                                                                                                   |                |                   |                              |
| 14027.238560                                      | <i>Zea mays</i> 9-cis-epoxycarotenoid dioxygenase 1, chloroplastic (Swissprot ID: O24592)                                         | 85.48%         | 6e-177            | - 18.703                     |
| 14027.234358                                      | <i>Setaria italica</i> abscisic acid 8'-hydroxylase 3 (Nr ID: XP_004957014.1)                                                     | 70.33%         | 4e-163            | + 23.595                     |
| 14027.36785                                       | <i>Setaria italica</i> brassinosteroid-6-oxidase 2 cytochrome P450 85A1 (KO ID: K12640)                                           | 93.12%         | 2e-105            | + 24.019                     |
| <i>ROS scavenging regulatory mechanisms</i>       |                                                                                                                                   |                |                   |                              |
| 14027.104252                                      | <i>Flaveria pringlei</i> NADP-dependent malic enzyme, chloroplastic (Swissprot ID: P36444)                                        | 70.49%         | 5e-135            | Inf*                         |
| 14027.141579                                      | <i>Setaria italica</i> ubiquinol oxidase 2, mitochondrial-like (AOX) (Nr ID: XP_004953576.1)                                      | 80.65%         | 4e-87             | + 13.511                     |
| 14027.159513                                      | <i>Zea Mays</i> superoxide dismutase [Cu-Zn] (Swissprot ID: P23345)                                                               | 89.67%         | 2e-164            | + 11.777                     |
| 14027.172733                                      | <i>Setaria italica</i> superoxide dismutase [Fe] 1, chloroplastic-like (Nt ID: XM_004981985.2)                                    | 72.96%         | 1e-165            | - 11.799                     |
| <i>Osmolyte biosynthesis</i>                      |                                                                                                                                   |                |                   |                              |
| 14027.166473                                      | <i>Setaria italica</i> delta-1-pyrroline-5-carboxylate synthase (P5CS) (Nt ID: XM_004970516.2)                                    | 95.94%         | 8e-175            | + 44.106                     |
| 14027.197137                                      | <i>Brachypodium distachyon</i> delta-1-pyrroline-5-carboxylate dehydrogenase 12A1, mitochondrial (P5CSDH) (Nr ID: XP_010231104.1) | 92.46%         | 5e-138            | + 17.324                     |
| 14027.116788                                      | <i>Oryza sativa</i> subsp. <i>japonica</i> Betaine aldehyde dehydrogenase 1 (BADH) (Swissprot ID: O24174)                         | 85.80%         | 2e-94             | + 16.655                     |
| 14027.196396                                      | <i>Oryza sativa</i> subsp. <i>japonica</i> Group arginine decarboxylase 1 (ADC) (Swissprot ID: Q9SNN0)                            | 48.64%         | 2e-180            | + 18.455                     |
| <i>Photosynthesis and photorespiration</i>        |                                                                                                                                   |                |                   |                              |
| 14027.157747                                      | <i>Oryza sativa</i> subsp. <i>japonica</i> Group Ribulose biphosphate carboxylase small chain A (Swissprot ID: Q0INY7)            | 94.59%         | 3e-20             | - 13.548                     |
| 14027.70510                                       | <i>Adiantum capillus-veneris</i> ribulose-biphosphate carboxylase large subunit (rbcL) (Swissprot ID: P36476)                     | 94.33%         | 9e-180            | - 13.342                     |
| 14027.168328                                      | <i>Setaria italica</i> ribulose biphosphate carboxylase/oxygenase activase (Nt ID: XM_004960085.2)                                | 80.30%         | 4e-66             | - 10.404                     |
| 14027.153211                                      | <i>Oryza sativa</i> subsp. <i>japonica</i> chloroplastic pyruvate phosphate dikinase 1 (PPDK1) (Swissprot ID: Q6AVA8)             | 88.41%         | 1e-163            | + 28.312                     |
| 14027.170986                                      | <i>Setaria italica</i> phosphoenolpyruvate carboxylase kinase (PEPC kinase) (Nt ID: XM_004953094.3)                               | 83.33%         | 7e-05             | - 17.751                     |

| <i>Biomass digestibility and biofuel production</i> |                                                                                    |        |        |          |
|-----------------------------------------------------|------------------------------------------------------------------------------------|--------|--------|----------|
| 14027.76193                                         | <i>Setaria italica</i> cinnamyl alcohol dehydrogenase<br>(Nt ID: XM_004951572.2)   | 82.35% | 2e-132 | - 11.287 |
| 14027.238308                                        | <i>Setaria italica</i> triacylglycerol lipase SDP1-like<br>(Nr ID: XP_004970049.1) | 75.07% | 4e-168 | + 10.139 |

**Table 9.** Transcription factors responsive to salt in *A. donax*, resulted by a comparative analysis with the available database of rice transcription factors.

| <i>A. donax</i> ID | Rice ID    | % identity | E value   | Family    | G2-S4 vs G2-CK | G2-S3 vs G2-CK | G2-S4 vs G2-S3 | Regulation | Diff. Expr. |
|--------------------|------------|------------|-----------|-----------|----------------|----------------|----------------|------------|-------------|
| 14027.146299       | Os09g20350 | 91.67      | 1,00E-38  | AP2-EREBP | 1              | 0              | 0              | Up         | Salinity    |
| 14027.156597       | Os09g20350 | 81.82      | 5,00E-08  | AP2-EREBP | 1              | 0              | 0              | Down       | Salinity    |
| 14027.157270       | Os09g20350 | 95.77      | 3,00E-25  | AP2-EREBP | 1              | 0              | 0              | Up         | Salinity    |
| 14027.171527       | Os04g55560 | 92.73      | 2,00E-36  | AP2-EREBP | 1              | 0              | 0              | Up         | Salinity    |
| 14027.180316       | Os04g55560 | 85.48      | 3,00E-33  | AP2-EREBP | 1              | 0              | 0              | Up         | Salinity    |
| 14027.186619       | Os02g57790 | 85.71      | 4,00E-31  | C2H2      | 1              | 0              | 0              | Up         | Salinity    |
| 14027.192028       | Os07g39480 | 85.49      | 1,00E-131 | WRKY      | 1              | 0              | 0              | Up         | Salinity    |
| 14027.248285       | Os06g40330 | 88.71      | 1,00E-70  | MYB       | 1              | 0              | 0              | Up         | Salinity    |
| 14027.250058       | Os06g44750 | 91.49      | 7,00E-27  | AP2-EREBP | 1              | 0              | 0              | Up         | Salinity    |
| 14027.250059       | Os06g44750 | 91.49      | 4,00E-27  | AP2-EREBP | 1              | 0              | 1              | Down       | Salinity    |
| 14027.4111         | Os07g22770 | 89.39      | 2,00E-35  | AP2-EREBP | 1              | 1              | 0              | Down       | Salinity    |
| 14027.61430        | Os03g54170 | 94.37      | 1,00E-22  | MADS      | 1              | 0              | 0              | Down       | Salinity    |
| 14027.64311        | Os01g13030 | 84.55      | 6,00E-43  | AUX-IAA   | 1              | 0              | 0              | Down       | Salinity    |
| 14027.84501        | Os11g45950 | 89.06      | 1,00E-11  | NAC       | 1              | 0              | 0              | Down       | Salinity    |
| 9227.0             | Os06g44750 | 93.55      | 4,00E-31  | AP2-EREBP | 1              | 0              | 0              | Up         | Salinity    |

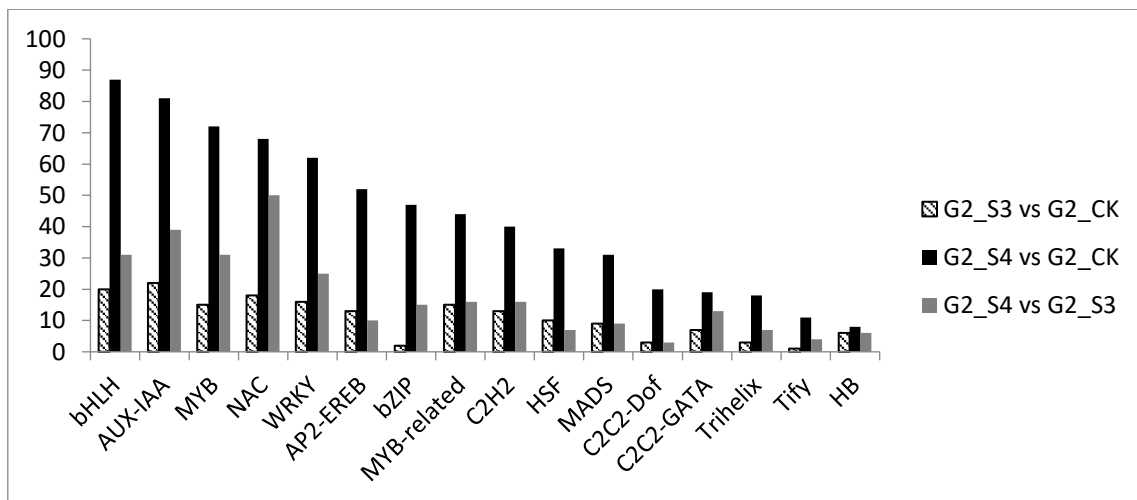


**Figure 9.** Distribution of transcription factors responsive to salt stress. Data are sorted by number of G2-S4 vs G2 CK DEGs. Only categories with more than 3 DEGs identified as transcription factors are shown.

#### 4.2.13 Retrieval and analysis of genes targeted as “salt stress responsive”

The GO terms were further analyzed in order to retrieve clusters specifically involved in the salt stress response, thus excluding all transcripts also regulated by different abiotic stress, such as water deprivation, cold, heavy metals and oxidative stresses (geneontology.org/). All the retrieved clusters are also found to be involved in salt-induced osmotic stress according to the finding that levels of NaCl higher than 100–150 mM cause osmotic stress, that normally arises up at salinity levels ranging between 50 and 100 mM NaCl (Shavrukov, 2012). The results shown in Table 10 reveal that among 9 clusters specifically regulated by salt, 7 are up regulated and 2 are down regulated in the G2-S3 vs G2-CK comparison. Among the up regulated genes, the CBL-interacting protein kinase 1 (CIPK1-SOS2 like) has been found (Table 10) thus suggesting that it induces specific signal transduction pathways under severe salt stress conditions. Instead, clusters related to plasma membrane Na<sup>+</sup>/K<sup>+</sup> transporter are down regulated by severe salt stress treatment (Table 10), both results being already highlighted in Table 6. A higher number of up and down regulated genes have been found among the G2-S4 vs G2-CK data set, they are being 29 and 7, respectively, for a total of 36 clusters (Table 11). Similarly, to G2-S3 vs G2-CK comparison, clusters encoding the CBL-interacting protein kinase 1 (CIPK1-SOS2 like) have been found up regulated under extreme salt stress S4 (Table 11, Table 7). Moreover, CBL-interacting protein kinase 24 SOS2 (homolog of *Oryza sativa* subsp. *Japonica* protein, Table 7) is specifically up regulated under extreme salt stress conditions (S4). Interestingly, clusters encoding homologs of the mitochondrial persulfide dioxygenase ETHE1 (ETHYLMALONIC ENCEPHALOPATHY PROTEIN1), that catalyzes the oxidation of persulfides derived from either cysteine or hydrogen sulfide to thiosulfate and sulfate (Höfler, 2016) have been found up regulated in S4 conditions. Finally, clusters mainly related to a probable *Oryza sativa* subsp. *Japonica* cation transporter HKT6 are down regulated under extreme salt conditions (Table 11). In order to support the relationship among the main specific salt responsive genes (CIPK1-SOS2 like, cation transporter HKT9, NHX1, NHX2, SOS2 and ETHE 1, Tab. 7, Table 11) and their orthologues, each *A. donax* cluster was aligned with fifteen orthologues from different plant sources and phylogenetic trees were constructed (Figure 10a, 10b, 10c, 10d, 10e and 10f). The sequence alignments allowed to classify the proteins within the respective protein family and, in the case of CIPK1-SOS2 like, of persulfide dioxygenase ETHE1 and CBL-interacting protein kinase 24 (SOS2) sequence alignment revealed the presence of specific protein functional domains (Table 10). The findings of the phylogenetic trees depicted that all the genes from different plant sources can be subcategorized into subgroups (Figure 10a, 10b, 10c, 10d, 10e and 10f) and that, all the giant reed genes were clustered into one of these subgroups.

**Table 10.** Salt stress related genes in G2-S3 vs G2-CK (GO:0009651 Response to salt stress)

| Gene_ID      | log <sub>2</sub> FoldChange | Swissprot Description                                                         |
|--------------|-----------------------------|-------------------------------------------------------------------------------|
| 14027.266446 | Inf*                        | CBL-interacting protein kinase 21 ( <i>Oryza sativa</i> subsp. japonica)      |
| 14027.182899 | 39.581                      | CBL-interacting protein kinase 1 ( <i>Oryza sativa</i> subsp. japonica)       |
| 14027.196826 | 35.123                      | CBL-interacting protein kinase 1 ( <i>Oryza sativa</i> subsp. japonica)       |
| 14027.182901 | 33.766                      | CBL-interacting protein kinase 1 ( <i>Oryza sativa</i> subsp. japonica)       |
| 14027.190185 | 25.043                      | CBL-interacting protein kinase 1 ( <i>Oryza sativa</i> subsp. japonica)       |
| 14027.194848 | 0,93616                     | Ankyrin repeat-containing protein NPR4 ( <i>Oryza sativa</i> subsp. Japonica) |
| 14027.149173 | 0,78963                     | V-type proton ATPase catalytic subunit A ( <i>Daucus carota</i> )             |
| 14027.230649 | -22.658                     | Probable cation transporter HKT6 ( <i>Oryza sativa</i> subsp. japonica)       |
| 14027.230650 | -26.106                     | Probable cation transporter HKT6 ( <i>Oryza sativa</i> subsp. japonica)       |

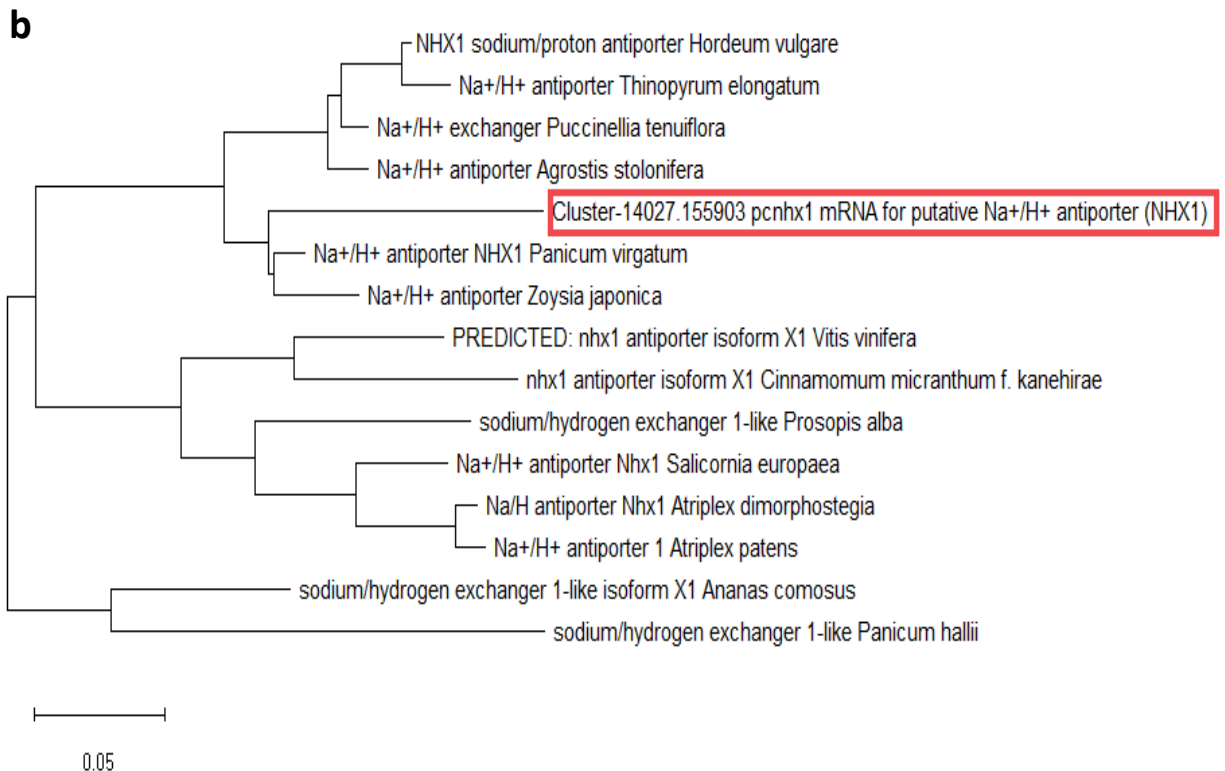
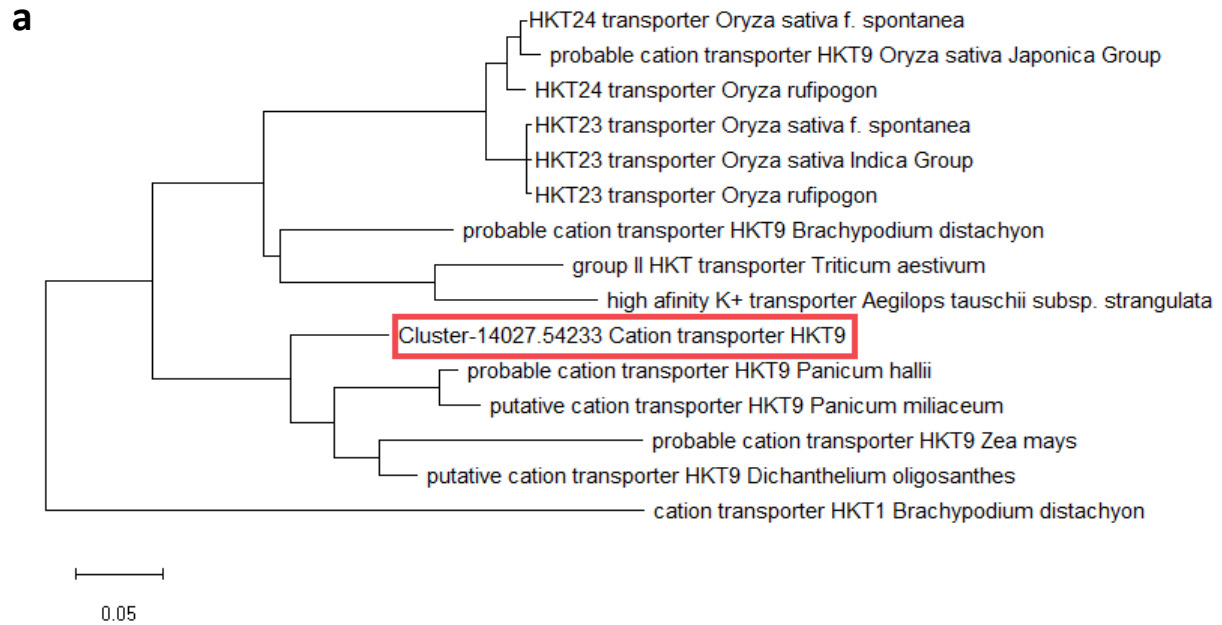
\*it means that the read count value of CK samples is zero

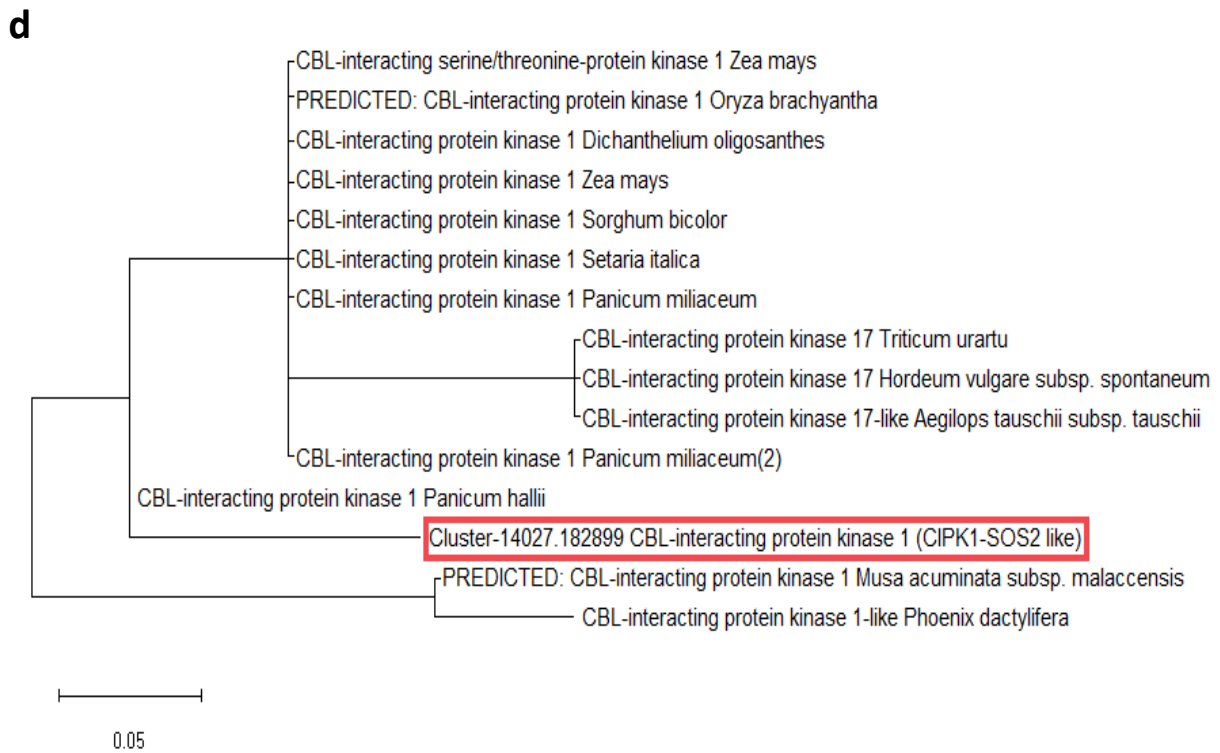
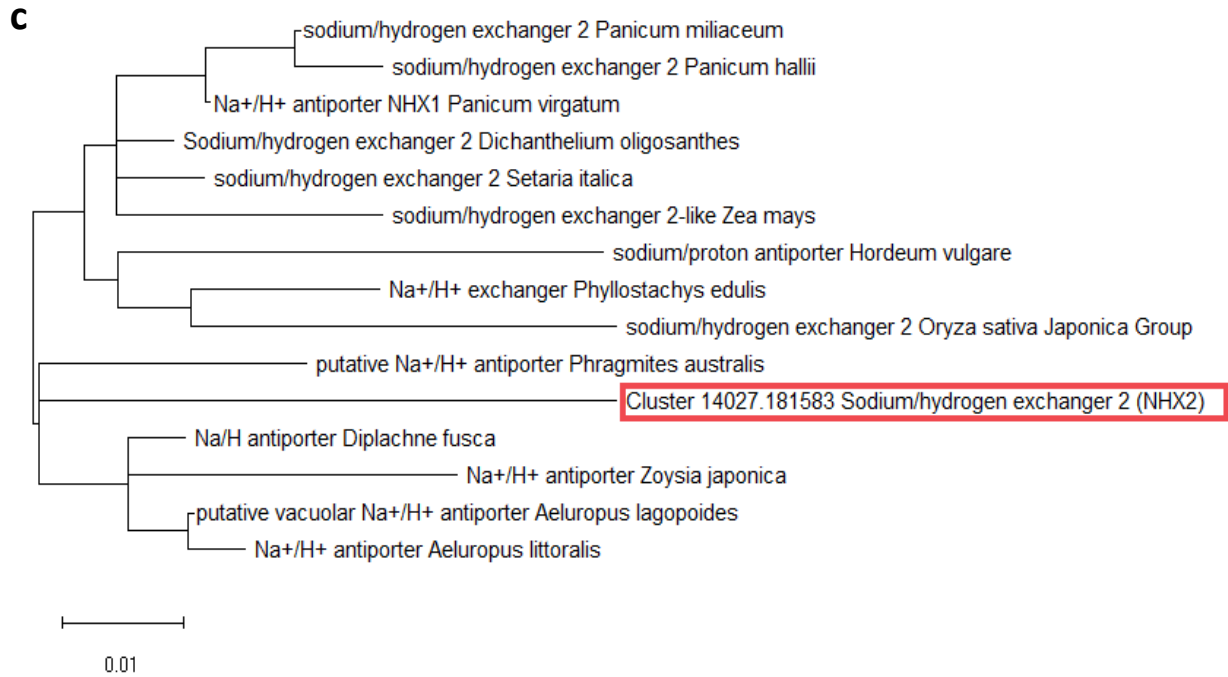
**Table 11.** Salt stress related genes in G2-S4 vs G2-CK (GO:0009651 Response to salt stress)

| Gene_ID      | log <sub>2</sub> FoldChange | Swissprot Description                                                                               |
|--------------|-----------------------------|-----------------------------------------------------------------------------------------------------|
| 14027.231692 | 54.475                      | NAD-dependent malic enzyme 62 kDa isoform ( <i>Solanum tuberosum</i> )                              |
| 14027.231386 | 49.507                      | Persulfide dioxygenase ETHE1 homolog ( <i>Arabidopsis thaliana</i> )                                |
| 14027.196826 | 42.577                      | CBL-interacting protein kinase 1 ( <i>Oryza sativa</i> subsp. Japonica)                             |
| 14027.190185 | 34.055                      | CBL-interacting protein kinase 1 ( <i>Oryza sativa</i> subsp. Japonica)                             |
| 14027.130203 | 25.169                      | Persulfide dioxygenase ETHE1 homolog ( <i>Arabidopsis thaliana</i> )                                |
| 14027.209414 | 24.094                      | Calcium-dependent protein kinase 1 ( <i>Oryza sativa</i> subsp. Japonica)                           |
| 14027.189242 | 16.044                      | Persulfide dioxygenase ETHE1 homolog ( <i>Arabidopsis thaliana</i> )                                |
| 14027.90003  | 14.432                      | Ankyrin repeat-containing protein NPR4 ( <i>Oryza sativa</i> subsp. Japonica)                       |
| 14027.190184 | 13.951                      | CBL-interacting protein kinase 1 ( <i>Oryza sativa</i> subsp. Japonica)                             |
| 14027.149173 | 13.206                      | V-type proton ATPase catalytic subunit A ( <i>Daucus carota</i> )                                   |
| 14027.146671 | 12.089                      | NAD-dependent malic enzyme 62 kDa isoform ( <i>Solanum tuberosum</i> )                              |
| 14027.198243 | 11.098                      | CBL-interacting protein kinase 24 ( <i>Oryza sativa</i> subsp. Japonica)                            |
| 14027.190190 | 3.837                       | CBL-interacting protein kinase 1 ( <i>Oryza sativa</i> subsp. Japonica)                             |
| 14027.211592 | 1,94                        | COBRA-like protein 1 ( <i>Oryza sativa</i> subsp. Japonica)                                         |
| 14027.158801 | 0,93                        | V-type proton ATPase catalytic subunit A ( <i>Daucus carota</i> )                                   |
| 14027.176822 | 0,92                        | CBL-interacting protein kinase 24 ( <i>Oryza sativa</i> subsp. Japonica)                            |
| 14027.129089 | 0,82                        | 3-isopropylmalate dehydratase small subunit 3 ( <i>Arabidopsis thaliana</i> )                       |
| 14027.163583 | 0,81                        | --                                                                                                  |
| 14027.176826 | 0,77                        | CBL-interacting protein kinase 1 ( <i>Oryza sativa</i> subsp. Japonica)                             |
| 14027.169731 | 0,76                        | Gamma carbonic anhydrase 2 ( <i>Arabidopsis thaliana</i> )                                          |
| 14027.181983 | 0,74                        | Mitochondrial-processing peptidase subunit alpha ( <i>Solanum tuberosum</i> )                       |
| 14027.180575 | 0,71                        | CBL-interacting protein kinase 24 ( <i>Oryza sativa</i> subsp. Japonica)                            |
| 14027.195126 | 0,68                        | 3-isopropylmalate dehydratase small subunit 3 ( <i>Arabidopsis thaliana</i> )                       |
| 14027.110430 | 0,67                        | ATP synthase subunit d ( <i>Arabidopsis thaliana</i> )                                              |
| 14027.135632 | 0,63                        | ATP synthase subunit d ( <i>Arabidopsis thaliana</i> )                                              |
| 14027.189399 | 0,59                        | Mitochondrial-processing peptidase subunit alpha ( <i>Solanum tuberosum</i> )                       |
| 14027.219001 | 0,55                        | Nascent polypeptide-associated complex subunit alpha-like protein 1 ( <i>Arabidopsis thaliana</i> ) |
| 14027.173498 | 0,53                        | Kynurenine formamidase ( <i>Bacillus weihenstephanensis</i> ) (strain KBAB4)                        |
| 14027.139505 | 0,52                        | NADH dehydrogenase [ubiquinone] 1 alpha subcomplex subunit 9 ( <i>Arabidopsis thaliana</i> )        |
| 14027.172033 | -0,74                       | Interferon-related developmental regulator 2 ( <i>Homo sapiens</i> )                                |
| 14027.230649 | -4.392                      | Probable cation transporter HKT6 ( <i>Oryza sativa</i> subsp. Japonica)                             |
| 14027.162962 | -11.339                     | Interferon-related developmental regulator 2 ( <i>Homo sapiens</i> )                                |



|              |         |                                                                         |
|--------------|---------|-------------------------------------------------------------------------|
| 14027.225205 | -25.336 | Interferon-related developmental regulator 1 ( <i>Sus scrofa</i> )      |
| 14027.142581 | -28.631 | --                                                                      |
| 14027.230647 | -43.229 | Probable cation transporter HKT6 ( <i>Oryza sativa</i> subsp. Japonica) |
| 14027.180958 | -45.185 | CBL-interacting protein kinase 1 ( <i>Oryza sativa</i> subsp. Japonica) |
| 14027.230650 | -55.502 | Probable cation transporter HKT6 ( <i>Oryza sativa</i> subsp. Japonica) |





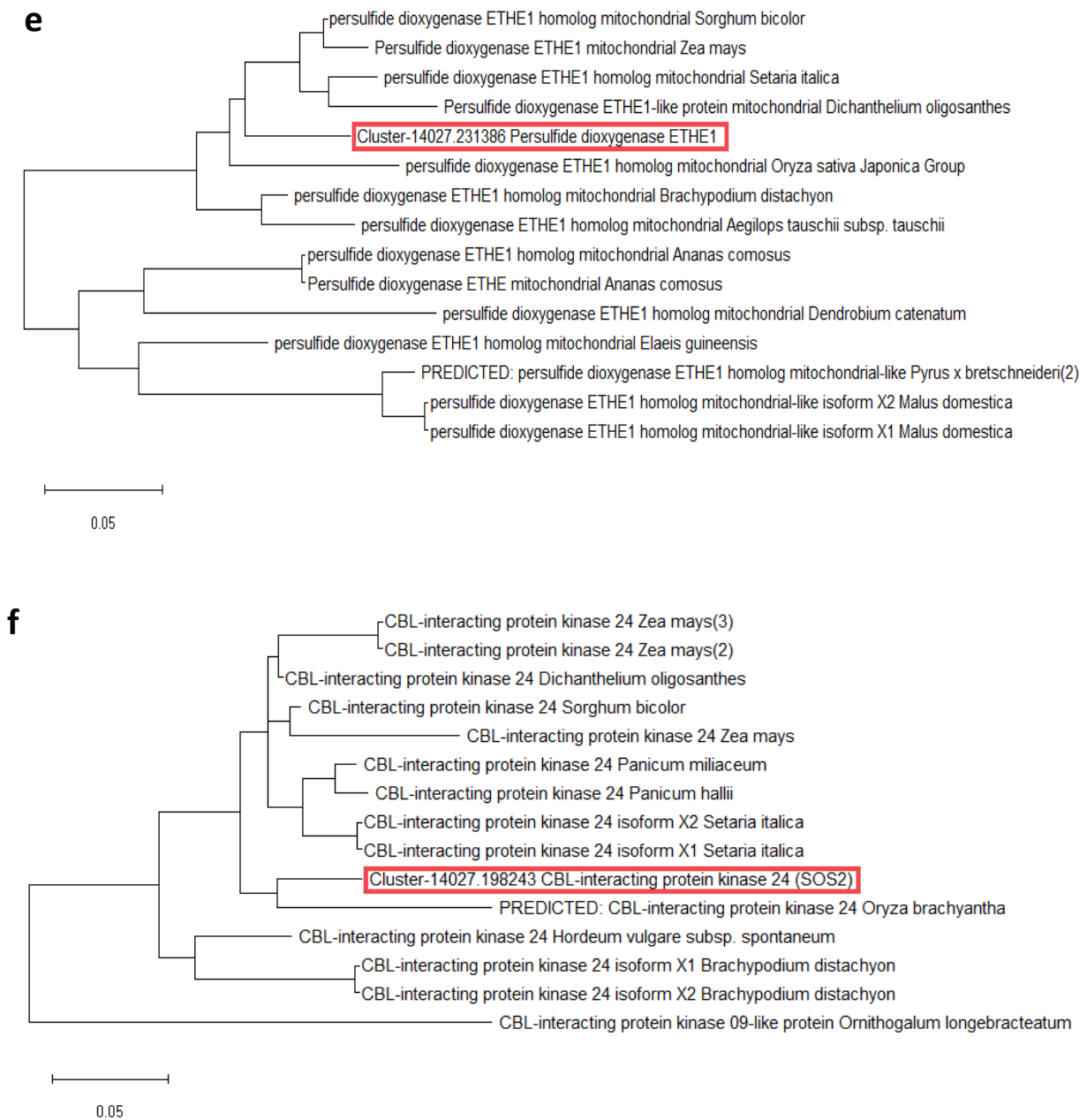


**Figure 10.** Phylogenetic relationship among *A. donax* salt responsive clusters and orthologues belonging to different plant sources. a cluster 14,027–155,903 homolog of *Phramites australis* Na<sup>+</sup>/H<sup>+</sup> antiporter (NHX1). b cluster 14,027–181,583 homolog of *Arabidopsis thaliana* Na<sup>+</sup>/H<sup>+</sup> exchanger 2 (NHX2). c cluster 14,027–182,899 homolog of *Oryza sativa* CBL-interacting protein kinase 1 (CIPK1-SOS2-like). d cluster 14,027–182,899 homolog of *Oryza sativa* CBL-interacting protein kinase 24 (SOS2). e cluster 14,027–54,233 homolog of *Setaria italica* cation transporter (HKT9). f cluster 14,027–231,386 homolog of *Arabidopsis thaliana* persulfide dioxygenase (ETHE1).

**Table 10.** Protein family and domain description

| Cluster ID   | Cluster description                                                                                   | Family Name - Description                                                                                                                  | Domain Name- Description                                                                               |
|--------------|-------------------------------------------------------------------------------------------------------|--------------------------------------------------------------------------------------------------------------------------------------------|--------------------------------------------------------------------------------------------------------|
| 14027.182899 | <i>Oryza sativa</i> subsp. japonica Group CBL-interacting protein kinase 1 (CIPK1-SOS2 like)          | PKc_like superfamily - Protein kinase family                                                                                               | STKc_SnRK3 - Catalytic domain of the Serine/Threonine Kinases, Sucrose nonfermenting 1-related protein |
| 14027.54233  | <i>Setaria italica</i> probable cation transporter HKT9                                               | 2a38euk superfamily - Potassium uptake protein, Trk family                                                                                 | -                                                                                                      |
| 14027.181583 | <i>Arabidopsis thaliana</i> Sodium/hydrogen exchanger 2 (NHX2)                                        | b_cpa1 superfamily; PRK05326 - Sodium/hydrogen exchanger family; potassium/proton antiporter                                               | -                                                                                                      |
| 14027.231386 | <i>Arabidopsis thaliana</i> Persulfide dioxygenase ETHE1                                              | Glyoxylase or a related metal-dependent hydrolase, beta-lactamase superfamily II                                                           | POD-like_MBL-fold - ETHE1 (PDO type I), persulfide dioxygenase A                                       |
| 14027.198243 | <i>Oryza sativa</i> subsp. Japonica CBL-interacting protein kinase 24 (SOS2)                          | AMPKA_C_like superfamily - C-terminal regulatory domain of 5'-AMP-activated protein kinase (AMPK) alpha subunit and similar domains family | CIPK_C - C-terminal regulatory domain of Calcineurin B-Like (CBL)-interacting protein kinases          |
| 14027.155903 | <i>Phragmites australis</i> pnhx1 mRNA for putative Na <sup>+</sup> /H <sup>+</sup> antiporter (NHX1) | b_cpa1 superfamily; PRK05326 - Sodium/hydrogen exchanger family; potassium/proton antiporter                                               | -                                                                                                      |

### 4.3 Discussion

Plants generate high yields if the growth demands are properly supplied as well as light and temperature fit to their optimum requirements. Yield-associated traits are inversely related to abiotic stress conditions such as salt during plant development. Under conditions of moderate salinity (EC 4-8 dS m<sup>-1</sup>), all important glycophytic crops reduce average yields by 50–80% (Panta et al., 2014). Plants have developed the ability to sense both the hyperosmotic component and the toxic ionic Na<sup>+</sup> component of salt stress (Deinlein et al., 2014). To date the molecular identities of plant hyperosmotic sensors and Na<sup>+</sup> sensors present at the plasma membrane have remained unknown. Recently, Choi et al. (Choi et al., 2014) suggested that Ca<sup>2+</sup>-dependent signaling plays a role in the systemic transmission of signaling as a Ca<sup>2+</sup> wave propagates preferentially through cortical and endodermal cells from roots to distal shoots. In salt tolerant plants, the cytosolic calcium perturbation activates the Salt Overly Sensitive (SOS) pathway (Liu and Zhu, 1998; Martinez-Atienza et al., 2007). The components of this pathway are the Ca<sup>2+</sup> sensor (SOS3) which accordingly changes its conformation in a Ca<sup>2+</sup>-dependent manner and interacts with SOS2, a serine/threonine protein kinase, forming the active SOS2-SOS3 complex. This interaction results in the activation through its phosphorylation of SOS1 (plasma membrane Na<sup>+</sup>/H<sup>+</sup> antiporter) which mediates the exclusion of Na<sup>+</sup> excess out of the cells. In addition, the SOS2-SOS3 complex activates NHX, the vacuolar Na<sup>+</sup>/H<sup>+</sup> exchanger resulting in the vacuolar sequestration of Na<sup>+</sup> excess thus further contributing to the restore of ion homeostasis (Zhu, 2002; Barragan et al., 2012). Consequently, the data suggest that the SOS pathway is only

partially activated under severe salt stress (up-regulation of CIPK1-SOS2-like protein and HKT9) and the down regulation of NHX indicates that the vacuolar sequestration of Na<sup>+</sup> excess seems to be impaired (Table 6). A specific response to extreme salt stress has been detected (Table 7), since the up regulation of CIPK1-SOS2 like and HKT9 (*Setaria italica* probable cation transporter HKT9) was accompanied by the up-regulation of NHX1 (*Arabidopsis thaliana* sodium/hydrogen exchanger 1) encoding the vacuolar Na<sup>+</sup>/H<sup>+</sup> antiporter. Moreover, CBL-interacting protein kinase 24 (homologs of *Oryza sativa* subsp. *Japonica* protein, Table 7), involved in the regulatory pathway for the control of intracellular Na<sup>+</sup> and K<sup>+</sup> homeostasis and salt tolerance, is specifically up regulated under extreme salt stress conditions (S4). It activates the vacuolar H<sup>+</sup>/Ca<sup>2+</sup> antiporter and operates in synergy with CBL4/SOS3 to activate the plasma membrane Na<sup>+</sup>/H<sup>+</sup> antiporter SOS1 (Cheng et al., 2004). As expected, the components of the SOS response are among the salt induced specific genes, indicating their key role in salt detoxification. In addition to that, several transcripts homologous to *Arabidopsis* NHX5 and NHX6 encoding endosomal Na<sup>+</sup>/H<sup>+</sup> antiporters are also up-regulated (data not shown). Although the relative log<sub>2</sub> fold changes of these clusters are below the +10.000 threshold we established at the beginning of the analysis, these results anyway suggest that the cellular components devoted to Na<sup>+</sup> excess expulsion, located in the tonoplast and in the endosomal membranes all together might participate in reducing the Na<sup>+</sup> cytoplasmic concentrations. The importance of these genes in salt stress relief is supported by the finding that *Arabidopsis nhx5 nhx6* double knockout showed reduced growth and increased sensitivity to salinity (Bassi et al., 2011). Downstream of aforementioned activation of Ca<sup>2+</sup> alteration induced by salinity, kinases become activated and may transduce the hyperosmotic signal to induce protein activities and gene transcription. The activation of transcription factors can occur by the direct binding with calmodulin-binding transcriptional activators (CAMTAs), GT-element binding proteins and MYBs (Mahajan and Tuteja, 2005; Deinlein et al., 2014). Transcription factors (TFs) are considered as the most important regulators controlling the expression of a broad range of target genes ultimately influencing the level of salt tolerance in plants. It is well documented that TFs belonging to the DREB, NAC, MYB, MYC, C2H2 zinc finger, bZIP, AP2/ERF (Ethylene Responsive Factor) and WRKY families are relevant in salt stress response (Golldack et al., 2014). In most cases, the overexpression of these transcription factors successfully enhanced salinity tolerance in many crops (Hanin et al., 2016). By comparing our results with those obtained in *A. donax* subjected to water deficit (Fu et al., 2016), slight differences can be observed in terms of TF subfamilies involved in salt and water stresses, but a greater number of all TFs for each family resulted differently regulated under both severe and extreme salt stress. Interestingly, a major involvement of AUX/IAA TFs is detected under salt stress with respect to *A. donax* plants subjected to drought thus indicating that a different regulation network is induced. Moreover, a total of 449 *A.*

*donax* unigenes correspond to high confidence rice homologs previously identified as salt or salt/drought responsive genes (Priya and Jain, 2013). Most of them (434) resulted also responsive to drought, indicating that the plant responses to these stresses probably overlap each other and that the downstream metabolic pathways can crosstalk. Significantly, few genes (15) specifically respond to salt treatments and they have been found especially (14 out of 15) among the G2-S4 vs G2-CK DEGs (Table 9), suggesting they might have a crucial role in the response to extreme salt conditions. Among these clusters, 9 (six up regulated and three downregulated) belong to the AP2-EREBP family (Chen et al., 2016). They have been implicated in various hormones-related signal transduction pathway including abscisic acid (ABA), ethylene and jasmonates (JAs) (Chen et al., 2016), which seem to be strongly involved in *A. donax* extreme salt stress response.

In our study, among the downregulated genes belonging to G2-S3 vs G2-CK DEGs, a homolog of *Setaria italica* protein TIFY 10B-like (LOC101761171) known to be a repressor of jasmonate (JA) responses, has been found (Table 5). As detailed below, an important attribute of JA is its ability to act both as a potent inhibitor of vegetative growth and as a positive regulator of reproductive and defensive processes (Pauwels et al., 2008). These antagonistic JA activities suggest that, in *A. donax* subjected to severe salt stress, the dilemma of plant “to grow or defend itself” seems to be resolved trying to growth in an unfavorable environment. A homolog of *Setaria italica* trihelix transcription factor GTL1 (LOC101762434) that acts as negative regulator of water use efficiency via the promotion of stomatal density and distribution (Yoo et al., 2010; Weng et al., 2012) has been found up-regulated in G2-S3 vs G2-CK DEGs (Table 5). It has been reported that GTL1 is expressed when *Arabidopsis* plants have sufficient available water but is downregulated by water deficit. *Arabidopsis thaliana* GTL1 loss-of-function mutations result in increased water deficit tolerance and higher integrated water use efficiency by reducing daytime transpiration without a demonstrable reduction in biomass accumulation. Moreover, GTL1 does not regulate ABA responsiveness, and the lower transpiration rates of *gtl1* defective plants are not caused by differences in stomatal aperture or ABA-induced stomatal closure (Yoo et al., 2010). The observed up-regulation of GTL1 under S3 severe salt stress reveals the susceptibility of *A. donax* plants to salt-induced water deficit and that it might be a target for gene knockout in order to genetically improve the *A. donax* performance in salty soil. Finally, homologs of *Setaria italica* bZIP *ABSCISIC ACID-INSENSITIVE 5*-like protein 7 functioning as transcriptional activator in the ABA-inducible expression of rd29B have been also found among the up-regulated clusters. Although their role is still unknown, rd29B proteins has potential to confer abiotic stress resistance in crop species grown in arid and semi-arid regions (Msanne et al., 2011).

The synthesis, sequestration, transportation, and turnover of hormones generate a net of signals that correlates plant growth in dependence on internal and external cues. Among these hormones, abscisic acid regulates important abiotic stress responses, in particular water balance and osmotic stress tolerance under drought and salt stress (Kuromori et al., 2018). ABA levels depend on the equilibrium between synthesis and degradation pathways. Several ABA biosynthetic genes have been isolated from different sources including zeaxanthin epoxidase (ABA1), 9-cis-epoxycarotenoid dioxygenase (NCED), ABA aldehyde oxidase (AOX) and ABA3/LOS5 (Xiong et al., 2001). The hydroxylation at the 8'-position of ABA is known as the key step of ABA catabolism, and this reaction is catalyzed by ABA 8'-hydroxylase, a cytochrome P450 (Saito et al., 2004). ABA signals are perceived by different cellular receptors operating in distinct cellular compartments (Figure 11a). The PYR/PYL/RCARs receptors bind ABA and inhibit type 2C protein phosphatases (PP2C) (Golldack et al., 2014). The PP2C inactivation leads to the accumulation of the active form of SNF1-RELATED PROTEIN KINASE (SnRK2) which in turn positively regulates ABA-responsive transcription factor as well the downstream ABA-responsive metabolic pathways. In this context, the analysis of G2-S3 vs G2-CK means to propose that plant responds to prolonged severe stress by lowering ABA levels (Table 5). However, ABA signal is probably persisting since ABA nucleoplasmatic receptors are up-regulated as well as the PP2C and SnRK2 which, as detailed before, active many downstream ABA-responsive processes (Golldack et al., 2014) (Figure 11a). Recently, the increase of leaf tissue ABA concentrations at two hours after plants were exposed to 50 mM of the ions was observed in maize indicating that ABA synthesis and accumulation are part of the early response to salt (Geilfus et al., 2018). Interestingly, the putative ortholog of AT1G78390, nine-cis-epoxycarotenoid dioxygenase 9 (NCED), is strongly upregulated in both *Arundo* shoots and roots during the early responses to water stress (Fu et al., 2016), this finding being in line with our suggestion that ABA might be not strictly involved in the response to a prolonged salt stress treatment. Brassinosteroids are growth-promoting plant hormones that act to enhance cell expansion and increase tolerance to stresses, including salinity, by mediating the synthesis of enzymatic or non-enzymatic antioxidant systems, proline, or lectins (Bajguz and Hayat, 2009). The specific induction under extreme salt stress (S4) but not in severe (S3) conditions of cytochrome P450 85A1 (LOC101770408) encoding brassinosteroid-6-oxidase 2, involved in active brassinosteroid biosynthesis might suggest a key role of these hormones in the case extreme environmental conditions are reached. Ethylene is biosynthesized by the plant in response to life-cycle events or environmental cues including among other diseases, mechanical stress, drought or flood. The phenotypes that can be observed with respect to ethylene signaling typically relate to the inhibition of plant growth and seasonal changes in a plant's life cycle. Ethylene is efficiently biosynthesized from 1-

aminocyclopropane-1-carboxylic acid (ACC) (Zhou et al., 2002). The mechanism of ethylene action, from perception to function, has been referred to as the “cleave and shuttle model” (Li et al., 2015) (Figure 11b). The most studied of the receptors is ethylene response 1 (ETR1) and downstream of ETR1 in *A. thaliana* is the kinase constitutive triple response 1 protein (CTR1) (Light et al., 2016). In absence of ethylene, this protein directly interacts with the ethylene receptors and it is required to be localized to the endoplasmic reticulum and be kinase active to be signaling active. CTR1 phosphorylates the putative metal transporter ethylene insensitive 2 (EIN2) that triggers its degradation by the Ub/26S proteasome (Light et al., 2015). In the presence of ethylene, CTR1 is inactivated by the interaction with ETR1 and the EIN2 dephosphorylated form is proteolytically cleaved to generate a C-terminal fragment called CEND EIN2. The CEND fragment localizes to the nucleus and initiates transcriptional regulation involving ethylene insensitive 3 (EIN3) and EIN3 like proteins (EIL1) (Figure 11b). Interestingly, transcripts encoding ACC oxidase have been found up-regulated both under severe and extreme salt stress, whereas homolog of *Arabidopsis thaliana* ETR is downregulated and clusters related to CTR1 and EIN3 are exclusively up-regulated in G2-S4 vs G2-CK samples (Table 7). In our opinion, this condition might describe a situation in which a low perception of emitted ethylene is attempted under extreme salt stress (down regulation of ETR1 expression), concomitantly to an increased expression of CTR1, of EIN2 and EIN3 with the aim to minimize the negative effect of ethylene upon plant growth. Salt also alters the expression of auxin responsive genes and auxin/IAA pathways in different plants (Wang et al., 2010) conferring higher tolerance to NaCl treatment (Bianco and Defez, 2009). Auxin is assumed to activate the proton pump of the plasma membrane pumping protons from the cytosol into the apoplast, resulting in wall loosening and an increase in wall extensibility (Bianco and Defez, 2009). In this respect, a homolog of *Zea mays* indole-3-acetaldehyde oxidase (AAO), involved in the biosynthesis of auxin, is upregulated in S4 samples and also in the G2-S4 vs G2-S3 comparison suggesting that IAA is synthesized in S4 extreme conditions (Table 8). Moreover, exclusively under extreme stress condition (Table 7) a homolog of auxin responsive GH3 gene family is also up-regulated. All the results, considering the role of GH3 genes in regulating levels of biologically active auxin through amino acid conjugation, thereby targeting them for degradation (Khan and Stone., 2007), indicate that auxin level might be finely tuned under S4 extreme stress condition. Globally, the high number of AUX/IAA transcription factors differently regulated in extreme salt environment accounts for a key role of auxins during long-term salt treatment (Figure 9). Finally, jasmonic acid-amido synthetase JAR1 is exclusively down regulated under extreme salt stress (Table 7), indicating that jasmonic acid signaling is likely impaired. The relationship between the salt stress response and the JA pathway is not well understood at molecular and cellular levels. However, large-scale transcriptomic studies have



shown JA signaling pathway is activated by salt stress leading to root growth inhibition in *Arabidopsis* (Valenzuela et al., 2016). The observed down regulation of JAR1 (Table 7) indicates that the pathway involved in the inhibition of root elongation might be not activated in *A. donax*, likely to address the plant demand to explore soil in the attempt of avoiding stress.

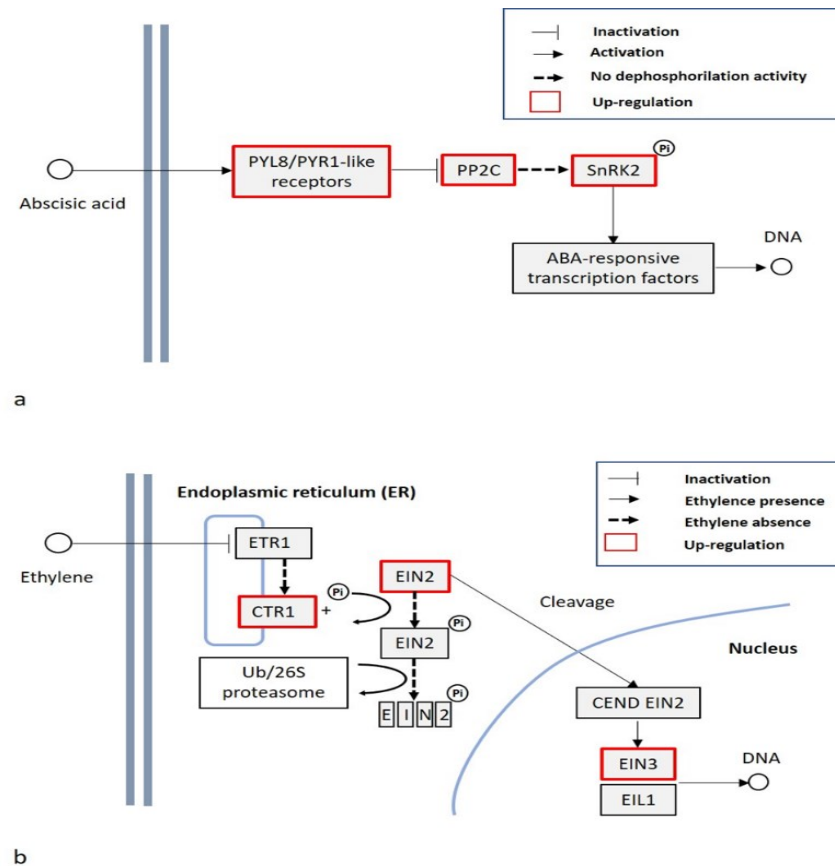


**Figure 11. Abscisic acid and ethylene signal pathways.** **a** abscisic acid receptor (PYL8), abscisic acid receptor (PYR1-like), serine/threonine-protein kinase (SnRK); protein phosphatase 2C (PP2C). The PYR/PYL/RCARs receptors bind ABA and inhibit type 2C protein phosphatases (PP2C). The active form of SnRK2 accumulates and positively regulates ABA-responsive metabolic pathways. **b** ethylene response 1 (ETR1), kinase constitutive triple response 1 protein (CTR1), putative metal transporter ethylene insensitive 2 (EIN2), EIN2 C-terminal fragment (CEND EIN2), ethylene insensitive 3 (EIN3) and EIN3 like proteins (EIL1). In absence of ethylene, CTR1 directly interacts with ETR1 and phosphorylates EIN2 that is in turn degraded. In the presence of ethylene, CTR1 is inactivated and the EIN2 dephosphorylated form is proteolytically cleaved to generate the CEND EIN2, initiating transcriptional regulation involving ethylene insensitive 3 (EIN3) and EIN3 like proteins (EIL1). See the text for details.

A consequence of high salt in the soil is the generation of a low water potential zone around the roots area making extremely difficult for the plants to obtain water and nutrients. Stomatal closure occurs in order to low water loss by transpiration, but it is at the same time responsible of sharp decrease in CO<sub>2</sub> availability for Calvin cycle and a depletion of oxidized NADP<sup>+</sup>. The overproduced

electrons are transferred to  $O_2$  to generate  $O_2^{\bullet-}$  and a series of dangerous oxygen reactive species (ROSs) causing unrestricted oxidation of various cellular components such as membrane lipids, proteins, and nucleic acid (Scandalios, 2005). Therefore, salinity tolerance is positively correlated with the induction of ROS scavenging enzymes such as superoxide dismutase (SOD), catalase (CAT), glutathione peroxidase (GPX), ascorbate peroxidase (APX), monodehydroascorbate reductase (MDHAR), dehydroascorbate reductase (DHAR) and glutathione transferases (GSTs) (Gupta and Huang, 2014). Moreover, under stress conditions, the activation of malate-oxalacetate (OAA) shuttle permits the transfer of reducing equivalents among compartments. In particular, the plastid NADP-malate dehydrogenase reduces oxalacetate to malate, thus regenerating the  $NADP^+$ . Malate is then translocated into the cytoplasm where is converted back in oxaloacetate, generating NADH by the cytosolic malate dehydrogenase. This called malate-valve appears to play a primary role under salinity constituting an important mechanism in salt acclimation (Gawronska et al., 2013). Drainage of electron flow towards the AOX oxidase pathway increases under salt stress (Zhang et al., 2016c) and prevents over-reduction of ubiquinone thus lowering excessive ROS generations. The malate-valve seems to be activated under S3 severe salt stress conditions (up-regulation of plastid NADP-malic dehydrogenase encoding gene), this result being consistent with a putative electron drainage from the over-reduced photosynthetic chain to other cellular compartments, in particular towards the mitochondria as homolog of the mitochondrial malate dehydrogenase (MHD) are also induced by salinity (Table 6). Under extreme salt stress, the unequivocal up regulation of the NADP-malic dehydrogenase and AOX oxidase is probably aimed to move the excess of reducing power from plastids to the cytosol and to avoid over-reduction of the mitochondrial respiratory chain. However, most of the other considered clusters related with the cellular antioxidant machinery have been found between both the down and up-regulated clusters. In our opinion, this is because under extreme stress conditions, which is certainly an emergency condition, a discerning regulation is needed both among and inside the cell compartments. To support our hypothesis, the SOD plastid pool comprising Cu/Zn SOD and Fe/SOD results differently regulated, with Cu/Zn SOD up regulated and Fe/SOD down regulated (Table 7 and 8). As multifunctional amino acid, proline seems to have diverse roles under stress conditions, such as stabilization of proteins, membranes, and subcellular structures, and protecting cellular functions by scavenging ROSs. Biosynthesis of proline occurs in the chloroplast or cytosol via glutamate pathway in which 1-delta-pyrroline-5-carboxylate synthase (P5CS) catalyzes the key regulatory and rate limiting reaction (Kaur and Asthir, 2015). During proline synthesis, 2 mol of NADPH per mole are consumed thus draining electrons from chloroplasts and contributing to the stabilization of redox balance and maintenance of cellular homeostasis when electron transport chain is saturated because of adverse conditions. Proline catabolism occurs predominantly in the

mitochondria involving proline dehydrogenase (PDH) or proline oxidase (POX) and 1-delta-pyrroline-5-carboxylate dehydrogenase (P5CSDH). The PDH and P5CSDH use NAD and FAD as electron acceptor, respectively, that deliver electrons to the respiratory chain to gain energy and resume growth after stress (Kaur and Asthir, 2015). The up-regulation of P5CS found in all comparisons suggests that that proline biosynthesis represents a pivotal mechanism to overcome the hypersaline conditions and adjust the osmotic status in *A. donax*. However, since PDH and P5CSDH resulted up regulated in extreme salt stress conditions (Table 7 and 8), we propose that S4 salt dose triggers a specific response that is not related to the mere proline synthesis to cope with osmotic stress. Regarding this aspect, it has been shown that proline catabolism is enhanced during stress recovery attempts. During this phase, it might function as signaling molecule proposed to regulate the expression of stress recovery genes (Szabados and Savoure, 2010). Therefore, under extreme salt stress, proline levels might be accurately regulated in order to accommodate the whole cell demand in terms of both osmotic potential and redox homeostasis adjustments. Polyamines play a crucial role in abiotic stress tolerance including salinity and increases in the level of polyamines are correlated with stress tolerance in plants (Yang et al., 2007; Zapata et al., 2008). The comparison of all data sets indicates that polyamines biosynthesis is induced during long term salt stress in *A. donax* having most likely a role in salt tolerance mechanism, especially under extreme stress condition (Table 6-8). Photosynthesis is the primary processes to be affected by salinity (Munns and Tester, 2008; Wang and Nii, 2000). Stomata close in response to leaf turgor declines, therefore supply of CO<sub>2</sub> to Rubisco (EC 4.1.1.39) is impaired thus inducing sharp alterations of photosynthetic metabolism. In *A. donax* under severe salt stress condition, CO<sub>2</sub> assimilation via the C<sub>3</sub> Calvin cycle seems to be impaired in favor of oxygen fixation through the photorespiration pathway. Moreover, the findings indicate that extreme salt treatment induces a down regulation of all C<sub>3</sub> Calvin cycle enzymes and a concomitant switch on of C<sub>4</sub> photosynthesis. The induction of PEPC activity and its expression following salt stress is documented in the facultative CAM plant *Mesembryanthemum crystallinum* and it is involved in the change from C<sub>3</sub> to CAM photosynthesis (Cushman and Bohnert, 1992). In *A. donax* leaves, the activation of C<sub>4</sub> pathway associated to a down-regulation of Rubisco biosynthesis, assembly and activation could be construed as an ultimate rescue attempt to overcome the long-term extreme conditions.

As concern metabolic pathways related to bioenergy production, it has been shown that lignin content in cell wall is inversely related to yield and conversion efficiency of polysaccharides into ethanol (Xie et al., 2018). Unfortunately, in the *A. donax* transcriptome subjected to both severe and extreme salt stress, several clusters involved in lignin biosynthesis are induced and this unwanted consequence of soil salinization might negatively affect biomass digestibility. This unfavorable

circumstance could be compensated by the fact that, after biomass saccharification, lignin residue can be used to produce biodegradable plastic and chemicals (Ragauskas, 2016). Furthermore, the induction of transcripts homologous to sucrose synthase (*Setaria italica* sucrose synthase) in the G2-S3 vs G2-CK comparison accounts for a probable increase in cellulose content that it has been shown to be without negative effects on growth (Coleman et al., 2009). Recently, the lipid fraction has been proposed as pivotal component of green biomass since it stores twice as much energy than cellulose per unit of weight (Ohlrogge et al., 2009). The up-regulation of key enzymes, such as triacylglycerol lipase and diacylglycerol kinase under severe salt stress supports the hypothesis that *A. donax* G2 response is trying to cope stress by inducing gene expression of pathways involved in biomass yield. The further analysis performed to identify genes which are regulated uniquely under salt stress conditions highlighted that a very small subset of clusters are up or down regulated by salt and not by other abiotic stress thus suggesting that the response pathways to different environmental cues often cross-talk and overlap each other in plants. As expected, the main salt-specific pathways are related to the SOS response (Liu and Zhu, 1998; Martinez-Atienza, 2007) and to the activation of ETHE1 (Krüßel, 2014) (Table S4). In *Arabidopsis* leaves, ETHE1 sulfur dioxygenase has a key function in the degradation of sulfur-containing amino acids and strongly affects the oxidation of branched-chain aminoacids as alternative respiratory substrates in situations of carbohydrate starvation (Krüßel, 2014). Therefore, ETHE1 could be relevant for stress tolerance against soil salinity in giant reed.

#### 4.4 Conclusions

The possibility to assign marginal land to bioenergy crop cultivation represents the main strategy to overcome the forthcoming conflict between land demand for feeding the world population and the request of new energy sources to sustain it. Salt affected soils are a widespread agricultural problem limiting crop production due to ionic, osmotic and oxidative stresses with negative impact on plant growth. In this work, the bioenergy crop *A. donax*, known to be able to growth in unfavorable environments, was subjected to two levels of long-term salt stress both doses being much higher than that used to define a soil area as “salinized”. To cultivate bioenergy crops in such soils might represent the unique possibility of their utilization, releasing suitable soil for crop cultivation. Moreover, considering that in S4 extreme salt treatment, the Na<sup>+</sup> is very close to that of seawater, we propose, as water-saving strategy, to irrigate the soil allocated to *A. donax* cultivation with opportune seawater dilutions. To fill the lack of information about the molecular mechanism involved in *A. donax* response to salt stress, we *de novo* sequenced, assembled and analyzed the *A. donax* G2 leaf transcriptome in response to the above detailed salt stresses. The response to salt and other

environmental constraints such as drought share similar attributes. However, we found that most of the *A. donax* annotated DEGs are homologs of genes belonging also to other species (*Setaria italica* and *Zea mays*) thus suggesting that long term salt stress regulates a specific set of genes providing a general overview of the prolonged salt stress transcriptional responses in *A. donax* (Table 6-8). The picture that emerges from the identification of functional genes related to salt stress is consistent with a dose-dependent response to salt. The number of DEGs under extreme salt stress is much higher than that observed in severe salt stress suggesting that a deep re-programming of the gene expression must occur in S4 samples, which, during the experiment, certainly grew in an “emergency” state. As concerns hormone regulation, the response to S3 severe salt stress seems not to be dependent by ABA levels as gene involved in its biosynthesis are not differently regulated whereas the clusters encoding the main catabolic enzyme are strongly up-regulated. Moreover, once *A. donax* plants were subjected to S4 extreme salt stress a clear down regulation of ABA biosynthetic genes is registered suggesting that ABA synthesis might have a key role during the onset of stressful conditions as demonstrated in other species (Geilfus et al., 2018) and in the case of water stress (Fu et al., 2016) but not in the case of long-term stress. Another distinct trait of the *A. donax* response to S4 extreme salt stress is the induction of clusters involved in brassinosteroid and IAA/AUX biosynthesis which probably have a key role in those more unfavorable conditions. Similarly, the down-regulation of gene involved in jasmonic acid biosynthesis suggests that JA signaling, leading to root growth inhibition, is repressed likely in the attempt to let the roots explore the surrounding soil more efficiently. The analysis of clusters related to ethylene biosynthesis and signaling indicated that, exclusively under S4 extreme salt stress, the gene transcription is modulated towards the minimization of ethylene negative effects upon plant growth. The *A. donax* leaves subjected to S3 severe salt stress respond to salt-induced oxidative stress by the induction of genes involved in ROS scavenging (APX) and in redistributing the reducing power excess among cell compartments (malate valve). Along with the clusters implicated in the malate valve, under S4 extreme salt stress, also gene encoding the alternative oxidase (AOX) have been found up regulated, highlighting once more that the induction of some pathways occurs in the case of more stringent environmental conditions. A clear involvement of proline and polyamines in coping the salt-induced osmotic stress can be suggested whereas sugars seem not to be involved as osmolytes protecting cell homeostasis. Certainly, the photosynthesis and photorespiration processes are strongly affected since under S3 severe salt treatment, genes involved in Rubisco assembly are down-regulated, and the fact that *A. donax* leaf are impeded to operate CO<sub>2</sub> fixation via C3 Calvin cycle is also supported by the up-regulation of genes involved in photorespiration (glycolate oxidase). Conversely, in S4 extreme salt treated samples, a dramatic change from C3 Calvin cycle to C4 photosynthesis is likely to occur as all gene regulation is addressed

to repress Rubisco synthesis and assembly, and to activate the primary CO<sub>2</sub> fixation to PEP in mesophyll cells (C4 pathway), this probably being the main finding of our work. Considered the distinct response to salt dose, either genes involved in S3 severe or in S4 extreme salt response could constitute useful markers of the physiological status of *A. donax* in salinized soil. Moreover, many of the unigenes identified in the present study have the potential to be used for the development of novel *A. donax* varieties with improved productivity and stress tolerance, in particular the knock out of the GTL1 gene acting as negative regulator of water use efficiency has been proposed as good target for genome editing experiments.

## 4.5 Methods

### 4.5.1 Plant material and application of salt stress

The experiment was conducted at the Department of Agriculture, Food and Environment (Di3A) of the University of Catania, initially using three different giant reed clones, namely G2, G18 and G20 ecotypes, originated from Caltagirone (Italy), (latitude 37°14', longitude 14°31'), Biancavilla (Italy) (latitude 37°38', longitude 14°52') and Capo D' Orlando (Italy) (latitude 38°08', longitude 14°43'), respectively, and collected for the *Giant reed Network* project (Cosentino et al., 2006). The trial started on July 7<sup>th</sup>, 2017, by transplanting *A. donax* rhizomes into 25 l pots (40 cm diameter and 30 cm height) containing a sandy soil as substrate. Before transplantation, the rhizomes were weighed using a laboratory scale and the number of buds was counted. For each ecotype, samples showing homogeneous rhizome weight and same bud number were used for transplanting. The individual rhizomes were then placed at 15 cm depth, one for each pot. The pots were arranged according to a randomized block factor scheme, performing three biological replicates for treatments. During the experiment, the irrigation was performed on a weekly basis, and until the first sprouts have been released, tap water (5 l per pot) has been used. Irrigation was carried out manually using a watering can, avoiding possible leaks by leaching. The first irrigation with saline water was carried out on August 3<sup>rd</sup>, 2017. Salt stress was imposed by adding different concentrations of NaCl to the irrigation water. In particular, S0 samples (no salt added), S3 (severe salt stress, 256.67 mM NaCl corresponding to 32 dS m<sup>-1</sup> electric conductivity, EC), S4 (extreme salt stress, 419.23 mM NaCl corresponding to 50 dS m<sup>-1</sup> electric conductivity, EC), this last concentration being very close to the seawater NaCl concentration (3%), where Na<sup>+</sup> molarity is about 460 mM and Cl<sup>-</sup> is around 540 mM (Mahajan and Tuteja, 2005). Before leaf harvest, the following morpho-biometric and physiological parameters were measured: number of culms, height of the main culm, number of green and senescent leaves, net photosynthesis and chlorophyll content measured in SPAD units (SPAD 502, Konica Minolta). Moreover, the measurement of the yielded biomass was also carried out (Cosentino et al., 2006). The collected data were submitted to ANOVA analysis, using CoStat 6.003

software. The averages were separated by the Student Newman Keuls (SNK) test when  $P \leq 0.05$ . On the basis of the aforementioned parameters suggesting contrasting behavior under salinity stress (S3 and S4 salt levels) among the clones under investigation, G2 was selected to perform the global transcriptomic analysis.

#### **4.5.2 Sample collection and RNA extraction**

In November 17<sup>th</sup>, 2017, fully expanded, no senescing G2 leaves (the 3<sup>rd</sup> leaf from the top) were harvested and immediately frozen with liquid nitrogen. Then, plant material, kept frozen by continuously liquid nitrogen adding, was ground using precooled mortar and pestle followed by RNA isolation using the Spectrum Plant Total RNA Extraction Kit (Sigma-Aldrich, St. Louis, MO, USA) according to the manufacturer's instructions. RNA degradation and contamination were monitored on 1% agarose gels. RNA purity and concentration were assayed using the NanoDrop spectrophotometer (ThermoFisher Scientific, Waltham, MA, USA). RNA integrity was assessed using the Agilent Bioanalyzer 2100 system (Agilent Technologies, Santa Clara, CA, USA). Before to be sequenced, the RNA samples were subjected to quality parameter evaluation. The average RNA Integrity Number (RIN) was of 8.0 and there was very slight genomic DNA contamination confirming that all the samples have such high quality level to be processed (Table 1).

#### **4.5.3 Library preparation for transcriptome sequencing**

A total amount of 1.5 µg RNA per sample was used as input material for the RNA sample preparations. Sequencing libraries were generated using NEBNext® Ultra™ RNA Library Prep Kit for Illumina® (New England Biolabs, Ipswich, MA, USA) following manufacturer's recommendations. Briefly, mRNA was purified from total RNA using poly-T oligo-attached magnetic beads. Fragmentation was carried out using divalent cations under elevated temperature in NEBNext First Strand Synthesis Reaction Buffer (5X). First strand cDNA was synthesized using random hexamer primer and M-MuLV Reverse Transcriptase (RNase H-). Second strand cDNA synthesis was subsequently performed using DNA Polymerase I and RNase H. Remaining overhangs were converted into blunt ends via exonuclease/polymerase activities. After adenylation of 3' ends of DNA fragments, NEBNext Adaptor with hairpin loop structure were ligated to prepare for hybridization. In order to select cDNA fragments of preferentially 150~200 bp in length, the library fragments were purified with AMPure XP system (Beckman Coulter, Beverly, MA, USA). Then 3 µl USER Enzyme by NEB was used with size-selected, adaptor-ligated cDNA at 37°C for 15 min followed by 5 min at 95 °C before PCR. Then PCR was performed with Phusion High-Fidelity DNA polymerase, Universal PCR primers and Index (X) Primer. At last, PCR products were purified (AMPure XP system) and library quality was assessed on the Agilent Bioanalyzer 2100 system.

#### 4.5.4 Clustering and next generation RNA sequencing

Cluster generation and sequencing were performed by Novogene Bioinformatics Technology Co., Ltd. (Beijing, China). The clustering of the index-coded samples was performed on a cBot Cluster Generation System using a PE Cluster kit cBot-HS (Illumina). After cluster generation, the library preparations were sequenced on Illumina HiSeq2000 platform to generate pair-end reads. Raw data (raw reads) of fastq format were firstly processed through in-house perl scripts. In this step, clean data were obtained by removing reads containing adapter, reads containing ploy-N and low-quality reads. At the same time, Q20, Q30, GC-content and sequence duplication level of the clean data were calculated. All the downstream analyses were based on clean data with high quality (Table 1).

#### 4.5.5 *De novo* transcriptome assembling and gene functional annotation

*De novo* transcriptome assembly was accomplished using Trinity (r20140413p1 version) with `min_kmer_cov:5` parameters ( $k=25$ ). Then Hierarchical Clustering was performed by Corset (v1.05 version) to remove redundancy (parameter `-m 10`). Afterwards the longest transcripts of each cluster were selected as Unigenes. Gene function was annotated based on the following databases: National Center for Biotechnology Information (NCBI) non-redundant protein sequences (Nr), NCBI non-redundant nucleotide sequences (Nt), Protein family (Pfam), Clusters of Orthologous Groups of proteins (KOG/COG), Swiss-Prot, Kyoto Encyclopedia of Genes and Genomes (KEGG), Ortholog database (KO) and Gene Ontology (GO) (Table 2).

#### 4.5.6 Identification of clusters specifically involved in the salt stress response

In order to discriminate among clusters specifically regulated by salt treatment from those also involved in the response to other abiotic stress (oxidative, water deprivation stress, cold, heavy metals), the GO term lists relative to each comparison (G2\_S3 vs G2\_CK and G2\_S4 vs G2\_CK) were filtered and exclusively salt-regulated clusters were extrapolated. For the identification of transcription factors responsive to salt stress in *A. donax*, we mined the available salt stress-responsive transcription factor database of rice (SRTFDB) (Yoo et al., 2010) by Blastn searches with an *e* value cutoff of  $1e^{-5}$ .

#### 4.5.7 Multiple sequence alignment and phylogenetic analysis

Multiple alignment analysis of fifteen amino acid sequences of selected proteins (CIPK1-SOS2 like, cation transporter HKT9, NHX1, NHX2, SOS2 and ETHE 1) was carried out by MUSCLE by executing MEGA X 10.0.5 (<https://www.megasoftware.net/>). The phylogenetic tree was created using MEGA X 10.0.5 by the ML (maximum likelihood) method following the Jones, Taylor and Thornton (JTT) substitution model and 1000 bootstrap replicate with other default parameters.



#### 4.5.8 Quantification of gene expression and differential expression analysis

Gene expression levels were estimated by RSEM (v1.2.26 version) with bowtie2 mismatch 0 parameters in order to map to Corset filtered transcriptome. For each sample, clean data were mapped back onto the assembled transcriptome and readcount for each gene was then obtained from the mapping results. Differential expression analysis between control and salt stressed samples was performed using the DESeq R package (1.12.0 version,  $\text{padj} < 0.05$ ). The resulting  $p$ -values were adjusted using the Benjamini and Hochberg's approach for controlling the false discovery rate. Genes with an adjusted  $p$ -value  $< 0.05$  found by DESeq were assigned as differentially expressed. The GO enrichment analysis of the differentially expressed genes (DEGs) was implemented by the Goseq R packages (1.10.0, 2.10.0 version, corrected P-Value  $< 0.05$  based) Wallenius non-central hypergeometric distribution (Young et al., 2010). Furthermore, to analyze the *Arundo donax* transcriptome all of the unigenes were submitted to the KEGG pathway database for the systematic analysis of gene functions. KOBAS software (v2.0.12 version, corrected P-Value  $< 0.05$ ) was used to test the statistical enrichment of differential expression genes in KEGG pathways.

#### 4.5.9 Real-time validation of selected DEG candidates using qRT-PCR

Total RNA (2.5  $\mu\text{g}$ ) extracted from sample leaves as described above, was reversed transcribed using the SuperScript<sup>TM</sup> Vilo<sup>TM</sup> cDNA synthesis kit by ThermoFisher Scientific, according to the manufacturer's instructions. Real-time qRT-PCR was performed for a total of ten DEGs with PowerUp SYBR Green Master mix by ThermoFisher Scientific and carried out in the Bio-Rad iQ5 Thermal Cycler detection system. All the genes were normalized with *A. donax* 26 S proteasome non-ATPase regulatory subunit 11 gene (RPN6) that was reported to be a suitable housekeeping gene in abiotic stress conditions (Poli et al., 2017). All reactions were performed in triplicate and fold change measurements calculated with the  $2^{-\Delta\Delta\text{CT}}$  method. Sequences of primers used for real-time PCR are provided in Table 4.

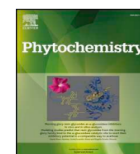
## 5 Transcriptional response of giant reed (*Arundo donax* L.) low ecotype to long-term salt stress by Unigene-based RNAseq



Contents lists available at ScienceDirect

Phytochemistry

journal homepage: [www.elsevier.com/locate/phytochem](http://www.elsevier.com/locate/phytochem)



### Transcriptional response of giant reed (*Arundo donax* L.) low ecotype to long-term salt stress by unigene-based RNAseq



Angelo Sicilia, Danilo Fabrizio Santoro, Giorgio Testa, Salvatore Luciano Cosentino, Angela Roberta Lo Piero\*

*Department of Agriculture, Food and Environment, University of Catania, Via Santa Sofia 98, 95123, Catania, Italy*

### Abstract

The giant reed is a fast growing herbaceous non-food crop considered as eligible alternative energy source to reduce the usage of fossil fuels. Tolerance of this plant to abiotic stress has been demonstrated across a range of stressful conditions, thus allowing cultivation in marginal or poorly cultivated land in order not to compromise food security and to overcome land use controversies. In this work, we *de novo* sequenced, assembled and analyzed the *A. donax* low G34 ecotype leaf transcriptome (RNAseq analysis) subjected to severe long-term salt stress (256.67 mM NaCl corresponding to 32 dS m<sup>-1</sup> electric conductivity). In order to shed light upon the response to high salinity of this non model plant, we analyzed clusters related to salt sensory and signaling transduction, transcription factors, hormone regulation, Reactive Oxygen Species (ROS) scavenging and osmolyte biosynthesis, all of them showing different regulation compared to untreated plants. The analysis of clusters related to ethylene biosynthesis and signaling indicated that gene transcription is modulated towards the minimization of ethylene negative effects upon plant growth. Certainly, the photosynthesis is strongly affected since genes involved in Rubisco biosynthesis and assembly are down-regulated. However, a shift towards C4 photosynthesis is likely to occur as gene regulation is aimed to activate the primary CO<sub>2</sub> fixation to PEP (phosphoenolpyruvate). The analysis of “carbon metabolism” category revealed that G34 ecotype under salt stress induces the expression of glycolysis and Krebs cycle related genes, this being consistent with the hypothesis that some sort of salt avoidance might be occurred in *A. donax* G34 low ecotype. By comparing our results with findings obtained with other giant reed ecotype, we identified several differences in the response to salt that are in accordance with the possibility that heritable phenotypic differences among clones of *A. donax* might be accumulated especially in ecotypes originating from distant geographical areas, despite their asexual reproduction modality. Additionally, 26,838 simple sequence repeat (SSR) markers were identified and validated. This SSR dataset definitely expands the marker catalogue of *A. donax* facilitating the genotypic characterization of this species

**Keywords:** *Arundo donax*, Poaceae, RNA-Seq, *de novo* assembly, Giant reed, Bioenergy crops, Salt stress, Low ecotype, SSR.

## 5.1 Introduction

The energy issue has become of fundamental importance in the last few decades and it represents an extremely complex problem to deal with due to a combination of different causes. Phenomena such as the demographic explosion recorded in the last century followed by a strong urbanization, as well as the improvement of the economic conditions of ever-wider groups of population led to a significant increase in global energy demand. The use of fossil fuels of organic origin and non-renewable energy sources became increasingly unsustainable from an environmental, political and economic point of view. For these reasons, many countries in the world, including the United States (US) and the European Union (EU), have begun to develop new energy policies with the aim of using alternative and sustainable energy sources (REN21, 2016). Among the various renewable energy sources, the production of energy from biomass (bioenergy) is becoming increasingly important since it is one of the most widely available renewable sources on our planet. Second generation biofuels are produced from organic materials not intended for food use including perennial herbaceous plants and fast-growing trees. As cellulosic feedstocks cannot be produced on arable lands due to their competition with the cultivation of food crops, a recommended strategy is to grow them on “marginal lands”, overcoming risks for food security. The marginal lands are usually described as unproductive or unsuitable for crop production due to poor soil properties, bad quality underground water, drought, undesired topology and unfavorable climatic conditions (Tang et al. 2010). Salt affected soils are also considered marginal due to high salinity and sodicity (Shahid and Al-Shankiti 2013). *Arundo donax* L. (Poaceae), common name “giant cane” or “giant reed”, grows in soil rich in water, especially near channels, rivers, lakes, ponds and marshes, where it shows the maximum biomass yields. *Arundo donax* L. was studied in sufficient depth, in terms of biomass production potential in warm-temperate and semi-arid areas (Monti and Cosentino 2015; Fernando et al. 2015). The adaptability of the plants to different kinds of environments, soils and growing conditions, in combination with the high biomass production confers on *A. donax* many advantages when compared to other energy crops. The desirable traits include aspects of crop phenology, canopy and leaf photosynthesis, biomass partitioning, nutrient and water use efficiency and heat, cold and salt tolerance (Jones et al. 2015). In particular, the growth and physiological responses of giant cane to salinity (NaCl) have been evaluated across a range of salinities (0–42 dS m<sup>-1</sup>) (Nackley and Kim 2015). Classic growth analysis showed >80% reduction in overall growth at the highest salt concentration, and the plants at 40 dS m<sup>-1</sup> grew without chlorosis, maintaining net assimilation rates 7–12 μmol m<sup>-2</sup> s<sup>-1</sup>, confirming that *A. donax* is a halophyte plant (Williams et al. 2009; Quinn et al. 2015). Salinity is one of the most brutal environmental stresses that hamper crop productivity worldwide (Flowers 2004; Munns and Tester 2008; Gupta and Huang 2014). It impairs plant growth and development via water stress, cytotoxicity

due to excessive uptake of ions such as sodium ( $\text{Na}^+$ ) and chloride ( $\text{Cl}^-$ ), and nutritional imbalance (Isayenkov and Maathuis 2019). Additionally, salinity is typically accompanied by oxidative stress due to the generation of reactive oxygen species (ROS) (Tsugane et al. 1999; Isayenkov 2012). Plants develop various physiological and biochemical mechanisms in order to survive in soils with high salt concentration. Principle mechanisms include ion homeostasis and compartmentalization, ion transport and uptake, biosynthesis of osmoprotectants and compatible solutes, activation of antioxidant enzymes and synthesis of antioxidant compounds, synthesis of polyamines, generation of nitric oxide (NO), and hormone modulation (Gupta and Huang 2014). Nevertheless, decoding of salt stress response mechanisms in plants remains restricted due to the complexity of the response process and the genetic variability among plant species. Moreover, our knowledge of the genetic bases of salt tolerance is largely based on genetic studies in model or crop species (Hanin et al. 2016). *De novo* RNA sequencing (RNA-Seq) assembly facilitates the study of transcriptomes for non-model plant species for which the genome sequence is not available by enabling an almost exhaustive survey of their transcriptomes and allowing the discovery of virtually all expressed genes in a plant tissue under abiotic stress. In 2019, the first transcriptome of G2 *A. donax* ecotype subjected to two levels (S3, severe and S4, extreme) of long-term salt stress has been reported (Sicilia et al. 2019). A deeper re-programming of the gene expression has been found in those plants grew at extreme salt level than in those subjected to severe salt stress, probably representing for them an “*emergency*” state, considering that in the highest salt treatment, the  $\text{Na}^+$  concentration was very close to that of seawater. That study allowed identifying several expressed genes that could be preferential targets for functional studies, for metabolic engineering or for tailoring growth habit/development of the giant reed to higher bioenergy yield (Sicilia et al. 2019). Because of its sterility, *A. donax* has developed asexual vegetative reproduction, allowing its rapid spread throughout the world. New plants can be generated every year directly from rhizomes and for this reason, genetic diversity has been very low, as expected for an agamic-reproducing plant (Balogh et al. 2012). Regarding the genotypic diversity among clonal populations sampled in different regions, data reveal moderate differences (Haddadchi et al. 2013; Khudamrongsawat et al. 2004; Ahmad et al. 2008). A likely explanation for different levels of variation reported in different regions could be the use of particular type of molecular markers to detect genotypic variation, e.g., ISSRs detect more polymorphic bands per primer than RAPDs (Esselman et al. 1999; Behera et al. 2008), and the fact that ploidy levels may vary among regions. Pilu and co-workers (2014) conducted a genetic analysis on 100 Italian clones using SSR markers with the aim of characterizing the population of *A. donax* on Italian territory. They observed quite a low genetic diversity among the clones although suggested the presence of three distinct populations. All these studies suggest that, despite the expected and reported low genetic diversity,

genetic and phenotypic differences might be accumulated among ecotypes due to their different geographic origin and distribution. Heritable phenotypic differences among clones of *A. donax* have been reported that could be explored to improve several plant characteristics such as number of culms, culm diameter and height (Cosentino et al. 2006). For these reasons, the genetic improvement of this plant, aiming to obtain better performance as an energy crop in several conditions, needs to be mainly based on clonal selection. For the same reasons a deep knowledge of the global transcriptomic response of different giant reed ecotypes to salt is needed that might lead to the discovery of still unidentified candidate genes to employ in genome editing experiments. In this work, considering the frequent occurrence of soil salinity in the Mediterranean area and the potential use of marginal soil for energy crop cultivation, we *de novo* sequenced, assembled and analyzed the *A. donax* low G34 ecotype leaf transcriptome (RNAseq analysis) subjected to severe long-term salt stress (32 dS m<sup>-1</sup>). G34 ecotype was chosen because it is normally lower than other ecotypes, this phenotypic characteristic probably being caused by genetic and epigenetic marks it has accumulated from its origin on.

## **5.2 Results**

### **5.2.1 Effect of salt stress upon *A. donax* morpho-biophysiological parameters**

As described in the Methods section, *A. donax* G34 ecotype morpho-biometric and physiological parameters were measured at sampling date after being subjected to prolonged salt stress imposition (S3 samples). The results showed that both the leaf number per pot, the stem number and the main stem height per pot were reduced by salt stress (Figure 12a, 12b and 12c). Similarly, physiological parameters such as SPAD unit, net photosynthesis and biomass yield per pot significantly decreased under salt stress conditions (S3) compared with untreated S0 samples (Figure 12a, 12b and 12c) thus indicating the effectiveness of the treatment to induce gene expression reprogramming.

### **5.2.2 Transcript assembly and annotation**

In this study, we carried out a comprehensive identification of transcriptional responses of *A. donax* G34 clone to prolonged severe salt stress by RNA-Seq (see experimental design in Materials and Methods). Raw reads were filtered to remove reads containing adapters or reads of low quality, so that the downstream analyses are based on a total of 430 million clean reads with an average of ~71.5 million reads (~10.7 G) per sample, the average percentage of Q30 and GC being 94.3 % and 54.3 %, respectively (Table 12).

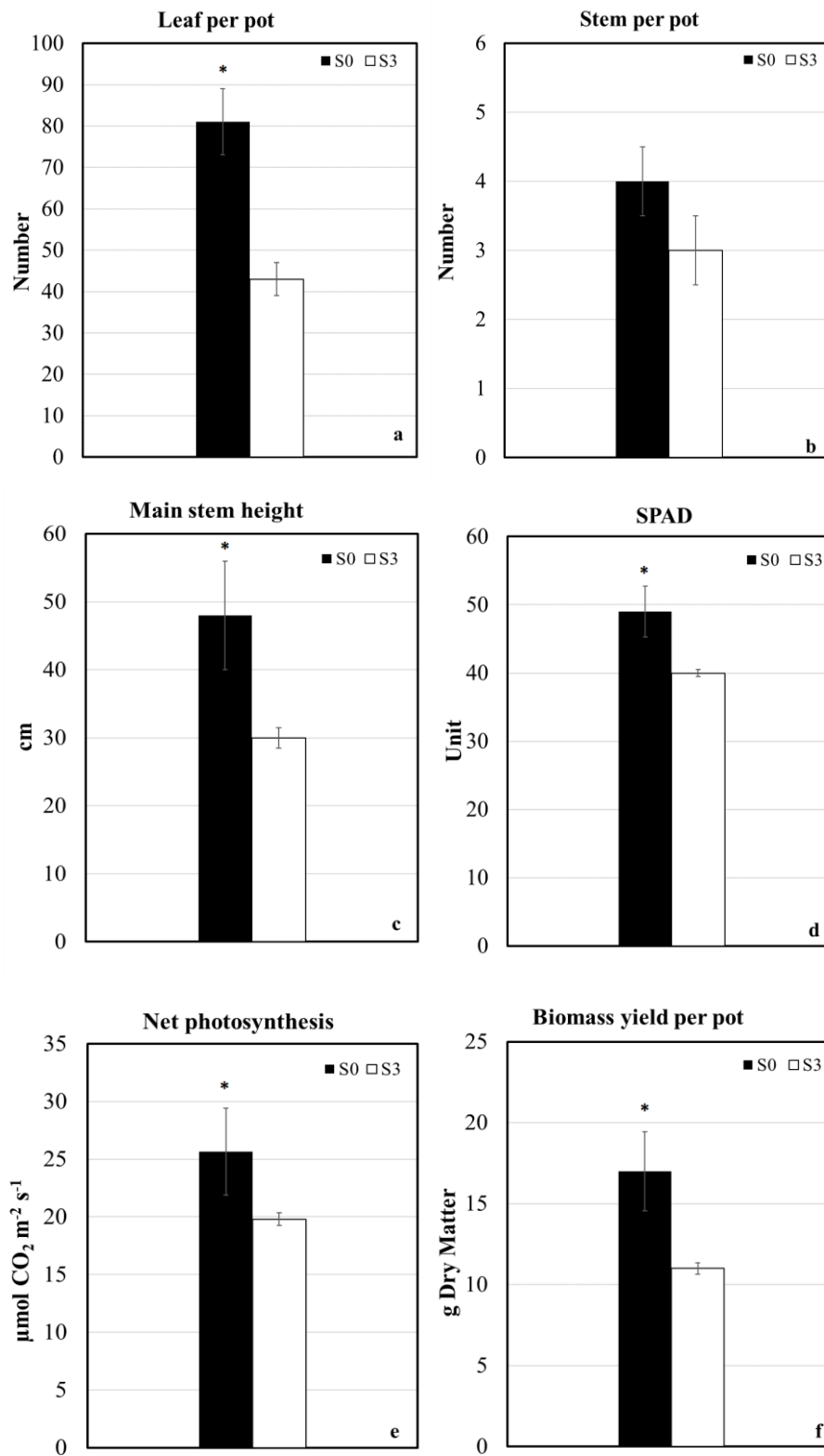


**Figure 12.** Effect of salt stress upon G34 ecotype morpho-biometric and physiological parameters. a Leaf number per pot. b Stem number per pot. d Main stem height. d SPAD. e Net photosynthesis. f Dry biomass.

*De novo* assembly of clean reads resulted in 273,717 transcripts and 193,070 unigenes with N50 length of 1957 and 1858, respectively (Table 12), in line with previous N50 reports (Sablok et al. 2014; Fu et al. 2016; Sicilia et al. 2019), indicating that a good coverage of the transcriptome has been achieved. To evaluate the assembly consistency, the filtered unique reads were mapped back to the final assembled leaf transcriptome and the average read mapping rate using the alignment software Bowtie2 was 66.0%. (Table 12).

**Table 12.** Summary statistics of the RNA quality and sequencing results

|                              |             |
|------------------------------|-------------|
| Average RIN                  | 7.6         |
| Clean reads                  | 430 million |
| N° of transcripts            | 273,717     |
| N° of Unigenes               | 193,070     |
| Average of read mapping rate | 66,0        |
| Transcripts N50 (bp)         | 1957        |
| Unigenes N50 (bp)            | 1858        |
| Q30 (%)                      | 94.3        |
| GC content (%)               | 54.3        |

Both transcript and Unigene length distributions are reported in Supplementary Figure 13. These data showed that the throughput and sequencing quality were high enough to warrant further analysis.

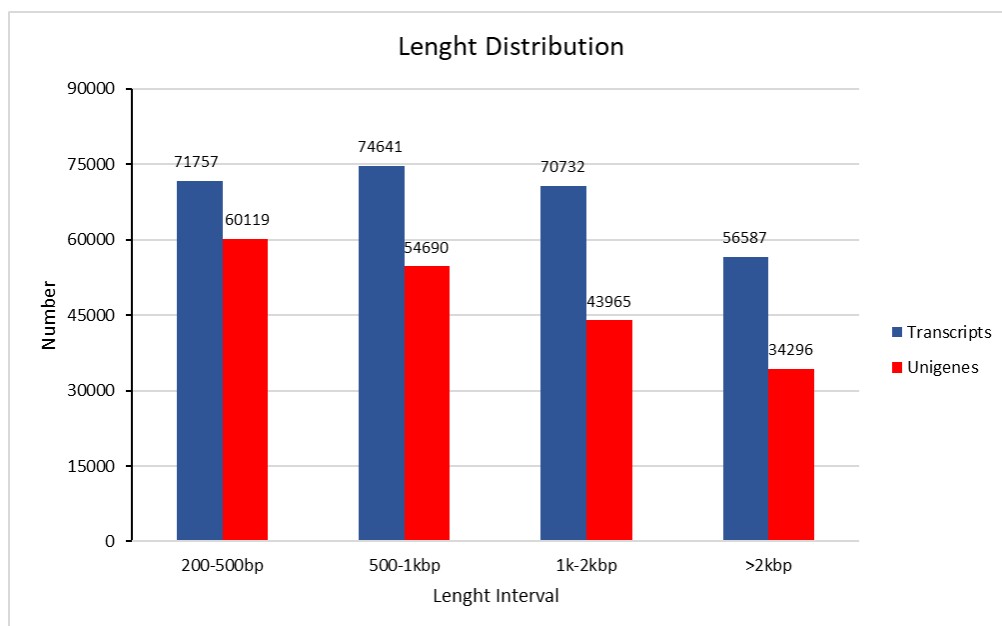


**Figure 13.** Overview of the number of transcripts and unigenes in different length intervals

To achieve comprehensive gene functional annotation, all assembled unigenes were blasted against public databases, including National Center for Biotechnology Information (NCBI), Protein family (Pfam), Clusters of Orthologous Groups of proteins (KOG/COG), Swiss-Prot, Ortholog database (KO) and Gene Ontology (GO) (Table 13). A total of 105,782 unigenes were annotated in at least one searched database, accounting for 54.78 % of the obtained total unigenes. Among them, 28,524 (14.77%) and 35,773 (18.53%) assembled unigenes showed identity with sequences in the Nr and Nt databases, respectively. The percentage of assembled unigenes homologous to sequences in KO, Swiss-Prot, Pfam, GO and KOG databases were 19.99, 30.17, 13.75, 38.76 and 16.25%, respectively (Table 13).

**Table 13.** The number and percentage of successful annotated genes

| Database                           | Number of unigenes | Percentage % |
|------------------------------------|--------------------|--------------|
| Annotated in Nr                    | 28,524             | 14.77        |
| Annotated in Nt                    | 35,773             | 18.53        |
| Annotated in KO                    | 38,604             | 19.99        |
| Annotated in SwissProt             | 58,260             | 30.17        |
| Annotated in Pfam                  | 26,543             | 13.75        |
| Annotated in GO                    | 74,840             | 38.76        |
| Annotated in KOG                   | 31,378             | 16.25        |
| Annotated in at least one Database | 105,782            | 54.78        |

### 5.2.3 Identification of differentially expressed genes (DEGs)

The characterization of *A. donax* transcriptional response to salt stress was carried out by the identification of the unigenes whose expression level changed upon NaCl treatment. A total of 1778 differentially expressed genes (DEGs) were identified from the G34-S3 vs G34-CK comparison, 977 up-regulated genes and 801 down-regulated genes (Figure 14). Validation of expression levels for ten selected DEG candidates was carried out by quantitative real-time PCR (qRT-PCR) and reported in Sicilia et al. (2019) being part of the same sequencing project. The results show high congruence between RNA-Seq results and qRT-PCR (coefficient of determination  $R^2 = 0.91$ ) indicating the reliability of RNA-Seq quantification of gene expression (Figure 6).



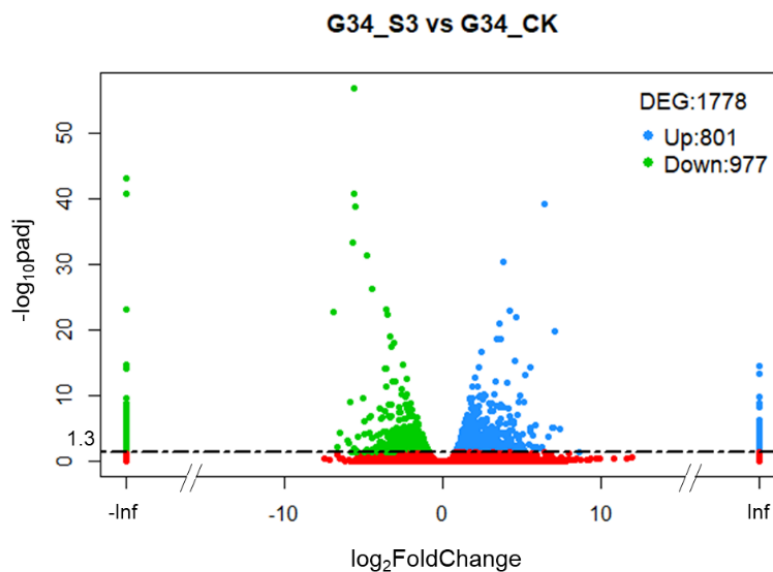


**Figure 14.** Volcano plot showing the DEGs of G34-S3 vs G34-CK comparison. The up-regulated genes with statistically significance are represented by blue dots, the green dots represent the down-regulated genes and the red dots are DEGs with  $-\log_{10}padj < 1.3$ , adopting  $\log_2FoldChange$  threshold of 0.58 (1.5 fold change). The X-axis is the gene expression change, and the Y-axis is the pvalue adjusted after normalization

#### 5.2.4 Functional classification of DEGs

Gene Ontology (GO) terms, Clusters of Orthologous Groups of proteins (KOG) classification and Kyoto Encyclopedia of Genes and Genomes (KEGG) pathway functional enrichment was performed to identify possible biological processes or pathways involved in salt stress response. Considering the G34-S3 vs G34-CK sample set (Figure 15), “oxidation-reduction process” (100 up- and 42 down-regulated genes), “transmembrane transport” (59 up- and 31 down-regulated genes) and “carbohydrate metabolic process” (33 up- and 20 down-regulated genes) are the three most enriched GO terms in the Biological Process (BP) ontology. “Oxidoreductase activity” (78 up- and 19 down-regulated genes) is the most enriched GO terms in the Molecular Function (MF) category indicating that genes acting in this process might play crucial roles in the response to salt treatment (Figure 15). “Chloroplast” (9 up- and 3 down-regulated genes), “chloroplast part” ( 5 up- and 5 down-regulated genes), “chloroplast stroma” ( 2 up- and 11 down-regulated genes) and “chloroplast thylakoid” ( 1 up- and 7 down-regulated genes) are the most enriched GO terms in the Cellular Component ontology clearly indicating that this organelle is mainly involved under salt stress condition (Figure 15). To predict and classify possible functions, all unigenes were aligned to the KOG database and were assigned to the KOG categories. Among the KOG categories, the cluster for “general function” (16%) represented the largest group, followed by “posttranslational modification, protein turnover, chaperones” (13.4%) and “signal transduction mechanisms” (9.3%). “Translation, ribosomal

structure and biogenesis” (8%), “RNA processing and modification” (6.4%) and “transcription” (5.6%) were the largest next categories (data not shown).

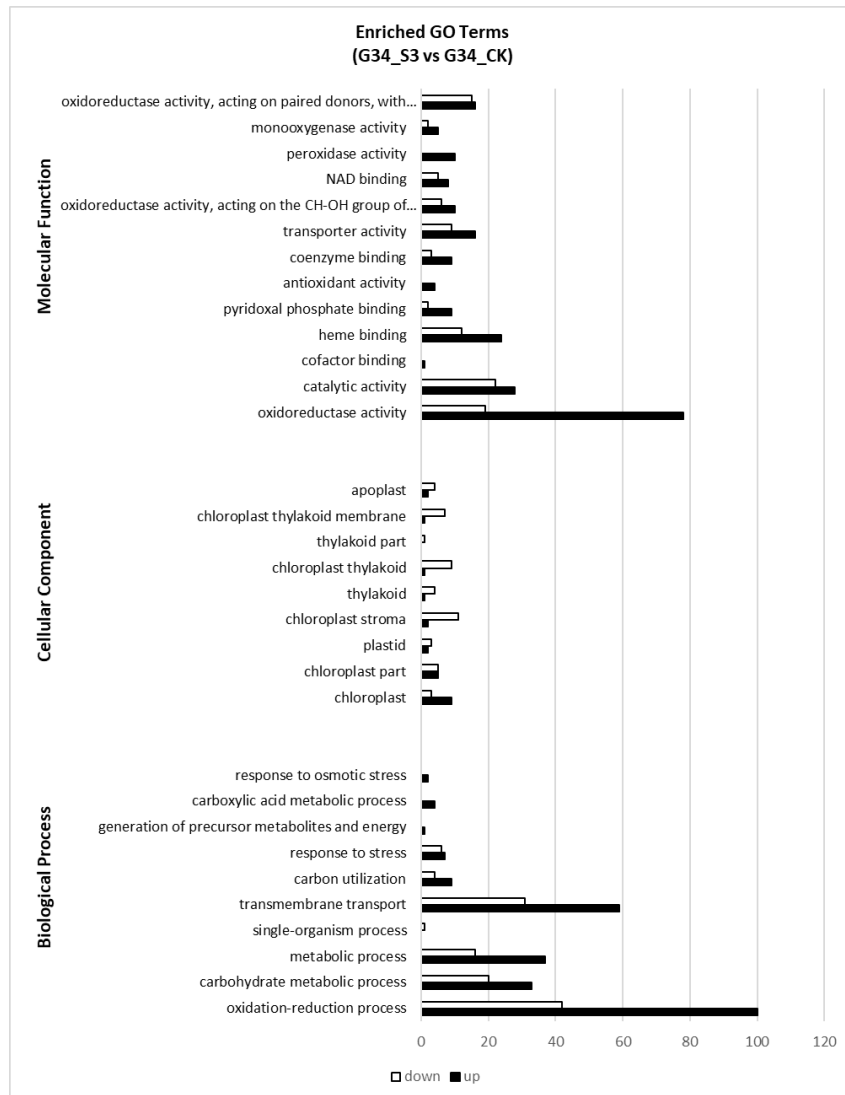


**Figure 15.** GO enrichment analysis for the DEGs in *A. donax* (G34-S3 vs G34-CK) The X-axis indicates the numbers related to the total number of GO terms, and the Y-axis indicates the subcategories.

BP, biological processes; CC, cellular components; MF, molecular functions

The set of DEGs originated from G34-S3 vs G34-CK comparison was also mapped onto KEGG pathways. Table 14 shows the main forty KEGG pathway terms sorted by a decreasing gene number involved in the pathway.

**Table 14.** Distribution of KEGG pathways for DEGs in G34-S3 vs G34-CK data sample set.

| <b>Enriched Pathway terms</b>                       | <b>G34-S3 vs G34-CK</b> |
|-----------------------------------------------------|-------------------------|
| Carbon metabolism                                   | 25                      |
| Starch and sucrose metabolism                       | 20                      |
| Biosynthesis of amino acids                         | 15                      |
| Citrate cycle (TCA cycle)                           | 14                      |
| Carbon fixation in photosynthetic organisms         | 13                      |
| Protein processing in endoplasmic reticulum         | 13                      |
| Glycolysis / Gluconeogenesis                        | 12                      |
| Cysteine and methionine metabolism                  | 11                      |
| Glycerophospholipid metabolism                      | 9                       |
| Oxidative phosphorylation                           | 9                       |
| Pyruvate metabolism                                 | 9                       |
| Ribosome                                            | 8                       |
| Plant-pathogen interaction                          | 8                       |
| Peroxisome                                          | 8                       |
| Amino sugar and nucleotide sugar metabolism         | 8                       |
| Glyoxylate and dicarboxylate metabolism             | 8                       |
| Plant hormone signal transduction                   | 7                       |
| Glutathione metabolism                              | 7                       |
| Arginine and proline metabolism                     | 7                       |
| Ubiquinone and other terpenoid-quinone biosynthesis | 7                       |
| RNA degradation                                     | 7                       |
| Phagosome                                           | 7                       |
| Cyanoamino acid metabolism                          | 6                       |
| Lysosome                                            | 6                       |
| Phenylpropanoid biosynthesis                        | 5                       |
| Aminoacyl-tRNA biosynthesis                         | 5                       |
| 2-Oxocarboxylic acid metabolism                     | 5                       |
| Carotenoid biosynthesis                             | 4                       |
| alpha-Linolenic acid metabolism                     | 4                       |
| Phenylalanine metabolism                            | 4                       |
| Purine metabolism                                   | 3                       |
| Tyrosine metabolism                                 | 3                       |
| Drug metabolism - cytochrome P450                   | 3                       |
| Photosynthesis                                      | 3                       |
| Phenylalanine, tyrosine and tryptophan biosynthesis | 3                       |
| Glycine, serine and threonine metabolism            | 3                       |
| Porphyrin and chlorophyll metabolism                | 3                       |
| Fructose and mannose metabolism                     | 2                       |
| RNA transport                                       | 2                       |
| Alanine, aspartate and glutamate metabolism         | 2                       |

Overall, the results show that the maximum number of DEGs were observed in the “carbon metabolism” pathway, followed by the “starch and sucrose metabolism” and “biosynthesis of amino acids” indicating that a deep reprogramming of these metabolisms under severe salt treatment occurred as also suggested by the involvement of other related pathways such as “citrate cycle”, “carbon fixation”, “glycolysis / gluconeogenesis” and “pyruvate metabolism”. “Plant hormone signal

transduction”, which comprises the transcripts of several hormone-responsive proteins involved in regulation and signal transduction and two other important pathways, including ‘phenylalanine metabolism’ and ‘plant-pathogen interaction’ were also found to be regulated by salt in our study (Table 14). Other examples of relevant pathways, which are known to be involved in responses to abiotic stresses in giant reed (Fu et al. 2016), are “protein processing in endoplasmic reticulum”, “arginine and proline metabolism” and “oxidative phosphorylation” (Table 14).

### 5.2.5 Identification of functional genes related to salt stress tolerance

To unravel the *A. donax* G34 salt stress response, we analyzed the RNA-Seq datasets from the G34-S3 vs G34-CK comparison, focusing on genes known to be related to soil salinity, from salt sensory and signal to the main downstream metabolisms that might be affected by salt (Gupta and Huang 2014). Those clusters showing a threshold of +/- 10.000 log<sub>2</sub>fold change have been considered as DEGs (up- or down-regulated) in the *A. donax* transcriptome (Table 15). Table 15 also shows that the majority of the *A. donax* sequences aligned with high level of homology with those from related species *S. italica*, confirming a high level of global sequence similarity within the *Poaceae* family as indicated by Evangelistella and coworkers (2017).

### 5.2.6 Salt sensory and signaling mechanisms

The analysis of different expressed genes between G34-S3 and G34-CK revealed that homologous to *Oryza sativa* (CBL-interacting protein kinases 1) CIPK1-SOS2-like is up-regulated in the salt treated samples, whereas genes homologous to the *Phragmites australis* NHX1 and *Arabidopsis* NHX2 (Na<sup>+</sup>/H<sup>+</sup> antiporters) are down regulated in response to severe S3 salt stress (Table 15). CIPK1-SOS2-like protein is a serine/threonine protein kinase involved in the activation of plasma membrane Na<sup>+</sup>/H<sup>+</sup> antiporter (SOS1) which mediates the exclusion of Na<sup>+</sup> excess out of the cells. Consequently, the data suggest that the plant response to severe salt stress is likely to increase the activation upon the existing Na<sup>+</sup>/H<sup>+</sup> antiporter (SOS1) by the CIPK1-SOS2 like phosphorylating activity. The down regulation of NHXs indicates that the vacuolar sequestration of Na<sup>+</sup> excess seems to be impaired in the G34 *A. donax* ecotype subjected to severe salt stress condition. A cluster coding for cation transporter to adjust the K<sup>+</sup> homeostasis (Zhu, 2002; Barragan et al. 2012) such as HKT6 was found downregulated (Zhu, 2002; Barragan et al. 2012), probably suggesting that the plasma membrane Na<sup>+</sup>/K<sup>+</sup> exchange as well is defective (Table 15).

### 5.2.7 Hormone regulation of salt stress response

We focused our attention on the main plant hormones involved in salt stress response, such as abscisic acid, brassinosteroid, ethylene, auxin/IAA and jasmonic acid (JA) (Golldack et al. 2014; Gupta and Huang 2014). Regarding the hormone regulation in G34 ecotype (G34-S3 vs G34-CK) we found that genes involved in ethylene biosynthesis and regulation such as transcripts encoding ACC oxidase, namely the ethylene-forming enzyme (homolog of *Saccharum arundinaceum* 1-aminocyclopropane-1-carboxylate oxidase), and homolog of CTR1 (*Arabidopsis thaliana* serine/threonine-protein kinase), implicated in quenching the ethylene signal, are both up-regulated under salt stress (Table 15). Despite the importance of abscisic acid (ABA) in salt stress response, no genes involved in ABA biosynthesis, degradation or perception have been found differentially regulated. In addition, the components of auxin and jasmonic acid signal transduction and regulation do not result differentially regulated in salt stress conditions. As regards brassinosteroid, homolog of *Setaria italica* cytochrome P450 710A1-like (LOC101770311), involved in steroids biosynthesis process (Bajguz et al. 2009), is up-regulated indicating that brassinosteroid signaling increased in response to S3 severe salt treatment (Table 15).

### 5.2.8 ROS scavenging regulatory mechanisms

The analysis of G34-S3 vs G34-CK revealed that, among the antioxidant enzymes, GST 23-like is up-regulated concordantly with GST role in salt stress relief (Puglisi et al. 2013; Lo Cicero et al. 2015). G34 ecotype also shows the downregulation of superoxide dismutase [Fe]<sup>2+</sup> thus suggesting that the “neutralization” of superoxide ions in the chloroplast is impaired (Table 15). However, homologs of *Setaria italica* chloroplastic NADP<sup>+</sup>-dependent malic enzyme that catalyzes the oxidative decarboxylation of L-malate to yield pyruvate, CO<sub>2</sub> and NADPH, and chloroplastic *Setaria italica* malate dehydrogenase (MDH) were up-regulated under salt stress conditions (Table 15) suggesting that components of the “malate valve” are induced in response to severe salt stress (Zhang et al. 2012).

### 5.2.9 Osmolyte biosynthesis

The accumulation of compatible osmolytes, such as proline, polyamines and sugar alcohols plays a key role in maintaining the low intracellular osmotic potential of plants and in preventing the harmful effects of salinity stress (Hoque et al. 2008; Deinlein et al. 2014; Gupta and Huang. 2014;). In our study, 1-delta-pyrroline-5-carboxylate synthase (P5CS), the key enzyme of proline biosynthesis, was found up regulated in salt stressed samples (Table 15) suggesting that proline accumulation might represent a pivotal mechanism to overcome the hypersaline conditions and to adjust the osmotic status in *A. donax*. Due to their cationic nature, polyamines can interact with

proteins, nucleic acids, membrane phospholipids and cell wall constituents, either activating or stabilizing these molecules (Yang et al. 2007; Zapata et al. 2008). Considering the G34-S3 vs G34-CK data set, a cluster encoding *Setaria italica* polyamine oxidase 2 (polyamine degradative enzyme) is up-regulated suggesting that polyamines degradation is induced during long term salt stress in *A. donax*, they having probably not a primary role in the salt tolerance mechanism in G34 ecotype (Table 15).

**Table 15.** List of DEGs related to salt stress response identified in G34-S3 vs G34-CK comparison

| <i>Cluster ID</i>                                 | <i>Database description</i>                                                                                                  | <i>Percent identity</i> | <i>Evalue</i> | <i>log<sub>2</sub> fold change</i> |
|---------------------------------------------------|------------------------------------------------------------------------------------------------------------------------------|-------------------------|---------------|------------------------------------|
| <i>Salt sensory and signaling mechanisms</i>      |                                                                                                                              |                         |               |                                    |
| 14027.182899                                      | <i>Oryza sativa</i> subsp. <i>japonica</i> Group CBL-interacting protein kinase 1 (CIPK1-SOS2 like), (Nt ID: XM_015766590.1) | 93.33%                  | 4e-23         | + Inf*                             |
| 14027.155903                                      | <i>Phragmites australis</i> pcnhx1 mRNA for putative Na <sup>+</sup> /H <sup>+</sup> antiporter (NHX1), (Nt ID: AB211145.1)  | 93.40%                  | 3e-54         | - 12.753                           |
| 14027.181583                                      | <i>Arabidopsis thaliana</i> Sodium/hydrogen exchanger 2 (NHX2), (Swissprot ID: Q56XP4)                                       | 77.78%                  | 8e-79         | - 11.093                           |
| 14027.230649                                      | <i>Oryza sativa</i> probable cation transporter HKT6 (Nr ID: XP_015626193.1)                                                 | 71.87%                  | 1e-154        | - 15,51                            |
| <i>Hormone regulation of salt stress response</i> |                                                                                                                              |                         |               |                                    |
| 14027.99729                                       | <i>Saccharum arundinaceum</i> 1-aminocyclopropane-1-carboxylate oxidase (ACC oxidase) (Nr ID: ABM74187.1)                    | 91.46%                  | 1e-122        | + 18.071                           |
| 14027.223665                                      | <i>Arabidopsis thaliana</i> serine/threonine-protein kinase CTR1, (Swissprot ID: Q05609)                                     | 89.36%                  | 1e-02         | + Inf*                             |
| 14027.220930                                      | <i>Setaria italica</i> cytochrome P450 710A1-like (Nt ID: XM_004968550.2)                                                    | 87.92%                  | 3e-147        | + 42.918                           |
| <i>ROS scavenging regulatory mechanisms</i>       |                                                                                                                              |                         |               |                                    |
| 14027.54848                                       | <i>Setaria italica</i> glutathione transferase GST 23-like, (Nr ID: XP_004966104.1)                                          | 79.46%                  | 2e-57         | + 16.425                           |
| 14027.156319                                      | <i>Setaria italica</i> superoxide dismutase [Fe] 2, chloroplastic-like, (Nt ID: XM_004964461.2)                              | 93.24%                  | 3e-86         | - 10.398                           |
| 14027.223022                                      | <i>Setaria italica</i> malate dehydrogenase, chloroplastic (MDH), (Nt ID: XM_012847145.2)                                    | 97.50%                  | 3e-170        | + 11.012                           |
| 14027.169726                                      | <i>Setaria italica</i> NADP-dependent malic enzyme, chloroplastic (Nr ID: XP_004960887.1)                                    | 81.69%                  | 3e-154        | + 15,508                           |
| <i>Osmolyte biosynthesis</i>                      |                                                                                                                              |                         |               |                                    |
| 14027.146844                                      | <i>Setaria italica</i> delta-1-pyrroline-5-carboxylate synthase (P5CS) (Nt ID: XM_004961829.3)                               | 91.92%                  | 6e-168        | + 28.543                           |
| 14027.160267                                      | <i>Setaria italica</i> polyamine oxidase 2 (Nt ID: XM_004960065.2)                                                           | 95.00%                  | 5e-137        | + 20.021                           |
| <i>Photosynthesis and photorespiration</i>        |                                                                                                                              |                         |               |                                    |
| 14027.153819                                      | <i>Pisum sativum</i> RuBisCO large subunit-binding protein subunit alpha, chloroplastic (Swissprot ID: P08926)               | 74.89%                  | 4e-110        | - 39.871                           |
| 14027.193818                                      | <i>Setaria italica</i> peroxisomal (S)-2-hydroxy-acid oxidase (Nt ID: XM_004958250.2)                                        | 92.51%                  | 5e-156        | + 14.194                           |
| 14027.158029                                      | <i>Setaria italica</i> phosphoenolpyruvate carboxylase kinase (PEPC kinase) (Nr ID: XP_004976235.1)                          | 84.05%                  | 2e-127        | - 32.125                           |
| 14027.157747                                      | <i>Oryza sativa</i> subsp. <i>japonica</i> Group Ribulose biphosphate carboxylase small chain A (Swissprot ID: Q0IN7)        | 94.59%                  | 3e-20         | - 10.522                           |

### 5.2.10 Photosynthesis and photorespiration

The analysis of G34-S3 vs G34-CK DEGs reveals that homologs of large subunits of ribulose-1,5-bisphosphate carboxylase/oxygenase (Rubisco) is not represented neither in the up-regulated or in the down regulated clusters, whereas homolog of *Oryza sativa* subsp. *japonica* Group Ribulose bisphosphate carboxylase small chain A is down regulated (Table 15). Furthermore, homologs of *Pisum sativum* Rubisco large subunit-binding protein subunit alpha, required for the correct assembly of Rubisco, have been discovered among the down-regulated genes, indicating that the processes of Rubisco synthesis and assembly could be strongly affected under S3 salt stress (Table 15). Moreover, clusters encoding glycolate oxidase (*Setaria italica* peroxisomal (S)-2-hydroxy-acid oxidase, LOC101764130), which is a key enzyme of the glycolate recovery pathway induced by photorespiration, is up-regulated in G34-S3 vs G34-CK comparison suggesting that CO<sub>2</sub> assimilation via the C3 Calvin cycle might be impaired in favor of oxygen fixation through the photorespiration pathway (Table 15). This result is consistent with the decrease of net photosynthesis showed in Figure 12. However, homolog of *Setaria italica* phosphoenolpyruvate carboxylase kinase (LOC101779241), that is a phosphoenolpyruvate carboxylase (PEPC) inactivating enzyme, was found down-regulated. PEPC forms oxaloacetate, a four-carbon dicarboxylic acid through the carboxylation of phosphoenolpyruvate (PEP) and is involved in carbon fixation process. Thus, giant reed G34 ecotype responds to severe salt stress by tending to maximize the catalytic efficiency of PEPC (Table 15).

### 5.2.11 Transcription factors

In our study, DEGs encoding TFs were identified and divided in 14 subfamilies, as showed in Figure 15, which reports the number of DEGs belonging to each subfamily. The results showed that under severe stress condition, an average of 9 TFs for each family are differently regulated. In particular, 21 DEGs belong to bHLH, 19 to WRKY and 16 to AUX/IAA families, respectively, indicating that they probably play a key role in regulating the changes of transcriptional regulation in response to salt (Figure 15).

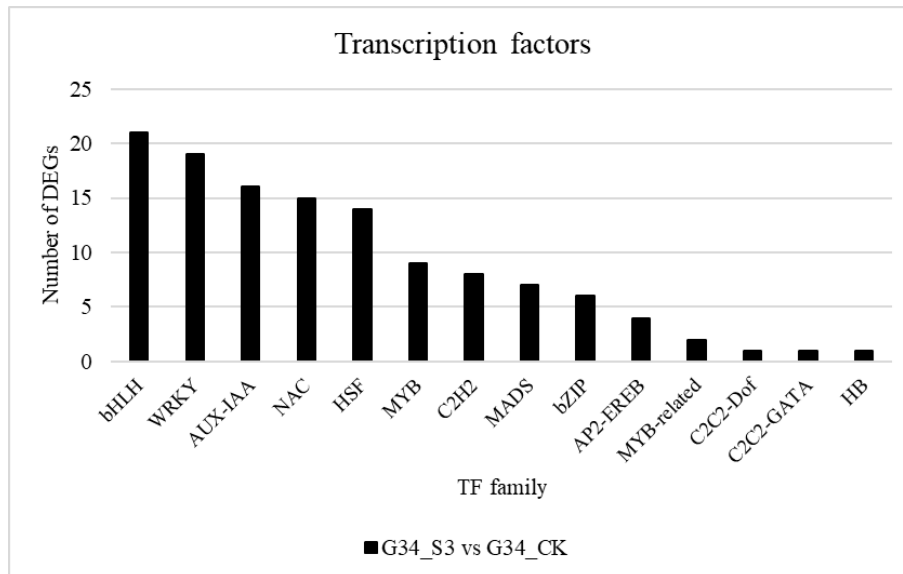


**Figure 15.** Distribution of transcription factors responsive to salt stress. Data are sorted by number of G34-S3 vs G34-CK DEGs

A comparative analysis performed using the available database of rice transcription factors under salt stress led to the identification of 27 *A. donax* unigenes, corresponding to high confidence rice TF homologs previously identified as salt or salt/drought genes (Table 16) (Priya and Jain 2013). Probably because of the altered water potential under salt stress, the majority of these genes (26) are also responsive to drought. Only one gene is specifically responding to salt (Table 16), it belongs to the WRKY family and is strongly down-regulated.

### 5.2.12 Comparison between G34 and G2 giant reed ecotypes

We also compared the aforementioned results with those obtained by the specular analysis performed upon the G2 ecotype (Sicilia et al. 2019). The results highlighted that there are three clusters, differentially expressed in the G34-S3 vs G34-CK, which are also included in the G2 ecotype DEG list (Table 17). In particular, clusters encoding the *Arabidopsis thaliana* serine/threonine protein kinase CTR1, the *Oryza sativa* ribulose biphosphate carboxylase small chain A, and the *Setaria italica* phosphoenolpyruvate carboxylase kinase (PEPC kinase) are differently regulated in both ecotypes. However, these clusters become differentially expressed in the G2 ecotype at higher salt dose (extreme salt stress, S4, 419.23 mM NaCl corresponding to 50 dS m<sup>-1</sup> electric conductivity) thus indicating that G34 ecotype senses the surrounding salt and modifies the related gene expression at lower concentration (severe salt stress, S3, 256.67 mM NaCl corresponding to 32 dS m<sup>-1</sup> electric conductivity).



**le 16.** Transcription factors responsive to salt, to drought or both stresses in *A. donax*

| <i>A. donax</i> unigene_ID | Rice_ID        | E-value   | Hit Score | Family      | Regulation | Differentially expressed gene |
|----------------------------|----------------|-----------|-----------|-------------|------------|-------------------------------|
| 14027.97807                | LOC_Os01g09080 | 6.00E-27  | 62        | WRKY        | Down       | Salinity;Drought              |
| 14027.10532                | LOC_Os01g14440 | 8.00E-11  | 35        | WRKY        | Up         | Salinity;Drought              |
| 14027.15302                | LOC_Os01g34060 | 5.00E-31  | 69        | MYB-related | Down       | Salinity;Drought              |
| 14027.12954                | LOC_Os01g42260 | 2.00E-21  | 53        | LUG         | Up         | Salinity;Drought              |
| 14027.14492                | LOC_Os01g61080 | 1.00E-134 | 243       | WRKY        | Up         | Salinity;Drought              |
| 14027.7232                 | LOC_Os01g68700 | 1.00E-110 | 202       | bHLH        | Up         | Salinity;Drought              |
| 14027.14591                | LOC_Os01g74410 | 5.00E-23  | 55        | MYB         | Down       | Salinity;Drought              |
| 14027.15916                | LOC_Os02g02424 | 9.00E-54  | 107       | C2H2        | Up         | Salinity;Drought              |
| 14027.15229                | LOC_Os02g08440 | 1.00E-48  | 98        | WRKY        | Up         | Salinity;Drought              |
| 14027.25148                | LOC_Os02g35770 | 9.00E-18  | 47        | HB          | Down       | Salinity;Drought              |
| 14027.78029                | LOC_Os02g39140 | 3.00E-39  | 83        | bHLH        | Up         | Salinity;Drought              |
| 14027.15954                | LOC_Os03g21060 | 5.00E-64  | 124       | NAC         | Down       | Salinity;Drought              |
| 14027.14325                | LOC_Os03g26210 | 2.00E-26  | 61        | bHLH        | Down       | Salinity;Drought              |
| 14027.16813                | LOC_Os04g36054 | 5.00E-45  | 93        | ARF         | Up         | Salinity;Drought              |
| 14027.33142                | LOC_Os04g52810 | 7.00E-18  | 47        | NAC         | Up         | Salinity;Drought              |
| 14027.20029                | LOC_Os05g41760 | 8.00E-67  | 129       | AP2-EREBP   | Up         | Salinity;Drought              |
| 14027.1767                 | LOC_Os05g46020 | 1.00E-96  | 179       | WRKY        | Up         | Salinity;Drought              |
| 14027.7979                 | LOC_Os06g10350 | 8.00E-09  | 31        | MYB         | Up         | Salinity;Drought              |
| 14027.17627                | LOC_Os06g44010 | 5.00E-64  | 124       | WRKY        | Up         | Salinity;Drought              |
| 14027.25148                | LOC_Os06g45140 | 2.00E-19  | 50        | bZIP        | Down       | Salinity;Drought              |
| 14027.3911                 | LOC_Os06g46270 | 2.00E-61  | 120       | NAC         | Up         | Salinity;Drought              |
| 14027.14269                | LOC_Os07g41370 | 8.00E-16  | 43        | MADS        | Down       | Salinity;Drought              |
| 14027.12249                | LOC_Os07g48596 | 9.00E-39  | 82        | G2-like     | Up         | Salinity;Drought              |
| 14027.17591                | LOC_Os08g03520 | 1.00E-84  | 159       | CSD         | Up         | Salinity;Drought              |
| 14027.98589                | LOC_Os08g43090 | 2.00E-30  | 68        | bZIP        | Up         | Salinity;Drought              |
| 14027.26535                | LOC_Os09g28210 | 1.00E-139 | 250       | bHLH        | Up         | Salinity;Drought              |
| 14027.23859                | LOC_Os12g40570 | 2.00E-47  | 97        | WRKY        | Down       | Salinity                      |

### 5.2.13 Retrieval and analysis of genes targeted as “salt stress responsive”

The GO terms were further analyzed in order to retrieve clusters specifically involved in the salt stress response, thus excluding all transcripts also regulated by different abiotic stress, such as water deprivation, cold, heavy metals and oxidative stresses (geneontology.org/). All the retrieved clusters are also found to be involved in salt-induced osmotic stress according to the finding that levels of NaCl higher than 100–150 mM cause osmotic stress (Shavrukov, 2012). The results shown in Table 18 reveal that only 2 clusters, besides the one encoding the aforementioned WRKY, are specifically regulated by salt. The CBL-interacting protein kinase 1 (CIPK1-SOS2 like) has been found up-regulated (Table 18) thus suggesting that it activates specific signal transduction pathways under severe salt stress conditions. Instead, clusters related to cation transporter HKT6 is down regulated by severe salt stress treatment (Table 18), both results being already highlighted in Table 15.

**Table 17.** Comparison of DEGs related to salt stress response in G34-S3 vs G34-CK, G2-S3 vs G2-CK and G2-S4 vs S2-CK sample sets.

| Cluster ID                                        | Database description                                                                                                     | Percent identity | Evalue | log <sub>2</sub> fold change<br>G34_S3<br>vs<br>G34 CK | log <sub>2</sub> fold change<br>G2_S3<br>vs<br>G2 CK | log <sub>2</sub> fold change<br>G2_S4<br>vs<br>G2 CK |
|---------------------------------------------------|--------------------------------------------------------------------------------------------------------------------------|------------------|--------|--------------------------------------------------------|------------------------------------------------------|------------------------------------------------------|
| <i>Hormone regulation of salt stress response</i> |                                                                                                                          |                  |        |                                                        |                                                      |                                                      |
| 14027.223665                                      | <i>Arabidopsis thaliana</i> serine/threonine-protein kinase CTR1, (Swissprot ID: Q05609)                                 | 65.84%           | 2e-171 | +Inf*                                                  | --**                                                 | + 11.918                                             |
| <i>Photosynthesis and photorespiration</i>        |                                                                                                                          |                  |        |                                                        |                                                      |                                                      |
| 14027.157747                                      | <i>Oryza sativa</i> , subsp. <i>Japonica</i> Group Ribulose biphosphate carboxylase small chain A (Swissprot ID: P18566) | 97.30%           | 6e-18  | -10.522                                                | --**                                                 | - 17.834                                             |
| 14027.158029                                      | <i>Setaria italica</i> phosphoenolpyruvate carboxylase kinase (PEPC kinase) (Nr ID: XP_004976235.1)                      | 77.15%           | 7e-123 | - 32.125                                               | --**                                                 | - 40.627                                             |

### 5.2.14 Identification of functional genes related to “carbon metabolism” and “starch and sucrose metabolism”

Since “carbon metabolism” and “starch and sucrose metabolism” are the most represented KEGG pathways, among the DEGs related to these pathways we searched for genes encoding enzymes involved in glycolysis and Krebs cycle (Table 19).

**Table 18.** Salt stress related genes (GO:0009651 Response to salt stress)

| Gene ID     | log <sub>2</sub> FoldChange | padj     | Swissprot Description                                                                      |
|-------------|-----------------------------|----------|--------------------------------------------------------------------------------------------|
| 14027.1829  | Inf                         | 6.07E-07 | <i>CBL-interacting protein kinase 1 OS=Oryza sativa subsp. japonica GN=CIPK1 PE=2 SV=1</i> |
| 14027.23065 | -15.51                      | 0.000488 | <i>Probable cation transporter HKT6 OS=Oryza sativa subsp. japonica GN=HKT6 PE=2 SV=2</i>  |

In this further analysis, as detailed above, those clusters showing a threshold of +/- 10.000 log<sub>2</sub>fold change have been considered as DEGs (up- or down-regulated) in the *A. donax* transcriptome. For each cluster, the alignment of *A. donax* sequence has been performed and the score of these alignments was reported (% identity and *e* value). Table 19 shows that homolog of *Setaria italica* hexokinase-7 (HXK7), *Setaria italica* ATP-dependent 6-phosphofructokinase 2 (PFK2), *Setaria italica* 2,3-bisphosphoglycerate-independent phosphoglycerate mutase, *Setaria italica* glyceraldehyde-3-phosphate dehydrogenase 3 (GAPCP3) are strongly up-regulated under severe salt stress conditions. These clusters are all components of the glycolysis pathway where HK generates the hexose phosphate pool of the plant cell, PFK catalyzes the conversion of fructose 6-phosphate (F6P) into fructose-1,6-bisphosphate (F1,6BP), and the last two clusters encode the enzymes involved in the steps of oxidation of glyceraldehyde 3-phosphate and the conversion of 3-phosphoglycerate into 2-phosphoglycerate and leading to phosphoenolpyruvate (PEP) (Table 19). Surprisingly, clusters related to *Ricinus communis* chloroplastic pyruvate kinase isozyme A, catalyzing the irreversible synthesis of pyruvate and ATP, are strongly down regulated in salt stress condition thus indicating that probably an accumulation of PEP might occur to the detriment of pyruvate formation (Table 19). Moreover, homologs of *Arabidopsis thaliana* dihydrolipoyllysine-residue acetyltransferase component of pyruvate dehydrogenase complex are up regulated under salt stress condition suggesting that acetyl CoA is actively produced in order to feed the downstream Krebs cycle. This hypothesis is supported by the fact that clusters encoding *Oryza brachyantha* pyruvate dehydrogenase (acetyl-transferring) kinase, known to negatively regulate the pyruvate dehydrogenase activity by phosphorylation (Zou et al. 1999), was found sharply downregulated (Table 19). Transcripts encoding most of the enzymes involved in the Krebs cycle (citrate synthase, isocitrate dehydrogenase, succinate dehydrogenase and fumarase) are up regulated in salt treated samples, unequivocally indicating that this pathway and its intermediate products assume a crucial role during the response of G34 *A. donax* ecotype to severe salt stress (Table 19). Phosphoenolpyruvate carboxykinase (PEPCK) homologs (*Setaria italica*) catalyzing the reversible conversion of oxaloacetate to phosphoenolpyruvate and CO<sub>2</sub> was also strongly induced by salt stress probably leading to an increase of CO<sub>2</sub> e PEP in the cytosol, where PEPCK appears to be exclusively located (Ku et al. 1980; Chapman et al. 1983; Watanabe et al. 1984;). As regards the “starch and sucrose metabolism” pathway, genes involved in the starch biosynthesis such as *Setaria italica* 1,4-alpha-glucan-branching enzyme 2 and *Setaria italica* glucose-1-phosphate adenylyltransferase large subunit have been found up-regulated in G34-S3 vs G34-CK sample set and, the finding that clusters related to starch catabolism such as *Setaria italica* alpha-1,4 glucan phosphorylase are also up regulated is probably related to their reported role in abiotic stress tolerance (Table 19) (Zeeman et al. 2004).

**Table 19.** Comparison of DEGs related to KEGG pathways identified in G34-S3 vs G34-CK, G2-S3 vs G2-CK and G2-S4 vs G2-CK sample sets

| <i>Cluster ID</i>                    | <i>Database description</i>                                                                                                                                   | <i>Percent identity</i> | <i>Evalue</i> | <i>log<sub>2</sub> fold change G34_S3 vs G34_CK</i> | <i>log<sub>2</sub> fold change G2_S3 vs G2_CK</i> | <i>log<sub>2</sub> fold change G2_S4 vs G2_CK</i> |
|--------------------------------------|---------------------------------------------------------------------------------------------------------------------------------------------------------------|-------------------------|---------------|-----------------------------------------------------|---------------------------------------------------|---------------------------------------------------|
| <i>Carbon metabolism</i>             |                                                                                                                                                               |                         |               |                                                     |                                                   |                                                   |
| 14027.261590                         | <i>Setaria italica</i> hexokinase-7 (HXK7), (Nt ID: XM_004960833.3)                                                                                           | 92.50%                  | 2e-162        | +24.834                                             | +17.252                                           | + 34.025                                          |
| 14027.261776                         | <i>Setaria italica</i> ATP-dependent 6-phosphofructokinase 2 (PFK2), (Nr ID: XP_004975916.1)                                                                  | 79.82%                  | 2e-54         | +44.432                                             | --*                                               | + 24.309                                          |
| 14027.70763                          | <i>Setaria italica</i> glyceraldehyde-3-phosphate dehydrogenase 3 (GAPCP3), (Nr ID: XP_010930058.1)                                                           | 75,83%                  | 2e-73         | +28.263                                             | +28.878                                           | + 49.616                                          |
| 14027.30626                          | <i>Setaria italica</i> 2,3-bisphosphoglycerate-independent phosphoglycerate mutase (PFAM ID: PF10143)                                                         | 67.57%                  | 2e-10         | +Inf**                                              | --                                                | + Inf**                                           |
| 14027.52780                          | <i>Ricinus communis</i> pyruvate kinase isozyme A, chloroplastic (Swissprot ID: Q43117)                                                                       | 66.85%                  | 4e-179        | -Inf***                                             | --                                                | - 16.659                                          |
| 14027.212884                         | <i>Oryza brachyantha</i> pyruvate dehydrogenase (acetyl-transferring) kinase (Nr ID: XP_006658015.1)                                                          | 94.07%                  | 4e-88         | -18.890                                             | --                                                | --                                                |
| 14027.146727                         | <i>Arabidopsis thaliana</i> dihydrolipoyllysine-residue acetyltransferase component 2 of pyruvate dehydrogenase complex, mitochondrial (Swissprot ID: Q8RWN9) | 70.49%                  | 3e-180        | +12,376                                             | --                                                | + 14.354                                          |
| 14027.202505                         | <i>Setaria italica</i> citrate synthase 4 (CSY4), (Nt ID: XM_004951531.1)                                                                                     | 95.00%                  | 9e-149        | +11.237                                             | --                                                | + 11.496                                          |
| 14027.155073                         | <i>Setaria italica</i> isocitrate dehydrogenase, mitochondrial (Nt ID: XM_004967640.3)                                                                        | 97.49%                  | 2e-175        | +19,652                                             | --                                                | --                                                |
| 14027.190285                         | <i>Zea mays</i> succinate dehydrogenase flavoprotein subunit, mitochondrial (SDH) (Nt ID: EU970939.1)                                                         | 97.89%                  | 2e-173        | +12.117                                             | --                                                | + 26.218                                          |
| 14027.187091                         | <i>Setaria italica</i> fumarate hydratase 1, mitochondrial (Nt ID: XM_004984384.2)                                                                            | 97.50%                  | 2e-145        | +17.773                                             | --                                                | + 18.953                                          |
| 14027.150469                         | <i>Setaria italica</i> phosphoenolpyruvate carboxykinase (PEPCK), (Nr ID: XP_004984967.1)                                                                     | 100.00%                 | 3e-93         | +26.480                                             | +36.401                                           | + 36.731                                          |
| <i>Starch and sucrose metabolism</i> |                                                                                                                                                               |                         |               |                                                     |                                                   |                                                   |
| 14027.194053                         | <i>Setaria italica</i> 1,4-alpha-glucan-branching enzyme 2 (Nt ID: XM_004952572.1)                                                                            | 60.11%                  | 1e-60         | +17.373                                             | --                                                | + 33.943                                          |
| 14027.222866                         | <i>Setaria italica</i> glucose-1-phosphate adenylyltransferase large subunit, (Nr ID: XP_006654841.1)                                                         | 62.22%                  | 6e-145        | +23.167                                             | --                                                | + 38.907                                          |
| 14027.204584                         | <i>Setaria italica</i> alpha-1,4 glucan phosphorylase (Nr ID: XP_004981704.1)                                                                                 | 93.51%                  | 4e-98         | +10.353                                             | --                                                | + 20.785                                          |

Considering the availability of unreported data, a similar analysis was also performed in the giant reed G2 ecotype and the results are in Table 19. It is interesting that the majority of the clusters that are differentially expressed in the G34 ecotype under severe salt stress (S3), are not differently regulated (neither up- nor downregulated) in the G2 ecotype grown under the same salt dose (G2-S3 vs G2-CK). Clusters encoding for the hexokinase, glyceraldehyde-3-phosphate dehydrogenase and phosphoenolpyruvate carboxykinase (PEPCK) represent the exceptions and in these cases a similar regulation (up- or down regulation) is observable (Table 19). However, most of the clusters differently regulated under severe salt stress (S3) in the G34 ecotype are also listed among the G2-S4 vs G2-CK data set, clearly indicating that G34 ecotype response to severe salt stress (S3) resembles to the G2 ecotype response subjected to higher salt dose (extreme salt stress, S4, 419.23 mM NaCl corresponding to 50 dS m<sup>-1</sup> electric conductivity, EC).

### 5.2.15 Identification and distribution of SSR

The 193,070 unigenes, were screened for repeated motifs to explore the SSR profile in the *A. donax* leaf transcriptome. The motif distribution was screened both in untranslated regions (both 5'-UTR and 3'-UTR) and in coding regions (CDS), since many of the sequenced mRNA transcripts contained untranslated regions (UTRs) and occasional remaining introns. A total of 26,838 SSRs were obtained from 24,304 unigenes, consequently 2,534 sequences contained more than one SSR marker. In addition, 881 sequences revealed composed SSR formation (Table 20). We further investigated the distribution of SSR classes in the unigenes (CDS, 5' UTR, and 3' UTR). Out of the total SSRs, 9,463 (35.26%) were located in the UTR and CDS regions, of which 5,062 (53.49%), 1,690 (17.85%), and 2,711 (28.65%) SSRs were located in the 5' UTR, CDS, and 3' UTR, respectively. The remaining SSRs (17,375 SSRs; 64.74%) have not an ascertained position because it was not possible to identify the UTR and CDS regions of the transcripts containing them. In Table 21 is reported the frequency in percentage of each motif. Most of repeated motifs (10,188 SSRs) are mono-base repetitions (37.95 %), followed by tri-base (9,441 SSRs; 35.17 %) and di-base motifs (5,970 SSRs; 22.24 %). As regard the SSRs located in CDS region, most of them (1,423 SSRs) are tri-base repetition (84.20 %), followed by mono-base repetitions (120 SSRs; 7.10 %). In 5'-UTR region most of the SSRs are tri-base repetitions (2,465 SSRs; 48.69 %) followed by mono-base repetitions (1,151 SSRs; 22.73 %), while in 3'-UTR regions 1,476 SSRs (54.44 %) are mono-base repetitions and 623 SSR (22.98 %) are di-base repetitions. The most abundant nucleotide patterns found in the analysis are the following: A/T (6,096 SSRs; 22.71 %) and C/G (4,092 SSRs; 15.24 %) for mono-nucleotides, AG/CT (1,820 SSRs; 6.78 %) for di-nucleotides and CCG/CGG (1,405 SSRs; 5.23 %) for tri-nucleotides (Table 21).

**Table 20.** Summary statistics of SSRs analysis

|                                                  |         |
|--------------------------------------------------|---------|
| Total number of sequences examined               | 193,070 |
| Total number of identified SSRs                  | 26,838  |
| Number of SSR containing sequences               | 24,304  |
| Number of sequences containing more than one SSR | 2,534   |
| Number of SSRs present in compound formation     | 881     |

**Table 21.** SSR nucleotide patterns

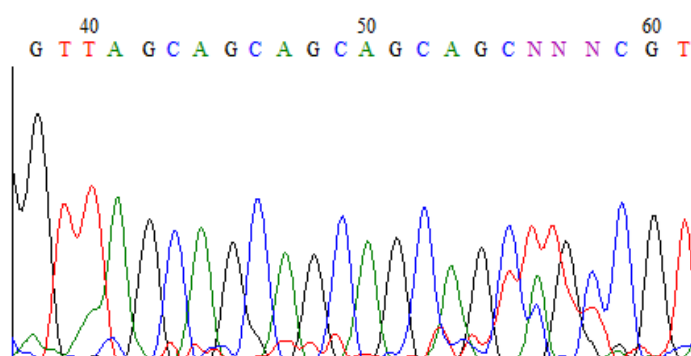
| Nucleotide motif | Number of SSRs | Frequency (%) |
|------------------|----------------|---------------|
| A/T              | 6,096          | 22.71         |
| C/G              | 4,092          | 15.24         |
| AC/GT            | 544            | 2.02          |
| AG/CT            | 1,820          | 6.78          |
| AT/AT            | 434            | 1.61          |
| CG/CG            | 186            | 0.69          |
| AAC/GTT          | 90             | 0.33          |
| AAG/CTT          | 237            | 0.88          |
| AAT/ATT          | 58             | 0.21          |
| ACC/GGT          | 96             | 0.35          |
| ACG/CGT          | 82             | 0.30          |
| ACT/AGT          | 13             | 0.05          |
| AGC/CTG          | 385            | 1.43          |
| AGG/CCT          | 383            | 1.42          |
| ATC/ATG          | 68             | 0.25          |
| CCG/CGG          | 1,405          | 5.23          |
| AAAT/ATTT        | 6              | 0,02          |
| AAGG/CCTT        | 3              | 0,01          |
| ATCC/ATGG        | 9              | 0,03          |

### 5.2.16 Validation of SSRs

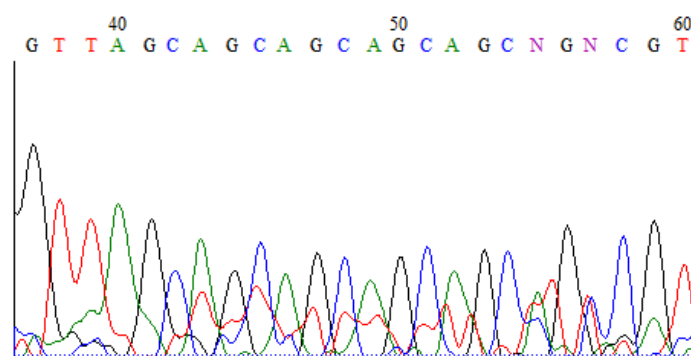
As described in Methods section, SSR validation was conducted by amplifying and sequencing five microsatellite regions randomly chosen in 5'-UTR, CDS and 3'-UTR sequences (Table 22). The repeated motifs are embedded in sequences belonging to genes homologous to: *Setaria italica* serine/arginine repetitive matrix protein 2 (SRRM2), *Setaria italica* high mobility group nucleosome-binding domain-containing protein 5 (HMGN5), *Setaria italica* protein SHORT-ROOT 1 (SHR1), *Setaria italica* myb-related protein MYBAS1-like (myba), *Setaria italica* squamosa promoter-binding-like protein 2 (SPL1). For all the microsatellites analyzed, both the repeated motifs and the number of repetitions were confirmed by sequence analysis. In fact, five repetitions of AGC motif were detected in SRRM2 and HMGN5, six repetitions of AGC motif were detected in SHR1, four repetitions of AGC motif were detected in myba and five repetitions of GCA motif were detected in SPL1 (Figure 16a, 16b, 16c, 16d, 16e), showing a perfect congruence with the RNA-seq experiment and allowing the validation.

**Table 22.** SSR patterns and primer sequences for SSRs validation

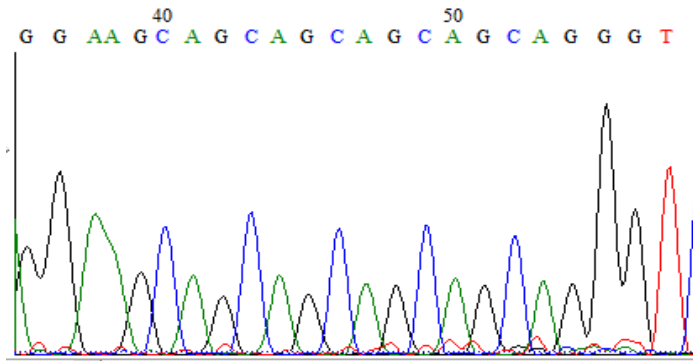
| Unigene ID   | SSR | Repetitions | Primer name  | Primer sequence            |
|--------------|-----|-------------|--------------|----------------------------|
| 14027.192887 | AGC | 5           | Ad_SRRM2 For | 5'-CGCAAACGCTCCAAGAAACA-3' |
|              |     |             | Ad_SRRM2 Rev | 5'-GCCCCTCCCTTTTCTCTTCC-3' |
| 14027.42287  | AGC | 5           | Ad_HMGN5 For | 5'-CATTCGAGGTCGTGGGCAG-3'  |
|              |     |             | Ad_HMGN5 Rev | 5'-TCTCCTTCTCCTTCCGCTCA-3' |
| 14027.58603  | AGC | 6           | Ad_SHR1 For  | 5'-GAGCATGCACACGCCTTATG-3' |
|              |     |             | Ad_SHR1 Rev  | 5'-TCTTGGTACGGCTCCAGGTA-3' |
| 14027.124297 | AGC | 4           | Ad_myba For  | 5'-AAGATCTGAAGAGCAGGCGG-3' |
|              |     |             | Ad_myba Rev  | 5'-TAAGAAATCCCAGCGGCGTT-3' |
| 14027.96747  | GCA | 5           | Ad_SPL1 For  | 5'-TCTGTCAGACAACCAGACGC-3' |
|              |     |             | Ad_SPL1 Rev  | 5'-ACCATGGTATTGCTGCAGCT-3' |



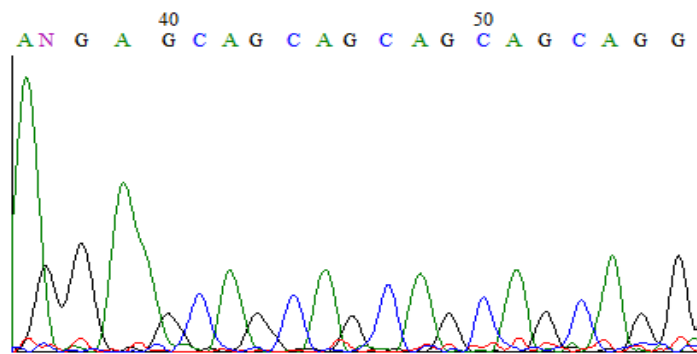
**a. G2\_SSRM2**



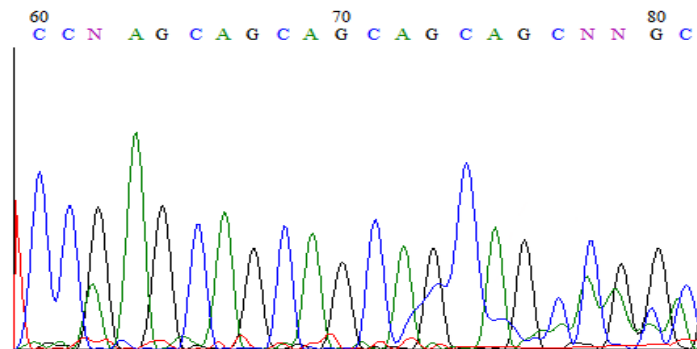
**a. G34\_SSRM2**



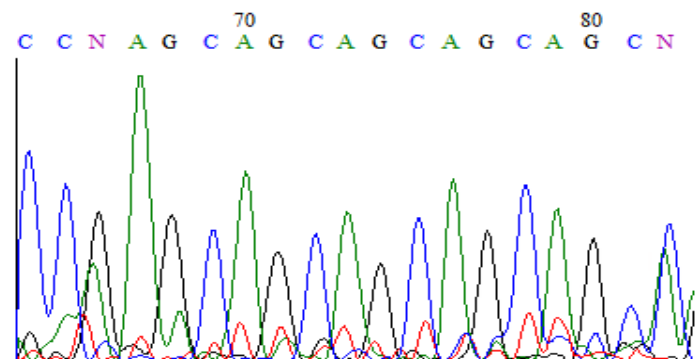
**b. G2\_HMG5**



**b. G34\_MHG5**

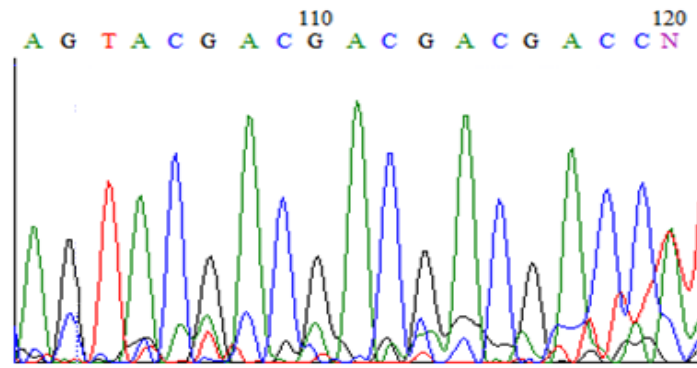


**c. G2\_SHR1**

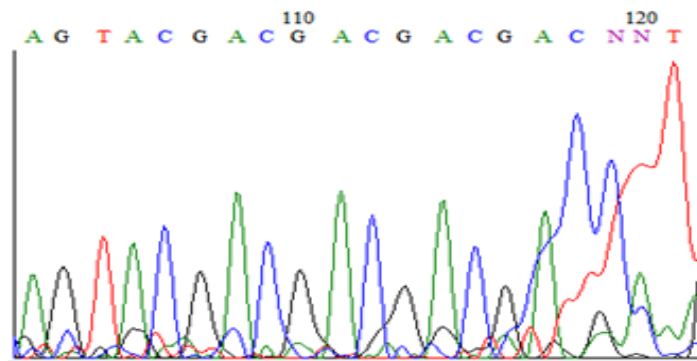


**c. G34\_SHR1**

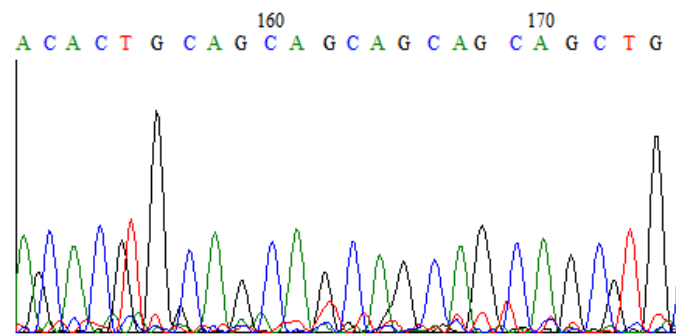




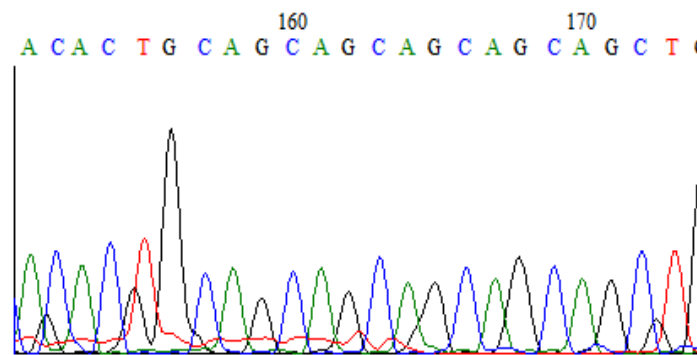
**d. G2\_Myba**



**d. G34\_Myba**



**e. G2\_SPL1**



**e. G34\_SPL1**

**Figure 16.** Sequence of regions analyzed for SSRs validation and electropherograms of Sanger sequencing. **a** SRRM2. **b** HMG5. **c** SHR1. **d** Myba. **e** SPL1.

### 5.3 Discussion

Abiotic and biotic stresses severely affect plant and crop growth and reproduction. Therefore, determining the critical molecular mechanisms and cellular processes in response to stresses will provide knowledge for addressing both climate change and food crises. RNA sequencing (RNA-Seq) using next-generation sequencing (NGS) is a revolutionary tool that has been used extensively in plant stress research in view of the great potential to reveal unprecedented complexity of the transcriptomes. The transcriptome sequencing of an organism provides quick insights into the gene space, opportunity to isolate genes of interest, development of functional markers, quantitation of gene expression, and comparative genomic studies. Useful *A. donax* genomic resources were provided by the work of Sablok et al. (2014) which used tissue-specific NGS of four different organs (leaf, culm, bud and root) of one *A. donax* ecotype. The analysis of transcripts putatively involved in stress in *A. donax* led to the identification of genes related to salt and heavy metal tolerance, particularly interesting considering the tolerance of *A. donax* to these stresses. Successively, the shoot transcriptome was obtained from an *A. donax* invasive ecotype in order to establish a molecular dataset allowing studies of the abiotic stress capabilities of this plant (Barrero et al. 2015). Fu et al. (2016) have reported the first characterization of *A. donax* transcriptome in response to drought. They obtained by Illumina-based RNA-seq the whole root and shoot transcriptomes of young *A. donax* plants subjected to osmotic/water stress with 10 and 20 % polyethylene glycol (PEG). Evangelistella and colleagues (2017) provided a *de novo* assembly and annotation of the leaf transcriptome of *A. donax* releasing a more complete gene expression catalogue to allow a comprehensive comparison among various assemblies. This last genomic resource was generated using three ecotypes originating from distant geographical locations (Greece, Croatia, and Portugal). A global comparison of homology between the transcriptomes of *A. donax* and four other species of the *Poaceae* family revealed a high level of global sequence similarity within this family (Evangelistella et al 2017). Recently, the first transcriptome of *A. donax* subjected to two level of long-term salt stress has been reported (Sicilia et al. 2019). The picture that emerged from the identification of differentially expressed genes is consistent with a salt dose-dependent response. Here, we describe the results of the RNA sequencing and *de novo* assembly of a low ecotype of giant reed subjected to an extended and severe salt stress (S3 dose). Although G34 clone was naturally lower than the giant reed ecotypes described in literature (Sicilia et al. 2019), it had a fair performance under salt stress, showing minimal reduction of main stem height (-37 %) and biomass yield (-35 %) (Figure 12) values compared to those registered for the other giant reed clones such as G2 (-48 % and - 50 %, respectively) (Sicilia et al. 2019) Moreover, the number of DEGs reported in G34 ecotype is much lesser than that reported for G2 ecotype under the same salt dose (3,852 DEGs) (Sicilia et al 2019) indicating that a refined

and focused modulation of gene expression is achieved to cope the unfavorable conditions. In salt tolerant plants, the cytosolic calcium perturbation activates the Salt Overly Sensitive (SOS) pathway (Liu and Zhu, 1998; MartinezAtienza et al. 2007). The components of this pathway are the  $\text{Ca}^{2+}$  sensor (SOS3) which accordingly changes its conformation in a  $\text{Ca}^{2+}$ -dependent manner and interacts with SOS2, a serine/threonine protein kinase, forming the active SOS2-SOS3 complex. This interaction results in the activation through its phosphorylation of SOS1 (plasma membrane  $\text{Na}^+/\text{H}^+$  antiporter) which mediates the exclusion of  $\text{Na}^+$  excess out of the cells. In addition, the SOS2-SOS3 complex activates NHX, the vacuolar  $\text{Na}^+/\text{H}^+$  exchanger resulting in the vacuolar sequestration of  $\text{Na}^+$  excess thus further contributing to the restore of ion homeostasis (Zhu, 2002; Barragan et al. 2012). The data suggest that the SOS pathway is only partially activated in giant reed G34 ecotype under severe salt stress as indicated by the sharp up-regulation of CIPK1-SOS2-like protein. The down regulation of NHXs and HKT6 highlights that both the vacuolar sequestration of  $\text{Na}^+$  excess and the  $\text{Na}^+$  extrusion out of the cell across the plasma membrane seem to be impaired. The giant reed response to salt seems to be restricted to a dramatic enhancement of phosphorylating activity upon existing SOS1 antiporter provoking its activation (Table 15). As expected, the components of the SOS response are among the few salt related specific DEGs, indicating their key role in the specific response to salt. Transcription factors (TFs) are considered as the most important regulators controlling the expression of a broad range of target genes ultimately influencing the level of salt tolerance in plants. It is well documented that TFs belonging to the DREB, NAC, MYB, MYC, C2H2 zinc finger, bZIP, AP2/ERF (Ethylene Responsive Factor) and WRKY families are relevant in salt stress response (Golldack et al. 2014). By comparing our results with those obtained in *A. donax* subjected to water deficit (Fu et al. 2016), slight differences can be observed in terms of TF subfamilies involved in salt and water stresses. Interestingly, a major involvement of AUX/IAA TFs is detected under salt stress with respect to *A. donax* plants subjected to drought thus indicating that a different regulation network is induced (Fu et al. 2016). Similarly, the same transcription factor families are involved in the G2 ecotype of giant reed under salinity, but a greater number of all TFs for each family resulted differently regulated under extreme salt stress in G2 ecotype (S4) (Sicilia et al. 2019). Moreover, a total of 27 *A. donax* unigenes correspond to high confidence rice homologs previously identified as salt or salt/drought responsive genes (Table 16) (Priya and Jain, 2013). Most of them (26) resulted also responsive to drought, indicating that the plant responses to these stresses probably overlap each other and that the downstream metabolic pathways can crosstalk. Significantly, a single gene belonging to WRKY transcription factor family specifically responds to salt treatment suggesting it might have a crucial role in the response to severe stress in the G34 ecotype (Gupta and Huang, 2014). The synthesis, sequestration, transportation, and turnover of hormones generate a

net of signals that correlates plant growth in dependence on internal and external cues. Among these hormones, abscisic acid regulates important abiotic stress responses, in particular water balance and osmotic stress tolerance under drought and salt stress (Kuromori and Seo, 2018). The analysis of G34-S3 vs G34-CK indicates that the ABA-activated signal transduction cascade is not influenced by salt treatment as none of the components was among the DEGs of G34-S3 vs G34-CK. Recently, the increase of leaf tissue ABA concentrations at two hours after plants were exposed to 50 mM of the ions was observed in maize indicating that ABA synthesis and accumulation are part of the early response to salt (Geilfus et al. 2018). Interestingly, the putative ortholog of AT1G78390, nine-cis-epoxycarotenoid dioxygenase 9 (NCED), is strongly upregulated in both *Arundo* shoots and roots during the early responses to water stress (Fu et al. 2016), this finding being in line with our opinion that ABA is not strictly involved in the response to long term salt stress. Ethylene is biosynthesized by the plant in response to life-cycle events or environmental cues including among other diseases, mechanical stress, drought or flood. The phenotypes that can be observed with respect to ethylene signaling typically relate to the inhibition of plant growth and seasonal changes in a plant's life cycle. Ethylene is efficiently biosynthesized from 1-aminocyclopropane-1-carboxylic acid (ACC) (Zhou et al. 2002). The mechanism of ethylene action, from perception to function, has been referred to as the "cleave and shuttle model" (Li et al. 2015). The most studied of the receptors is ethylene response 1 (ETR1) and downstream of ETR1 in *A. thaliana* is the kinase constitutive triple response 1 protein (CTR1) (Light et al. 2016). In absence of ethylene, CTR1 phosphorylates the putative metal transporter ethylene insensitive 2 (EIN2) that triggers EIN2 degradation by the Ub/26S proteasome (Li et al. 2015). In the presence of ethylene, CTR1 is inactivated and the EIN2 dephosphorylated form is proteolytically cleaved to generate a C-terminal fragment that localizes to the nucleus and initiates transcriptional regulation. Interestingly, transcripts encoding ACC oxidase have been found up-regulated under severe salt stress, whereas homolog of *Arabidopsis thaliana* CTR1 is sharply up-regulated in G34-S3 vs G34-CK samples (Table 15). In our opinion, this condition might describe a situation in which a low perception of emitted ethylene is attempted under severe salt stress (activation of CTR1) with the aim to minimize the negative effect of ethylene upon plant growth. These attempts to minimize the effect of emitted deleterious hormone were also observed in *A. donax* G2 ecotype subjected to salt stress. However, this kind of response was triggered when the G2 ecotype was subjected to extreme salt stress (S4) (Sicilia et al. 2019), indicating that more stringent conditions are needed in the G2 ecotype to prevent the negative effects of ethylene (Table 17). A consequence of high salt in the soil is the generation of a low water potential zone around the roots area making extremely difficult for the plants to obtain water and nutrients. Stomatal closure occurs in order to low water loss by transpiration, but it is at the same time responsible of sharp decrease in CO<sub>2</sub>

availability for Calvin cycle and a depletion of oxidized  $\text{NADP}^+$ . The overproduced electrons are transferred to  $\text{O}_2$  to generate  $\text{O}_2^{\bullet-}$  and a series of dangerous oxygen reactive species (ROSs) causing unrestricted oxidation of various cellular components such as membrane lipids, proteins, and nucleic acid (Scandalios, 2005). Therefore, salinity tolerance is positively correlated with the induction of ROS scavenging enzymes such as superoxide dismutase (SOD), catalase (CAT), glutathione peroxidase (GPX), ascorbate peroxidase (APX), monodehydroascorbate reductase (MDHAR), dehydroascorbate reductase (DHAR) and glutathione transferases (GSTs) (Gupta and Huang 2014). Moreover, malate is a versatile compound in plant metabolism (Lance and Rustin 1984) that can easily be transported across subcellular membranes and can be used as a substrate for mitochondrial ATP production or provision of NADH to the cytosol. Malate/oxaloacetate shuttles acting in combination with malate dehydrogenases (MDHs) as key enzymes (also termed malate valves) connect cellular compartments each other. They are powerful systems for balancing metabolic fluxes by enabling indirect transfer of reducing equivalents, and therefore, they play a key role in plant metabolism. The malate valve is strictly regulated during day light (Zhang et al. 2012). The activation of NADP-MDH is only enabled when NADPH increases because it is not consumed in the Calvin cycle due to a lack of  $\text{CO}_2$  or ATP. Under these conditions, the NADP-MDH uses the excess NADPH generated via the photosynthetic electron transport chain to convert oxaloacetate to malate, regenerating the electron acceptor  $\text{NADP}^+$ . Therefore, an electron drainage flux from an over-reduced photosynthetic chain to other cellular compartments can occur. In addition to the NADP-dependent MDH, namely component of the “light” malate valve, chloroplasts contain a redox-independent activity of NAD-MDH functioning as part of the “dark” malate valve and playing an important role during metabolism in the dark. In chloroplasts during darkness, ATP and NADPH for anabolism are generated independently via plastidial glycolysis (ATP), and plastidial oxidative pentose phosphate pathway (NADPH). The “dark” malate valve is here required to export the NADH that is formed during glycolysis at the substrate phosphorylation steps that require a continuous supply of  $\text{NAD}^+$ . The regeneration of  $\text{NAD}^+$ , which allows for continued ATP production via glycolysis, is possible due to the activity of NAD-MDH for indirect export of NADH in the form of malate exchanged with oxaloacetate. In our experiment, both the “light” and “dark” malate-valve seem to be activated as both the up-regulation of plastid NADP-malic dehydrogenase and NAD-MDH are observed, probably aimed to move the excess of reducing power from chloroplasts to the cytosol and to avoid over-reduction of the chloroplast glycolysis. As multifunctional amino acid, proline seems to have diverse roles under stress conditions, such as stabilization of proteins, membranes, and subcellular structures, and protecting cellular functions by scavenging ROSs. Biosynthesis of proline occurs in the chloroplast or cytosol via glutamate pathway in which 1-delta-pyrroline-5-carboxylate synthase

(P5CS) catalyzes the key regulatory and rate limiting reaction (Kaur and Asthir, 2015). During proline synthesis, 2 mol of NADPH per mole are consumed thus draining electrons from chloroplasts and contributing to the stabilization of redox balance and maintenance of cellular homeostasis when electron transport chain is saturated because of adverse conditions. The up-regulation of P5CS suggests that that proline biosynthesis represents either a crucial mechanism to adjust the osmotic status or a way for NADP<sup>+</sup> restoring in *A. donax*. Photosynthesis is the primary processes to be affected by salinity (Munns and Tester, 2008; Wang and Nii, 2000). Stomata close in response to leaf turgor declines, therefore supply of CO<sub>2</sub> to Rubisco (EC 4.1.1.39) is impaired thus inducing sharp alterations of photosynthetic metabolism. In *A. donax* under severe salt stress condition, CO<sub>2</sub> assimilation via the C<sub>3</sub> Calvin cycle seems to be impaired in favor of oxygen fixation through the photorespiration pathway (Table 15). In particular, the downregulation of PEPC kinase caused by salt stress indicates that mechanisms aimed to block the PEPC phosphorylation/inactivation occur in G34 ecotype maximizing the role of PEP as CO<sub>2</sub> acceptor catalyzed by PEPC. To reinforce this hypothesis, transcripts of chloroplastic pyruvate kinase (PK) are sharply down regulated indicating that carbon metabolism is directed towards PEP accumulation. A similar phenomenon has been reported in the facultative halophyte *Mesembryanthemum crystallinum* during adaptation to salinity where the transition from C<sub>3</sub> photosynthesis to Crassulacean acid metabolism (CAM) is associated with the increase in activity of key enzymes of C<sub>4</sub> cycle such as PEPC (Chu et al. 1990). In *A. donax* leaves, the activation of C<sub>4</sub> pathway has been recently reported (Sicilia et al. 2019), however, in G2 ecotype the downregulation of PEPC kinase occurs at extreme salt concentration (S4) as an ultimate rescue attempt to overcome the long-term stress conditions (Table 17). It had been reported that the transcript abundance of components of the glycolytic, mitochondrial respiration, and pentose phosphate pathways generally decreases in NaCl stress (Jiang et al. 2007; Zhong et al. 2016). Phosphofructokinase (PFK), pyruvate kinase (PK) and phosphoenolpyruvate kinase (PEPC) gene expression has been found significantly decreased in cucumber leaves when exposed to salt stress. Salt stress also significantly reduced isocitrate dehydrogenase, malate dehydrogenase and succinate dehydrogenase and their levels of transcription, causing a decreased production of organic acids and to a decline in metabolic rate (Wu et al. 2013; Fougere et al. 1991). Exogenous putrescine reversed the salt stress and increased gene expression of the key enzymes involved in the glycolysis pathway and Krebs cycle promoting the release of more energy currency (ATP and ADP) (Zhong et al. 2016). Table 19 reports that G34 ecotype subjected to salt stress responds by inducing, without any exogenous treatment, most of the genes involved in glycolysis and Krebs cycle thus encouraging carbohydrates to enter the glycolytic pathway and the Krebs cycle in order to supply more energy for plant metabolism and allowing the plant to tolerate the salt stress. The internal tolerance to salt stress

observed in the G34 ecotype is achieved at severe salt stress (S3 dose), whereas a similar response was observed in G2 ecotype only when it was subjected to higher salt concentration (S4 dose) (Table 19).

## 5.4 Conclusions

In this work, *A. donax*, G34 ecotype was subjected to long-term salt stress at salt level being much higher than that used to define a soil area as “salinized”. G34 ecotype was selected because of its characteristic to be shorter than other *A. donax* ecotypes when grown in pots. As *A. donax* reproduces itself asexually, this attribute should depend exclusively upon accumulated genetic and epigenetics marks that can influence other traits such as the response to salt stress as pleiotropic effect. Indeed, the genetic diversity of G34 is testified by the obtained peculiar results (both morpho-physiological and transcriptomic data) indicating that some sort of the stress avoidance occurred. G34 ecotype does not induce the entire SOS pathway, but the only CIPK1-SOS2 component is strongly activated. The analysis of clusters related to ethylene biosynthesis and signaling indicated that the gene transcription is modulated towards the minimization of ethylene negative effects upon plant growth. The *A. donax* leaves subjected to S3 severe salt stress respond to salt-induced oxidative stress by the induction of genes involved in redistributing the reducing power excess among cell compartments (“light” and “dark” malate valve). A clear involvement of proline in coping the salt-induced osmotic stress can be suggested as well as a crucial role of proline biosynthesis as NADPH consumer might be evocated. Certainly, the photosynthesis is strongly affected since genes involved in Rubisco biosynthesis and assembly are down-regulated, however, a shift C3 Calvin cycle to C4 photosynthesis is likely to occur as gene regulation is aimed to activate the primary CO<sub>2</sub> fixation to PEP in mesophyll cells (C4 pathway). The analysis of carbon metabolism revealed that G34 ecotype under salt stress activates the gene expression of glycolysis and Krebs cycle genes known to be a typical response to face salt stress. Interestingly, a similar response was achieved by the G2 ecotype subjected to a much higher salt dose suggesting that G34 ecotype more promptly tries to counteract the stressful conditions. In this respect, also the attempt to mitigate the detrimental effect of ethylene by activating CTR1 is started up by G34 ecotype under severe salt stress. Therefore, the results of our work are in accordance with the possibility that heritable phenotypic differences among clones of *A. donax* might be accumulated especially in ecotypes originating from distant geographical areas (Nackley and Kim 2015). Additionally, 26,838 simple sequence repeat (SSR) markers were identified and validated. This SSR array certainly enlarges the already available SSR catalogue (Evangelistella et al. 2017) which includes 8,364 SSRs, thus suggesting the future possibility to study genetic variability of this species more accurately.

## 5.5 Experimental

### 5.5.1 Plant material and application of salt stress

The experiment was conducted at the Department of Agriculture, Food and Environment (Di3A) of the University of Catania, using G34 giant reed clone originated in Birgi (Italy) (latitude 38°01', longitude 12°32') and collected for the Giant reed Network project (Cosentino et al. 2006). The trial started on July 7<sup>th</sup>, 2017, by transplanting *A. donax* rhizomes into 25 l pots (40 cm diameter and 30 cm height) containing a sandy soil as substrate and kept in open air. Before transplantation, the rhizomes were weighed using a laboratory scale and the number of buds was counted, and those showing homogeneous rhizome weight and same bud number were used for transplanting. The pots were arranged according to a randomized block factor scheme, performing three biological replicates for treatments with a total of six experimental units. During the experiment, the irrigation was performed on a weekly basis, and until the first sprouts have been released, tap water (5 l per pot) has been used. The first irrigation with salted water was carried out on August 3<sup>rd</sup>, 2017. Salt stress was imposed by adding 256.67 mM NaCl corresponding to 32 dS m<sup>-1</sup> electric conductivity to the irrigation water (S3 samples), whereas control samples (CK) were irrigated with tap water without salt addition (S0 samples). Before leaf harvest, the following morpho-biometric and physiological parameters were measured: number of culms, height of the main culm, number of green and senescent leaves, net photosynthesis and chlorophyll content measured in SPAD units (SPAD 502, Konica Minolta). Moreover, the measurement of the yielded biomass was also carried out (Cosentino et al. 2006). R software was used for standard deviation calculation. The collected data were submitted to ANOVA analysis using R Studio. The averages with pvalue  $\leq 0.05$  were separated by the TukeyHSD test.

### 5.5.2 Sample collection and RNA extraction

On November 17<sup>th</sup>, 2017, fully expanded, no senescing G34 leaves (the 3<sup>rd</sup> leaf from the top) were harvested and immediately frozen with liquid nitrogen. RNA isolation was performed using the Spectrum Plant Total RNA Extraction Kit (Sigma-Aldrich, St. Louis, MO, USA) according to the manufacturer's instructions. RNA degradation and contamination were monitored on 1% agarose gels. RNA purity and concentration were assayed using the NanoDrop spectrophotometer (ThermoFisher Scientific, Waltham, MA, USA). RNA integrity was assessed using the Agilent Bioanalyzer 2100 system (Agilent Technologies, Santa Clara, CA, USA). Before to be sequenced, the RNA samples were subjected to quality parameter evaluation. The average RNA Integrity Number (RIN) was of 7.6 and there was very slight genomic DNA contamination confirming that all the samples have such high-quality level to be processed (Table 12).



### 5.5.3 Library preparation for transcriptome sequencing

A total amount of 1.5 µg RNA per sample was used as input material for library preparations. Sequencing libraries were generated using NEBNext® Ultra™ RNA Library Prep Kit for Illumina® (New England Biolabs, Ipswich, MA, USA) following manufacturer's recommendations as described in Sicilia et al. (2019).

### 5.5.4 Clustering and next generation RNA sequencing

Cluster generation and sequencing were performed by Novogene Bioinformatics Technology Co., Ltd. (Beijing, China). The clustering of the index-coded samples was performed on a cBot Cluster Generation System using a PE Cluster kit cBot-HS (Illumina). After cluster generation, the library preparations were sequenced on Illumina HiSeq2000 platform to generate pair-end reads. Raw data (raw reads) of fastq format were firstly processed through in-house perl scripts. In this step, clean data were obtained by removing reads containing adapter, reads containing poly-N and low quality reads. At the same time, Q20, Q30, GC-content and sequence duplication level of the clean data were calculated. All the downstream analyses were based on clean data with high quality.

### 5.5.5 *De novo* transcriptome assembling and gene functional annotation

*De novo* transcriptome assembly was accomplished using Trinity (r20140413p1 version) with `min_kmer_cov:5` parameters ( $k=25$ ). Then Hierarchical Clustering was performed by Corset (v1.05 version) to remove redundancy (parameter `-m 10`). Afterwards the longest transcripts of each cluster were selected as Unigenes. As part of a wider sequencing project, the flow chart of the G34 ecotype *de novo* transcriptome assembly is reported in Sicilia et al. (2019).

### 5.5.6 Identification of clusters specifically involved in the salt stress response

In order to discriminate among clusters specifically regulated by salt treatment from those also involved in the response to other abiotic stress (oxidative, water deprivation, cold, heavy metals), the GO term lists relative to G34-S3 vs G34-CK (severe salt stress samples versus control samples) comparison were filtered and exclusively salt-regulated clusters were extrapolated. For the identification of transcription factors responsive to salt stress in *A. donax*, we mined the available salt stress-responsive transcription factor database of rice (SRTFDB) (Priya and Jain 2013) by Blastn searches with an *e* value cutoff of  $1e^{-5}$ .

### 5.5.7 Quantification of gene expression and differential expression analysis

Gene expression levels were estimated by RSEM (v1.2.26 version) with bowtie2 mismatch 0 parameters in order to map to Corset filtered transcriptome. For each sample, clean data were mapped back onto the assembled transcriptome and readcount for each gene was then obtained from the mapping results. Differential expression analysis between control and salt stressed samples was performed using the DESeq R package (1.12.0 version,  $\text{padj} < 0.05$ ). The resulting  $p$ -values were adjusted using the Benjamini and Hochberg's approach for controlling the false discovery rate. Genes with an adjusted  $p$ -value  $< 0.05$  found by DESeq were assigned as differentially expressed, adopting  $\log_2\text{FoldChange}$  threshold of 0.58 (1.5 fold change). The GO enrichment analysis of the differentially expressed genes (DEGs) was implemented by the Goseq R packages (1.10.0, 2.10.0 version, corrected P-Value  $< 0.05$  based) Wallenius non-central hyper-geometric distribution (Young et al. 2010). Furthermore, to analyze the *Arundo donax* transcriptome, all of the unigenes were submitted to the KEGG pathway database for the systematic analysis of gene functions. KOBAS software (KEGG Orthology-Based Annotation System, v2.0.12 version, corrected P-Value  $< 0.05$ ) was used to annotate sequences by KEGG Orthology terms.

### 5.5.8 Real-time validation of selected DEG candidates using qRT-PCR

Selected DEGs were validated using qRT-PCR as described in Sicilia et al. (2019). Briefly, total RNA (2.5  $\mu\text{g}$ ) extracted from sample leaves as described above, was reversed transcribed using the SuperScript<sup>TM</sup> Vilo<sup>TM</sup> cDNA synthesis kit by ThermoFisher Scientific, according to the manufacturer's instructions. Real-time qRT-PCR was performed for a total of ten DEGs with PowerUp SYBR Green Master mix by ThermoFisher Scientific and carried out in the Bio-Rad iQ5 Thermal Cycler detection system. All the genes were normalized with *A. donax* 26 S proteasome non-ATPase regulatory subunit 11 gene (RPN6) that was reported to be a suitable housekeeping gene in abiotic stress conditions (Poli et al. 2017). All reactions were performed in triplicate and fold change measurements calculated with the  $2^{-\Delta\Delta\text{CT}}$  method.

### 5.5.9 SSR detection and validation

Picard - tools v1.41 and samtools v0.1.18 were used to sort, remove duplicated reads and merge the bam alignment results of each sample. MISA (v1.0, default parameters; minimum number of repeats of each unit size is: 1-10; 2-6; 3-5; 4-5; 5-5; 6-5) was used for the SSR detection in the unigenes. These markers include repetitions of one, two, three, four, five or six bases with 10, 6, 5.5 and 5 uninterrupted repetitions. TransDecoder v3.0.0 was used in order to have the best 5'-UTR, CDS and 3'-UTR regions. Afterwards, the positions of transcribed domains were combined with the SSRs positions, in order to assign the microsatellites within the ORFs (Open Reading frames). SSRs

validation was conducted by amplifying and sequencing five microsatellite regions chosen randomly in 5'-UTR, CDS and 3'-UTR (EST-SSR) coding sequences. The five primer sets were designed using the primer-BLAST software (<https://www.ncbi.nlm.nih.gov/tools/primer-blast/>) and their sequences and amplicons are listed in Supplementary Table S1. DNA extraction was performed by using the DNeasy<sup>®</sup> Plant Mini Kit (Qiagen, Hilden, Germany) according to the producer instruction. The PCR was performed on a 50 µl total volume, according BIOTAQ<sup>™</sup> DNA Polymerase (BIOLINE, Singapore) protocol. PCR products were then subjected to a 3% agarose gel electrophoresis, running at a voltage of 90 volt for 3 hours. Bands showing the expected size were excised and purified using the PureLink<sup>™</sup> Quick Gel Extraction & PCR Purification Combo Kit (Invitrogen by Thermo Fisher Scientific, Lithuania) according to the producer's instructions. The isolated DNA was sequenced by Eurofins Genomics (Ebersberg, Germany) and checked for repeated motifs.

## 6 Global leaf and root transcriptome reprogramming in response to cadmium reveals tolerance mechanisms in *Arundo donax* L.

Danilo Fabrizio Santoro, Angelo Sicilia, Giorgio Testa, Salvatore Luciano Cosentino, Angela Roberta Lo Piero\*

Department of Agriculture, Food and Environment, University of Catania, Via Santa Sofia 98, 95123 Catania (Italy)

\*corresponding author: rlopiero@unict.it

### Abstract

The expected increase of sustainable energy demand has shifted the attention towards bioenergy crops. Due to their know tolerance against abiotic stress and relatively low supply request, they have been proposed as election crops to be cultivated in marginal lands without disturbing the part of lands employed for agricultural purposes. *Arundo donax* L. is a promising bioenergy crop whose behaviour under water and salt stress has been recently studied at transcriptomic levels. As the anthropogenic activities produced in the last years a worrying increase of cadmium contamination worldwide, the aim of our work was to decipher the global transcriptomic response of *A. donax* leaf and root in the perspective of its cultivation in contaminated soil. In our study, RNA-seq libraries yielded a total of 416 million clean reads and 10.4 Gb per sample. *De novo* assembly of clean reads resulted in 378,521 transcripts and 126,668 unigenes with N50 length of 1812 bp and 1555 bp, respectively. Differential gene expression analysis revealed 5,303 deregulated transcripts (3,206 up- and 2,097 down regulated) specifically observed in the Cd-treated roots compared to Cd-treated leaves. Among them, we identified genes related to “Protein biosynthesis”, “Phytohormone action”, “Nutrient uptake”, “Cell wall organisation”, “Polyamine metabolism”, “Reactive oxygen species metabolism” and “Ion membrane transport”. Globally, our results indicate that ethylene biosynthesis and the downstream signal cascade are strongly induced by cadmium stress. In accordance to ethylene role in the interaction with the ROS generation and scavenging machinery, the transcription of several genes (NADPH oxidase 1, superoxide dismutase, ascorbate peroxidase, different glutathione S-transferases and catalase) devoted to cope the oxidative stress is strongly activated. Several small signal peptides belonging to *ROTUNDIFOLIA*, *CLAVATA3*, and C-TERMINALLY ENCODED PEPTIDE 1 (CEP) are also among the up-regulated genes in Cd-treated roots functioning as messenger molecules from root to shoot in order to communicate the stressful status to the upper part of the plants. Finally, the main finding of our work is that genes involved in cell wall remodelling and lignification are decisively up-regulated in giant reed roots this being a mechanism of cadmium avoidance adopted by giant cane and strongly supporting its cultivation in cadmium contaminated soils in a perspective to save agricultural soil for food and feed crops.

**Keywords:** *Arundo donax* L., bioenergy crops, RNA-seq, *de novo* assembly, leaf and root transcriptome, heavy metals, cadmium.

## 6.1 Introduction

Nowadays, globe climate change has become one of the most urgent problems humans have to deal with due to the ongoing Green House Gas (GHG) emissions into the atmosphere. Fossil fuels based on organic origin and non-renewable energy sources are by now unsustainable, thereby new energy policies relying on the use of sustainable energy sources should be considered in order to meet the global energy demand (REN21, 2016). Among the different renewable energy sources, biomass is becoming an interesting candidate because of its peculiarity to be converted in a variety of products, such as solid fuels, liquid fuels, heat, electricity, and hydrogen. In particular, second generation of biofuels (biomass) is produced from organic origin by using perennial herbaceous plants and fast-growing trees, which are able to limit GHG levels by producing sustainable energy (Muench and Guenther 2013; Ross and Ahlgren 2018). Biomass derived from bioenergy crops has the capability to be cultivated on marginal land, this fact being very attractive in order not to compete with feed and food crops for land use (Lewandowski et al. 2016) also in the perspective that the global world's population is expected to reach 9.7 billion by 2050 (ONU, 2019) thus determining a considerable increase for agricultural land availability (Rivera et al. 2017). Such marginal sites have little or no agricultural or industrial value, are characterized by little potential for profit and often have poor soil or other undesirable characteristics such as high salt content, inadequate water supply or heavy metal (HM) contaminations. Although some HMs are categorized as essential elements because of their positive impact on the plant growth and crop yield (e.g., B, Cu, Co, Fe, Mn, Ni, Zn), some of them, such as Cd, Hg, Pb and As do not play any role in plant metabolism and can operate by reducing the crop productivity in the case their levels reach toxic concentrations (Edelstein and Ben-Hur 2017). Heavy metal pollution has mainly brought about by the use of pesticides and fertilizers in agriculture, compost wastes, smelting industry, mining activities and transport. Among all HMs, given both its high toxicity even at low level and its high rate of widespread capacity in lands, cadmium has led to contaminated soils worldwide (Tchounwou et al. 2012; Mahar et al. 2016) and in particular in Europe where its concentration in the topsoil raised from  $< 0.01$  to 14.1 ppm in the last years (Pan et al. 2010). Moreover, due to its high solubility in soil, cadmium can be easily extracted by the plant root system (Sidhu et al. 2019) from where it is accumulated in the above-ground regions inhibiting plant growth and causing a threat to animal and human health through the food chain (Gall et al. 2015). Cadmium accumulation-related molecules include many transporters, chelators, some amino acids and organic acids, and the genes encoding the corresponding proteins/enzymes were functionally characterized in both *A. thaliana* and *O. sativa* (Fan et al. 2021). The family of NRAMP metal ion transporters represents an important group of transmembrane protein involved in metal transport and homeostasis and it was supposed to be the major transporter family of  $\text{Cd}^{2+}$  from the soil into root cells (Nevo and

Nelson 2006). The mechanisms by which Cd exerts toxicity in plants include: a) substitution of some essential metal ion (e.g.  $Zn^{2+}$  and  $Fe^{2+}$ ) or blocking functional groups which leads to inactivation of biomolecules (Stohs and Bagchi 1995); b) a tight binding of metal ions with thiol groups of proteins which destroys their structure and function (Yadav, 2010); c) generation of reactive oxygen species (ROS), which brings to oxidative stress (Sharma and Dietz 2009; Dalcorsio et al. 2013). *Arundo donax* L. also known as giant reed, is a perennial rhizomatous grass species, genus *Arundo*, belonging to *Poaceae* family. Among rhizomatous grasses dedicated to energy production, *A. donax* represents one of the most promising bioenergy crops (Lewandowski et al 2003; Angelini et al. 2009) because of its high biomass production, both low irrigation and nitrogen input requirements, and its high tolerance to abiotic stress conditions, including herbicide, salinity and heavy metals (Bajguz and Hayat 2009; Zhang et al. 2016). Notably, it has been proposed as species to be employed for phytoremediation (Fernando et al. 2016) due to its ability to accumulate and tolerate high doses of heavy metals, such as Ni, Cd and As (Papazoglou et al. 2007; Mirza et al. 2011). Transcriptomic analysis represents a powerful tool to elucidate the molecular mechanisms by which plants accumulate, translocate and detoxify Cd ions and for this reason a huge number of genes involved in Cd tolerance in different crop species, such as maize or rice (Cheng et al. 2014) were uncovered. Moreover, RNA Sequencing (RNA-Seq) and *de novo* assembly of the transcriptome allow the discover and the quantitative determination of all the expressed genes for those species whose genome sequence is not available yet. Genomic resources of *A. donax* were provided by sequencing RNA extracted from different organs (leaf, culm, bud and root) of giant reed ecotypes subjected to either normal (Sablock et al. 2014; Barrero et al. 2015; Evangelistella et al. 2017) or under water stress condition (Fu et al. 2016). More recently, the analysis of the transcriptional response of giant reed was analysed after a long-term period of salt stress in two different *A. donax* ecotypes (Sicilia et al. 2019; Sicilia et al. 2020). Overall, these studies contributed both to the drafting of candidate gene list that can be used in molecular breeding projects and in revealing the role of genes in the abiotic stress response. However, the transcriptional response of *A. donax* subjected to cadmium treatments is still incomplete and the molecular mechanism of cadmium effects on giant reed metabolic process remains poorly understood. Recently, Shaheen et al. (2018) evaluated the effects of increasing concentrations of cadmium on the expression of selected genes (carotenoid hydroxylase, amidase, glutathione reductase, bHLH, NRAMP and YSL) in *Arundo donax* L. cultivated in hydroponic solution. The highest expression for these genes was observed in plants exposed to the highest Cd concentration (100 mg/L). Moreover, the activity of several enzymes involved in the ROS scavenging (SOD, CAT, POD) was also measured revealing their activation at the highest cadmium concentration and confirming the onset of a secondary oxidative stress (Shaheen et al. 2018). A study conducted in

cohorts of *A. donax* strongly suggests that phytochelatin encoding genes (*AdPCS1*, *AdPCS2*, and *AdPCS3*) most likely contribute to Cd detoxification in *A. donax* and the presence of multiple PCS isoforms seems to be advantageous both to provide higher general levels of phytochelatin biosynthesis and to increase flexibility in HM resistance (Li et al. 2019). In this study, considering the frequency of cadmium in soils of Mediterranean basin and the perspective of potential use of marginal land to cultivate bioenergy crops, we sequenced and *de novo* assembled the giant reed leaf and root transcriptome after a prolonged period of cadmium treatment by using RNA-Seq technique. The aim of our work was to gain novel insight into the cadmium stress tolerance and to shed new light on the distinct role of leaf and root in the dynamics of heavy metal stress response in plants.

## 6.2 Material and methods

### 6.2.1 Plant material and application of cadmium nitrate

The experiment was conducted at the Department of Agricultural, Food and Environment (Di3A) of the University of Catania, using G10 ecotype coming from Fondachello (Italy) (latitude N 37°45', longitude E 15°11'), collected for the Giant reed Network project (Cosentino et al. 2006). The trial started on May 4<sup>th</sup> 2020, by filling each pot with 8 kg of clay soil and kept in open air. The contamination of each pots was achieved by using 4 ppm (4 mg/kg) of cadmium nitrate Cd(NO<sub>3</sub>)<sub>2</sub> for treated plants and 5.774 grams of NH<sub>4</sub>NO<sub>3</sub> for control plants, so as to equilibrate the N concentration between the two conditions. The aforementioned concentration is higher than the reference threshold established by the European Union directive 86/278/EEC on Environment protection which establishes the maximum concentration of cadmium on soil should range between 1 and 3 ppm (European Commission, 1986). Cadmium contents above 3 mg/kg are generally thought to indicate contaminated soil (Akbar et al. 2006). Afterwards, one litre of tap water was added to each pot to allow the element adsorption by soil colloids. Successively, in each pot a single *A. donax* stem node was transplanted and the irrigation was performed three times a week by adding one litre of tap water to avoid Cd(NO<sub>3</sub>)<sub>2</sub> leaching. The pots were arranged according to a randomized block factor scheme, considering three biological replicates for each treatment, with a total of six experimental units. Before sampling (July 28<sup>th</sup>, 2020), the following morpho-biometric and physiological parameters were evaluated: number of culms per pots, height of the main culm, net photosynthesis efficiency measured by LCI-T portable photosynthesis system (ADC BioScientific Ltd). Moreover, the measurement of biomass was performed (Cosentino et al. 2006). R software was used for standard deviation analysis. The data were submitted to one-way ANOVA test using R Studio. The averages with pvalue ≤0.05 were separated by the TukeyHSD test.

### **6.2.2 Sample collection and RNA extraction**

On July 28<sup>th</sup> 2020, fully expanded, no senescing G10 leaves and roots were harvested and immediately frozen with liquid nitrogen. RNA isolation was carried out by using the Spectrum Plant Total RNA Extraction kit (Sigma-Aldrich, St. Louis, MO, USA) according to the manufacturer's instructions. RNA degradation and contamination were monitored by electrophoresis with 1% agarose gel. RNA purity and concentration were assayed using the NanoDrop spectrophotometer (ThermoFisher Scientific, Waltham, MA, USA). Before to be sequenced, the RNA samples were subjected to quality parameter evaluation. RNA integrity was assessed using the Agilent Bioanalyzer 2100 system (Agilent Technologies, Santa Clara, CA, USA).

### **6.2.3 Library preparation for transcriptome sequencing**

One µg of RNA was used as input material for library preparations. Sequencing libraries were generated using NEBNext<sup>®</sup> Ultra<sup>™</sup> RNA Library Prep Kit for Illumina<sup>®</sup> (New England Biolabs, Ipswich, MA, USA) following manufacturer's recommendations. Briefly, mRNA was purified from total RNA using poly-T oligo-attached magnetic beads. Fragmentation was carried out using divalent cations under elevated temperature in NEBNext First Strand Synthesis Reaction Buffer (5X). First strand cDNA was synthesized using random hexamer primer and M-MuLV Reverse Transcriptase (RNase H) as synthesizing enzyme. Second strand cDNA synthesis was subsequently performed using RNase H to insert breaks into the RNA molecule and DNA Polymerase I as synthesizing enzyme. Remaining overhangs were converted into blunt ends via exonuclease/polymerase activities. After adenylation of 3' ends of DNA fragments, NEBNext Adaptor with hairpin loop structure were ligated to prepare for hybridization. In order to select cDNA fragments of preferentially 150~200 bp in length, the library fragments were purified with AMPure XP system (Beckman Coulter, Beverly, MA, USA). Then 3 µl USER Enzyme by NEB were used with size-selected, adaptor-ligated cDNA at 37 °C for 15 min followed by 5 min at 95 °C before PCR. Then PCR was performed with Phusion High-Fidelity DNA polymerase, Universal PCR primers and Index (X) Primer. Finally, PCR products were purified (AMPure XP system) and library quality was assessed on the Agilent Bioanalyzer 2100 system.



#### **6.2.4 Clustering and next generation RNA sequencing**

Cluster generation and sequencing were performed by Novogene (UK) company Limited (25 Cambridge Park, Milton Road, Cambridge, CB4 0FW, United Kingdom). The clustering of the index-coded samples was performed on a cBot Cluster Generation System using a PE Cluster kit cBot-HS (Illumina). After cluster generation, the library preparations were sequenced on Illumina HiSeq2000 platform to generate pair-end reads. Raw data (raw reads) in fastq format were firstly processed through in-house perl scripts. In this step, clean data were obtained by removing reads containing adapters, reads containing poly-N and low-quality reads. At the same time, Q20, Q30, GC-content and sequence duplication level of the clean data were calculated. All the downstream analyses were based on clean data with high quality (Table 23).

#### **6.2.5 *De novo* assembly and gene functional annotation**

*De novo* transcriptome assembly was made up by Trinity software (2.6.6 version) with  $\text{min\_Kmer\_Cov} = 3$  and  $\text{min\_glue} = 4$ . Hierarchical Clustering was carried out by Corset (4.6 version) in order to remove redundancy (parameter -m 10), so that the longest transcript of each cluster has been selected as Unigene. The assembly assessment and gene prediction have been performed by Benchmarking Universal Single-Copy Orthologous (BUSCO software, 3.0.2 version), whereas the gene functional annotation was obtained by exploiting seven different databases: National Centre for Biotechnology Information (NCBI), non-redundant protein sequences (Nr, Diamond software, 0.8.22 version, e-value threshold  $1e-5$ ), NCBI non-redundant nucleotide sequences (Nt, NCBI blast software, 2.9.0 version, e-value threshold  $1e-5$ ), Protein family (Pfam, hmmscan software, HMMER 3.1 version, e-value threshold 0.01), Cluster of Orthologous Groups of Proteins (KOG/COG, Diamond software, 0.8.22 version, e-value threshold  $1e-5$ ), Swiss-Prot (Diamond software, 0.8.22 version, e-value threshold  $1e-5$ ), Kyoto Encyclopedia of Genes and Genome (KEGG, Diamond and KAAS software, 0.8.22 version, e-value threshold  $1e-5$ ) and Gene Ontology (GO, blast2GO software, b2g4pipe\_v2.5 version, e-value threshold  $1e-6$ ). To identify the transcription factor, iTAK (hmmscan software) tool was used to infer the TF families (Pérez-Rodríguez et al. 2009; Jin et al. 2014).

## 6.2.6 Quantification of gene expression and differential expression analysis

Gene expression level was estimated by RSEM software (1.2.28 version) by mapping back each clean read onto assembled transcriptome and readcounts for each gene were then obtained from the mapping results. Furthermore, the readcounts of each gene have been used as input data for DESeq2 (1.26 version,  $\text{padj} \leq 0.05$ ), to obtain differentially expressed genes (DEGs). Comparisons were made to identify the set of differentially expressed genes between control (CK) and cadmium (Cd) treatments for each tissue (Cd\_L\_vs CK\_L; Cd\_R vs CK\_R). Moreover, the core of our analysis was performed on the comparison between the Cd-treated samples of the two tissues indicated as Cd\_R vs Cd L\*. In this comparison, the Cd-treated root vs Cd-treated leaf DEGs (Cd\_R vs Cd L\*) were obtained by subtracting the DEGs belonging to the CK\_R vs CK\_L comparison (tissue specific DEGs in control conditions) to the Cd\_R vs Cd\_L. An adjusted p-value cutoff of 0.05 and a log<sub>2</sub>fold change (Log<sub>2</sub>FC) threshold of 1 was adopted to filter the significantly up- and down-regulated genes. A correlation analysis was performed in order to demonstrate experiment repeatability and to reveal differences in gene expression among samples. Principal Component Analysis 3D plot and a heatmap were obtained by using R language, considering as input data the readcounts of each sample, including biological replicates.

## 6.2.7 Real-Time validation of selected DEG candidates using qRT-PCR

Total RNA (2.5 µg) purified from leaves and roots as described above, was reverse transcribed using SuperScript™ Vilo™ cDNA synthesis kit by ThermoFischer Scientific, according to manufacturer's instructions. Real-time qRT-PCR was carried out for a total of 8 DEGs with PowerUp SYBR Green Master mix by ThermoFischer Scientific in the Bio-Rad iQ5 Thermal Cyclers detection system. All the genes have been normalized with *cyclin-dependent kinase C-2* (CDKC-2, XM\_004962139), being a suitable housekeeping gene (Guo et al. 2007). All reactions were performed in duplicate and fold change measurements calculated with the  $2^{-\Delta\Delta\text{CT}}$  method.

## 6.2.8 Gene ontology and KEGG enrichment analysis

Based on differentially expressed genes (DEGs), the GO enrichment was accomplished by using blast2go (b2g4pipe\_v2.5 version) software (e-value = 1e-6). Furthermore, to analyse the *Arundo donax* L. transcriptome, all the unigenes were submitted to KEGG database for the systematic analysis of gene function. KOBAS software (v.3.0, corrected p-value  $\leq 0.05$ ) has been applied to test the statistical enrichment of differentially expressed genes in KEGG pathway. Moreover, a pathway analysis was conducted using MapMan3.6.0RC1 (<https://mapman.gabipd.org/>). All the unigenes were annotated and mapped using Mercator4 V2.0, an on-line tool of MapMan (<https://www.plabipd.de/portal/mercator4>) which accurately assigns hierarchical ontology providing

visual representation of genes in different plant processes. The significant DEGs ( $p_{adj} < 0.05$ ), with the corresponding  $\log_2$ FoldChange values, were used as dataset to align with the Mercator map. In order to analyse the main gene families and pathways affected by cadmium treatment, DEGs (Cd\_R vs Cd\_L\* comparison) belonging to “Phytohormone action”, “Transcription factors”, “Nutrient uptake”, “Cell wall”, “Polyamine metabolism”, “ROS scavenging” and “Heavy metal transporter” categories were aligned to the *Arabidopsis thaliana* genome (Phytozome genome ID: 167, NCBI taxonomy ID: 3702) accessed through Phytozome 13 ([https://phytozome-next.jgi.doe.gov/info/Athaliana\\_TAIR10](https://phytozome-next.jgi.doe.gov/info/Athaliana_TAIR10)). The DEGs showing a threshold of  $\pm 2.000$   $\log_2$ FoldChange and an e-value  $\leq 0.05$  were selected.

### 6.2.9 KEGG classification of heavy metal and salt common genes

In order to elucidate the core response of *A. donax* to both salt (Sicilia et al., 2019; Sicilia et al., 2020) and cadmium stress, the significant DEGs ( $p_{adj} \leq 0.05$ ) belonging to both S3\_vs\_CK (specifically deregulated DEGs under severe salt stress, 256.67 mM NaCl), and S4\_vs\_CK (specifically deregulated DEGs under extreme salt stress, 419.23 mM NaCl) comparisons (Sicilia et al., 2019; Sicilia et al., 2020) were filtered considering a threshold of  $\pm 2.00$   $\log_2$ FoldChange and merged, thus resulting in a “list of salt deregulated DEGs”. The same procedure was adopted to retrieve the significant DEGs ( $p_{adj} \leq 0.05$ ) belonging to Cd\_R vs Cd\_L\*, Cd\_L vs Cd\_CK and Cd\_R vs Cd\_CK comparisons, resulting in a “list of cadmium deregulated DEGs”. A KO ID (KEGG ORTHOLOGY Database, <https://www.genome.jp/kegg/ko.html>) was assigned to each DEG, then, the two lists were compared by using the KO ID as common annotation code. The aforementioned comparison generated a merged DEG list where only DEGs whose KO ID was in both the “list of salt deregulated DEGs” and “list of cadmium deregulated DEGs” were included. Finally, genes were grouped by concordant type of regulation (up-regulated or down-regulated in both stresses).

## 6.3 Results

### 6.3.1 Effect of cadmium upon *A. donax* morpho-biometric and physiological parameters

As described in the Material and Methods section, both morpho-biometric and physiological parameters of *A. donax* G10 ecotype were evaluated at sampling date after being subjected to 4 ppm (4 mg/kg) of cadmium nitrate. A picture of giant reed G10 ecotype at sampling time is shown in Figure 17. Considering the average values of the three biological replicates, we observed that both the main stem height and biomass dry weight per pot were reduced in those samples subjected to Cd treatment (Figure 18A, 18B). Moreover, the net photosynthesis efficiency was also significantly reduced in treated samples compared to the untreated samples, reaching values of  $8.64 \mu\text{mol CO}_2 \text{ m}^{-2} \text{ s}^{-1}$  and  $14.91 \mu\text{mol CO}_2 \text{ m}^{-2} \text{ s}^{-1}$ , respectively (Figure 18C). The alteration of the aforementioned parameters indicated the effectiveness of the cadmium dose to induce response in G10 giant reed ecotype.

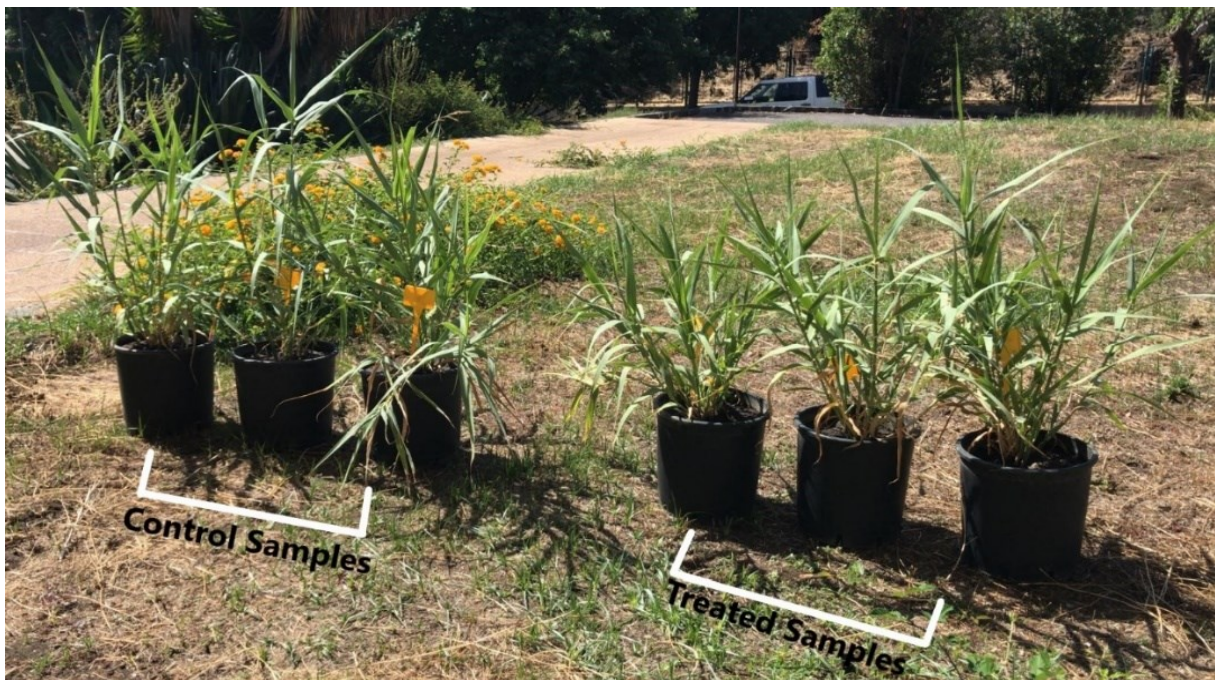


**Figure 17.** Picture of giant reed plants at sampling date (July 28<sup>th</sup>, 2020)

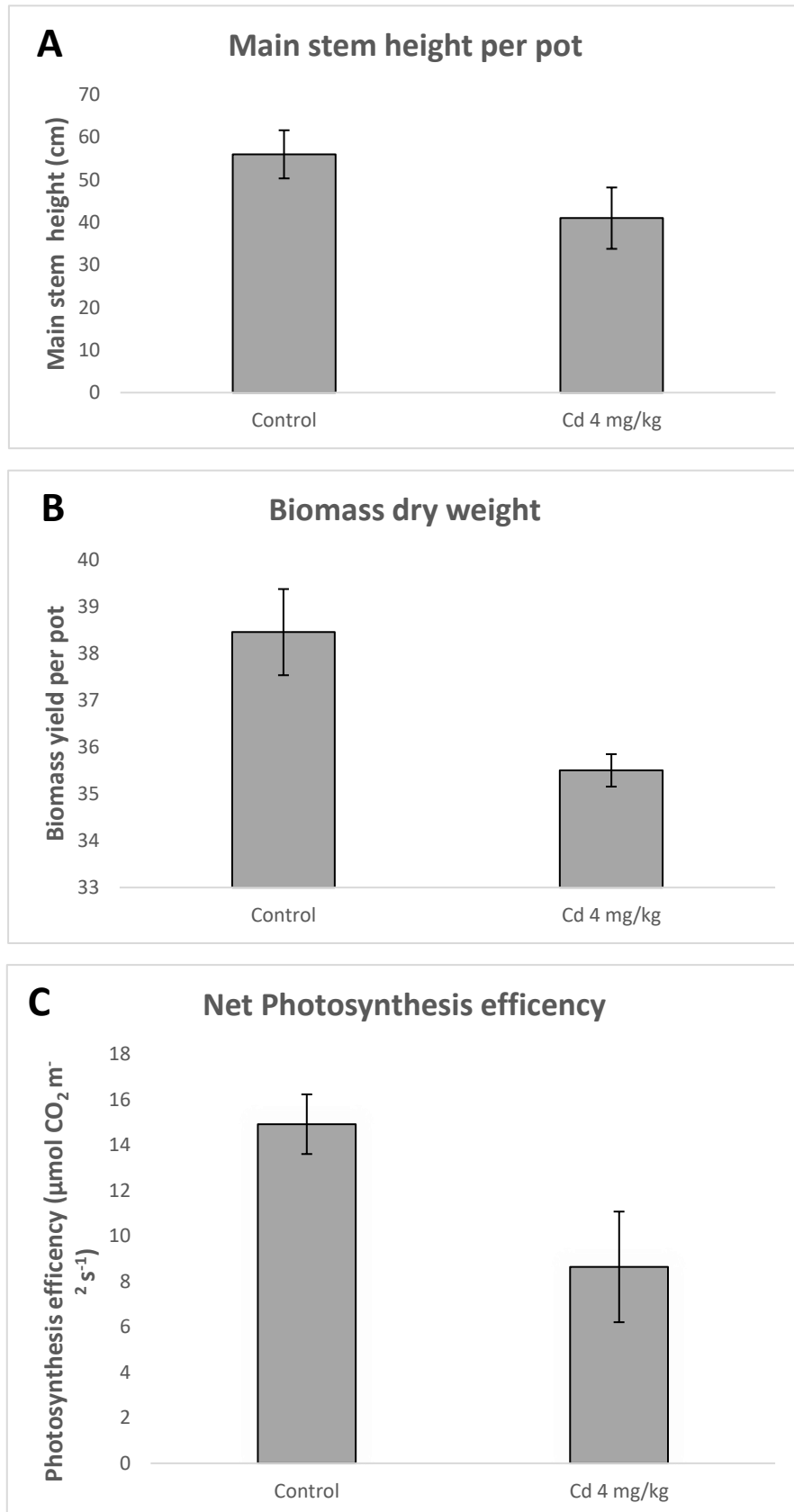


**Figure 18.** Effect of cadmium treatment on morpho-biometric and physiological parameters of G10 ecotype of *A. donax*. A) Main stem height per pot. B) Biomass dry weight. C) Net photosynthesis efficiency.

### 6.3.2 Transcript assembly and annotation

In the present study, we have performed a comprehensive identification of the transcriptional responses of *A. donax* G10 ecotype in both leaves and roots by RNA-Seq approach. A flowchart of the pipeline for the *A. donax* leaf and root transcriptome sequencing and *de novo* assembly is reported in Figure 19. Before sequencing, RNA integrity was checked and the average RNA integrity number (RIN) was 7.05, thus indicating that all the samples had adequate quality to be further processed and sequenced (Table 23). After sequencing, raw reads were filtered to remove reads containing adapters or reads of low quality, so that the downstream analysis was based on a total of 416 million of clean reads with an average value of ~ 34.7 million reads (10.4 Gb) per each sample, the average percentage of Q30 and GC being 94.37 and 55.08 %, respectively (Table 23). *De novo* assembly of clean reads resulted in 378,521 transcripts and 126,668 unigenes with N50 length of 1812 bp and 1555 bp, respectively (Table 23), in line with previously reported N50 values (Evangelistella et al. 2017; Fu et al. 2016; Sicilia et al. 2019; Sicilia et al. 2020). To evaluate the assembly consistency, the filtered unique reads were mapped back into the reconstructed transcriptome, and the average read mapping rate using the alignment software bowtie2 was equal to 69.0 % (Table 23). In addition, both transcript and unigene length distributions were reported (Figure 20). Consequently, these results indicated that the sequencing quality was reliable to perform downstream analysis.

**Table 23.** Summary statistics of the RNA quality and sequencing results

|                     |             |
|---------------------|-------------|
| Average RIN         | 7.05        |
| Clean reads         | 416 million |
| N° Transcripts      | 378,521     |
| N° Unigenes         | 126,668     |
| Mapping rate        | 69.0        |
| Transcript N50 (bp) | 1,812       |
| Unigenes N50 (bp)   | 1,555       |
| Q30 (%)             | 94.37       |
| GC content (%)      | 55.08       |

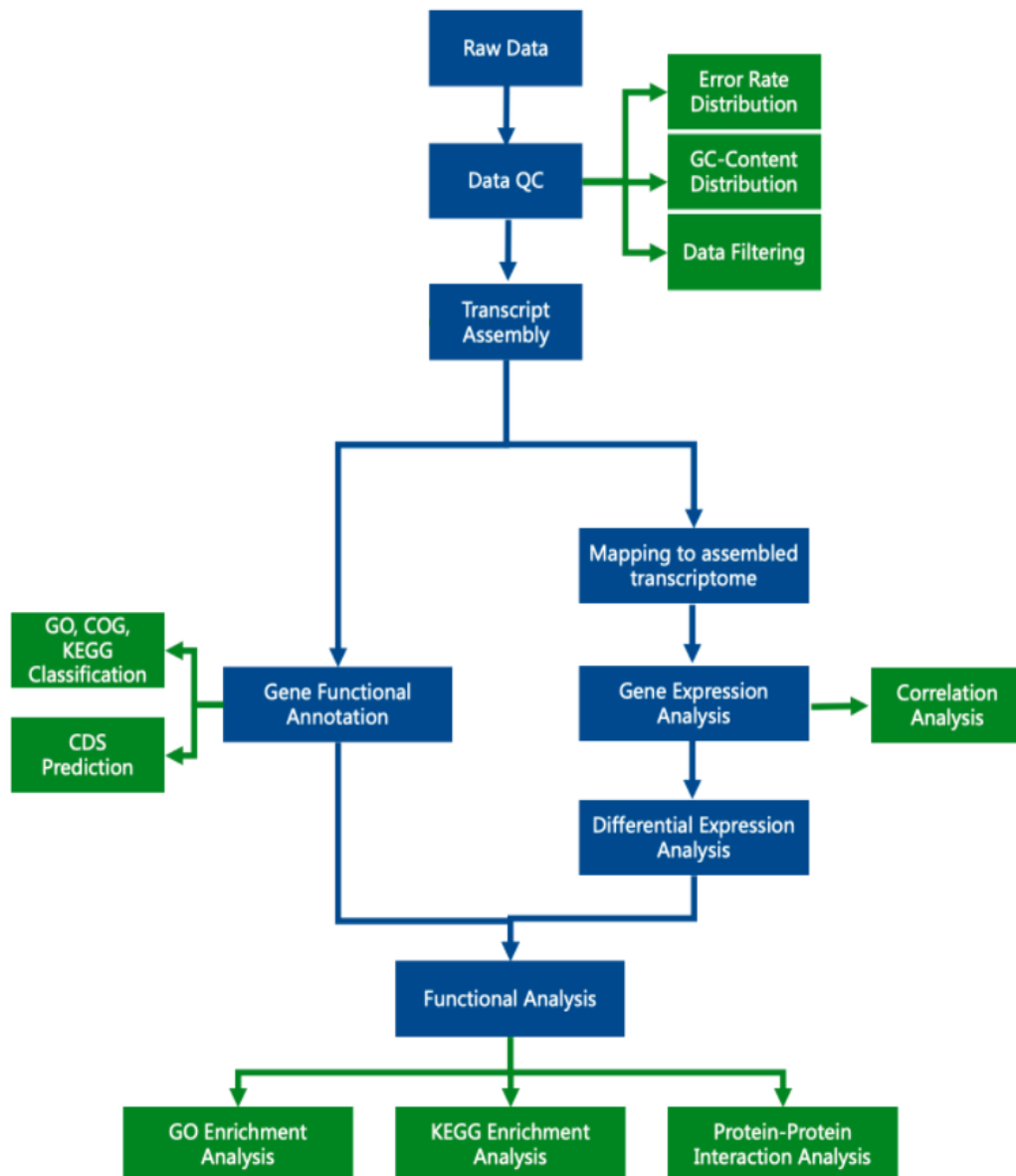


**Figure 19.** Flowchart of *de novo* assembly and analysis of leaves and roots transcriptome of *A. donax*. Firstly, after the full expanded leaves and roots has been sampled, total RNA extraction and cDNA library preparation was carried out. The RNA integrity and purity were evaluated before the Illumina sequencing. The sequencing data were subjected to data quality control to ensure an accurate and reliability results of both reads and bases. The clean read filtered from raw reads has been assembled as to get the reference sequence. *De novo* assembly was carried out by Trinity software with minKmerCov equal to 3, of which the contigs of shared reads has been filtered out by Corset. In addition, Corset works for hierarchical clustering by removing transcripts redundancy, and selecting the longest transcripts as Unigenes. The mapping rate was evaluated by mapped back each clean data onto the Corset assembled transcriptome by RESEM. Finally, to get an reliability gene functional annotation, CDS/EST prediction, differential expression analysis, protein-protein interaction analysis, GO and KEGG enrichment analysis were carried out.

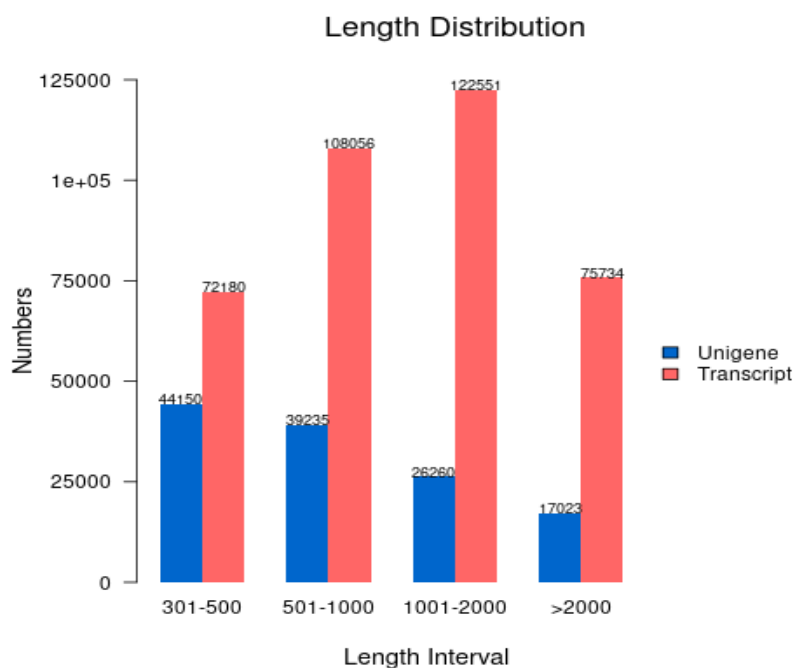


**Figure 20.** Length distribution of Transcripts and Unigenes

All assembled unigenes were blasted into public databases, including National Center for Biotechnology Information (NCBI), Protein family (Pfam), Clusters of Orthologous Groups of proteins (KOG/COG), SwissProt, Ortholog database (KO) and Gene Ontology (GO) (Table 24). A total of 88,139 unigenes were annotated in at least one searched database, the frequency of unigenes annotated in at least one database was 69.58 %. Among them, 73,588 (58.08 %) and 63,917 (50.46 %) assembled unigenes showed identity with sequences in the Nr and Nt database, respectively. The distribution of assembled unigenes homologous to sequences in KO, Swiss-Prot, Pfam, GO and KEGG database were 21.67, 40.83, 41.54, 41.54 and 13.71%, respectively (Table 24).

**Table 24.** The number and frequency of successful annotated genes

| Database                           | Number of unigenes | Frequency % |
|------------------------------------|--------------------|-------------|
| Annotated in NR                    | 73,588             | 58.09       |
| Annotated in NT                    | 63,917             | 50.46       |
| Annotated in KO                    | 27,461             | 21.67       |
| Annotated in SwissProt             | 51,724             | 40.83       |
| Annotated in PFAM                  | 52,630             | 41.54       |
| Annotated in GO                    | 52,627             | 41.54       |
| Annotated in KOG                   | 17,370             | 13.71       |
| Annotated in at least one database | 88,139             | 69.58       |



### 6.3.3 Identification of differentially expressed genes (DEGs)

The characterization of root and leaf *A. donax* transcriptome was accomplished by the identification of those unigenes whose expression level changed upon cadmium treatment. Based on the experimental design, a total of 162 genes showed differential expression in response to Cd treatment, 107 of them differentially expressed in root (Cd\_R vs CK\_R) and the remaining 55 differentially expressed in leaf (Cd\_L vs CK\_L). Among the 107 DEGs found in root, 36 were up-regulated and 71 down-regulated. In leaf, 19 genes resulted up-regulated and 36 down-regulated (Figure 21A). No DEGs were found in common between root and leaf. The higher number of DEGs in root with respect of the leaf suggested that root, representing the interface between soil and plant, is subjected to a wider reprogramming of the gene expression than leaves. DEGs identified in biological replicates clustered together in both organs, indicating good reproducibility of treatment (Figure 22). Moreover, samples either belonging to control or treated samples clustered very close, thus probably explaining the low number of DEGs retrieved when comparing stressed and control samples (Figure 22, 23). On the contrary, a total of 5303 genes were counted as differentially expressed when the Cd\_R vs Cd\_L\* comparison was analyzed (Figure 21B). This result was obtained by subtracting the DEGs found in the comparison CK\_R vs CK\_L (all genes that are differentially expressed because they are tissue specific and not related to cadmium treatment) to the total DEGs retrieved by the comparison Cd\_R vs Cd\_L. Among the 5303 DEGs, 3206 were up-regulated (showing a higher expression in root than in leaf) and 2097 were down-regulated (showing a lower expression in root than in leaf). Validation of RNAseq experiment was performed by measuring the expression levels of eight selected DEGs by quantitative real-time PCR (qRT-PCR) (Figure 24, Table 25). The results show high congruence between RNA-Seq and qRT-PCR (coefficient of determination  $R^2 = 0.91$ ), which accounts for the high reliability of RNA-Seq quantification of gene expression.

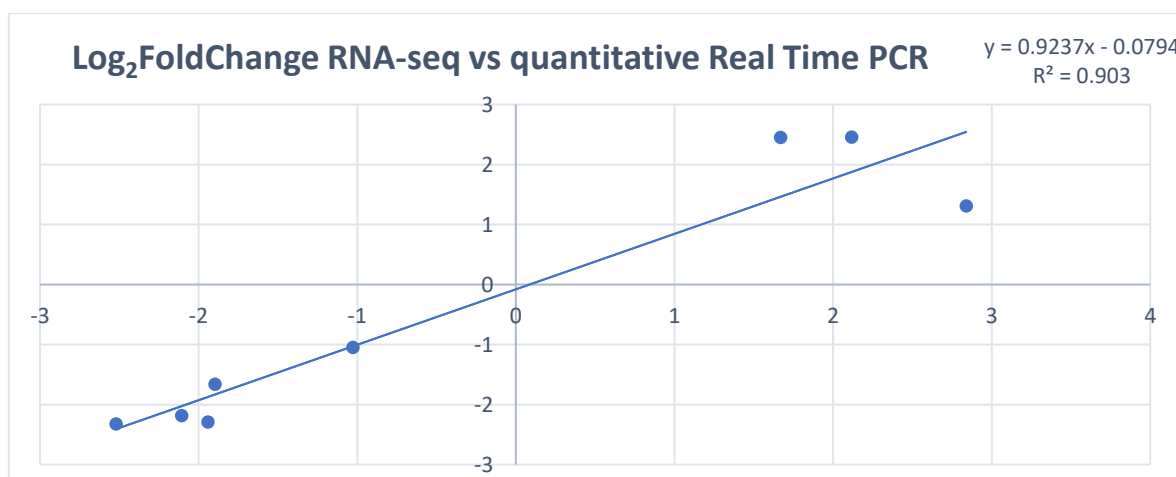
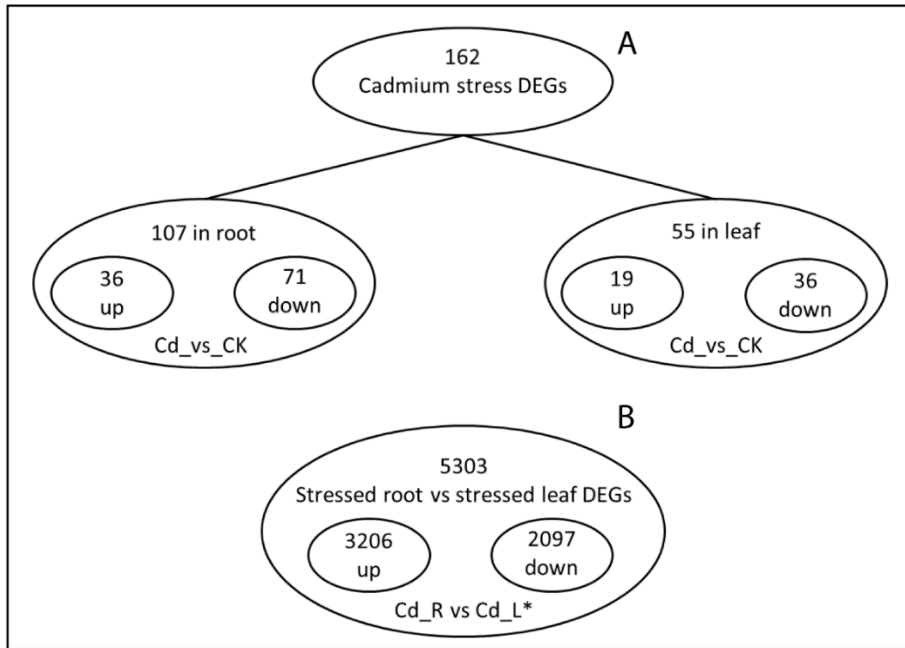
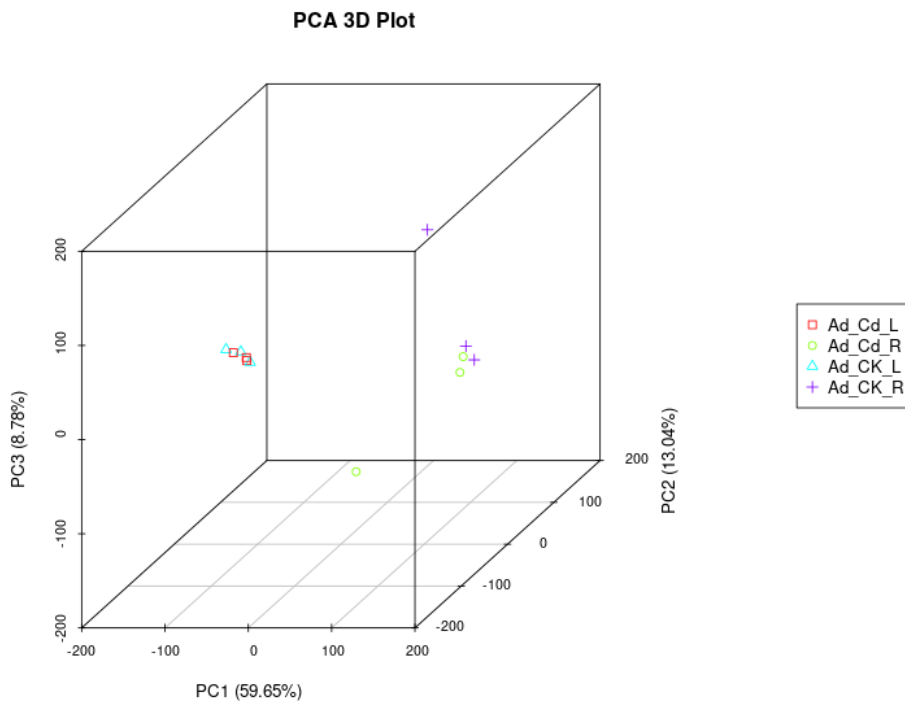


Figure 24. Validation of *A. donax* DEGs by Real Time qRT-PCR



**Figure 21.** Summary of DEGs in roots and leaves of *A. donax* upon cadmium treatment. **A** Number of up-/down-regulated genes by Cd in different tissues (root treated vs control samples; leaf treated vs control samples). **B** Number of regulated genes between different tissues in stressed conditions. \* The stressed root vs stressed leaf DEGs were obtained by subtracting the DEGs belonging to the CK\_R vs CK\_L comparison to the Cd\_R vs Cd\_L comparison.



**Figure 22.** Three-dimension PCA for RNAseq correlation. Principal Component coordinates were calculated using samples readcount.

### Cluster analysis of differentially expressed genes

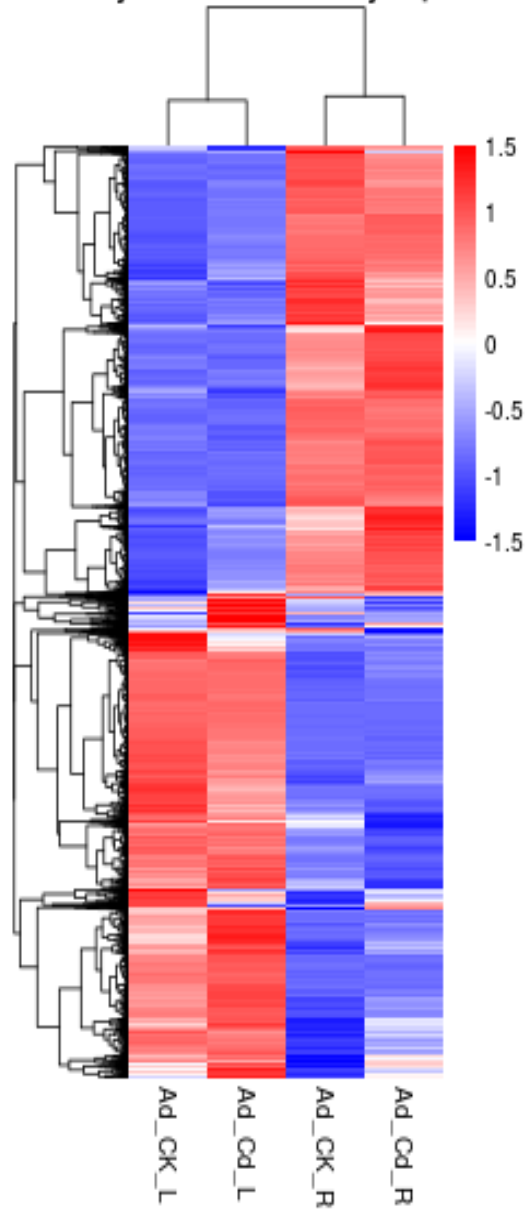


**Figure 23.** Hierarchical clustering map for differential expression genes

**Table 25.** List of DEGs and sequences primers used for Real Time qRT-PCR validation.

| Pattern                      | Cluster ID  | Annotation                                    | log <sub>2</sub> FC<br>Illumina | log <sub>2</sub> FC<br>rt-PCR |
|------------------------------|-------------|-----------------------------------------------|---------------------------------|-------------------------------|
| G10_Cd vs G10_CK Root / Up   | 14691.18708 | Glycine                                       | 2.1175                          | 2.46                          |
| G10_CK_L vs G10_CK_R /Up     | 14691.61095 | UGT85A23_7-deoxyloganetin glucosyltransferase | 1.6694                          | 2.45                          |
| G10_Cd_L vs G10_Cd_R /Up     | 14691.31660 | BAE44                                         | 2.8394                          | 1.31                          |
| G10_Cd vs G10_CK Root / Down | 14691.76303 | ABC_transporter                               | -1.8982                         | -1.662                        |
| G10_Cd vs G10_CK Root / Down | 14691.49288 | Xylanase                                      | -1.0277                         | -1.05                         |
| G10_Cd vs G10_CK Leave/ Down | 14691.50971 | Sucrose 1-fructosyltransferase                | -2.5204                         | -2.32                         |
| G10_Cd vs G10_CK Root/ Down  | 14691.50971 | Sucrose 1-fructosyltransferase                | -1.9425                         | -2.29                         |
| G10_Cd_L vs G10_Cd_R /Down   | 14691.10370 | GQ55                                          | -2.1064                         | -2.183                        |
| All                          | 14691.35187 | Cyclin dependent kinase                       |                                 |                               |

| Cluster ID  | Primer F 5'→3'        | Primer R 5'→3'        |
|-------------|-----------------------|-----------------------|
| 14691.18708 | CGGCATTGGCGGGTATAAAG  | ATTATCGCCGCCACCAGAG   |
| 14691.61095 | CCTGACCAACGGATACCTCG  | ACCATGAAGTCGTTCTGGGTC |
| 14691.31660 | AGTTTGATGGTGATGAGCCGC | GCCACTCCAGGTGCTTCAAC  |
| 14691.76303 | GTTCTACACCTGCTCCGACG  | CGATAGCACGTACGAGGACC  |
| 14691.49288 | ATCCACGTCAGGTTCTACGG  | GGGATCACGCCGTAGTAGAG  |
| 14691.50971 | CATCGACTTCTACCCCGTCG  | GTAGTAGTCGTGGCGGTCG   |
| 14691.50971 | CATCGACTTCTACCCCGTCG  | GTAGTAGTCGTGGCGGTCG   |
| 14691.10370 | GGCCTTACCACCTCTCAAG   | AACAGTGGCCCCGAGAAATC  |
| 14691.35187 | CATACGGCAAGTGTTTCATGG | TCCTTGAGCTGGATGACGTTC |
| 14691.18708 | CGGCATTGGCGGGTATAAAG  | ATTATCGCCGCCACCAGAG   |
| 14691.61095 | CCTGACCAACGGATACCTCG  | ACCATGAAGTCGTTCTGGGTC |

### 6.3.4 Functional classification of DEGs

Gene Ontology (GO) terms, Clusters of Orthologous Groups of protein (KOG) classification and Kyoto Encyclopedia of Genes and Genomes (KEGG) pathway functional enrichment were carried out to identify biological processes or pathways involved in cadmium stress response. Considering Cd\_R vs CK\_R dataset (Figure 25A), “transmembrane transport” (GO:0055085) (4 up- and 4 down-regulated genes), “peptidase activity” (GO:0008233) (1 up- and 4 down-regulated genes) and “lipid binding” (GO:0008289) (0 up- and 5 down-regulated genes) are the three most enriched GO terms. “Intracellular” (GO:0005622) (5 up- and 10 down-regulated genes), “DNA-binding transcription factor activity” (GO:0003700) (1 up- and 6 down-regulated genes) and “catabolic process” (GO:0009056) (1 up- and 3 down-regulated genes) are the most enriched GO terms of Cd\_L vs CK\_L comparison (Figure 25B). As concerns the Cd\_R vs Cd\_L\* sample data set (Figure 25C), “ion binding” (GO:0043167) (451 up- and 295 down-regulated genes), “oxidoreductase activity” (GO:0016491) (156 up- and 103 down-regulated genes), “cellular protein modification process” (GO:0006464) (167 up- and 91 down-regulated genes), “ribosome biogenesis” (GO:0042254) (152 up- and 27 down-regulated genes) and “kinase activity” (GO:0016301) (111 up- and 68 down-regulated genes) are the most enriched GO terms. To predict any possible functions, all identified unigenes (126,668) were aligned to the KOG database to assign their corresponding KOG category (Figure 26). Among the KOG categories, those clusters encoding for “Translation, ribosomal structure and biogenesis” (15.24 %), “Post-translation modification, protein turnover, chaperones” (14.38 %), “General function predict only” (11.59 %) represented the largest group, followed by “Intracellular trafficking, secretion, and vesicular transport” (6.88 %), “Energy production and conversion” (6.84 %), “Signal transduction mechanisms” (6.67 %), “RNA processing and modification” (5.49 %), “Amino acid transport and metabolism” (5.25 %), “Carbohydrate transport and metabolism” (4.68 %), “Transcription” (4.55 %) and “Lipid transport and metabolism” (4.42 %) were the most numerous categories (Figure 26). The sets of DEGs originated from the above-described three comparisons (Cd\_R vs CK\_R, Cd\_L vs CK\_L and Cd\_R vs Cd\_L\*) were mapped onto KEGG enrichment pathways. The main KEGG pathway terms were plotted in the Figure 27. Considering both Cd\_R vs CK\_R and Cd\_L vs CK\_L sample data sets, we observed pathways represented by few DEGs each: “Oxidative phosphorylation”, “Arginine and proline metabolism” and “Monoterpenoid biosynthesis” in Cd\_R vs CK\_R comparison, and “Thiamine metabolism” and “Carotenoid biosynthesis” in Cd\_L vs CK\_L comparison (Figure 27). As concerning Cd\_R vs Cd\_L\* comparison “Plant hormone signal transduction”, “Phenylpropanoid biosynthesis”, “Starch and sucrose metabolism”, “Toll-like receptor signalling pathway” and “Glycolysis/Gluconeogenesis” were the five most represented KEGG pathways (Figure 27).

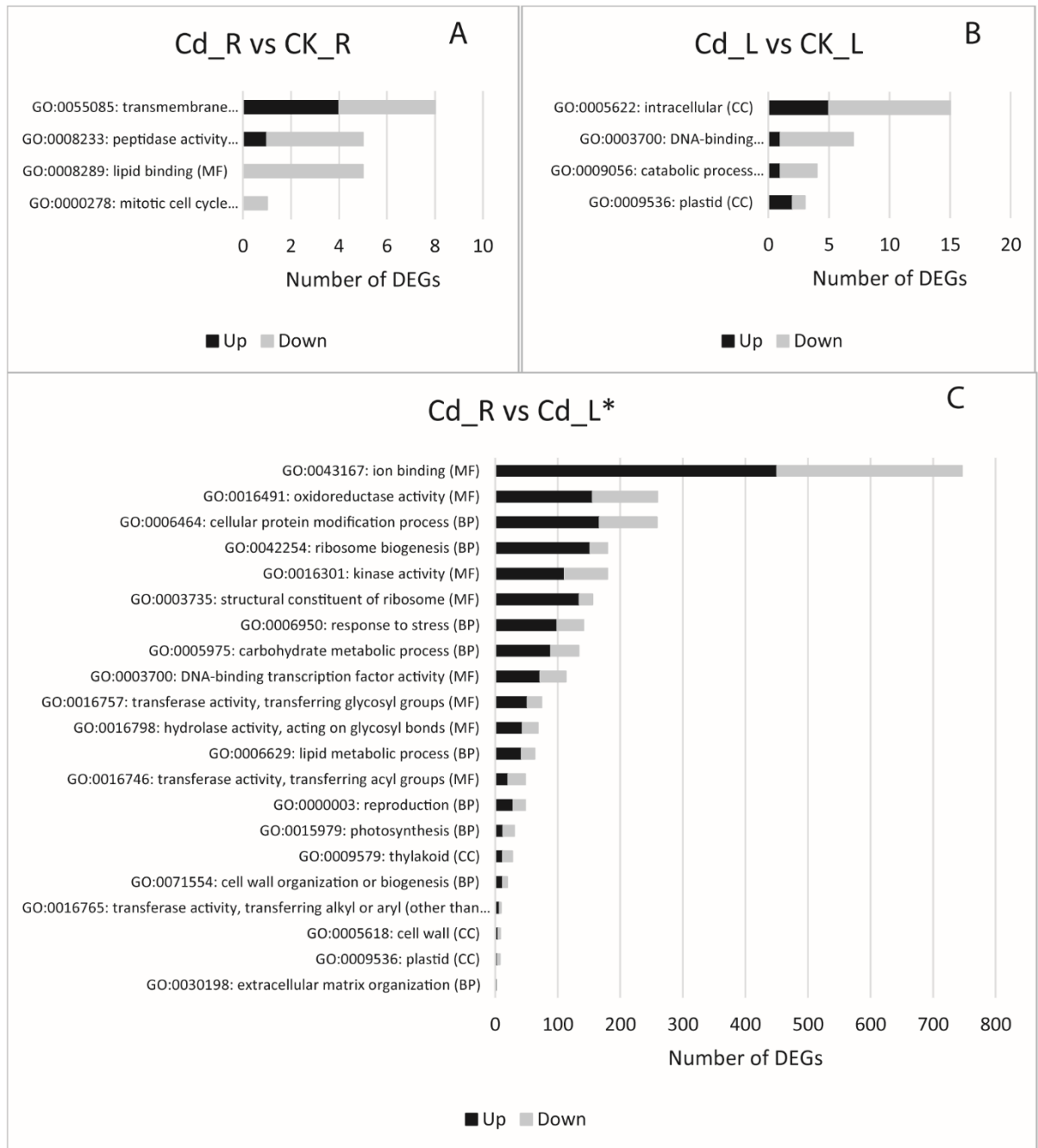


**Figure 25.** Gene Ontology (GO) enrichment for the DEGs of (A) Cd\_R vs CK\_R, (B) Cd\_L vs CK\_L and (C) Cd\_R vs Cd\_L\*. The X-axis indicates the number of DEGs and the Y-axis indicates the subcategories. BP: Biological Process; MF: Molecular Function; CC: Cellular Component.

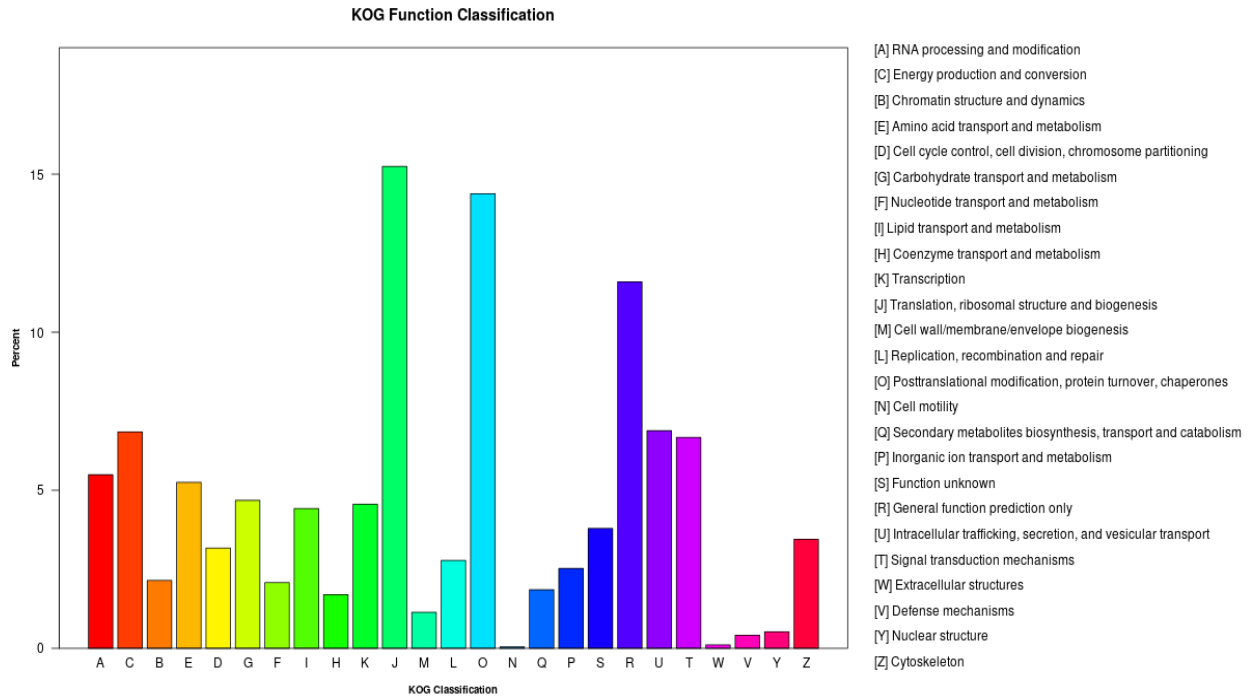


**Figure 26.** KOG functional characterization

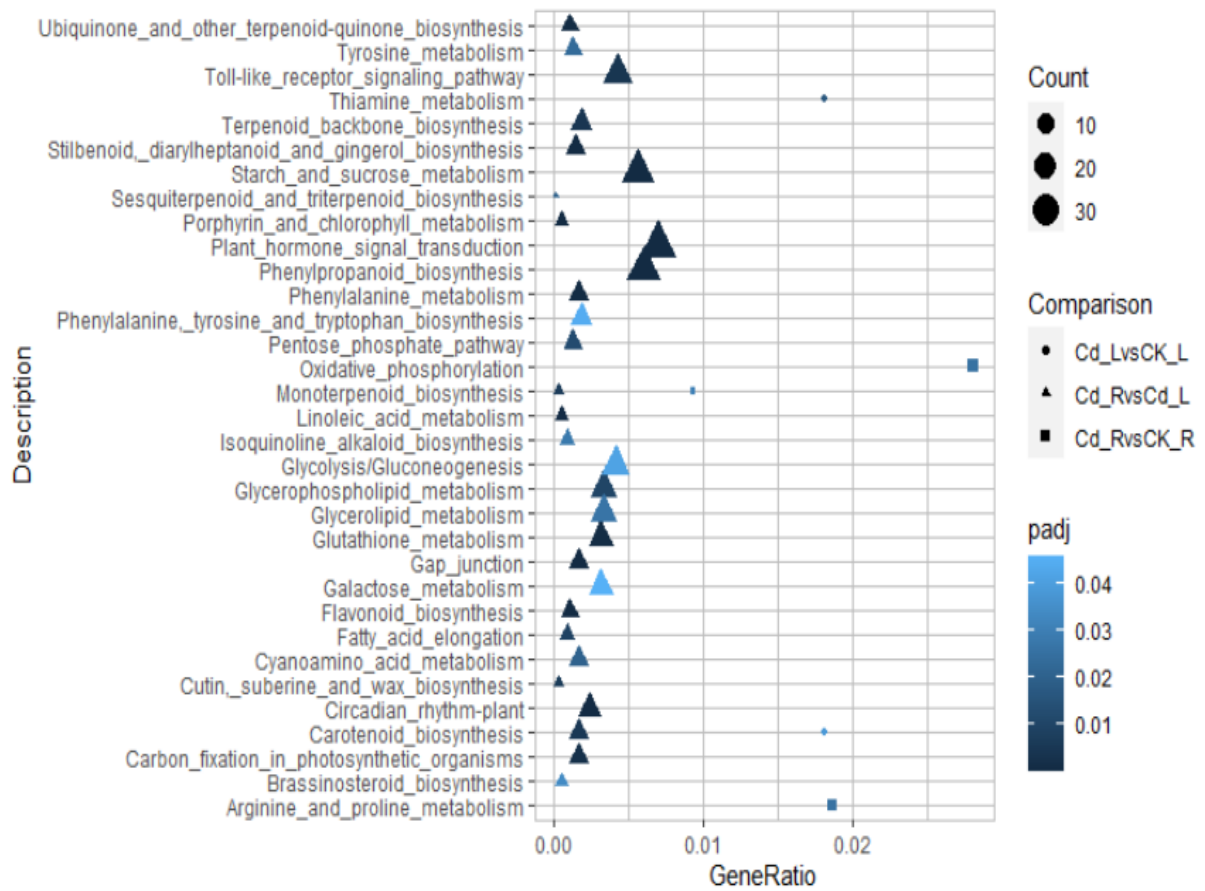


**Figure 27.** Distribution of Kyoto Encyclopedia of Genes and Genomes (KEGG) pathways for differential expressed genes (DEGs) in the Cd\_R vs CK\_R, Cd\_L vs CK\_L and Cd\_R vs Cd\_L\* comparisons.

### 6.3.5 Identification of transcription factor families involved in plant response to cadmium

Transcription factors (TFs) have been identified as candidate targets for ameliorating plant tolerance in case of cadmium treatment. Therefore, DEGs encoding for TFs were retrieved from each comparison (Cd\_R vs CK\_R, Cd\_L vs CK\_L and Cd\_R vs Cd\_L\*), grouped according to the belonging family and sorted for their corresponding abundance (Figure 28). As result of the analysis, the five more abundant transcription factor families resulted “Ethylene responsive transcription factor” (ERF) (29 DEGs), “bzip” (27 DEGs), “WRKY” (23 DEGs), “bHLH” (15 DEGs) and “MYB” (13 DEGs) (Figure 28). When different comparisons were considered, two bHLH (both up-regulated) and two ERF (1 up- and 1 down-regulated) TFs were found in the Cd\_R vs CK\_R dataset and one ERF, two bZIP and one WRKY (all down-regulated) were found in the Cd\_L vs CK\_L dataset. On the contrary, a higher number of DEGs were found in the Cd\_R vs Cd\_L\* dataset: 26 DEGs belonging to ERF family (21 up- and 5 down-regulated), 25 to bZIP family (14 up- and 11-down regulated), 22 to WRKY family (17 up- and 5 down-regulated), 13 to bHLH family (10 up- and 3 down-regulated) and 13 to MYB family (7 up- and 6 down-regulated).

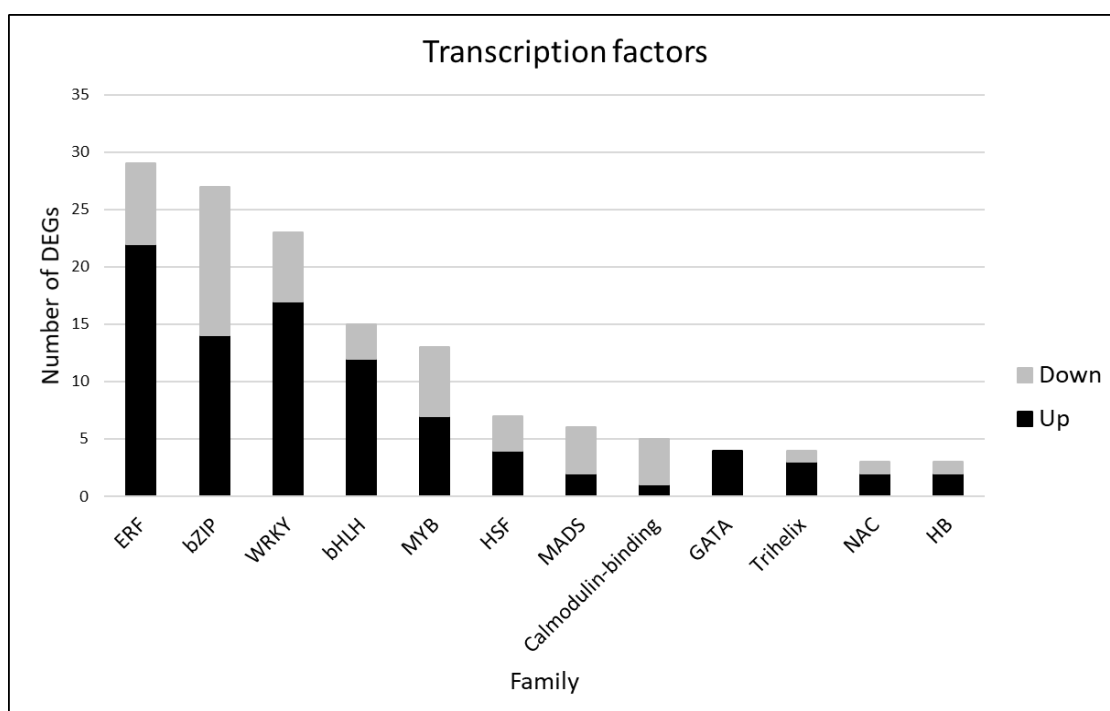


**Figure 28.** DEGs encoding for TFs. The bars represent the overall TFs found in the three comparisons (Cd\_R vs CK\_R, Cd\_L vs CK\_L and Cd\_R vs Cd\_L\*).



### 6.3.6 Main Processes affected by cadmium treatment

To have a comprehensive view of the metabolic changes occurring in *A. donax* L. under Cd treatment, all the significant DEGs of the Cd\_R vs Cd\_L\* comparison were mapped to the MapMan 3.5.1R2 pathways. The analysis indicated that the five most enriched metabolic pathways are “Protein biosynthesis”, “Phytohormone action”, “Nutrient uptake”, “Cell wall organisation” and “Polyamine metabolism” (Table 26).

**Table 26.** Number of DEGs of the Cd\_R vs Cd\_L\* comparison assigned to the top five MapMan 3.5.1R2 pathways. The significant DEG assignment is indicated by pvalue  $\leq 0.05$ .

| Pathway Mapman         | n° of DEGs | Up  | Down | pvalue                 |
|------------------------|------------|-----|------|------------------------|
| Protein biosynthesis   | 130        | 128 | 2    | $3.25 \times 10^{-23}$ |
| Phytohormone action    | 56         | 45  | 11   | $7.61 \times 10^{-06}$ |
| Nutrient uptake        | 18         | 15  | 3    | $1.23 \times 10^{-03}$ |
| Cell wall organisation | 17         | 15  | 2    | $1.17 \times 10^{-02}$ |
| Polyamine metabolism   | 4          | 0   | 4    | $4.80 \times 10^{-02}$ |

The DEGs belonging to these pathways resulted mostly up-regulated in treated root compared to the treated leaf (Cd\_R vs Cd\_L\*), except for genes of “Polyamine metabolism” that resulted all down-regulated in root compared with the leaf. In addition, considering their crucial role in heavy metal stress response, the coding sequence of each transcripts belonging to “Oxidative stress”, “Heavy metal ATPase 3 (HMA3) transporters” and “NRAMP transporters” categories along with the clusters resulted from the MapMan analysis (Table 26) have been aligned against the *Arabidopsis thaliana* genome (TAIR10) and the score of these alignments was reported (identity score and e-value) thus providing valuable indications of the cluster similarity with the reported genes (Table 27). Congruously, Table 27 reports clusters whose e-value was  $< 0.05$  and showing a threshold of  $\pm 2.000 \log_2$  fold change. The complete list of DEGs belonging to these pathways is reported in table 28. Regarding the “Phytohormone” category, nine-cis-epoxycarotenoid dioxygenase 9 catalyzing the first step of abscisic-acid (ABA) biosynthesis from carotenoids is down regulated in cadmium treated giant reed roots (Cd\_R vs Cd\_L\*) (Table 27). Moreover, abscisic acid 8'-hydroxylase 1 – related involved in the first step of the oxidative degradation of (+)-ABA was up-regulated in the Cd\_R vs Cd\_L\* comparison, suggesting that cadmium treatment suppresses ABA synthesis and promotes its degradation in giant reed root thus quenching the signal cascade induced by this hormone. Indole-3-pyruvate monooxygenase YUCCA2-related encoding an enzyme involved in auxin biosynthesis and

converting the indole-3-pyruvic acid (IPA) to indole-3-acetic acid (IAA) resulted up regulated in the cadmium treated roots with respect to treated leaf (Cd\_R vs Cd\_L\*). Similarly, the gene encoding 1-aminocyclopropane-1-carboxylate oxidase (ACO) encoding an enzyme synthesizing the plant hormone ethylene was up-regulated in giant reed roots treated with cadmium. Gibberellin 20 oxidase 2, encoding a key oxidase enzyme in the biosynthesis of gibberellins, considered potent signaling molecules to enhance growth and developmental processes under abiotic stress conditions (Colebrook et al. 2014), was also found up-regulated in the Cd\_R vs Cd\_L\* comparison. Signalling peptides, also known as peptide hormones, along with classical phytohormones, are involved in plant intracellular signalling. C-terminally encoded peptide (CEP), two genes encoding ROTUNDIFOLIA like proteins, and a transcript encoding CLAVATA3/ESR-RELATED 25 were among the sharply up-regulated genes in the cadmium treated root (Cd\_R vs Cd\_L\*). As concerns the “Transcription factors” category, several transcripts encoding Ethylene-Responsive Transcription (ERT) factors which have been reported to be involved in the ethylene signalling transduction pathway in plant abiotic stress response (Nakano et al. 2006) were found sharply up regulated in the Cd\_R vs Cd\_L\*. Therefore, the results indicate that ethylene-triggered signal cascade plays a crucial role in giant reed root under cadmium treatment. Interestingly, the WRKY gene family is also over-represented in the “Transcription factor” category (Table 27) and in particular WRKY9, that is involved in increased root suberin deposition (Krishnamurthy et al. 2021), WRKY33 that controls the apoplastic barrier formation in roots (Krishnamurthy et al. 2020) and WRKY50 positively regulating resistance against necrotrophic pathogens (Hussain et al. 2018) were found up-regulated in cadmium treated giant reed roots (Cd\_R vs Cd\_L\*). Conversely, WRKY46 that seems to be involved in hypersensitivity to drought and salt stress (Ding et al. 2015) was down regulated (Table 27). The analysis of the “Cell wall” category reveals that transcripts encoding alpha expansin 11, that causes loosening and extension of plant cell walls by disrupting non-covalent bonding between cellulose microfibrils and matrix glucans (Wang et al. 2013) were up-regulated in the Cd\_R vs Cd\_L\* comparison. The genes encoding cinnamoyl Coa reductase, laccase and membrane-associated progesterone binding protein 3 involved in lignin biosynthesis were strongly induced in cadmium treated roots. Moreover, pectin methylesterase 61 and invertase/pectin methylesterase inhibitor gene have been found up-regulated in Cd-treated root thus confirming the overall results related to “Cell wall” category that this cellular district is target of deep remodeling under cadmium stress (Wormit and Usadel 2018). Regarding the “Nutrient uptake” category, transcripts related with nitrogen metabolism, such as nitrate reductase and high affinity nitrate transporter 2.5 were upregulated by cadmium treatment in giant reed roots, being they involved in nitrogen assimilation and uptake, respectively. Furthermore, phosphate transporter encoding genes involved in phosphate uptake at plasma membrane level were also

upregulated whereas vacuolar iron transporter required for iron sequestration into vacuoles was downregulated in cadmium treated roots. Overall, these results support that cadmium treatment induced an imbalance of the main nutrient levels which can cause disturbances in plant growth. Polyamines (PAs) are ubiquitous low molecular weight aliphatic cations that are present in all organisms; the major PAs in plants are putrescine, spermidine, and spermine, and to a lesser extent, cadaverine. Cadaverine, a structurally different diamine, has an independent biosynthetic pathway as it is synthesized from lysine by lysine decarboxylase (LDC) (Rajpal and Tomar 2020). Agmatine deiminase catalyzes the hydrolysis of agmatine into N-carbamoylputrescine in the arginine decarboxylase (ADC) pathway of putrescine biosynthesis. In the “Polyamine metabolism” category, lysine decarboxylase gene was upregulated whereas agmatine deiminase was downregulated in cadmium treated roots, suggesting that under heavy metal stress, the pathway leading to cadaverine is preferentially undertaken in giant reed root. The amount of cadmium inside the root cells depends on the balance between metal intrusion or uptake, normally determined by general metal transporters belonging to the NRAMP family, and metal extrusion. The efflux systems, namely heavy metal ATPase 3 (HMA3) transporters translocate cadmium both outside the cell and into the vacuole (Nazar et al. 2012; Hohabubul et al. 2021). The analysis of “Metal transporter” group revealed that transcript encoding NRAMP1 transporter was upregulated whilst HMA3 transporter encoding gene were downregulated in the cadmium treated root thus indicating that the mechanisms to avoid cadmium entrance and residence are not implemented in our conditions. As concerns the ROS scavenging regulatory mechanisms, the analysis of Cd\_R vs Cd\_L\* revealed that superoxide dismutase (SOD), ascorbate peroxidase (APX), catalase and NADPH oxidase 1 encoding genes are all up-regulated suggesting that H<sub>2</sub>O<sub>2</sub> could be the main ROS the *A. donax* roots have to cope with under cadmium treatment. Moreover, many transcripts encoding glutathione transferases (GSTs) are also up-regulated (Table 27) concordantly with their role in abiotic stress relief (Lo Piero et al. 2010; Puglisi et al. 2013). Moreover, transcripts encoding glutaredoxin-C5, small redox enzyme of approximately one hundred amino-acid residues involved in the reduction of specific disulfides such as glutathionylated proteins (Couturier et al. 2011) were found strongly induced in cadmium treated roots. Finally, the “Protein biosynthesis” category encompasses a plethora of genes involved in ribosome constitution (ribosomal proteins) and DNA-directed RNA polymerase II subunit that resulted up regulated indicating that this pathway is sharply activated by cadmium treatment in giant reed roots (data not shown).

**Table 27.** List of DEG related to cadmium stress response identified in Cd\_R vs Cd\_L\* sample data set

| Cluster                      | Annotation                                                                             | Gene identifier | Log <sub>2</sub> FC | Identity % | e-Value   |
|------------------------------|----------------------------------------------------------------------------------------|-----------------|---------------------|------------|-----------|
| <i>Phytohormone action</i>   |                                                                                        |                 |                     |            |           |
| 14691.43609                  | nine-cis-epoxycarotenoid dioxygenase                                                   | AT1G78390.1     | -3.2009             | 69         | 1.18E-179 |
| 14691.50813                  | Abscissic acid 8'-hydroxylase 1-related                                                | AT4G19230.1     | 2.0026              | 72         | 0         |
| 14691.49474                  | Indole-3-pyruvate monooxygenase YUCCA2-related                                         | AT5G25620.2     | -2.6551             | 60         | 2.7E-74   |
| 14691.13200                  | auxin efflux carrier component 9 (PIN)                                                 | AT5G57090.1     | 6,7678              | 53         | 1.50e-52  |
| 14691.11710                  | 1-Aminocyclopropane-1-carboxylate oxidase 5l                                           | AT1G77330.1     | 3.3103              | 63         | 9.05E-115 |
| 14691.10785                  | ETHYLENE-INSENSITIVE 2 (EIN2)                                                          | AT5G03280.1     | 1.9616              | 54         | 3.91e-46  |
| 14691.11833                  | gibberellin 20 oxidase 2                                                               | AT5G51810.1     | 2.9104              | 60         | 6.4E-162  |
| 14691.10408                  | ROTUNDIFOLIA like 8                                                                    | AT2G39705.1     | 7.0488              | 68         | 1.12E-09  |
| 14691.12312                  | ROTUNDIFOLIA like 15                                                                   | AT1G68825.1     | 6.1578              | 69         | 4.21E-10  |
| 15957.0                      | CLAVATA3/ESR-RELATED 25                                                                | AT3G28455.1     | 6.0686              | 83         | 1.21E-4   |
| 14691.82632                  | C-TERMINALLY ENCODED PEPTIDE 1                                                         | AT5G66815.1     | 9.4341              | 74         | 4.30E-04  |
| <i>Transcription factors</i> |                                                                                        |                 |                     |            |           |
| 14691.27999                  | Ethylene-Responsive Transcription Factor CRF5-Related                                  | AT2G20880.1     | 2.4027              | 92         | 3.47E-35  |
| 14691.77282                  | Ethylene-Responsive Transcription Factor ERF003                                        | AT5G25190.1     | 7.1758              | 70         | 1.54E-12  |
| 15337.0                      | AP2-Like Ethylene-Responsive Transcription Factor AIL1                                 | AT1G72570.1     | 7.117               | 87         | 5.02E-117 |
| 14691.5263                   | Ethylene-Responsive Transcription Factor ERF071-Related                                | AT2G47520.1     | 5.4749              | 78         | 1.22E-12  |
| 14691.17960                  | Ethylene-Responsive Transcription Factor CRF1-Related                                  | AT3G14230.1     | 3.9041              | 96         | 4.31E-11  |
| 14691.397                    | octadecanoid-responsive Arabidopsis AP2/ERF 59                                         | AT1G06160.1     | 5.2872              | 61         | 2.22E-19  |
| 14691.11372                  | related to AP2 11                                                                      | AT5G19790.1     | 3.196               | 90         | 2.84E-14  |
| 14691.28900                  | ERF domain protein 11                                                                  | AT1G28370.1     | 2.4679              | 74         | 1.49E-03  |
| 14691.32159                  | DNA-binding superfamily protein member of the ERF (ethylene response factor) subfamily | AT1G15360.1     | -2.39               | 93         | 2.47E-12  |
| 14691.82651                  | bZIP transcription factor family protein                                               | AT1G68640.1     | 2.4872              | 63         | 3.05E-101 |
| 14691.13800                  | Basic-leucine zipper (bZIP) transcription factor family protein                        | AT2G42380.2     | 3.7627              | 72         | 2.05E-42  |
| 19280.1                      | WRKY DNA-binding protein 31                                                            | AT4G22070.1     | 6.1847              | 72         | 4.18E-63  |
| 14691.7381                   | WRKY DNA-binding protein 9                                                             | AT1G68150.1     | 5.7632              | 63         | 4.79E-42  |

|                             |                                                             |             |         |    |           |
|-----------------------------|-------------------------------------------------------------|-------------|---------|----|-----------|
| 14691.78281                 | WRKY DNA-binding protein 33                                 | AT2G38470.1 | 5.4276  | 84 | 6.74E-29  |
| 32613.0                     | WRKY DNA-binding protein 46                                 | AT2G46400.1 | -2.1896 | 70 | 5.80E-14  |
| 14691.59464                 | WRKY family transcription factor                            | AT2G44745.1 | -4.8279 | 77 | 4.73E-60  |
| 14691.7255                  | WRKY DNA-binding protein 50                                 | AT5G26170.1 | 4.2467  | 72 | 1.92E-25  |
| 14691.57513                 | Transcription factor BHLH66-Related                         | AT4G30980.1 | 2.4623  | 98 | 3.22E-24  |
| 14691.57184                 | Helix-loop-helix DNA-binding domain (HLH)                   | AT4G05170.1 | -2.2109 | 83 | 1.35E-21  |
| 14691.73182                 | Transcription factor BHLH71-RELATED                         | AT1G22490.1 | 7.0841  | 82 | 3.30E-15  |
| 14691.61708                 | MYB domain PROTEIN 11-RELATED                               | AT2G47460.1 | -2.8152 | 85 | 2.61E-15  |
| 14691.15951                 | myb domain protein 24                                       | AT5G40350.1 | 5.4902  | 82 | 3.71E-55  |
| 14691.40443                 | Transcription factor RAX2                                   | AT2G36890.1 | -2.2491 | 78 | 6.01E-21  |
| <i>Nutrient uptake</i>      |                                                             |             |         |    |           |
| 14691.17907                 | nitrate transporter 2.5                                     | AT1G12940.1 | 3.835   | 68 | 0         |
| 14691.36103                 | nitrate reductase 1                                         | AT1G77760.1 | 4.0674  | 61 | 8.24E-145 |
| 14691.51441                 | phosphate transporter 1.7                                   | AT3G54700.1 | 2.1772  | 71 | 1.34E-81  |
| 14691.45899                 | phosphate transporter 1.4                                   | AT2G38940.1 | 2.0997  | 76 | 0         |
| 14691.23657                 | vacuolar iron transporter 1                                 | AT2G01770.1 | -2.4401 | 71 | 3.72E-58  |
| <i>Cell wall</i>            |                                                             |             |         |    |           |
| 20197.0                     | pectin methylesterase 61                                    | AT3G59010.1 | 5.3189  | 65 | 3.93E-65  |
| 14691.66836                 | Plant invertase/pectin methylesterase inhibitor superfamily | AT5G09760.1 | 4.3545  | 62 | 1.03E-108 |
| 14691.14990                 | cinnamoyl coa reductase 1                                   | AT2G33570.1 | 3.4503  | 64 | 2.51E-149 |
| 14691.6397                  | laccase-8                                                   | AT3G09220.1 | 3,9852  | 42 | 2.24e-74  |
| 14691.27253                 | membrane-associated progesterone binding protein 3          | AT3G48890.1 | 2.2593  | 84 | 2.72E-16  |
| 14691.76733                 | alpha expansin 11                                           | AT1G20190.1 | 6.7503  | 73 | 6.73E-132 |
| 14691.8155                  | EG45-LIKE domain containing protein 1 -related              | AT4G30380.1 | 7.2163  | 61 | 3.44E-36  |
| <i>Polyamine metabolism</i> |                                                             |             |         |    |           |
| 14691.48898                 | Agmatine deiminase                                          | AT5G08170.1 | -3.3113 | 72 | 1.82E-49  |
| 14691.6139                  | Putative lysine decarboxylase family protein                | AT2G28305.1 | 4.1682  | 82 | 1.93E-115 |
| <i>ROS scavenging</i>       |                                                             |             |         |    |           |
| 14691.12641                 | NADPH oxidase 1                                             | AT1G09090.1 | 7.1387  | 50 | 5.55e-4   |
| 14691.9595                  | Superoxide dismutase                                        | AT1G08830.2 | 6.7735  | 55 | 2.49e-46  |
| 14691.24413                 | Ascorbate peroxidase 3                                      | AT4G35000.1 | 3.4836  | 84 | 7.24e-59  |

|                                 |                                            |                 |         |    |          |
|---------------------------------|--------------------------------------------|-----------------|---------|----|----------|
| 14691.9539                      | Glutathione S-transferase                  | AT1G78340.<br>1 | 9.5248  | 52 | 9.61e-66 |
| 10504.0                         | Catalase                                   | AT1G07890.<br>6 | 6.3794  | 39 | 3.30e-4  |
| 14691.81808                     | Glutaredoxin-C5                            | AT5G14070.<br>1 | 7.2257  | 55 | 4.69e-35 |
| <i>Heavy metal transporters</i> |                                            |                 |         |    |          |
| 14691.35424                     | Cadmium / zinc-transporting<br>ATPase HMA3 | AT4G30120.<br>1 | -3.7045 | 55 | 2.90e-42 |
| 27204.0                         | Metal transporter Nramp1                   | AT1G80830.<br>1 | 3.6765  | 57 | 2.06e-70 |

**Table 28.** List of significant DEGs of the Cd\_R vs Cd\_L\* comparison

| BindCode                    | Id                  | Description                                          | BinName                                                                                                                                               | Cd_R vs Cd_L |
|-----------------------------|---------------------|------------------------------------------------------|-------------------------------------------------------------------------------------------------------------------------------------------------------|--------------|
| <i>Polyamine metabolism</i> |                     |                                                      |                                                                                                                                                       |              |
| 8.1.1.2                     | cluster-14691.48898 | Agmatine deiminase                                   | Polyamine metabolism.putrescine biosynthesis.plastidial/nuclear pathway.agmatine iminohydrolase                                                       | -3.3113      |
| 8.1.1.2                     | cluster-14691.45377 | Agmatine deiminase                                   | Polyamine metabolism.putrescine biosynthesis.plastidial/nuclear pathway.agmatine iminohydrolase                                                       | -1.4654      |
| 8.1.1.2                     | cluster-14691.45378 | Agmatine deiminase                                   | Polyamine metabolism.putrescine biosynthesis.plastidial/nuclear pathway.agmatine iminohydrolase                                                       | -1.5005      |
| 8.5.2.2                     | cluster-14691.48693 | Polyamine oxidase 2                                  | Polyamine metabolism. polyamine degradation.FAD-dependent polyamine oxidase activities.peroxisomal polyamine oxidase (PAO2/3/4)                       | -1.4462      |
| <i>Phytohormone action</i>  |                     |                                                      |                                                                                                                                                       |              |
| 11.1.1.4                    | cluster-14691.43609 | neoxanthin cleavage protein                          | Phytohormone action.abscisic acid.biosynthesis.neoxanthin cleavage protein                                                                            | -3.2009      |
| 11.1.1.6                    | cluster-14691.60538 | xanthoxin oxidase molybdopterin sulfurase (ABA3)     | Phytohormone action.abscisic acid.biosynthesis.xanthoxin oxidase molybdopterin sulfurase (ABA3)                                                       | -1.1117      |
| 11.1.2.1.1.2                | cluster-14691.49163 | protein phosphatase 2C 6                             | Phytohormone action.abscisic acid.perception and signalling.receptor activities.cytoplasm-localized receptor complex.regulatory phosphatase component | -1.2224      |
| 11.1.2.3                    | cluster-14691.16178 | signal transducer of abscisic acid perception (RHA2) | Phytohormone action.abscisic acid.perception and signalling.signal transducer (RHA2)                                                                  | 1.3468       |
| 11.1.3.2                    | cluster-14691.50813 | abscisic acid hydroxylase                            | Phytohormone action.abscisic acid.conjugation and degradation.abscisic acid hydroxylase                                                               | 2.0026       |
| 11.2.1.1.2                  | cluster-14691.49474 | putative indole-3-pyruvate monooxygenase YUCCA9      | Phytohormone action. auxin. biosynthesis. indole-3-pyruvic acid (IPyA) pathway.flavin-dependent monooxygenase (YUCCA)                                 | -2.6551      |
| 11.2.2.2                    | cluster-14691.15466 | auxin-responsive protein IAA9-like                   | Phytohormone action.auxin.perception and signal transduction.transcriptional repressor (IAA/AUX)                                                      | 1.9826       |
| 11.2.4.1.1                  | cluster-14691.35301 | putative auxin efflux carrier component 4            | Phytohormone action.auxin.transport.polar auxin transport.auxin transporter (PIN)                                                                     | -1.6076      |
| 11.2.4.1.1                  | cluster-14691.35301 | putative auxin efflux carrier component 4            | Phytohormone action.auxin.transport.polar auxin transport.auxin transporter (PIN)                                                                     | -1.6076      |

|            |                     |                                                                        |                                                                                                                                      |         |
|------------|---------------------|------------------------------------------------------------------------|--------------------------------------------------------------------------------------------------------------------------------------|---------|
| 11.2.4.1.1 | cluster-14691.31627 | auxin efflux carrier component 1a                                      | Phytohormone action.auxin.transport.polar auxin transport.auxin transporter (PIN)                                                    | 2.0014  |
| 11.2.4.1.1 | cluster-14691.13200 | probable auxin efflux carrier component 9                              | Phytohormone action.auxin.transport.polar auxin transport.auxin transporter (PIN)                                                    | 6.7678  |
| 11.2.4.2   | cluster-14691.13007 | auxin efflux transporter (PILS)                                        | Phytohormone action.auxin.transport.auxin efflux transporter (PILS)                                                                  | 8.9229  |
| 11.4.1.2   | cluster-14691.6139  | cytokinin phosphoribohydrolase                                         | Phytohormone action.cytokinin.biosynthesis.cytokinin phosphoribohydrolase                                                            | 4.1682  |
| 11.4.1.2   | cluster-14691.40808 | cytokinin riboside 5'-monophosphate phosphoribohydrolase LOGL1         | Phytohormone action.cytokinin.biosynthesis.cytokinin phosphoribohydrolase                                                            | 1.2273  |
| 11.4.2.5   | cluster-14691.16490 | A-type cytokinin ARR response negative regulator                       | Phytohormone action.cytokinin.perception and signal transduction.A-type ARR response negative regulator                              | 1.955   |
| 11.4.2.5   | cluster-14691.55777 | Two-component response regulator ORR10                                 | Phytohormone action.cytokinin.perception and signal transduction.A-type ARR response negative regulator                              | 1.5482  |
| 11.4.3.1   | cluster-14691.64014 | UDP-dependent glycosyl transferase                                     | Phytohormone action.cytokinin.conjugation and degradation.UDP-dependent glycosyl transferase                                         | 1.3384  |
| 11.5.1.2   | cluster-14691.52687 | 1-aminocyclopropane-1-carboxylate (ACC) oxidase                        | Phytohormone action. ethylene. biosynthesis.1-aminocyclopropane-1-carboxylate (ACC) oxidase                                          | -1.3363 |
| 11.5.1.2   | cluster-14691.11710 | 1-aminocyclopropane-1-carboxylate (ACC) oxidase                        | Phytohormone action.ethylene.biosynthesis.1-aminocyclopropane-1-carboxylate (ACC) oxidase                                            | 3.3103  |
| 11.5.1.2   | cluster-14691.30304 | 1-aminocyclopropane-1-carboxylate (ACC) oxidase                        | Phytohormone action. ethylene. biosynthesis.1-aminocyclopropane-1-carboxylate (ACC) oxidase                                          | 1.0988  |
| 11.5.2.4   | cluster-14691.2106  | ethylene signal modulator (ARGOS)                                      | Phytohormone action.ethylene.perception and signal transduction.signal modulator (ARGOS)                                             | 4.7361  |
| 11.5.2.6   | cluster-14691.10785 | ethylene signal transducer (EIN2)                                      | Phytohormone action.ethylene.perception and signal transduction.signal transducer (EIN2)                                             | 1.9616  |
| 11.5.2.8   | cluster-14691.10463 | ethylene signal transducer (EIN3/EIL)                                  | Phytohormone action.ethylene.perception and signal transduction.signal transducer (EIN3/EIL)                                         | 1.756   |
| 11.5.2.9   | cluster-14691.44992 | EIN3-substrate-adaptor of SCF ubiquitin protein ligase complex (EBF)   | Phytohormone action.ethylene.perception and signal transduction.EIN3-substrate-adaptor of SCF ubiquitin protein ligase complex (EBF) | 1.131   |
| 11.6.1.5   | cluster-14691.11833 | gibberellin 20-oxidase                                                 | Phytohormone action.gibberellin.biosynthesis.gibberellin 20-oxidase                                                                  | 2.9104  |
| 11.6.2.3   | cluster-14691.29389 | substrate adaptor of gibberellin signalling SCF ubiquitin ligase (SLY) | Phytohormone action.gibberellin.perception and signal transduction.substrate adaptor of SCF ubiquitin ligase (SLY)                   | 1.1021  |
| 11.6.3.1   | cluster-14691.77995 | gibberellin modification enzyme (ELA)                                  | Phytohormone action.gibberellin.modification and degradation.gibberellin modification enzyme (ELA)                                   | 2.8169  |
| 11.7.1.2   | cluster-14691.65388 | 13-lipoxygenase (LOX)                                                  | Phytohormone action.jasmonic acid.biosynthesis.13-lipoxygenase (LOX)                                                                 | -2.6763 |



|             |                     |                                                 |                                                                                                                                                      |         |
|-------------|---------------------|-------------------------------------------------|------------------------------------------------------------------------------------------------------------------------------------------------------|---------|
| 11.7.1.4    | cluster-14691.51153 | allene oxidase cyclase (AOC)                    | Phytohormone action.jasmonic acid.biosynthesis.allene oxidase cyclase (AOC)                                                                          | -1.2624 |
| 11.7.1.9    | cluster-14691.64123 | acyl-CoA thioesterase (ACH)                     | Phytohormone action.jasmonic acid.biosynthesis.acyl-CoA thioesterase (ACH)                                                                           | -1.2535 |
| 11.7.1.9    | cluster-14691.60961 | acyl-CoA thioesterase (ACH)                     | Phytohormone action.jasmonic acid.biosynthesis.acyl-CoA thioesterase (ACH)                                                                           | -1.2882 |
| 11.7.2.1.2  | cluster-37109.0     | component JAZ of jasmonic acid receptor complex | Phytohormone action.jasmonic acid.perception and signal transduction.receptor complex.component JAZ                                                  | 7.2083  |
| 11.8.2.2    | cluster-14691.19269 | salicylic acid receptor protein (NPR1)          | Phytohormone action.salicylic acid.perception and signal transduction.receptor protein (NPR1)                                                        | 1.834   |
| 11.9.2.3    | cluster-14691.77771 | strigolactone signal modulator (SMXL)           | Phytohormone action.strigolactone.perception and signal transduction.signal modulator (SMXL)                                                         | 4.1699  |
| 11.10.1.1.1 | cluster-18430.0     | PIP/PIPL precursor polypeptide                  | Phytohormone action.signalling peptides.NCRP (non-cysteine-rich-peptide) category.PIP/PIPL-peptide activity.PIP/PIPL-precursor polypeptide           | 6.0251  |
| 11.10.1.2.1 | cluster-14691.75189 | pythosulfokine precursor polypeptide (PSK)      | Phytohormone action.signalling peptides.NCRP (non-cysteine-rich-peptide) category.pythosulfokine activity.pythosulfokine precursor polypeptide (PSK) | 3.8334  |
| 11.10.1.2.2 | cluster-14691.70969 | pythosulfokine peptide receptor (PSKR)          | Phytohormone action.signalling peptides.NCRP (non-cysteine-rich-peptide) category.pythosulfokine activity.pythosulfokine peptide receptor (PSKR)     | 2.0616  |
| 11.10.1.2.2 | cluster-14691.50727 | pythosulfokine peptide receptor (PSKR)          | Phytohormone action.signalling peptides.NCRP (non-cysteine-rich-peptide) category.pythosulfokine activity.pythosulfokine peptide receptor (PSKR)     | 1.2574  |
| 11.10.1.3.1 | cluster-14691.1727  | CEP precursor polypeptide                       | Phytohormone action.signalling peptides.NCRP (non-cysteine-rich-peptide) category.CEP-peptide activity.CEP-precursor polypeptide                     | 8.343   |
| 11.10.1.3.1 | cluster-14691.1486  | CEP precursor polypeptide                       | Phytohormone action.signalling peptides.NCRP (non-cysteine-rich-peptide) category.CEP-peptide activity.CEP-precursor polypeptide                     | 9.0142  |
| 11.10.1.3.1 | cluster-14691.1485  | CEP precursor polypeptide                       | Phytohormone action.signalling peptides.NCRP (non-cysteine-rich-peptide) category.CEP-peptide activity.CEP-precursor polypeptide                     | 7.4807  |
| 11.10.1.3.1 | cluster-14691.1826  | CEP precursor polypeptide                       | Phytohormone action.signalling peptides.NCRP (non-cysteine-rich-peptide) category.CEP-peptide activity.CEP-precursor polypeptide                     | 8.6158  |
| 11.10.1.3.1 | cluster-14691.82632 | CEP precursor polypeptide                       | Phytohormone action.signalling peptides.NCRP (non-cysteine-rich-peptide) category.CEP-peptide activity.CEP-precursor polypeptide                     | 9.4341  |

|              |                     |                                  |                                                                                                                                           |        |
|--------------|---------------------|----------------------------------|-------------------------------------------------------------------------------------------------------------------------------------------|--------|
| 11.10.1.6.1  | cluster-15002.0     | DVL/RTFL precursor polypeptide   | Phytohormone action.signalling peptides.NCRP (non-cysteine-rich-peptide) category.DVL/ROT-peptide activity.DVL/RTFL-precursor polypeptide | 6.1596 |
| 11.10.1.6.1  | cluster-14691.10408 | DVL/RTFL precursor polypeptide   | Phytohormone action.signalling peptides.NCRP (non-cysteine-rich-peptide) category.DVL/ROT-peptide activity.DVL/RTFL-precursor polypeptide | 7.0488 |
| 11.10.1.6.1  | cluster-14691.12312 | DVL/RTFL precursor polypeptide   | Phytohormone action.signalling peptides.NCRP (non-cysteine-rich-peptide) category.DVL/ROT-peptide activity.DVL/RTFL-precursor polypeptide | 6.1578 |
| 11.10.1.10.1 | cluster-18065.0     | CLE precursor polypeptide        | Phytohormone action.signalling peptides.NCRP (non-cysteine-rich-peptide) category.CLE-peptide activity.CLE-precursor polypeptide          | 5.962  |
| 11.10.1.10.1 | cluster-16580.0     | CLE precursor polypeptide        | Phytohormone action.signalling peptides.NCRP (non-cysteine-rich-peptide) category.CLE-peptide activity.CLE-precursor polypeptide          | 6.2232 |
| 11.10.1.10.1 | cluster-15957.0     | CLE precursor polypeptide        | Phytohormone action.signalling peptides.NCRP (non-cysteine-rich-peptide) category.CLE-peptide activity.CLE-precursor polypeptide          | 6.0686 |
| 11.10.1.10.1 | cluster-14691.3219  | CLE precursor polypeptide        | Phytohormone action.signalling peptides.NCRP (non-cysteine-rich-peptide) category.CLE-peptide activity.CLE-precursor polypeptide          | 6.5871 |
| 11.10.1.10.1 | cluster-16063.0     | CLE precursor polypeptide        | Phytohormone action.signalling peptides.NCRP (non-cysteine-rich-peptide) category.CLE-peptide activity.CLE-precursor polypeptide          | 6.1112 |
| 11.10.1.12.1 | cluster-14691.8155  | PNP precursor polypeptide        | Phytohormone action.signalling peptides.NCRP (non-cysteine-rich-peptide) category.PNP-peptide activity.PNP precursor polypeptide          | 7.2163 |
| 11.10.2.3.1  | cluster-14691.13389 | EPF/EPFL precursor polypeptide   | Phytohormone action.signalling peptides.CRP (cysteine-rich-peptide) category.EPF/EPFL-peptide activity.EPF/EPFL-precursor polypeptide     | 6.7622 |
| 11.10.2.3.3  | cluster-27720.0     | EPF-peptide receptor (TMM)       | Phytohormone action.signalling peptides.CRP (cysteine-rich-peptide) category.EPF/EPFL-peptide activity.EPF-peptide receptor (TMM)         | 5.2643 |
| 11.10.2.4.1  | cluster-14691.807   | RALF/RALFL precursor polypeptide | Phytohormone action.signalling peptides.CRP (cysteine-rich-peptide) category.RALF/RALFL-peptide activity.RALF/RALFL-precursor polypeptide | 7.0076 |
| 11.10.2.4.2  | cluster-14691.36401 | RALF-peptide receptor (CrRLK1L)  | Phytohormone action.signalling peptides.CRP (cysteine-rich-peptide) category.RALF/RALFL-peptide activity.RALF-peptide receptor (CrRLK1L)  | 1.542  |

| <i>Cell wall organization</i> |                     |                                                                                                                                                                                             |                                                                      |         |
|-------------------------------|---------------------|---------------------------------------------------------------------------------------------------------------------------------------------------------------------------------------------|----------------------------------------------------------------------|---------|
| 21.1.2.2                      | cluster-14691.74878 | Cell wall organisation.cellulose.cellulose-hemicellulose network assembly.regulatory protein (COB)                                                                                          | regulatory protein (COB) of cellulose-hemicellulose network assembly | 2.7791  |
| 21.2.1.1.4                    | cluster-14691.74646 | Cell wall organisation. hemicellulose. xyloglucan. biosynthesis. 1,2-alpha-fucosyltransferase (FUT)                                                                                         | 1,2-alpha-fucosyltransferase (FUT)                                   | 2.7483  |
| 21.2.2.1.1                    | cluster-14691.32672 | Cell wall organisation. hemicellulose. xylan.biosynthesis.galacturonosyltransferase                                                                                                         | galacturonosyltransferase                                            | 1.4428  |
| 21.2.4.1                      | cluster-14691.74366 | Cell wall organisation.hemicellulose.mixed-linked glucan.D-glucan synthase (CSLF)                                                                                                           | D-glucan synthase (CSLF)                                             | 3.3029  |
| 21.3.1.2.1                    | cluster-20197.0     | Cell wall organisation.pectin.homogalacturonan.modification and degradation.pectin methylesterase                                                                                           | pectin methylesterase                                                | 5.3189  |
| 21.3.1.2.1                    | cluster-14691.66836 | Cell wall organisation.pectin.homogalacturonan.modification and degradation.pectin methylesterase                                                                                           | pectin methylesterase                                                | 4.3545  |
| 21.3.2.1.3                    | cluster-14691.14990 | Cell wall organisation.pectin.rhamnogalacturonan I.biosynthesis.beta-1,4-galactosyltransferase                                                                                              | beta-1,4-galactosyltransferase                                       | 3.4503  |
| 21.3.2.2.4.1                  | cluster-14691.51009 | Cell wall organisation.pectin.rhamnogalacturonan I.modification and degradation.alpha-L-arabinofuranosidase activities.bifunctional alpha-L-arabinofuranosidase and beta-D-xylosidase (ASD) | bifunctional alpha-L-arabinofuranosidase and beta-D-xylosidase (ASD) | 1.3766  |
| 21.3.5.4                      | cluster-14691.47175 | Cell wall organisation.pectin.modification and degradation.pectin acetylerase                                                                                                               | pectin acetylerase                                                   | -1.0174 |
| 21.4.2.1                      | cluster-14691.4464  | Cell wall organisation.cell wall proteins.expansin activities.alpha-class expansin                                                                                                          | alpha-class expansin                                                 | 6.4851  |
| 21.4.2.1                      | cluster-14691.76733 | Cell wall organisation.cell wall proteins.expansin activities.alpha-class expansin                                                                                                          | alpha-class expansin                                                 | 6.7503  |
| 21.6.1.5                      | cluster-14691.6990  | Cell wall organisation.lignin.monolignol biosynthesis.cinnamoyl-CoA reductase (CCR)                                                                                                         | cinnamoyl-CoA reductase (CCR)                                        | 5.7272  |
| 21.6.1.9                      | cluster-14691.27253 | Cell wall organisation.lignin.monolignol biosynthesis.Cyt-P450 hydroxylase scaffold protein (MSBP)                                                                                          | Cyt-P450 hydroxylase scaffold protein (MSBP)                         | 2.2593  |

|                        |                     |                                                                                                       |                                                                                                 |        |
|------------------------|---------------------|-------------------------------------------------------------------------------------------------------|-------------------------------------------------------------------------------------------------|--------|
| 21.6.3.2               | cluster-14691.48618 | Cell wall organisation.lignin.monolignol glycosylation and deglycosylation.coniferin beta-glucosidase | coniferin beta-glucosidase                                                                      | 2.0831 |
| 21.6.3.2               | cluster-14691.24845 | Cell wall organisation.lignin.monolignol glycosylation and deglycosylation.coniferin beta-glucosidase | coniferin beta-glucosidase                                                                      | 2.8676 |
| 21.9.3.1               | cluster-14691.32159 | Cell wall organisation.cutin and suberin.biosynthesis regulation.transcription factor (SHN)           | cutin and suberin biosynthesis transcription factor (SHN)                                       | -2.39  |
| 21.9.3.1               | cluster-14691.1688  | Cell wall organisation.cutin and suberin.biosynthesis regulation.transcription factor (SHN)           | cutin and suberin biosynthesis transcription factor (SHN)                                       | 1.3845 |
| <i>Nutrient uptake</i> |                     |                                                                                                       |                                                                                                 |        |
| 25.1.1.1               | cluster-14691.1727  | systemic nitrogen signalling polypeptide (CEP)                                                        | Nutrient uptake.nitrogen assimilation.systemic nitrogen signalling.signalling polypeptide (CEP) | 8.343  |
| 25.1.1.1               | cluster-14691.1486  | systemic nitrogen signalling polypeptide (CEP)                                                        | Nutrient uptake.nitrogen assimilation.systemic nitrogen signalling.signalling polypeptide (CEP) | 9.0142 |
| 25.1.1.1               | cluster-14691.1485  | systemic nitrogen signalling polypeptide (CEP)                                                        | Nutrient uptake.nitrogen assimilation.systemic nitrogen signalling.signalling polypeptide (CEP) | 7.4807 |
| 25.1.1.1               | cluster-14691.1826  | systemic nitrogen signalling polypeptide (CEP)                                                        | Nutrient uptake.nitrogen assimilation.systemic nitrogen signalling.signalling polypeptide (CEP) | 8.6158 |
| 25.1.1.1               | cluster-14691.82632 | systemic nitrogen signalling polypeptide (CEP)                                                        | Nutrient uptake.nitrogen assimilation.systemic nitrogen signalling.signalling polypeptide (CEP) | 9.4341 |
| 25.1.2.5               | cluster-14691.17907 | nitrate transporter (NRT2)                                                                            | Nutrient uptake.nitrogen assimilation.nitrate uptake system.nitrate transporter (NRT2)          | 3.835  |
| 25.1.3.1               | cluster-14691.36103 | nitrate reductase                                                                                     | Nutrient uptake.nitrogen assimilation.nitrate assimilation.nitrate reductase                    | 4.0674 |
| 25.1.3.1               | cluster-14691.46130 | nitrate reductase                                                                                     | Nutrient uptake.nitrogen assimilation.nitrate assimilation.nitrate reductase                    | 1.3803 |
| 25.1.6                 | cluster-14691.70929 | aspartate aminotransferase                                                                            | Nutrient uptake.nitrogen assimilation.aspartate aminotransferase                                | 1.4308 |
| 25.3.1.2               | cluster-14691.54581 | phosphate signalling regulatory protein (SPX)                                                         | Nutrient uptake.phosphorus assimilation.phosphate signalling.regulatory protein (SPX)           | 1.5155 |
| 25.3.1.2               | cluster-14691.81540 | phosphate signalling regulatory protein (SPX)                                                         | Nutrient uptake.phosphorus assimilation.phosphate signalling.regulatory protein (SPX)           | 6.5835 |
| 25.3.1.2               | cluster-14691.81539 | phosphate signalling regulatory protein (SPX)                                                         | Nutrient uptake.phosphorus assimilation.phosphate signalling.regulatory protein (SPX)           | 6.2975 |
| 25.3.2.1               | cluster-14691.51441 | phosphate transporter (PHT1)                                                                          | Nutrient uptake.phosphorus assimilation.phosphate uptake.phosphate transporter (PHT1)           | 2.1772 |

| 25.3.2.1                        | cluster-14691.45899 | phosphate transporter (PHT1)                   | Nutrient uptake.phosphorus assimilation.phosphate uptake.phosphate transporter (PHT1)                              | 2.0997        |
|---------------------------------|---------------------|------------------------------------------------|--------------------------------------------------------------------------------------------------------------------|---------------|
| 25.3.2.1                        | cluster-14691.52580 | phosphate transporter (PHT1)                   | Nutrient uptake.phosphorus assimilation.phosphate uptake.phosphate transporter (PHT1)                              | 1.5945        |
| 25.4.2.4.3                      | cluster-14691.23657 | iron transporter (VIT)                         | Nutrient uptake.metal homeostasis.iron.iron storage.iron transporter (VIT)                                         | -2.4401       |
| 25.4.2.4.3                      | cluster-14691.23657 | iron transporter (VIT)                         | Nutrient uptake.metal homeostasis.iron.iron storage.iron transporter (VIT)                                         | -2.4401       |
| 25.4.2.5.3                      | cluster-14691.15172 | metal chelator nicotianamine transporter (TCR) | Nutrient uptake.metal homeostasis.iron.long-distance iron transport.metal chelator nicotianamine transporter (TCR) | -1.1134       |
| <i>ROS scavenger</i>            |                     |                                                |                                                                                                                    |               |
| Gene identifier                 | Id                  | Description                                    |                                                                                                                    | Cd_R vs Cd_L* |
| AT1G09090.1                     | cluster-14691.12641 | NADPH oxidase 1                                |                                                                                                                    | 7.1387        |
| AT1G08830.2                     | cluster-14691.9595  | Superoxide dismutase                           |                                                                                                                    | 6.7735        |
| AT4G35000.1                     | cluster-14691.24413 | Ascorbate peroxidase 3                         |                                                                                                                    | 3.4836        |
| AT1G78340.1                     | cluster-14691.9539  | Glutathione S-transferase                      |                                                                                                                    | 9.5248        |
| AT1G07890.6                     | cluster-10504       | Catalase                                       |                                                                                                                    | 6.3794        |
| AT5G14070.1                     | cluster-14691.81808 | Glutaredoxin-C5                                |                                                                                                                    | 7.2257        |
| <i>Heavy metal transporters</i> |                     |                                                |                                                                                                                    |               |
| AT4G30120.1                     | cluster-14691.35424 | Cadmium / zinc-transporting ATPase HMA3        |                                                                                                                    | -3.7045       |
| AT1G80830.1                     | cluster-27204       | Metal transporter Nramp1                       |                                                                                                                    | 3.6765        |

### 6.3.7 Analysis of the *A. donax* response to salt and cadmium treatments

The availability of transcriptomic data enabled the identification of genes that are implicated in *A. donax* response to both salt (Sicilia et al., 2019; Sicilia et al., 2020) and cadmium stress. In details, a DEG list containing deregulated genes in both stress conditions was obtained by using the KEGG ORTHOLOGY database (see Materials and Methods). The KEGG ORTHOLOGY database represents a reference resource for gene and protein annotation and allowed to overcome the species-specific annotation of other databases potentially leading to bias in the analysis (Kanehisa et al., 2016). Figure 29 reports the classification of common DEGs and their numerical distribution. Based on this analysis 162 DEGs were successfully classified and most of them (156) were up-regulated in both stress conditions whereas only 6 DEGs were down-regulated. In particular, the most abundant KO category was (ko01000) Enzymes (51 up-regulated and 4 down regulated DEGs), followed by (ko03011) Ribosome (46 up-regulated DEGs), (ko04147) Exosome (17 up-regulated DEGs), (ko04131) Membrane trafficking (15 up-regulated DEGs) and (ko02000) Transporters (13 up-regulated and 1 down-regulated DEGs) (Figure 29). Among the DEGs included in the “Transcription factor” category AP2-like factor and EREBP-like factor were found up-regulated, along with aminocyclopropane carboxylate oxidase (ACO) confirming the crucial role of ethylene in giant reed abiotic stress response. Moreover, the “Ribosome” category (46 up-regulated DEGs) contains an elevated number of genes encoding ribosomal proteins indicating that “Protein biosynthesis” is an extremely involved pathway in both conditions. The complete list containing the KO description of each DEG involved in both salt stress condition is in Table 29.

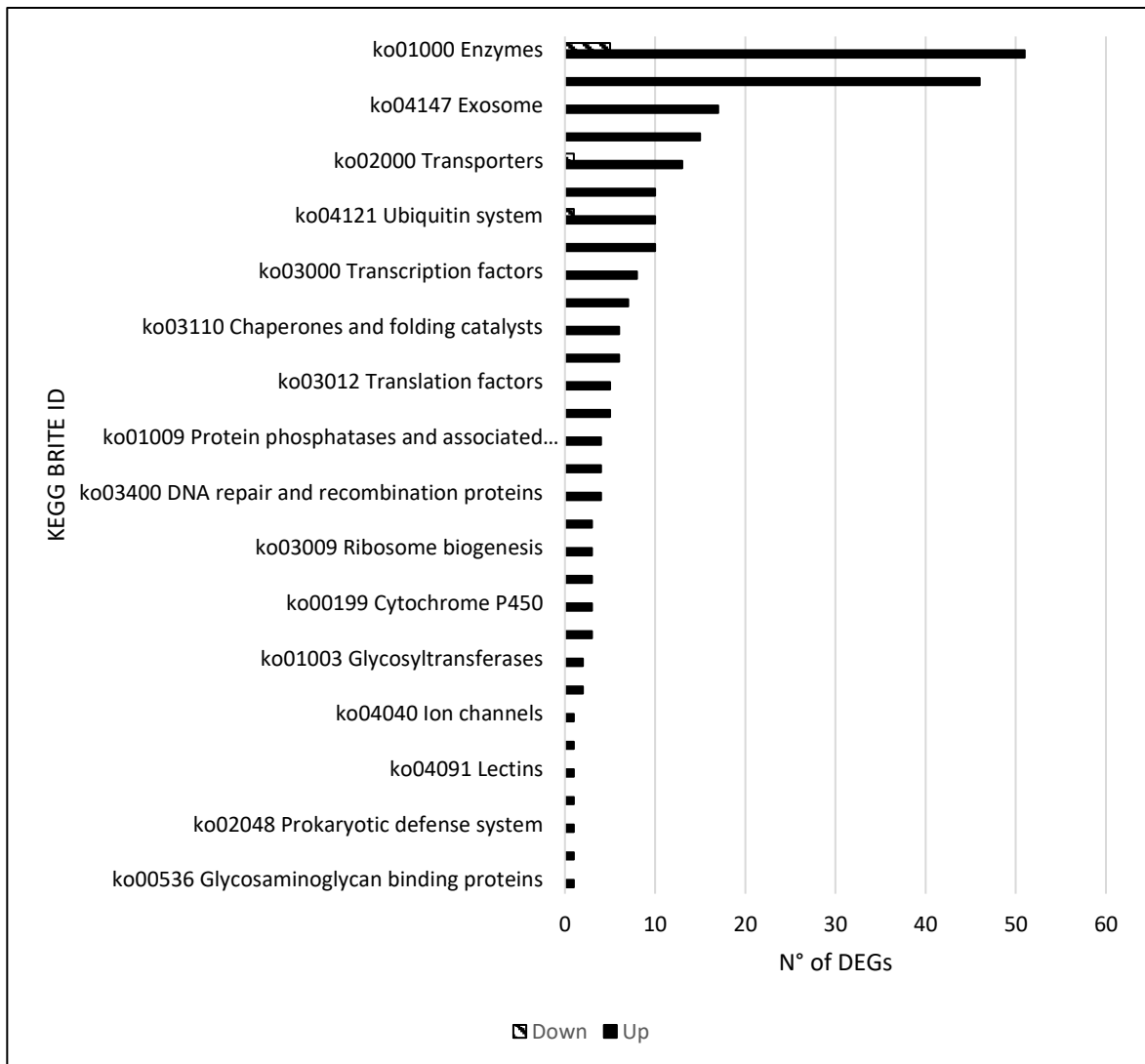


**Figure 29.** KO classification of DEGs found in common between salt and cadmium stress in *A. donax* ecotypes.

**Table 29.** KO Description of DEGs found in common between salt and cadmium treatment

| KO ID  | KO Description                        | Salt                |            |          | Cadmium             |              |
|--------|---------------------------------------|---------------------|------------|----------|---------------------|--------------|
|        |                                       | Log <sub>2</sub> FC | Comparison | Genotype | Log <sub>2</sub> FC | Comparison   |
| K00430 | peroxidase                            | Inf                 | S4 vs CK   | G2       | 10.434              | Cd_R vs Cd_L |
| K15382 | solute carrier family 50              | Inf                 | S4 vs CK   | G2       | 9.911               | Cd_R vs Cd_L |
| K07088 | uncharacterized protein               | Inf                 | S3 vs CK   | G34      | 8.9229              | Cd_R vs Cd_L |
| K02865 | large subunit ribosomal protein L10Ae | Inf                 | S4 vs CK   | G2       | 7.8562              | Cd_R vs Cd_L |
| K03263 | translation initiation factor 5A      | Inf                 | S4 vs CK   | G2       | 7.6995              | Cd_R vs Cd_L |
| K00799 | glutathione S-transferase             | Inf                 | S4 vs CK   | G2       | 7.5861              | Cd_R vs Cd_L |
| K05917 | sterol 14-demethylase                 | Inf                 | S3 vs CK   | G34      | 7.2344              | Cd_R vs Cd_L |
| K03676 | glutaredoxin 3                        | Inf                 | S4 vs CK   | G2       | 7.2257              | Cd_R vs Cd_L |
| K01802 | peptidylprolyl isomerase              | Inf                 | S4 vs CK   | G2       | 7.1581              | Cd_R vs Cd_L |
| K09285 | AP2-like factor, ANT lineage          | Inf                 | S4 vs CK   | G2       | 7.117               | Cd_R vs Cd_L |
| K02995 | small subunit ribosomal protein S8e   | Inf                 | S4 vs CK   | G2       | 7.0032              | Cd_R vs Cd_L |
| K02937 | large subunit ribosomal protein L7e   | Inf                 | S4 vs CK   | G2       | 6.998               | Cd_R vs Cd_L |
| K02932 | large subunit ribosomal protein L5e   | Inf                 | S4 vs CK   | G2       | 6.9106              | Cd_R vs Cd_L |
| K02975 | small subunit ribosomal protein S25e  | Inf                 | S4 vs CK   | G2       | 6.9098              | Cd_R vs Cd_L |
| K13126 | polyadenylate-binding protein         | Inf                 | S4 vs CK   | G2       | 6.7458              | Cd_R vs Cd_L |
| K03257 | translation initiation factor 4A      | Inf                 | S4 vs CK   | G2       | 6.7163              | Cd_R vs Cd_L |
| K02973 | small subunit ribosomal protein S23e  | Inf                 | S4 vs CK   | G2       | 6.593               | Cd_R vs Cd_L |
| K08054 | calnexin                              | Inf                 | S4 vs CK   | G2       | 6.5876              | Cd_R vs Cd_L |
| K08341 | GABA(A) receptor-associated protein   | Inf                 | S4 vs CK   | G2       | 6.5392              | Cd_R vs Cd_L |
| K02896 | large subunit ribosomal protein L24e  | Inf                 | S4 vs CK   | G2       | 6.4609              | Cd_R vs Cd_L |
| K02912 | large subunit ribosomal protein L32e  | Inf                 | S4 vs CK   | G2       | 6.4116              | Cd_R vs Cd_L |



|        |                                                         |     |          |    |        |              |
|--------|---------------------------------------------------------|-----|----------|----|--------|--------------|
| K02133 | F-type H <sup>+</sup> -transporting ATPase subunit beta | Inf | S4 vs CK | G2 | 6.403  | Cd_R vs Cd_L |
| K02991 | small subunit ribosomal protein S6e                     | Inf | S4 vs CK | G2 | 6.3814 | Cd_R vs Cd_L |
| K02997 | small subunit ribosomal protein S9e                     | Inf | S4 vs CK | G2 | 6.3723 | Cd_R vs Cd_L |
| K19040 | E3 ubiquitin-protein ligase ATL10/75/76/77/78           | Inf | S3 vs CK | G2 | 6.3708 | Cd_R vs Cd_L |
| K02183 | calmodulin                                              | Inf | S4 vs CK | G2 | 6.3128 | Cd_R vs Cd_L |
| K07936 | GTP-binding nuclear protein Ran                         | Inf | S4 vs CK | G2 | 6.3073 | Cd_R vs Cd_L |
| K02958 | small subunit ribosomal protein S15e                    | Inf | S4 vs CK | G2 | 6.2958 | Cd_R vs Cd_L |
| K01183 | chitinase                                               | Inf | S4 vs CK | G2 | 6.2888 | Cd_R vs Cd_L |
| K02883 | large subunit ribosomal protein L18e                    | Inf | S4 vs CK | G2 | 6.2491 | Cd_R vs Cd_L |
| K17302 | coatamer, subunit beta'                                 | Inf | S4 vs CK | G2 | 6.2418 | Cd_R vs Cd_L |
| K05863 | solute carrier family 25                                | Inf | S4 vs CK | G2 | 6.2367 | Cd_R vs Cd_L |
| K02966 | small subunit ribosomal protein S19e                    | Inf | S4 vs CK | G2 | 6.2149 | Cd_R vs Cd_L |
| K02955 | small subunit ribosomal protein S14e                    | Inf | S4 vs CK | G2 | 6.2029 | Cd_R vs Cd_L |
| K02934 | large subunit ribosomal protein L6e                     | Inf | S4 vs CK | G2 | 6.0777 | Cd_R vs Cd_L |
| K02962 | small subunit ribosomal protein S17e                    | Inf | S4 vs CK | G2 | 6.0526 | Cd_R vs Cd_L |
| K02969 | small subunit ribosomal protein S20e                    | Inf | S4 vs CK | G2 | 5.9959 | Cd_R vs Cd_L |
| K03232 | elongation factor 1-beta                                | Inf | S4 vs CK | G2 | 5.9423 | Cd_R vs Cd_L |
| K02915 | large subunit ribosomal protein L34e                    | Inf | S4 vs CK | G2 | 5.9413 | Cd_R vs Cd_L |
| K07374 | tubulin alpha                                           | Inf | S4 vs CK | G2 | 5.9236 | Cd_R vs Cd_L |
| K01915 | glutamine synthetase                                    | Inf | S4 vs CK | G2 | 5.9167 | Cd_R vs Cd_L |
| K02951 | small subunit ribosomal protein S12e                    | Inf | S4 vs CK | G2 | 5.9042 | Cd_R vs Cd_L |
| K02891 | large subunit ribosomal protein L22e                    | Inf | S4 vs CK | G2 | 5.9013 | Cd_R vs Cd_L |
| K02918 | large subunit ribosomal protein L35e                    | Inf | S4 vs CK | G2 | 5.8555 | Cd_R vs Cd_L |
| K02922 | large subunit ribosomal protein L37e                    | Inf | S4 vs CK | G2 | 5.8485 | Cd_R vs Cd_L |
| K02901 | large subunit ribosomal protein L27e                    | Inf | S4 vs CK | G2 | 5.7705 | Cd_R vs Cd_L |

|        |                                                  |     |          |     |        |              |
|--------|--------------------------------------------------|-----|----------|-----|--------|--------------|
| K02940 | large subunit ribosomal protein L9e              | Inf | S4 vs CK | G2  | 5.7541 | Cd_R vs Cd_L |
| K01363 | cathepsin B                                      | Inf | S4 vs CK | G2  | 5.7446 | Cd_R vs Cd_L |
| K07375 | tubulin beta                                     | Inf | S4 vs CK | G2  | 5.7182 | Cd_R vs Cd_L |
| K02974 | small subunit ribosomal protein S24e             | Inf | S4 vs CK | G2  | 5.7135 | Cd_R vs Cd_L |
| K02910 | large subunit ribosomal protein L31e             | Inf | S4 vs CK | G2  | 5.7101 | Cd_R vs Cd_L |
| K02981 | small subunit ribosomal protein S2e              | Inf | S4 vs CK | G2  | 5.669  | Cd_R vs Cd_L |
| K02889 | large subunit ribosomal protein L21e             | Inf | S4 vs CK | G2  | 5.6395 | Cd_R vs Cd_L |
| K02957 | small subunit ribosomal protein S15Ae            | Inf | S4 vs CK | G2  | 5.6123 | Cd_R vs Cd_L |
| K09264 | MADS-box transcription factor, plant             | Inf | S3 vs CK | G34 | 5.5709 | Cd_R vs Cd_L |
| K10406 | kinesin family member C2/C3                      | Inf | S3 vs CK | G2  | 5.5524 | Cd_R vs Cd_L |
| K04730 | interleukin-1 receptor-associated kinase 1       | Inf | S4 vs CK | G2  | 5.5046 | Cd_R vs Cd_L |
| K02898 | large subunit ribosomal protein L26e             | Inf | S4 vs CK | G2  | 5.4975 | Cd_R vs Cd_L |
| K02983 | small subunit ribosomal protein S30e             | Inf | S4 vs CK | G2  | 5.4957 | Cd_R vs Cd_L |
| K10523 | speckle-type POZ protein                         | Inf | S3 vs CK | G34 | 5.4711 | Cd_R vs Cd_L |
| K03234 | elongation factor 2                              | Inf | S4 vs CK | G2  | 5.4658 | Cd_R vs Cd_L |
| K02917 | large subunit ribosomal protein L35Ae            | Inf | S4 vs CK | G2  | 5.453  | Cd_R vs Cd_L |
| K02921 | large subunit ribosomal protein L37Ae            | Inf | S4 vs CK | G2  | 5.4419 | Cd_R vs Cd_L |
| K02964 | small subunit ribosomal protein S18e             | Inf | S4 vs CK | G2  | 5.4343 | Cd_R vs Cd_L |
| K10355 | actin, other eukaryote                           | Inf | S4 vs CK | G2  | 5.3752 | Cd_R vs Cd_L |
| K09580 | protein disulfide-isomerase A1                   | Inf | S4 vs CK | G2  | 5.3616 | Cd_R vs Cd_L |
| K06630 | 14-3-3 protein epsilon                           | Inf | S4 vs CK | G2  | 5.3289 | Cd_R vs Cd_L |
| K11253 | histone H3                                       | Inf | S4 vs CK | G2  | 5.2497 | Cd_R vs Cd_L |
| K08770 | ubiquitin C                                      | Inf | S4 vs CK | G2  | 5.2436 | Cd_R vs Cd_L |
| K02900 | large subunit ribosomal protein L27Ae            | Inf | S4 vs CK | G2  | 5.2076 | Cd_R vs Cd_L |
| K09419 | heat shock transcription factor, other eukaryote | Inf | S4 vs CK | G2  | 5.2054 | Cd_R vs Cd_L |

|        |                                                          |     |          |     |        |              |
|--------|----------------------------------------------------------|-----|----------|-----|--------|--------------|
| K02942 | large subunit ribosomal protein LP1                      | Inf | S4 vs CK | G2  | 5.1688 | Cd_R vs Cd_L |
| K09874 | aquaporin NIP                                            | Inf | S3 vs CK | G2  | 5.0152 | Cd_R vs Cd_L |
| K13508 | glycerol-3-phosphate acyltransferase                     | Inf | S3 vs CK | G2  | 4.7781 | Cd_R vs Cd_L |
| K11593 | eukaryotic translation initiation factor 2C              | Inf | S4 vs CK | G2  | 4.7445 | Cd_R vs Cd_L |
| K14411 | RNA-binding protein Musashi                              | Inf | S4 vs CK | G2  | 4.4911 | Cd_R vs Cd_L |
| K14445 | solute carrier family 13                                 | Inf | S4 vs CK | G2  | 4.4542 | Cd_R vs Cd_L |
| K10400 | kinesin family member 15                                 | Inf | S3 vs CK | G2  | 4.3389 | Cd_R vs Cd_L |
| K09422 | myb proto-oncogene protein, plant                        | Inf | S4 vs CK | G2  | 4.2149 | Cd_R vs Cd_L |
| K10534 | nitrate reductase (NAD(P)H)                              | Inf | S3 vs CK | G2  | 4.0674 | Cd_R vs Cd_L |
| K01580 | glutamate decarboxylase                                  | Inf | S3 vs CK | G2  | 3.9925 | Cd_R vs Cd_L |
| K07198 | 5'-AMP-activated protein kinase, catalytic alpha subunit | Inf | S3 vs CK | G34 | 3.9206 | Cd_R vs Cd_L |
| K04079 | molecular chaperone HtpG                                 | Inf | S4 vs CK | G2  | 3.8041 | Cd_R vs Cd_L |
| K02324 | DNA polymerase epsilon subunit 1                         | Inf | S3 vs CK | G2  | 3.6283 | Cd_R vs Cd_L |
| K00434 | L-ascorbate peroxidase                                   | Inf | S4 vs CK | G2  | 3.4836 | Cd_R vs Cd_L |
| K09286 | EREBP-like factor                                        | Inf | S3 vs CK | G34 | 3.196  | Cd_R vs Cd_L |
| K01953 | asparagine synthase (glutamine-hydrolysing)              | Inf | S4 vs CK | G2  | 3.1901 | Cd_R vs Cd_L |
| K07904 | Ras-related protein Rab-11A                              | Inf | S4 vs CK | G2  | 3.1051 | Cd_R vs Cd_L |
| K03327 | multidrug resistance protein, MATE family                | Inf | S3 vs CK | G2  | 2.9987 | Cd_R vs Cd_L |
| K14638 | solute carrier family 15                                 | Inf | S3 vs CK | G2  | 2.8241 | Cd_R vs Cd_L |
| K10728 | topoisomerase (DNA) II binding protein 1                 | Inf | S4 vs CK | G2  | 2.7112 | Cd_R vs Cd_L |
| K11294 | nucleolin                                                | Inf | S4 vs CK | G2  | 2.5034 | Cd_R vs Cd_L |
| K14431 | transcription factor TGA                                 | Inf | S3 vs CK | G2  | 2.4872 | Cd_R vs Cd_L |
| K00606 | 3-methyl-2-oxobutanoate hydroxymethyltransferase         | Inf | S4 vs CK | G2  | 2.4466 | Cd_R vs Cd_L |
| K16055 | trehalose 6-phosphate synthase/phosphatase               | Inf | S4 vs CK | G2  | 2.1966 | Cd_R vs Cd_L |
| K01681 | aconitate hydratase                                      | Inf | S3 vs CK | G34 | 2.183  | Cd_R vs Cd_L |

|        |                                                                  |        |          |     |        |              |
|--------|------------------------------------------------------------------|--------|----------|-----|--------|--------------|
| K05350 | beta-glucosidase                                                 | Inf    | S4 vs CK | G2  | 2.0831 | Cd_R vs Cd_L |
| K08235 | xyloglucan:xyloglucosyl transferase                              | Inf    | S4 vs CK | G2  | 2.0641 | Cd_R vs Cd_L |
| K18857 | alcohol dehydrogenase class-P                                    | Inf    | S4 vs CK | G2  | 2.0633 | Cd_R vs Cd_L |
| K03875 | F-box and leucine-rich repeat protein 1                          | Inf    | S3 vs CK | G34 | 2.0537 | Cd_R vs Cd_L |
| K01126 | glycerophosphoryl diester phosphodiesterase                      | Inf    | S4 vs CK | G2  | 2.0529 | Cd_R vs Cd_L |
| K03231 | elongation factor 1-alpha                                        | 8.9593 | S4 vs CK | G2  | 5.3995 | Cd_R vs Cd_L |
| K02930 | large subunit ribosomal protein L4e                              | 8.3622 | S4 vs CK | G2  | 6.5541 | Cd_R vs Cd_L |
| K02987 | small subunit ribosomal protein S4e                              | 8.3265 | S4 vs CK | G2  | 6.1851 | Cd_R vs Cd_L |
| K02908 | large subunit ribosomal protein L30e                             | 8.0795 | S4 vs CK | G2  | 5.2829 | Cd_R vs Cd_L |
| K02882 | large subunit ribosomal protein L18Ae                            | 7.9064 | S4 vs CK | G2  | 5.9678 | Cd_R vs Cd_L |
| K08245 | phytepsin                                                        | 7.5212 | S4 vs CK | G2  | 5.6198 | Cd_R vs Cd_L |
| K02885 | large subunit ribosomal protein L19e                             | 7.2192 | S4 vs CK | G2  | 6.3364 | Cd_R vs Cd_L |
| K02993 | small subunit ribosomal protein S7e                              | 7.0177 | S4 vs CK | G2  | 6.3395 | Cd_R vs Cd_L |
| K02894 | large subunit ribosomal protein L23e                             | 6.8401 | S4 vs CK | G2  | 6.2566 | Cd_R vs Cd_L |
| K06966 | uncharacterized protein                                          | 6.4127 | S4 vs CK | G2  | 4.1682 | Cd_R vs Cd_L |
| K02868 | large subunit ribosomal protein L11e                             | 6.2509 | S4 vs CK | G2  | 6.5062 | Cd_R vs Cd_L |
| K14753 | guanine nucleotide-binding protein subunit beta-2-like 1 protein | 6.1957 | S4 vs CK | G2  | 6.8244 | Cd_R vs Cd_L |
| K08900 | mitochondrial chaperone BCS1                                     | 5.8181 | S4 vs CK | G2  | 6.1916 | Cd_R vs Cd_L |
| K00128 | aldehyde dehydrogenase (NAD <sup>+</sup> )                       | 5.5637 | S4 vs CK | G2  | 6.7617 | Cd_R vs Cd_L |
| K13993 | HSP20 family protein                                             | 5.1609 | S4 vs CK | G2  | 3.9902 | Cd_R vs Cd_L |
| K16282 | E3 ubiquitin-protein ligase RHA2                                 | 4.8702 | S4 vs CK | G2  | 2.7342 | Cd_R vs Cd_L |
| K13719 | ubiquitin thioesterase OTU1                                      | 4.6021 | S4 vs CK | G2  | 2.7915 | Cd_R vs Cd_L |
| K08176 | MFS transporter, PHS family, inorganic phosphate transporter     | 4.3392 | S4 vs CK | G2  | 5.1623 | Cd_R vs Cd_L |
| K09753 | cinnamoyl-CoA reductase                                          | 4.2547 | S4 vs CK | G2  | 5.7272 | Cd_R vs Cd_L |
| K10144 | RING finger and CHY zinc finger domain-containing protein 1      | 3.9614 | S4 vs CK | G2  | 2.2587 | Cd_R vs Cd_L |

|        |                                                                  |        |          |    |        |              |
|--------|------------------------------------------------------------------|--------|----------|----|--------|--------------|
| K10268 | F-box and leucine-rich repeat protein 2/20                       | 3.5591 | S4 vs CK | G2 | 4.1648 | Cd_R vs Cd_L |
| K02984 | small subunit ribosomal protein S3Ae                             | 3.3401 | S4 vs CK | G2 | 5.5661 | Cd_R vs Cd_L |
| K01895 | acetyl-CoA synthetase                                            | 3.2589 | S4 vs CK | G2 | 2.0557 | Cd_R vs Cd_L |
| K09589 | steroid 3-oxidase                                                | 2.9684 | S3 vs CK | G2 | 2.3625 | Cd_R vs Cd_L |
| K01057 | 6-phosphogluconolactonase                                        | 2.9531 | S4 vs CK | G2 | 3.4516 | Cd_R vs Cd_L |
| K15283 | solute carrier family 35, member E1                              | 2.9414 | S3 vs CK | G2 | 2.5924 | Cd_R vs CK_R |
| K00827 | alanine-glyoxylate transaminase                                  | 2.9104 | S4 vs CK | G2 | 4.0328 | Cd_R vs Cd_L |
| K01051 | pectinesterase                                                   | 2.9027 | S4 vs CK | G2 | 6.9387 | Cd_R vs Cd_L |
| K08679 | UDP-glucuronate 4-epimerase                                      | 2.8918 | S4 vs CK | G2 | 3.4676 | Cd_R vs Cd_L |
| K09843 | (+)-abscisic acid 8'-hydroxylase                                 | 2.8267 | S4 vs CK | G2 | 2.0026 | Cd_R vs Cd_L |
| K00366 | ferredoxin-nitrite reductase                                     | 2.8171 | S3 vs CK | G2 | 4.4632 | Cd_R vs Cd_L |
| K14209 | solute carrier family 36 (proton-coupled amino acid transporter) | 2.7449 | S4 vs CK | G2 | 2.5934 | Cd_R vs Cd_L |
| K07052 | uncharacterized protein                                          | 2.6965 | S4 vs CK | G2 | 2.4726 | Cd_R vs Cd_L |
| K19042 | E3 ubiquitin-protein ligase BOI and related proteins             | 2.5414 | S4 vs CK | G2 | 3.6713 | Cd_R vs Cd_L |
| K14498 | serine/threonine-protein kinase SRK2                             | 2.5268 | S4 vs CK | G2 | 5.1093 | Cd_R vs Cd_L |
| K07466 | replication factor A1                                            | 2.5203 | S4 vs CK | G2 | 5.7118 | Cd_R vs Cd_L |
| K02866 | large subunit ribosomal protein L10e                             | 2.4986 | S4 vs CK | G2 | 6.3831 | Cd_R vs Cd_L |
| K07937 | ADP-ribosylation factor 1                                        | 2.4709 | S4 vs CK | G2 | 4.7146 | Cd_R vs Cd_L |
| K14290 | exportin-1                                                       | 2.3984 | S4 vs CK | G2 | 2.2948 | Cd_R vs Cd_L |
| K02575 | MFS transporter, NNP family, nitrate/nitrite transporter         | 2.3974 | S4 vs CK | G2 | 3.835  | Cd_R vs Cd_L |
| K01087 | trehalose 6-phosphate phosphatase                                | 2.3515 | S4 vs CK | G2 | 5.986  | Cd_R vs Cd_L |
| K01176 | alpha-amylase                                                    | 2.3483 | S4 vs CK | G2 | 5.3483 | Cd_R vs Cd_L |
| K10357 | myosin V                                                         | 2.3462 | S4 vs CK | G2 | 2.4613 | Cd_R vs Cd_L |
| K00844 | hexokinase                                                       | 2.3193 | S4 vs CK | G2 | 6.6885 | Cd_R vs Cd_L |
| K03549 | KUP system potassium uptake protein                              | 2.3032 | S4 vs CK | G2 | 3.3147 | Cd_R vs Cd_L |

|        |                                                           |         |          |    |         |              |
|--------|-----------------------------------------------------------|---------|----------|----|---------|--------------|
| K05894 | 12-oxophytodienoic acid reductase                         | 2.2828  | S4 vs CK | G2 | 2.0146  | Cd_R vs Cd_L |
| K13947 | auxin efflux carrier family                               | 2.2762  | S4 vs CK | G2 | 6.1606  | Cd_R vs Cd_L |
| K00558 | DNA (cytosine-5)-methyltransferase 1                      | 2.2557  | S4 vs CK | G2 | 3.838   | Cd_R vs Cd_L |
| K05933 | aminocyclopropanecarboxylate oxidase                      | 2.2325  | S4 vs CK | G2 | 3.3103  | Cd_R vs Cd_L |
| K17987 | next to BRCA1 gene 1 protein                              | 2.2079  | S4 vs CK | G2 | 6.4743  | Cd_R vs Cd_L |
| K01507 | inorganic pyrophosphatase                                 | 2.1397  | S4 vs CK | G2 | 3.0467  | Cd_R vs CK_R |
| K13448 | calcium-binding protein CML                               | 2.1314  | S4 vs CK | G2 | 2.8402  | Cd_R vs Cd_L |
| K07195 | exocyst complex component 7                               | 2.1003  | S4 vs CK | G2 | 2.2522  | Cd_R vs Cd_L |
| K11000 | callose synthase                                          | 2.0534  | S4 vs CK | G2 | 5.4922  | Cd_R vs Cd_L |
| K13495 | cis-zeatin O-glucosyltransferase                          | 2.0344  | S4 vs CK | G2 | 2.2481  | Cd_R vs Cd_L |
| K05016 | chloride channel 7                                        | 2.0305  | S4 vs CK | G2 | 2.3656  | Cd_R vs Cd_L |
| K01534 | Cd <sup>2+</sup> /Zn <sup>2+</sup> -exporting ATPase      | -2.3251 | S4 vs CK | G2 | -5.2971 | Cd_R vs Cd_L |
| K10143 | E3 ubiquitin-protein ligase RFW2                          | -2.6062 | S4 vs CK | G2 | -2.5064 | Cd_R vs Cd_L |
| K14709 | solute carrier family 39 (zinc transporter), member 1/2/3 | -3.1644 | S4 vs CK | G2 | -2.5601 | Cd_R vs Cd_L |
| K00901 | diacylglycerol kinase (ATP)                               | -3.1786 | S3 vs CK | G2 | -2.3161 | Cd_R vs Cd_L |
| K01658 | anthranilate synthase component II                        | -4.7779 | S4 vs CK | G2 | -2.4936 | Cd_R vs Cd_L |
| K01653 | acetolactate synthase I/III small subunit                 | -Inf    | S4 vs CK | G2 | -3.9009 | Cd_R vs Cd_L |

## 6.4 Discussion

Anthropogenic activities such as metal industries, mining application of pesticides and fertilizers led to dangerous Cd accumulation in arable soil worldwide (Nazar et al. 2012). The high solubility of Cd in the soil associated with the plant capability to absorb it represents a threat to humans as final consumers of putatively contaminated fruit and vegetables. The strategy to allocate cadmium contaminated soil to bioenergy crop might turn out to be successful as it potentially solve the increasing demand of sustainable energy sources which can be achieved without impairing the quote of agricultural lands. *Arundo donax* L. is considered a tolerant to several abiotic stress and recently, due to its ability to accumulate high concentration of HMs (Papazoglou et al. 2007; Mirza et al. 2011) has been proposed as a potential phytoremediation species. In order to elucidate the response of giant reed to cadmium, in this work we sequenced and *de novo* assembled the *A. donax* L. leaf and root transcriptome after a prolonged soil treatment with 4 mg/Kg cadmium nitrate. Cadmium concentrations in uncontaminated soil usually is 0.5 mg/Kg and cadmium contents above 3 mg/kg are generally thought to indicate contaminated soil (Akbar et al. 2006). Based on the measurement of trace cadmium concentration under non-phytotoxic cadmium treatment, Bonanno (2012) showed that giant reed roots act as main accumulation centre (root to shoot ratio is 6.6 :1), whereas stem functions as transition centre given the involvement in ion translocation from root to leaves. Taken into account these observations which preliminarily indicated that root is the frontline in encountering potentially toxic cadmium levels, we focused our analysis on a Cd\_R vs Cd\_L\* comparison originated by subtracting the DEGs belonging to the CK\_R vs CK\_L comparison (root specific DEGs under control conditions) to the Cd\_R vs Cd\_L comparison (root specific DEGs under cadmium treatment) thus obtaining a pool of DEGs specifically up or down-regulated (compared to leaf DEGs) in treated roots. Based on differentially gene expression data, the up regulation of the NRAMP1 transporter, a crucial group of transmembrane protein involved in the uptake of a broad range of ions (Mn, Zn, Cu, Fe, Ni, Co and Cd), suggest that giant reed roots reinforce their ability to adsorb ions in the presence of cadmium which interferes with the essential mineral supply (Nazar et al. 2012). Moreover, the down regulation of HMA3 transporter encoding gene, that regulates cadmium efflux out the citosol towards the vacuole or outside the cell (Mohabubul et al. 2021), indicates that the mechanisms to avoid cadmium residence in root cells are not implemented in our conditions. Once in the citosol, Cd has to be detoxified in order to avoid the onset of cellular damage. It has been shown that the major mechanism of cadmium detoxification is based on phytochelatins, a family of cysteine-rich oligopeptides synthesized from glutathione (GSH) by the enzyme phytochelatin synthase (PCS), that chelate the HMs to form complexes readily stored in the vacuoles (Song et al. 2014). Recently, three giant reed PCS genes have been characterized both in the species

of provenance and in transgenic model organisms (Li et al. 2019). These genes, namely *AdPCS1-3*, are expressed in all organs (root, rhizome, node, internode, leaf sheath and blade) in normal condition. In response to 500  $\mu\text{M}$   $\text{CdSO}_4$  treatment, all the PCS genes showed an increase of expression in roots whereas any change in leaf gene expression was observed (Li et al. 2019). Although these results clearly indicate that *A. donax* genome contains at least three PCS genes constitutively expressed in all plant organs and whose expression is induced in roots under cadmium treatment, none PCSs was found among the DEGs (data not shown) suggesting that the detoxification process through metal chelation was not triggered in our conditions. After the stress perception, phytohormones are the chemical messengers that play a pivotal role in the induction and regulation of diverse signal transduction pathways in response to cadmium stress (Saini et al. 2021). Higher endogenous ABA concentration are reported to mitigate the damaging effects of Cd stress by promoting root-to-shoot Cd translocation through the apoplast and accumulation more Cd in the shoots (Lu et al. 2020). Our results suggested that abscisic acid biosynthesis is inhibited whereas the main gene involved in ABA degradation is up-regulated in giant reed Cd-treated roots (Table 27), probably causing Cd to be detained in the roots. Auxin is recognized as a crucial phytohormone in regulating every aspect of plant root development during normal and stress conditions (Saini et al. 2021). In *Arabidopsis thaliana*, significantly enhanced expression of auxin biosynthesis gene YUCCA6 was observed upon Cd treatment (Fattorini et al. 2017). Moreover, reduced transcript levels of auxin efflux carrier pin-formed 1 (PIN1) were detected under Cd exposure in the post-embryonic roots decreasing auxin transport in the root apex thus altering auxin homeostasis (Fattorini et al. 2017). In our study, both auxin biosynthesis and transport transcript (YUCCA2 and PIN) were found among the up-regulated genes in Cd-treated giant reed roots suggesting that giant reed roots attempt not to alter auxin homeostasis preventing the alteration of root architecture as observed in tobacco (Luo et al. 2020). Furthermore, our results strongly indicate that ethylene biosynthesis and the downstream signalling cascade are up regulated in Cd-treated roots (Table 27). In accordance, the enhanced transcript levels of 1-aminocyclopropane-1-carboxylate (ACO) and ethylene signalling genes (EIN) were observed under As application to the rice roots (Huang et al. 2012) and elevated transcript level accumulation of ethylene receptor 2 (ETR2) gene was also observed under Cd application in *Arabidopsis thaliana* indicating Cd-mediated induction of ethylene production and signalling (Schellingen et al. 2014). Several studies indicated that ethylene modulates the ROS machinery by regulating the activities of both ROS producing and scavenging enzymes, this being considered the crucial reaction following HM stress in plants (Steffens, 2014). Ethylene stimulates the production of ROS by activating nicotinamide adenine dinucleotide phosphate (NADPH) oxidases under HM toxicity (Montero-Palmero et al. 2014) and also modulates antioxidant defense systems in plants exposed to HM stress.



NADPH oxidase 1 transcript was among the up regulated genes in Cd-treated roots and the activation of catalase, SOD, APX and GST expression (Table 27) is probably an attempt to overcome the Cd-induced oxidative stress. This result assumes an important significance since in several species it has been reported that the activation of ROS scavenging machinery is achieved in ethylene insensitive mutants (Saini et al. 2021) thus suggesting that this type of response could be specific of *A. donax* roots. However, we cannot exclude that the induction of YUCCA2 involved in auxin biosynthesis might be responsible of the regulation of reactive oxygen species (ROS) homeostasis as showed in transgenic potato over-expressing YUCCA6 gene (Kim et al. 2013). Oxidative stress can induce protein S-glutathionylation modulating protein function and to prevent irreversible oxidation of protein thiols (Dalle-Donne et al. 2009). High levels of oxidized glutathione (GSSG) can be sufficient to trigger protein S-glutathionylation by a thiol–disulphide exchange reaction between a protein thiol and GSSG. Interestingly, transcript encoding glutaredoxin-C5 is sharply up regulated in giant reed roots indicating that an active reactivation of protein function via the reduction of the cysteine sulphhydrylic groups might occur. Within the “Phytohormones” category, two genes encoding ROTUNDIFOLIA like proteins, which are small polypeptides acting as a regulatory molecules coordinating cellular responses involved in different aspects of cell differentiation, growth and development, were found sharply up regulated in the Cd\_R vs Cd\_L\* comparison. Their role is uncertain but probably they act by restricting polar cell proliferation in lateral organs and coordinating socket cell recruitment and differentiation at trichome sites (Valdivia et al. 2012). A transcript encoding CLAVATA3/ESR-RELATED 25 is among the sharply up-regulated genes in the cadmium treated root (Table 27), CLAVATA3/ESR represents a group of plant proteins acting as extracellular signal peptides involved in cell-to-cell communication in concert with different receptors in a range of processes during plant development (Strabala et al. 2006). A transcript encoding C-terminally encoded peptide (CEP) was strongly up-regulated in cadmium treated roots. CEP is a 15-amino acid post-translationally peptide which plays a pivotal role in lateral root formation and nodulation and its overexpression in *Medicago* results in the inhibition of lateral root formation and enhancement in nodule formation. Besides the role in root architecture, CEP genes also play a role in nitrate assimilation under N starvation conditions and results in the up regulation of the nitrate transporter gene NRT2.1 in roots specifically when nitrate is present in the rhizosphere (Ohkubo et al. 2017). Nitrate transporter are involved in the constitutive high-affinity transport system (cHATS) under low nitrate conditions. The principal role of this cHATS is to enable roots previously deprived of nitrate to absorb this ion and initiate induction of nitrate-inducible genes (Guan et al. 2021) Cd has been reported to inhibit NO<sub>3</sub><sup>-</sup> uptake in several plant species, under normal and high nitrate supply (Guan et al. 2015). Therefore, it is possible that nitrate uptake is inhibited under Cd stress in giant reed roots

mimicking low-nitrate conditions. Interestingly, the analysis of “Nutrient uptake” category revealed that nitrate transporter 2.5 genes are strongly up-regulated (Table 27) suggesting that mechanisms to enhance nitrogen supply are implemented in *A. donax* cadmium treated roots. Moreover, nitrate reductase encoding gene, involved in nitrate assimilation by reducing nitrate to nitrite, is up-regulated in cadmium treated samples probably to provide for more enzyme molecules that are supposed to be inhibited by cadmium (Singh et al. 2019). Under cadmium stress a decrease of mineral nutrient concentrations in plant leaf, such as Fe and P, has been observed and represents the key reason for the restraint of leaf photosynthesis (Nazar et al. 2019). In our work, transcript encoding the plasma membrane phosphate transporter are up-regulated in Cd-treated roots probably to face the unavailability of soluble phosphate sequestered in the soil as cadmium phosphate (Ruangcharus et al. 2020). The plant cell has a variety of mechanisms tools to avoid Cd stress. Mainly, cell wall remodeling might prevent Cd from entering and damaging the protoplast (Loix et al. 2017). At primary cell wall pectin, which contains most of the negative charges, can immobilize Cd very effectively. Furthermore, secondary cell wall lignification can serve to create a barrier to prevent cadmium entry. The utilization of different antibodies detecting methylated and demethylated forms of pectin in cadmium stressed in *Linum usitatissimum* hypocotyls has led to the identification of the presence of low-methylated pectin, which is particularly able to bind Cd ions due to the presence of free carboxyl groups in the outer face of the primary cell wall. This de-esterification was co-localized with an upregulation of PME activity. However, within the inner part of the primary cell wall a higher amount of methylated pectin was detected which was hypothesized to have a repellent function in keeping the cytosolic Cd away from the plasma membrane (Douchichle et al. 2007). In this perspective, the up regulation of both pectin methylesterase and pectin methylesterase inhibitor encoding genes might serve to finely regulate Cd sequestering at primary cell wall in giant cane root. At secondary cell wall level, lignification makes the cell wall less penetrable thus creating an effective barrier against the entry of Cd (Parrotta et al. 2015). The induction of the lignification process appeared as a key process useful to discriminate Cd-sensitive and -tolerant plants (Van De Mortel et al. 2006; Van De Mortel et al. 2008). The discovery of the upregulation of several WRKY transcription factors involved in cell wall lignification as well as the induction of cinnamoyl Coa reductase, laccase and membrane-associated progesterone binding protein 3 all of them involved in lignin biosynthesis (Table 27) clearly indicate that giant cane roots respond to cadmium treatment by avoiding its entrance into the cell.

## 6.5 Conclusions

The global analysis of our findings suggest that prolonged cadmium exposure stimulated a clear response at both morpho-physiological and transcriptomic levels. Hence, cadmium treated plants showed significantly reduced main stem height, biomass dry weight and the net photosynthesis efficiency. The quality of transcriptome sequencing and assembly was elevated and led to the identification of crucial metabolic pathways and to decipher the *A. donax* response to cadmium stress. Three main factors have to be taken in strong consideration in this concluding remarks: a) the used cadmium concentration (4 mg/Kg), slightly higher than allowed; b) the induction of lignification process clearly suggested by transcriptome analysis; c) the lack of phytochelatin transcripts among the DEGs. In our opinion, all these issues indicate that the induced stress condition can be sensed as “mild stress”. The low number of DEGs within the CK\_R vs Cd\_L and CK\_L vs Cd\_L comparisons seems to be in line with this hypothesis. The undertaken strategy was to analyse the Cd\_R vs Cd\_L\* comparison and it led us to focus on the main patterns involved in the Cd-treated giant cane root, it being the interface between plant and soil. Our results suggest that ethylene biosynthesis and signalling are strongly activated. In this respect, the identification of several genes differently regulated in both salt and cadmium conditions, such as genes involved in ethylene biosynthesis and signal transduction outlines those metabolic pathways and biochemical reactions as useful markers of abiotic stress in giant reed. Finally, the finding of DEGs encoding several small peptides functioning as messenger molecules between root and shoot in order to communicate the stressful status to the upper part of the plants (CEP, ROTUNDIFOLIA), the induction of the ROS scavenging machinery, and, above all, the remodelling of plant cell wall confirm the tolerance of giant cane towards cadmium stress and strongly support its cultivation in cadmium contaminated soils in a perspective to save agricultural soil for food and feed crops.

## 7 General conclusion

The possibility to cultivate bioenergy crops on marginal soils for sustainable energy production represents the main insight to overcome the upcoming food and energy crisis. Given that *Arundo donax* has become one of the most promising bioenergy crops for biomass production and industrial applications, a deep characterization of *A. donax* transcriptome in response to unfavorable conditions was accomplished. Although the responses of *A. donax* to a wide range of unfavorable conditions were reported worldwide, to date the molecular mechanisms of its resistance remain poorly understood. Thus, the characterization of the transcriptional changes under different abiotic stress conditions might shed novel light on its extremely adaptability to growth in unfavorable environments. Despite the potential role of *A. donax* for energy production on marginal lands has been established, the genomic resources available for undertaking the genetic improvement of this species are still limited. Salt affected soil is one of the most seriously problem to deal with due to its effects on crop growth and productivity. Firstly, we investigated the long-term salt stress response at doses being much higher than that used to define a soil area as salinized. To characterize the molecular mechanisms involved in *A. donax* salt stress response, we used RNA-Sequencing (RNA-Seq) technique to *de novo* assemble and analyze the *A. donax* leaf transcriptome of G2 and G34 ecotypes subjected to severe (S3) and extreme (S4) levels of salt stress conditions. Unfortunately, in this study we reported exclusively the data of G34 under severe salt concentration because we missed the samples subjected to S4 extreme salt stress treatment because of a fire occurred in the experimental field. Though *A. donax* propagates itself vegetatively, suggesting a low genetic diversity among each *A. donax* ecotypes, the comparative analysis of the G2 and G34 transcriptome shows different pattern not only under the same salt level but also in control condition; thus, these outcomes might explain the different response between G2 and G34 clones to salt stress condition. Interestingly, we observed a significant variation among ecotypes related to several important physiological traits, such as leaf number per plot, stem number per plot, main stem height, SPAD unit, net photosynthesis, and biomass yield per plot. These results were confirmed by RNA-Sequencing, whereby in case of salt stress response each ecotype shows a different transcriptomic re-programming in response to the salt stress imposition. The transcriptomic data generated in this study showed a dose-dependent response to salt stress. Notably, it is worth to mention that a re-modulation of the transcriptional machinery emerges in G2 ecotype subjected to S4 extreme salt stress than S3 severe salt stress, thus indicating that the “emergency” condition leads to the regulation of a specific dataset of DEGs putatively involved in the long-term salt stress response. Moreover, we observed that most of these unigenes are homologs of genes belonging to other species, such as *Setaria italica*, *Zea mays* and *Oryza sativa*, suggesting a genetic homology among these *Poaceae* species. As regards the G2 ecotype, the salt sensory

mechanism outlined as SOS pathway is partially activated under severe S3 salt stress; whilst in case of S4 extreme salt stress condition, the mechanism of ion vacuolar sequestration has also been reported regulated by the over-expression of the vacuolar ion channels. Comparing the G2 and G34 ecotype, the severe salt stress treatment resulted in a lower number of DEGs in G34 rather than in G2 ecotype; thus, it indicates as G34 ecotype re-adjusts its own transcriptomic machinery in a different way. In our opinion, G34 ecotype reduces salt stress perception likely by the strong induction of CIPK1-SOS2 component to respond immediately to salt stress exposure at lower salt dose. Regarding the hormone regulation, we observed a different response between severe S3 and extreme S4 salt stress condition. The characterization of G2 ecotype showed that S3 severe salt stress does not lead to any changes of the gene involved in ABA biosynthesis, whereas, a clear down-regulation of ABA biosynthetic genes occurred in S4 sample data set, suggesting that ABA accumulation does not participate in the long-term salt stress, but might have a fundamental role during the onset of stressful conditions as demonstrated in other species (Geilfu et al., 2018), as well as in case of water stress condition (Fu et al., 2016). To reinforce these outcomes, another distinctive characteristic of G2 ecotype subjected to S4 extreme salt stress is based on the regulation of clusters involved in brassinosteroid and IAA/AUX biosynthesis, suggesting the putative role of these hormones in re-shaping the transcriptional network in case of unfavorable conditions. Nonetheless, in case of S3 severe salt stress condition, G34 re-modulates the transcription network of genes related to the ethylene signaling towards the minimization of ethylene negative effects upon plant growth. Similarly, the same trend was observed in G2 ecotype upon S4 extreme salt stress imposition. It was also observed the induction of genes involved in ROS scavenging (APX) as well as in the redistributing the reducing power excess among cell compartments (malate valve) under S3 severe salt stress condition in both G2 and G34 ecotypes. Nevertheless, only in G2 ecotype subjected to S4 extreme salt stress genes implicated in the malate valve and alternative oxidase (AOX) resulted over-expressed. As concerns the osmolyte protection, we observed a clear involvement of proline and polyamine biosynthesis in all sample data sets, thus confirming that osmolyte biosynthesis represents a pivotal mechanism to get through the hypersaline conditions and to re-adjust the homeostasis status in *A. donax*. As concerns the photosynthesis processes, we observed that genes involved in Rubisco biosynthesis and assembly are down regulated in both ecotypes subjected to S3 severe salt stress, probably leading to impaired CO<sub>2</sub> fixation via C3 Calvin cycle. Noteworthy, a dramatic *switch* from C3 Calvin cycle to C4 Calvin cycle is likely to occur in exposed to harmful condition (G2 and G34 subjected to S4 extreme salt stress and S3 salt stress, respectively), since gene regulation is addressed to activate the primary CO<sub>2</sub> fixation to PEP in mesophyll cells (C4 Calvin cycle). Moreover, we observed the up regulation of a key enzyme of the glycolate recovery pathway involved in

photorespiration (C2 cycle) indicating that CO<sub>2</sub> assimilation via C3 Calvin cycle might be substitute in favor of oxygen fixation. Moreover, the analysis of carbon metabolism revealed the upregulation of glycolysis and Krebs cycle genes in G34 at S3 severe salt stress condition, while a similar response was achieved by the G2 ecotype subjected to the higher salt dose (S4). Finally, the SSR analysis highlighted a huge number of repeated motifs distributed among untranslated and coding genes. Among them, five SSRs were successfully validated, showing a reliable congruence with the experiment. Consequently, the SSR catalogue of this experiment could be used in experiments aimed to assess genetic diversity among ecotypes, to design genetic maps, in marker-assisted selection (MAS) and in comparative genomics. Furthermore, we hereby investigated the molecular basis of *A. donax* leaf and root transcriptome in response to cadmium stress to gain novel insight into the responsiveness to heavy metal stress. The results depicted a clear response at morpho-physiological levels upon the prolonged exposure to cadmium treatment. Given that roots act as interface between plant and soil, we focused on a Cd\_R vs Cd\_L\* comparison derived by subtracting the DEGs belonging to the CK\_R vs CK\_L (root-related DEGs under control conditions) to the Cd\_R vs Cd\_L comparison (root-related DEGs under cadmium stress conditions) in order to get those DEGs specifically involved in root cadmium stress response. Based on differentially gene expression, a strong induction of ethylene biosynthesis and signalling in treated roots emerged, suggesting that roots function as main “messenger” center to transmit the stressful status to the apical regions. Interestingly, the up-regulation of the NRAMP1 transporter in treated roots was observed, indicating their ability to uptake ions in case of cadmium exposure. In contrast, the down-regulation of HMA3 transporter encoding gene was registered thus indicating that Cd-treated roots do not regulate cadmium ions efflux from cytosol towards the vacuole or outside the cells. In order to cope with the onset cellular damage, it has been observed that Cd leads to the over-expression of small peptide molecules (CEP, ROTUNDIFOLIA) along with the induction of ROS scavenging enzymes (SOD, APX and GST) as the major mechanisms to communicate and overcome Cd-induced stress in Cd-treated roots. Based on transcriptomic data the abscisic acid biosynthesis is inhibited, whilst the main gene involved in ABA degradation is up-regulated in treated roots. Moreover, in our study, both auxin biosynthesis- and transport- related transcripts (YUCCA2 and PIN) have been found among the over-represented genes in Cd-treated roots, suggesting the pivotal role of roots in promoting auxin homeostasis under cadmium stress condition. The analysis of “Nutrient uptake” category indicates that both nitrate transporter encoding genes and nitrate reductase gene were strongly up-regulated in roots, hence suggesting that nitrogen balance is keep under surveillance in *A. donax* treated roots. Nevertheless, the main finding about our work rely on the over-regulation of several encoding genes involved in cell wall remodeling and lignification in Cd-treated roots, which might account for an

effective barrier against the entry of Cd ions into the cell. Considering the specific response to both salt and cadmium treatment, these findings might constitute useful markers of the physiological status of *A. donax* in salinized and contaminated soils. Since, the tolerance to both salinity and cadmium stress is orchestrated by several mechanisms, many of the unigenes identified in this study have the potential to be used for obtaining *A. donax* ecotypes with improved lignocellulosic biomass production and stress tolerance. Although, the generated databases could be used for future genetic and molecular studies as well as to allow the implementation of breeding strategies for *A. donax* bioenergy crop.

## Bibliographic

- Abdullah, H. M., Akbari, P., Paulose, B., Schnell, D., Qi, W., Park, Y., ... & Dhankher, O. P. (2016). Transcriptome profiling of *Camelina sativa* to identify genes involved in triacylglycerol biosynthesis and accumulation in the developing seeds. *Biotechnology for biofuels*, 9(1), 1-19.
- Aguirre, A. M., Bassi, A., & Saxena, P. (2013). Engineering challenges in biodiesel production from microalgae. *Critical reviews in biotechnology*, 33(3), 293-308.
- Ahmad, R., Jamil, S., Shahzad, M., Zörb, C., Irshad, U., Khan, N., Younas, M. and Khan, S.A (2017). Metabolic profiling to elucidate genetic elements due to salt stress. *CLEAN–Soil, Air, Water*, 45(12), 1600574.
- Ahmad, R., Liow, P. S., Spencer, D. F., & Jasieniuk, M. (2008). Molecular evidence for a single genetic clone of invasive *Arundo donax* in the United States. *Aquatic Botany*, 88(2), 113-120.
- Akalın, M. K., Tekin, K., & Karagöz, S. (2017). Supercritical fluid extraction of biofuels from biomass. *Environmental Chemistry Letters*, 15(1), 29-41.
- Akbar, K. F., Hale, W. H., Headley, A. D., & Athar, M. (2006). Heavy metal contamination of roadside soils of Northern England. *Soil Water Res*, 1(4), 158-163.
- Alexopoulou, E. (Ed.). (2018). *Perennial Grasses for Bioenergy and Bioproducts: Production, Uses, Sustainability and Markets for Giant Reed, Miscanthus, Switchgrass, Reed Canary Grass and Bamboo*. Academic Press.
- Allwright, M. R., & Taylor, G. (2016). Molecular breeding for improved second generation bioenergy crops. *Trends in Plant Science*, 21(1), 43-54.
- Angelini, L. G., Ceccarini, L., o Di Nasso, N. N., & Bonari, E. (2009). Comparison of *Arundo donax* L. and *Miscanthus x giganteus* in a long-term field experiment in Central Italy: Analysis of productive characteristics and energy balance. *Biomass and bioenergy*, 33(4), 635-643.
- Arneth, A., Barbosa, H., Benton, T., Calvin, K., Calvo, E., & Connors, S. (2019). Climate change and land: summary for policymakers. An IPCC Special Report on Climate Change, Desertification, Land Degradation, Sustainable Land Management, Food Security, and Greenhouse Gas Fluxes in Terrestrial Ecosystems, 43.
- Aro, E. M. (2016). From first generation biofuels to advanced solar biofuels. *Ambio*, 45(1), 24-31.
- Baeyens, J., Kang, Q., Appels, L., Dewil, R., Lv, Y., & Tan, T. (2015). Challenges and opportunities in improving the production of bio-ethanol. *Progress in Energy and Combustion Science*, 47, 60-88.
- Bajguz, A., & Hayat, S. (2009). Effects of brassinosteroids on the plant responses to environmental stresses. *Plant physiology and biochemistry*, 47(1), 1-8.
- Balogh, E., Herr Jr, J. M., Czakó, M., & Márton, L. (2012). Defective development of male and



- female gametophytes in *Arundo donax* L.(Poaceae). *Biomass and Bioenergy*, 45, 265-269.
- Barragán, V., Leidi, E.O., Andrés, Z., Rubio, L., De Luca, A., Fernández, J.A., Cubero, B. and Pardo, J.M. (2012). Ion exchangers NHX1 and NHX2 mediate active potassium uptake into vacuoles to regulate cell turgor and stomatal function in *Arabidopsis*. *The Plant Cell*, 24(3), 1127-1142.
- Barrero, R. A., Guerrero, F. D., Moolhuijzen, P., Goolsby, J. A., Tidwell, J., Bellgard, S. E., & Bellgard, M. I. (2015). Shoot transcriptome of the giant reed, *Arundo donax*. *Data in brief*, 3, 1-6.
- Bashri, G., & Prasad, S. M. (2015). Indole acetic acid modulates changes in growth, chlorophyll a fluorescence and antioxidant potential of *Trigonella foenum-graecum* L. grown under cadmium stress. *Acta physiologiae plantarum*, 37(3), 49.
- Bassil, E., Ohto, M.A., Esumi, T., Tajima, H., Zhu, Z., Cagnac, O., Belmonte, M., Peleg, Z., Yamaguchi, T. and Blumwald, E. (2011). The *Arabidopsis* intracellular Na<sup>+</sup>/H<sup>+</sup> antiporters NHX5 and NHX6 are endosome associated and necessary for plant growth and development. *The Plant Cell*, 23(1), 224-239.
- Bataille, C., Åhman, M., Neuhoff, K., Nilsson, L. J., Fishedick, M., Lechtenböhmer, S., ... & Rahbar, S. (2018). A review of technology and policy deep decarbonization pathway options for making energy-intensive industry production consistent with the Paris Agreement. *Journal of Cleaner Production*, 187, 960-973.
- Behera, T. K., Gaikward, A. B., Singh, A. K., & Staub, J. E. (2008). Relative efficiency of DNA markers (RAPD, ISSR and AFLP) in detecting genetic diversity of bitter melon (*Momordica charantia* L.). *Journal of the Science of Food and Agriculture*, 88(4), 733-737.
- Bentley, D.R., Balasubramanian, S., Swerdlow, H.P., Smith, G.P., Milton, J., Brown, C.G., Hall, K.P., Evers, D.J., Barnes, C.L., Bignell, H.R. and Boutell, J.M. (2008). Accurate whole human genome sequencing using reversible terminator chemistry. *nature*, 456(7218), 53-59.
- Bharwana, S. A., Ali, S., Farooq, M. A., Iqbal, N., Abbas, F., & Ahmad, M. S. A. (2013). Alleviation of lead toxicity by silicon is related to elevated photosynthesis, antioxidant enzymes suppressed lead uptake and oxidative stress in cotton. *J. Bioremed. Biodeg*, 4(4), 187.
- Bianco, C., & Defez, R. (2009). *Medicago truncatula* improves salt tolerance when nodulated by an indole-3-acetic acid-overproducing *Sinorhizobium meliloti* strain. *Journal of experimental botany*, 60(11), 3097-3107.
- Blanco-Canqui, H. (2010). Energy crops and their implications on soil and environment. *Agronomy journal*, 102(2), 403-419.
- Bockheim, J. G., & Gennadiyev, A. N. (2000). The role of soil-forming processes in the definition of taxa in Soil Taxonomy and the World Soil Reference Base. *Geoderma*, 95(1-2), 53-72.

- Bonanno, G. (2012). *Arundo donax* as a potential biomonitor of trace element contamination in water and sediment. *Ecotoxicology and Environmental Safety*, 80, 20-27.
- Bray, E. A. (2000). Response to abiotic stress. *Biochemistry & Molecular Biology of Plants*. American Society of Plant Physiologists, 1158-1203.
- Brennan, L., & Owende, P. (2010). Biofuels from microalgae—a review of technologies for production, processing, and extractions of biofuels and co-products. *Renewable and sustainable energy reviews*, 14(2), 557-577.
- Bruinsma, J. (2009, June). The resource outlook to 2050: by how much do land, water and crop yields need to increase by 2050. In *Expert meeting on how to feed the world in (Vol. 2050, pp. 24-26)*.
- Bucci, A., Cassani, E., Landoni, M., Cantaluppi, E., & Pilu, R. (2013). Analysis of chromosome number and speculations on the origin of *Arundo donax* L.(Giant Reed). *Cytology and Genetics*, 47(4), 237-241.
- Buonocore, E., Vanoli, L., Carotenuto, A., & Ulgiati, S. (2015). Integrating life cycle assessment and emergy synthesis for the evaluation of a dry steam geothermal power plant in Italy. *Energy*, 86, 476-487.
- Bustreo, C., Giuliani, U., Maggio, D., & Zollino, G. (2019). How fusion power can contribute to a fully decarbonized European power mix after 2050. *Fusion Engineering and Design*, 146, 2189-2193.
- Cai, X., Zhang, X., & Wang, D. (2011). Land availability for biofuel production. *Environmental science & technology*, 45(1), 334-339.
- Campbell, J. E., Lobell, D. B., Genova, R. C., & Field, C. B. (2008). The global potential of bioenergy on abandoned agriculture lands. *Environmental science & technology*, 42(15), 5791-5794.
- Carmo-Silva, A. E., & Salvucci, M. E. (2013). The regulatory properties of Rubisco activase differ among species and affect photosynthetic induction during light transitions. *Plant physiology*, 161(4), 1645-1655.
- Casneuf, T., Van de Peer, Y., & Huber, W. (2007). In situ analysis of cross-hybridisation on microarrays and the inference of expression correlation. *BMC bioinformatics*, 8(1), 1-13.
- Castelli, S., & de Sannazzaro, S. C. (2011). *Biomasse per la produzione di energia. Produzione, gestione e processi di trasformazione (Vol. 110)*. Maggioli Editore.
- Castiglia, D., Sannino, L., Marcolongo, L., Ionata, E., Tamburino, R., De Stradis, A., ... & Scotti, N. (2016). High-level expression of thermostable cellulolytic enzymes in tobacco transplastomic plants and their use in hydrolysis of an industrially pretreated *Arundo donax* L. biomass. *Biotechnology for biofuels*, 9(1), 1-16.
- Chakraborty, K., Sairam, R. K., & Bhattacharya, R. C. (2012). Differential expression of salt overly

- sensitive pathway genes determines salinity stress tolerance in Brassica genotypes. *Plant Physiology and Biochemistry*, 51, 90-101.
- Chapman, K. S., & Hatch, M. D. (1983). Intracellular location of phosphoenolpyruvate carboxykinase and other C4 photosynthetic enzymes in mesophyll and bundle sheath protoplasts of *Panicum maximum*. *Plant Science Letters*, 29(2-3), 145-154.
- Chen, L., Han, J., Deng, X., Tan, S., Li, L., Li, L., Zhou, J., Peng, H., Yang, G., He, G. and Zhang, W. (2016). Expansion and stress responses of AP2/EREBP superfamily in *Brachypodium distachyon*. *Scientific reports*, 6(1), 1-14.
- Chen, S., Li, J., Wang, S., Hüttermann, A., & Altman, A. (2001a). Salt, nutrient uptake and transport, and ABA of *Populus euphratica*; a hybrid in response to increasing soil NaCl. *Trees*, 15(3), 186-194.
- Cheng, H., Jiang, Z.Y., Liu, Y., Ye, Z.H., Wu, M.L., Sun, C.C., Sun, F.L., Fei, J. and Wang, Y.S. (2014). Metal (Pb, Zn and Cu) uptake and tolerance by mangroves in relation to root anatomy and lignification/suberization. *Tree physiology*, 34(6), 646-656.
- Cheng, N. H., Pittman, J. K., Zhu, J. K., & Hirschi, K. D. (2004). The protein kinase SOS2 activates the Arabidopsis H<sup>+</sup>/Ca<sup>2+</sup> antiporter CAX1 to integrate calcium transport and salt tolerance. *Journal of Biological Chemistry*, 279(4), 2922-2926.
- Chmielowska-Bąk, J., Gzyl, J., Rucińska-Sobkowiak, R., Arasimowicz-Jelonek, M., & Deckert, J. (2014). The new insights into cadmium sensing. *Frontiers in plant science*, 5, 245.
- Choi, W. G., Toyota, M., Kim, S. H., Hilleary, R., & Gilroy, S. (2014). Salt stress-induced Ca<sup>2+</sup> waves are associated with rapid, long-distance root-to-shoot signaling in plants. *Proceedings of the National Academy of Sciences*, 111(17), 6497-6502.
- Choong, G., Liu, Y., & Templeton, D. M. (2014). Interplay of calcium and cadmium in mediating cadmium toxicity. *Chemico-biological interactions*, 211, 54-65.
- Chu, C., Dai, Z., Ku, M. S., & Edwards, G. E. (1990). Induction of Crassulacean acid metabolism in the facultative halophyte *Mesembryanthemum crystallinum* by abscisic acid. *Plant Physiology*, 93(3), 1253-1260.
- Cicero, L.L., Madesis, P., Tsaftaris, A. and Piero, A.R.L. (2015). Tobacco plants over-expressing the sweet orange tau glutathione transferases (CsGSTUs) acquire tolerance to the diphenyl ether herbicide fluorodifen and to salt and drought stresses. *Phytochemistry*, 116, 69-77.
- Colebrook, E. H., Thomas, S. G., Phillips, A. L., & Hedden, P. (2014). The role of gibberellin signalling in plant responses to abiotic stress. *Journal of experimental biology*, 217(1), 67-75.
- Coleman, H. D., Yan, J., & Mansfield, S. D. (2009). Sucrose synthase affects carbon partitioning to increase cellulose production and altered cell wall ultrastructure. *Proceedings of the National*

Academy of Sciences, 106(31), 13118-13123.

- Cona, A., Rea, G., Angelini, R., Federico, R., & Tavladoraki, P. (2006). Functions of amine oxidases in plant development and defence. *Trends in plant science*, 11(2), 80-88.
- Corno, L., Pilu, R., & Adani, F. (2014). *Arundo donax* L.: a non-food crop for bioenergy and bio-compound production. *Biotechnology advances*, 32(8), 1535-1549.
- Cosentino, S. L., Copani, V., D'Agosta, G. M., Sanzone, E., & Mantineo, M. (2006). First results on evaluation of *Arundo donax* L. clones collected in Southern Italy. *Industrial Crops and Products*, 23(2), 212-222.
- Couturier, J., Ströher, E., Albetel, A.N., Roret, T., Muthuramalingam, M., Tarrago, L., Seidel, T., Tsan, P., Jacquot, J.P., Johnson, M.K. and Dietz, K.J. (2011). *Arabidopsis* chloroplastic glutaredoxin C5 as a model to explore molecular determinants for iron-sulfur cluster binding into glutaredoxins. *Journal of Biological Chemistry*, 286(31), 27515-27527.
- Cui, F., Liu, L., Zhao, Q., Zhang, Z., Li, Q., Lin, B., Wu, Y., Tang, S. and Xie, Q. (2012). *Arabidopsis* ubiquitin conjugase UBC32 is an ERAD component that functions in brassinosteroid-mediated salt stress tolerance. *The Plant Cell*, 24(1), 233-244.
- Curley, E. M., O'Flynn, M. G., & McDonnell, K. P. (2009). Nitrate leaching losses from *Miscanthus* × *giganteus* impact on groundwater quality. *Journal of agronomy*, 8(3), 107-112.
- Cushman, J. C., & Bohnert, H. J. (1992). Salt stress induction of crassulacean acid metabolism in a facultative CAM plant. In *Photosynthesis Research* (Vol. 34, No. 1, pp. 103-103). SPUIBOULEVARD 50, PO BOX 17, 3300 AA DORDRECHT, NETHERLANDS: KLUWER ACADEMIC PUBL.
- Da Silva, J. F., & Williams, R. J. P. (2001). *The biological chemistry of the elements: the inorganic chemistry of life*. Oxford University Press.
- Dabney, S. M., McGregor, K. C., Wilson, G. V., & Cullum, R. F. (2009). How management of grass hedges affects their erosion reduction potential.
- DalCorso, G., Manara, A., & Furini, A. (2013). An overview of heavy metal challenge in plants: from roots to shoots. *Metallomics*, 5(9), 1117-1132.
- Dalle-Donne, I., Rossi, R., Colombo, G., Giustarini, D., & Milzani, A. (2009). Protein S-glutathionylation: a regulatory device from bacteria to humans. *Trends in biochemical sciences*, 34(2), 85-96.
- Danelli, T., Cantaluppi, E., Tosca, A., Cassani, E., Landoni, M., Bosio, S., Adani, F. and Pilu, R. (2019). Influence of clonal variation on the efficiency of *Arundo donax* propagation methods. *Journal of Plant Growth Regulation*, 38(4), 1449-1457.
- Danelli, T., Laura, M., Savona, M., Landoni, M., Adani, F., & Pilu, R. (2020). Genetic Improvement

- of *Arundo donax* L.: Opportunities and Challenges. *Plants*, 9(11), 1584.
- Davenport, R. J., MUÑOZ-MAYOR, A. L. I. C. I. A., Jha, D., Essah, P. A., Rus, A. N. A., & Tester, M. (2007). The Na<sup>+</sup> transporter AtHKT1; 1 controls retrieval of Na<sup>+</sup> from the xylem in *Arabidopsis*. *Plant, cell & environment*, 30(4), 497-507.
- De Smet, S., Cuypers, A., Vangronsveld, J., & Remans, T. (2015). Gene networks involved in hormonal control of root development in *Arabidopsis thaliana*: a framework for studying its disturbance by metal stress. *International journal of molecular sciences*, 16(8), 19195-19224.
- De Stefano, R., Cappetta, E., Guida, G., Mistretta, C., Caruso, G., Giorio, P., ... & Tucci, M. (2018). Screening of giant reed (*Arundo donax* L.) ecotypes for biomass production under salt stress. *Plant Biosystems-An International Journal Dealing with all Aspects of Plant Biology*, 152(5), 911-917.
- Deenanath, E. D., Iyuke, S., & Rumbold, K. (2012). The bioethanol industry in Sub-Saharan Africa: history, challenges, and prospects. *Journal of Biomedicine and Biotechnology*, 2012.
- Deinlein, U., Stephan, A. B., Horie, T., Luo, W., Xu, G., & Schroeder, J. I. (2014). Plant salt-tolerance mechanisms. *Trends in plant science*, 19(6), 371-379.
- DeRose-Wilson, L., & Gaut, B. S. (2011). Mapping salinity tolerance during *Arabidopsis thaliana* germination and seedling growth. *PLoS One*, 6(8), e22832.
- DESA, U. (2019). *World Population Prospects 2019*. United Nations. Department of Economic and Social Affairs. *World Population Prospects 2019*.
- Dhir, S., Knowles, K., Pagan, C. L., & Mann, J. (2010). Optimization and transformation of *Arundo donax* L. using particle bombardment. *African Journal of Biotechnology*, 9(39), 6460-6469.
- Ding, Z. J., Yan, J. Y., Li, C. X., Li, G. X., Wu, Y. R., & Zheng, S. J. (2015). Transcription factor WRKY 46 modulates the development of *Arabidopsis* lateral roots in osmotic/salt stress conditions via regulation of ABA signaling and auxin homeostasis. *The Plant Journal*, 84(1), 56-69.
- Docimo, T., De Stefano, R., De Palma, M., Cappetta, E., Villano, C., Aversano, R., & Tucci, M. (2020). Transcriptional, metabolic and DNA methylation changes underpinning the response of *Arundo donax* ecotypes to NaCl excess. *Planta*, 251(1), 1-17.
- Domokos-Szabolcsy, E., Abdalla, N., Alshaal, T., Sztrik, A., Márton, L., & El-Ramady, H. (2014). In vitro comparative study of two *Arundo donax* L. ecotypes' selenium tolerance. *International Journal of Horticultural Science*, 20(3-4), 119-122.
- Doncheva, S., Amenos, M., Poschenrieder, C., & Barcelo, J. (2005). Root cell patterning: a primary target for aluminium toxicity in maize. *Journal of experimental botany*, 56(414), 1213-1220.
- Douchiche, O., Rihouey, C., Schaumann, A., Driouich, A., & Morvan, C. (2007). Cadmium-induced

- alterations of the structural features of pectins in flax hypocotyl. *Planta*, 225(5), 1301-1312.
- Dowling, Dame Ann, and Ramakrishnan Venki. (2018). Greenhouse Gas Removal. Report by the UK Royal Society and Royal Academy of Engineering
- Edelstein, M., & Ben-Hur, M. (2018). Heavy metals and metalloids: Sources, risks and strategies to reduce their accumulation in horticultural crops. *Scientia Horticulturae*, 234, 431-444.
- Ehret, D. L., Redmann, R. E., Harvey, B. L., & Cipywnyk, A. (1990). Salinity-induced calcium deficiencies in wheat and barley. *Plant and soil*, 128(2), 143-151.
- Elhawat, N., Alshaal, T., Domokos-Szabolcsy, É., El-Ramady, H., Márton, L., Czakó, M., Kátai, J., Balogh, P., Sztrik, A., Molnár, M. and Popp, J. (2014). Phytoaccumulation potentials of two biotechnologically propagated ecotypes of *Arundo donax* in copper-contaminated synthetic wastewater. *Environmental Science and Pollution Research*, 21(12), 7773-7780.
- El-Mashad, A. A. A., & Mohamed, H. I. (2012). Brassinolide alleviates salt stress and increases antioxidant activity of cowpea plants (*Vigna sinensis*). *Protoplasma*, 249(3), 625-635.
- Esselman EJ, Jianqiang L, Crawford DJ, Windus JL, Wolfe AD (1999) Clonal diversity in the rare *Calamagrostis porteri* ssp. *insperata* (Poaceae): comparative results for allozymes and random amplified polymorphic DNA (RAPD) and intersimple sequence repeat (ISSR) markers. *Molecular Ecology* 8: 443–451
- Estrela, R., & Cate, J. H. D. (2016). Energy biotechnology in the CRISPR-Cas9 era. *Current opinion in biotechnology*, 38, 79-84.
- European Commission. (2014.) State of Play on the Sustainability of Solid and Gaseous Biomass Used for Electricity, Heating and Cooling in the EU - Commission Staff Working Document. Igarss 2014.
- European commission. (2015). Progress Made in Cutting Emissions | Climate Action. European Commission.
- European Commission. Protection of the Environment, and in particular of the soil, when sewage sludge is used in agriculture. *Official Journal of the European Communities*. 1986;4:6–12.
- Evangelistella, C., Valentini, A., Ludovisi, R., Firrincieli, A., Fabbrini, F., Scalabrin, S., Cattonaro, F., Morgante, M., Mugnozza, G.S., Keurentjes, J.J. and Harfouche, A. (2017). De novo assembly, functional annotation, and analysis of the giant reed (*Arundo donax* L.) leaf transcriptome provide tools for the development of a biofuel feedstock. *Biotechnology for biofuels*, 10(1), 1-24.
- Fan, W., Liu, C., Cao, B., Ma, S., Hu, J., Xiang, Z., & Zhao, A. (2021). A meta-analysis of transcriptomic profiles reveals molecular pathways response to cadmium stress of Gramineae. *Ecotoxicology and Environmental Safety*, 209, 111816.

- Fan, W., Liu, C., Cao, B., Qin, M., Long, D., Xiang, Z., & Zhao, A. (2018). Genome-wide identification and characterization of four gene families putatively involved in cadmium uptake, translocation and sequestration in mulberry. *Frontiers in plant science*, 9, 879.
- Fargione, J. E., Plevin, R. J., & Hill, J. D. (2010). The ecological impact of biofuels. *Annual Review of Ecology, Evolution, and Systematics*, 41, 351-377.
- Farias, J.G., Antes, F.L., Nunes, P.A., Nunes, S.T., Schaich, G., Rossato, L.V., Miotto, A., Giroto, E., Tiecher, T.L., Dressler, V.L. and Nicoloso, F.T. (2013). Effects of excess copper in vineyard soils on the mineral nutrition of potato genotypes. *Food and Energy Security*, 2(1), 49-69.
- Fattorini, L., Ronzan, M., Piacentini, D., Della Rovere, F., De Virgilio, C., Sofo, A., Altamura, M.M. and Falasca, G. (2017). Cadmium and arsenic affect quiescent centre formation and maintenance in *Arabidopsis thaliana* post-embryonic roots disrupting auxin biosynthesis and transport. *Environmental and Experimental Botany*, 144, 37-48.
- Fawzy, S., Osman, A. I., Doran, J., & Rooney, D. W. (2020). Strategies for mitigation of climate change: a review. *Environmental Chemistry Letters*, 1-26.
- Fazio, S., & Monti, A. (2011). Life cycle assessment of different bioenergy production systems including perennial and annual crops. *Biomass and Bioenergy*, 35(12), 4868-4878.
- Feng, Q., Chaubey, I., Her, Y. G., Cibin, R., Engel, B., Volenec, J., & Wang, X. (2015). Hydrologic and water quality impacts and biomass production potential on marginal land. *Environmental Modelling & Software*, 72, 230-238.
- Fernando, A. L., Barbosa, B., Costa, J., & Papazoglou, E. G. (2016). Giant reed (*Arundo donax* L.): A multipurpose crop bridging phytoremediation with sustainable bioeconomy. In *Bioremediation and bioeconomy* (pp. 77-95). Elsevier.
- Fernando, A. L., Boléo, S., Barbosa, B., Costa, J., Duarte, M. P., & Monti, A. (2015). Perennial grass production opportunities on marginal Mediterranean land. *BioEnergy Research*, 8(4), 1523-1537.
- Ferretti, M., Ghisi, R., Merlo, L., Dalla Vecchia, F., & Passera, C. (1994). Effect of cadmium on photosynthesis and enzymes of photosynthetic sulphate and nitrate assimilation pathways in maize (*Zea mays*). *Photosynthetica*.
- Fidalgo, F., Azenha, M., Silva, A. F., de Sousa, A., Santiago, A., Ferraz, P., & Teixeira, J. (2013). Copper-induced stress in *Solanum nigrum* L. and antioxidant defense system responses. *Food and Energy Security*, 2(1), 70-80.
- Flowers, T. J. (2004). Improving crop salt tolerance. *Journal of Experimental botany*, 55(396), 307-319.
- FNR. (2017). Fachagentur Nachwachsende Rohstoffe e. V. BASISDATEN BIOENERGIE

DEUTSCHLAND 2017, 27.

- Fougere, F., Le Rudulier, D., & Streeter, J. G. (1991). Effects of salt stress on amino acid, organic acid, and carbohydrate composition of roots, bacteroids, and cytosol of alfalfa (*Medicago sativa* L.). *Plant physiology*, 96(4), 1228-1236.
- Fu, Y., Poli, M., Sablok, G., Wang, B., Liang, Y., La Porta, N., Velikova, V., Loreto, F., Li, M. and Varotto, C. (2016). Dissection of early transcriptional responses to water stress in *Arundo donax* L. by unigene-based RNA-seq. *Biotechnology for biofuels*, 9(1), 1-18.
- Gall, J. E., Boyd, R. S., & Rajakaruna, N. (2015). Transfer of heavy metals through terrestrial food webs: a review. *Environmental monitoring and assessment*, 187(4), 1-21.
- Gao, J., Sun, L., Yang, X., & Liu, J. X. (2013). Transcriptomic analysis of cadmium stress response in the heavy metal hyperaccumulator *Sedum alfredii* Hance. *PloS one*, 8(6), e64643.
- Gardner, W. K. (2016). Sodium, calcium and magnesium ratios in soils of NW Victoria, Australia may restrict root growth and crop production. *Journal of Plant Nutrition*, 39(9), 1205-1215.
- Gawronska, K., Romanowska, E., Miszalski, Z., & Niewiadomska, E. (2013). Limitation of C3-CAM shift in the common ice plant under high irradiance. *Journal of plant physiology*, 170(2), 129-135.
- Geilfus, C. M., Ludwig-Müller, J., Bárdos, G., & Zörb, C. (2018). Early response to salt ions in maize (*Zea mays* L.). *Journal of plant physiology*, 220, 173-180.
- Gessesse, B., Bewket, W., & Bräuning, A. (2015). Model-based characterization and monitoring of runoff and soil erosion in response to land use/land cover changes in the Modjo watershed, Ethiopia. *Land degradation & development*, 26(7), 711-724.
- Gharsallah, C., Fakhfakh, H., Grubb, D., & Gorsane, F. (2016). Effect of salt stress on ion concentration, proline content, antioxidant enzyme activities and gene expression in tomato cultivars. *AoB Plants*, 8.
- Gill, S. S., & Tuteja, N. (2010). Reactive oxygen species and antioxidant machinery in abiotic stress tolerance in crop plants. *Plant physiology and biochemistry*, 48(12), 909-930.
- Golldack, D., Li, C., Mohan, H., & Probst, N. (2014). Tolerance to drought and salt stress in plants: unraveling the signaling networks. *Frontiers in plant science*, 5, 151.
- Grabherr, M.G., Haas, B.J., Yassour, M., Levin, J.Z., Thompson, D.A., Amit, I., Adiconis, X., Fan, L., Raychowdhury, R., Zeng, Q. and Chen, Z. (2011). Full-length transcriptome assembly from RNA-Seq data without a reference genome. *Nature biotechnology*, 29(7), 644-652.
- Gressel, J. (2008). Transgenics are imperative for biofuel crops. *Plant science*, 174(3), 246-263.
- Groppa, M. D., & Benavides, M. P. (2008). Polyamines and abiotic stress: recent advances. *Amino acids*, 34(1), 35.



- Gu, C. S., Liu, L. Q., Deng, Y. M., Zhang, Y. X., Wang, Z. Q., Yuan, H. Y., & Huang, S. Z. (2017). De novo characterization of the *Iris lactea* var. *chinensis* transcriptome and an analysis of genes under cadmium or lead exposure. *Ecotoxicology and environmental safety*, 144, 507-513.
- Guan, M. Y., Fan, S. K., Fang, X. Z., & Jin, C. W. (2015). Modification of nitrate uptake pathway in plants affects the cadmium uptake by roots. *Plant signaling & behavior*, 10(3), e990794.
- Guan, M., Chen, M., & Cao, Z. (2021). NRT2. 1, a major contributor to cadmium uptake controlled by high-affinity nitrate transporters. *Ecotoxicology and Environmental Safety*, 218, 112269.
- Guarino, F., Cicatelli, A., Brundu, G., Improta, G., Triassi, M., & Castiglione, S. (2019). The use of MSAP reveals epigenetic diversity of the invasive clonal populations of *Arundo donax* L. *PLoS One*, 14(4), e0215096.
- Gude, V. G., & Martinez-Guerra, E. (2018). Green chemistry with process intensification for sustainable biodiesel production. *Environmental chemistry letters*, 16(2), 327-341.
- Guo, J., Song, J., Wang, F., & Zhang, X. S. (2007). Genome-wide identification and expression analysis of rice cell cycle genes. *Plant molecular biology*, 64(4), 349-360.
- Guo, M., Song, W., & Buhain, J. (2015). Bioenergy and biofuels: History, status, and perspective. *Renewable and sustainable energy reviews*, 42, 712-725.
- Gupta, A., & Verma, J. P. (2015). Sustainable bio-ethanol production from agro-residues: a review. *Renewable and sustainable energy reviews*, 41, 550-567.
- Gupta, B., & Huang, B. (2014). Mechanism of salinity tolerance in plants: physiological, biochemical, and molecular characterization. *International journal of genomics*, 2014.
- Gupta, K. J., Stoimenova, M., & Kaiser, W. M. (2005). In higher plants, only root mitochondria, but not leaf mitochondria reduce nitrite to NO, in vitro and in situ. *Journal of Experimental Botany*, 56(420), 2601-2609.
- Gupta, K., Dey, A., & Gupta, B. (2013). Polyamines and their role in plant osmotic stress tolerance. *Climate change and plant abiotic stress tolerance*, 1053-1072.
- Gurmani, A. R., Bano, A., Khan, S. U., Din, J., & Zhang, J. L. (2011). Alleviation of salt stress by seed treatment with abscisic acid (ABA), 6-benzylaminopurine (BA) and chlormequat chloride (CCC) optimizes ion and organic matter accumulation and increases yield of rice ('*Oryza sativa*'L.). *Australian Journal of Crop Science*, 5(10), 1278-1285.
- Haberl, H., Erb, K. H., Krausmann, F., Bondeau, A., Lauk, C., Müller, C., ... & Steinberger, J. K. (2011). Global bioenergy potentials from agricultural land in 2050: Sensitivity to climate change, diets and yields. *Biomass and bioenergy*, 35(12), 4753-4769.
- Haddadchi, A., Gross, C. L., & Fatemi, M. (2013). The expansion of sterile *Arundo donax* (Poaceae) in southeastern Australia is accompanied by genotypic variation. *Aquatic Botany*, 104, 153-161.

- Hanin, M., Ebel, C., Ngom, M., Laplaze, L., & Masmoudi, K. (2016). New insights on plant salt tolerance mechanisms and their potential use for breeding. *Frontiers in plant science*, 7, 1787.
- Haque, A. M., Gohari, G., El-Shehawi, A. M., Dutta, A. K., Elseehy, M. M., & Kabir, A. H. (2021). Genome-wide identification, characterization and expression profiles of heavy metal ATPase 3 (HMA3) in plants. *Journal of King Saud University-Science*, 101730.
- Hardion, L., Baumel, A., Verlaque, R., & Vila, B. (2014). Distinct evolutionary histories of lowland biota on Italian and Balkan peninsulas revealed by the phylogeography of *Arundo plinii* (Poaceae). *Journal of Biogeography*, 41(11), 2150-2161.
- Hardion, L., Verlaque, R., Baumel, A., Juin, M., & Vila, B. (2012). Revised systematics of Mediterranean *Arundo* (Poaceae) based on AFLP fingerprints and morphology. *Taxon*, 61(6), 1217-1226.
- Hardion, L., Verlaque, R., Rosato, M., Rossello, J. A., & Vila, B. (2015). Impact of polyploidy on fertility variation of Mediterranean *Arundo* L. (Poaceae). *Comptes rendus biologiques*, 338(5), 298-306.
- Hardion, L., Verlaque, R., Saltonstall, K., Leriche, A., & Vila, B. (2014). Origin of the invasive *Arundo donax* (Poaceae): a trans-Asian expedition in herbaria. *Annals of botany*, 114(3), 455-462.
- Hare, P. D., & Cress, W. A. (1997). Metabolic implications of stress-induced proline accumulation in plants. *Plant growth regulation*, 21(2), 79-102.
- Harvey, M. (2014). The food-energy-climate change trilemma: Toward a socio-economic analysis. *Theory, Culture & Society*, 31(5), 155-182.
- Harvey, M., & Pilgrim, S. (2011). The new competition for land: Food, energy, and climate change. *Food policy*, 36, S40-S51.
- Hasegawa, P. M., Bressan, R. A., Zhu, J. K., & Bohnert, H. J. (2000). Plant cellular and molecular responses to high salinity. *Annual review of plant biology*, 51(1), 463-499.
- Hasegawa, T., Sands, R. D., Brunelle, T., Cui, Y., Frank, S., Fujimori, S., & Popp, A. (2020). Food security under high bioenergy demand toward long-term climate goals. *Climatic Change*, 163(3), 1587-1601.
- Haworth, M., Centritto, M., Giovannelli, A., Marino, G., Proietti, N., Capitani, D., De Carlo, A. and Loreto, F. (2017b). Xylem morphology determines the drought response of two *Arundo donax* ecotypes from contrasting habitats. *Gcb Bioenergy*, 9(1), 119-131.
- Haworth, M., Cosentino, S.L., Marino, G., Brunetti, C., Scordia, D., Testa, G., Riggi, E., Avola, G., Loreto, F. and Centritto, M. (2017a). Physiological responses of *Arundo donax* ecotypes to drought: a common garden study. *Gcb Bioenergy*, 9(1), 132-143.

- Heaton, E. A., Dohleman, F. G., & Long, S. P. (2008). Meeting US biofuel goals with less land: the potential of *Miscanthus*. *Global change biology*, 14(9), 2000-2014.
- Hernandez, L. E., Garate, A., & Carpena-Ruiz, R. (1997). Effects of cadmium on the uptake, distribution and assimilation of nitrate in *Pisum sativum*. *Plant and Soil*, 189(1), 97-106.
- Hill, J., Nelson, E., Tilman, D., Polasky, S., & Tiffany, D. (2006). Environmental, economic, and energetic costs and benefits of biodiesel and ethanol biofuels. *Proceedings of the National Academy of sciences*, 103(30), 11206-11210.
- Ho, D. P., Ngo, H. H., & Guo, W. (2014). A mini review on renewable sources for biofuel. *Bioresource technology*, 169, 742-749.
- Hoogwijk, M., Faaij, A., Eickhout, B., De Vries, B., & Turkenburg, W. (2005). Potential of biomass energy out to 2100, for four IPCC SRES land-use scenarios. *Biomass and Bioenergy*, 29(4), 225-257.
- Hoque, M. A., Banu, M. N. A., Nakamura, Y., Shimoishi, Y., & Murata, Y. (2008). Proline and glycinebetaine enhance antioxidant defense and methylglyoxal detoxification systems and reduce NaCl-induced damage in cultured tobacco cells. *Journal of plant physiology*, 165(8), 813-824.
- Hossain, M. A., Piyatida, P., da Silva, J. A. T., & Fujita, M. (2012). Molecular mechanism of heavy metal toxicity and tolerance in plants: central role of glutathione in detoxification of reactive oxygen species and methylglyoxal and in heavy metal chelation. *Journal of Botany*, 2012.
- Hu, Y.F., Zhou, G., Na, X.F., Yang, L., Nan, W.B., Liu, X., Zhang, Y.Q., Li, J.L. and Bi, Y.R. (2013). Cadmium interferes with maintenance of auxin homeostasis in *Arabidopsis* seedlings. *Journal of Plant Physiology*, 170(11), 965-975.
- Huang, T. L., Nguyen, Q. T. T., Fu, S. F., Lin, C. Y., Chen, Y. C., & Huang, H. J. (2012). Transcriptomic changes and signalling pathways induced by arsenic stress in rice roots. *Plant molecular biology*, 80(6), 587-608.
- Huang, Y., Chen, Q., Deng, M., Japenga, J., Li, T., Yang, X., & He, Z. (2018). Heavy metal pollution and health risk assessment of agricultural soils in a typical peri-urban area in southeast China. *Journal of environmental management*, 207, 159-168.
- Hunter, M. C., Smith, R. G., Schipanski, M. E., Atwood, L. W., & Mortensen, D. A. (2017). Agriculture in 2050: recalibrating targets for sustainable intensification. *Bioscience*, 67(4), 386-391.
- Hussain Wani, S., Brajendra Singh, N., Haribhushan, A., & Iqbal Mir, J. (2013). Compatible solute engineering in plants for abiotic stress tolerance-role of glycine betaine. *Current genomics*, 14(3), 157-165.

- Hussain, A., Arif, S. M., & Aslam, M. (2017). Emerging renewable and sustainable energy technologies: State of the art. *Renewable and Sustainable Energy Reviews*, 71, 12-28.
- Hussain, R. M., Sheikh, A. H., Haider, I., Quareshy, M., & Linthorst, H. J. (2018). Arabidopsis WRKY50 and TGA transcription factors synergistically activate expression of PR1. *Frontiers in plant science*, 9, 930.
- IEA. (2017.) *Technology Roadmap: Delivering Sustainable Bioenergy*. IEA Publications.
- Im Kim, J., Baek, D., Park, H.C., Chun, H.J., Oh, D.H., Lee, M.K., Cha, J.Y., Kim, W.Y., Kim, M.C., Chung, W.S. and Bohnert, H.J. (2013). Overexpression of Arabidopsis YUCCA6 in potato results in high-auxin developmental phenotypes and enhanced resistance to water deficit. *Molecular plant*, 6(2), 337-349.
- Isayenkov, S. V. (2012). Physiological and molecular aspects of salt stress in plants. *Cytology and Genetics*, 46(5), 302-318.
- Isayenkov, S. V., & Maathuis, F. J. (2019). Plant salinity stress: many unanswered questions remain. *Frontiers in Plant Science*, 10, 80.
- Ishitani, M., Liu, J., Halfter, U., Kim, C. S., Shi, W., & Zhu, J. K. (2000). SOS3 function in plant salt tolerance requires N-myristoylation and calcium binding. *The Plant Cell*, 12(9), 1667-1677.
- Islam, E., Khan, M. T., & Irem, S. (2015). Biochemical mechanisms of signaling: perspectives in plants under arsenic stress. *Ecotoxicology and environmental safety*, 114, 126-133.
- Ismail, A. M., Heuer, S., Thomson, M. J., & Wissuwa, M. (2007). Genetic and genomic approaches to develop rice germplasm for problem soils. *Plant molecular biology*, 65(4), 547-570.
- Jacoby, R. P., Millar, A. H., & Taylor, N. L. (2010). Wheat mitochondrial proteomes provide new links between antioxidant defense and plant salinity tolerance. *Journal of proteome research*, 9(12), 6595-6604.
- Jalmi, S. K., & Sinha, A. K. (2015). ROS mediated MAPK signaling in abiotic and biotic stress-striking similarities and differences. *Frontiers in plant science*, 6, 769.
- Jalmi, S.K., Bhagat, P.K., Verma, D., Noryang, S., Tayyeba, S., Singh, K., Sharma, D. and Sinha, A.K. (2018). Traversing the links between heavy metal stress and plant signaling. *Frontiers in plant science*, 9, 12.
- Janicka-Russak, M., Kabała, K., Burzyński, M., & Kłobus, G. (2008). Response of plasma membrane H<sup>+</sup>-ATPase to heavy metal stress in *Cucumis sativus* roots. *Journal of Experimental Botany*, 59(13), 3721-3728.
- Janin, G., & Letzelter, B. (1977). [Giant reeds. Determination of average sample of a stalk in view of clonal selection [*Arundo donax*]]. [French]. *Papeterie*.
- Järup, L. (2003). Hazards of heavy metal contamination. *British medical bulletin*, 68(1), 167-182.

- Jayakannan, M., Bose, J., Babourina, O., Shabala, S., Massart, A., Poschenrieder, C., & Rengel, Z. (2015). The NPR1-dependent salicylic acid signalling pathway is pivotal for enhanced salt and oxidative stress tolerance in Arabidopsis. *Journal of Experimental Botany*, 66(7), 1865-1875.
- Jiang, Y., Yang, B., Harris, N. S., & Deyholos, M. K. (2007). Comparative proteomic analysis of NaCl stress-responsive proteins in Arabidopsis roots. *Journal of experimental botany*, 58(13), 3591-3607.
- Jin, E., & Sutherland, J. W. (2018). An integrated sustainability model for a bioenergy system: Forest residues for electricity generation. *Biomass and Bioenergy*, 119, 10-21.
- Jin, H. J., Zhao, J. C., Wu, L., Kim, J., & Yu, J. (2014). Cooperativity and equilibrium with FOXA1 define the androgen receptor transcriptional program. *Nature communications*, 5(1), 1-14.
- Jonak, C., Nakagami, H., & Hirt, H. (2004). Heavy metal stress. Activation of distinct mitogen-activated protein kinase pathways by copper and cadmium. *Plant physiology*, 136(2), 3276-3283.
- Jones, M. B., Finnan, J., & Hodkinson, T. R. (2015). Morphological and physiological traits for higher biomass production in perennial rhizomatous grasses grown on marginal land. *Gcb Bioenergy*, 7(2), 375-385.
- Jun, M., Fu, H. Y., Hong, J., Wan, X., Yang, C. S., & Ho, C. T. (2003). Comparison of antioxidant activities of isoflavones from kudzu root (*Pueraria lobata* Ohwi). *Journal of food science*, 68(6), 2117-2122.
- Kaleem, F., Shabir, G., Aslam, K., Rasul, S., Manzoor, H., Shah, S. M., & Khan, A. R. (2018). An overview of the genetics of plant response to salt stress: present status and the way forward. *Applied biochemistry and biotechnology*, 186(2), 306-334.
- Kanehisa, M., Sato, Y., Kawashima, M., Furumichi, M., & Tanabe, M. (2016). KEGG as a reference resource for gene and protein annotation. *Nucleic acids research*, 44(D1), D457-D462.
- Kaur, G., & Asthir, B. J. B. P. (2015). Proline: a key player in plant abiotic stress tolerance. *Biologia plantarum*, 59(4), 609-619.
- Kerepesi, I., & Galiba, G. (2000). Osmotic and salt stress-induced alteration in soluble carbohydrate content in wheat seedlings. *Crop science*, 40(2), 482-487.
- Keunen, E., Remans, T., Bohler, S., Vangronsveld, J., & Cuypers, A. (2011). Metal-induced oxidative stress and plant mitochondria. *International Journal of Molecular Sciences*, 12(10), 6894-6918.
- Khan, S., & Stone, J. M. (2007). Arabidopsis thaliana GH3. 9 influences primary root growth. *Planta*, 226(1), 21-34.
- Khudamrongsawat, J., Tayyar, R., & Holt, J. S. (2004). Genetic diversity of giant reed (*Arundo donax*) in the Santa Ana River, California. *Weed Science*, 52(3), 395-405.

- Ki-Moon, B. (2008). Kyoto Protocol Reference Manual. In United Nations Framework Convention on Climate Change (Vol. 130). UNFCCC.
- Knight, H., Trewavas, A. J., & Knight, M. R. (1997). Calcium signalling in *Arabidopsis thaliana* responding to drought and salinity. *The Plant Journal*, 12(5), 1067-1078.
- Kobayashi, N.I., Yamaji, N., Yamamoto, H., Okubo, K., Ueno, H., Costa, A., Tanoi, K., Matsumura, H., Fujii-Kashino, M., Horiuchi, T. and Nayef, M.A. (2017). OsHKT1; 5 mediates Na<sup>+</sup> exclusion in the vasculature to protect leaf blades and reproductive tissues from salt toxicity in rice. *The Plant Journal*, 91(4), 657-670.
- Koizumi, T. (2014). Biofuels and food security. In *Biofuels and Food Security* (pp. 103-121). Springer, Cham.
- Kováčik, J., & Klejdus, B. (2008). Dynamics of phenolic acids and lignin accumulation in metal-treated *Matricaria chamomilla* roots. *Plant cell reports*, 27(3), 605-615.
- Krishnamurthy, P., Vishal, B., Bhal, A., & Kumar, P. P. (2021). WRKY9 transcription factor regulates cytochrome P450 genes CYP94B3 and CYP86B1, leading to increased root suberin and salt tolerance in *Arabidopsis*. *Physiologia Plantarum*.
- Krishnamurthy, P., Vishal, B., Ho, W. J., Lok, F. C. J., Lee, F. S. M., & Kumar, P. P. (2020). Regulation of a cytochrome P450 gene CYP94B1 by WRKY33 transcription factor controls apoplastic barrier formation in roots to confer salt tolerance. *Plant Physiology*, 184(4), 2199-2215.
- Krübel, L., Junemann, J., Wirtz, M., Birke, H., Thornton, J.D., Browning, L.W., Poschet, G., Hell, R., Balk, J., Braun, H.P. and Hildebrandt, T.M. (2014). The mitochondrial sulfur dioxygenase ETHYLMALONIC ENCEPHALOPATHY PROTEIN1 is required for amino acid catabolism during carbohydrate starvation and embryo development in *Arabidopsis*. *Plant physiology*, 165(1), 92-104.
- Ku, M. S., Spalding, M. H., & Edwards, G. E. (1980). Intracellular localization of phosphoenolpyruvate carboxykinase in leaves of C4 and CAM plants. *Plant Science Letters*, 19(1), 1-8.
- Kukurba, K. R., & Montgomery, S. B. (2015). RNA sequencing and analysis. *Cold Spring Harbor Protocols*, 2015(11), pdb-top084970.
- Kuromori, T., Seo, M., & Shinozaki, K. (2018). ABA transport and plant water stress responses. *Trends in plant science*, 23(6), 513-522.
- Lal, R. (2009). Soils and world food security.
- Lance, C., & Rustin, P. (1984). The central role of malate in plant metabolism. *Physiologie végétale (Paris)*, 22(5), 625-641.

- Lansche, J., & Müller, J. (2012). Life cycle assessment of energy generation of biogas fed combined heat and power plants: Environmental impact of different agricultural substrates. *Engineering in Life Sciences*, 12(3), 313-320.
- Lewandowski, I., Clifton-Brown, J., Trindade, L.M., van der Linden, G.C., Schwarz, K.U., Müller-Sämman, K., Anisimov, A., Chen, C.L., Dolstra, O., Donnison, I.S. and Farrar, K. (2016). Progress on optimizing miscanthus biomass production for the European bioeconomy: Results of the EU FP7 project OPTIMISC. *Frontiers in plant science*, 7, 1620.
- Lewandowski, I., Scurlock, J. M., Lindvall, E., & Christou, M. (2003). The development and current status of perennial rhizomatous grasses as energy crops in the US and Europe. *Biomass and bioenergy*, 25(4), 335-361.
- Li, B., & Dewey, C. N. (2011). RSEM: accurate transcript quantification from RNA-Seq data with or without a reference genome. *BMC bioinformatics*, 12(1), 1-16.
- Li, M., Stragliati, L., Bellini, E., Ricci, A., Saba, A., Sanità di Toppi, L., & Varotto, C. (2019). Evolution and functional differentiation of recently diverged phytochelatin synthase genes from *Arundo donax* L. *Journal of experimental botany*, 70(19), 5391-5405.
- Li, W., Ma, M., Feng, Y., Li, H., Wang, Y., Ma, Y., Li, M., An, F. and Guo, H. (2015). EIN2-directed translational regulation of ethylene signaling in *Arabidopsis*. *Cell*, 163(3), 670-683.
- Light, K.M., Wisniewski, J.A., Vinyard, W.A. and Kieber-Emmons, M.T. (2016). Perception of the plant hormone ethylene: known-knowns and known-unknowns. *JBIC Journal of Biological Inorganic Chemistry*, 21(5), 715-728.
- Liu, J., & Zhu, J. K. (1998). A calcium sensor homolog required for plant salt tolerance. *Science*, 280(5371), 1943-1945.
- Liu, T.T., McConkey, B.G., Ma, Z.Y., Liu, Z.G., Li, X. and Cheng, L.L. (2011). Strengths, weaknessness, opportunities and threats analysis of bioenergy production on marginal land. *Energy Procedia*, 5, 2378-2386.
- Liu, Y.N., Xiao, X.Y. and Guo, Z.H. (2019). Identification of indicators of giant reed (*Arundo donax* L.) ecotypes for phytoremediation of metal-contaminated soil in a non-ferrous mining and smelting area in southern China. *Ecological Indicators*, 101, 249-260.
- Loix, C., Huybrechts, M., Vangronsveld, J., Gielen, M., Keunen, E., & Cuypers, A. (2017). Reciprocal interactions between cadmium-induced cell wall responses and oxidative stress in plants. *Frontiers in Plant Science*, 8, 1867.
- Lo Piero AR, Mercurio V, Puglisi I, Petrone G. Different roles of functional residues in the hydrophobic binding site of two sweet orange tau glutathione S-transferases, *FEBS Journal*. 2010; 277:255-262.

- Lord, R. A. (2015). Reed canarygrass (*Phalaris arundinacea*) outperforms Miscanthus or willow on marginal soils, brownfield and non-agricultural sites for local, sustainable energy crop production. *biomass and bioenergy*, 78, 110-125.
- Lu, C. and Kang, J. (2008). Generation of transgenic plants of a potential oilseed crop *Camelina sativa* by *Agrobacterium*-mediated transformation. *Plant cell reports*, 27(2), 273-278.
- Lu, Q., Chen, S., Li, Y., Zheng, F., He, B., & Gu, M. (2020). Exogenous abscisic acid (ABA) promotes cadmium (Cd) accumulation in *Sedum alfredii* Hance by regulating the expression of Cd stress response genes. *Environmental Science and Pollution Research*, 27(8), 8719-8731.
- Luo, Y., Wei, Y., Sun, S., Wang, J., Wang, W., Han, D., Shao, H., Jia, H. and Fu, Y. (2019). Selenium modulates the level of auxin to alleviate the toxicity of cadmium in tobacco. *International journal of molecular sciences*, 20(15), 3772.
- Luo, Z. B., He, J., Polle, A. and Rennenberg, H. (2016). Heavy metal accumulation and signal transduction in herbaceous and woody plants: paving the way for enhancing phytoremediation efficiency. *Biotechnology Advances*, 34(6), 1131-1148.
- Mahajan, S., & Tuteja, N. (2005). Cold, salinity and drought stresses: an overview. *Archives of biochemistry and biophysics*, 444(2), 139-158.
- Mahajan, S., & Tuteja, N. (2005). Cold, salinity and drought stresses: an overview. *Archives of biochemistry and biophysics*, 444(2), 139-158.
- Mahar, A., Ali, A., Lahori, A.H., Wahid, F., Li, R., Azeem, M., Fahad, S., Adnan, M., Khan, I.A. and Zhang, Z. (2020). Promising technologies for Cd-contaminated soils: drawbacks and possibilities. In *Environment, Climate, Plant and Vegetation Growth* (pp. 63-91). Springer, Cham.
- Mahar, A., Wang, P., Ali, A., Awasthi, M.K., Lahori, A.H., Wang, Q., Li, R. and Zhang, Z. (2016). Challenges and opportunities in the phytoremediation of heavy metals contaminated soils: a review. *Ecotoxicology and environmental safety*, 126, 111-121.
- Maischak, H., Zimmermann, M. R., Felle, H. H., Boland, W., & Mithöfer, A. (2010). Alamethicin-induced electrical long distance signaling in plants. *Plant signaling & behavior*, 5(8), 988-990.
- Malone, J. M., Virtue, J. G., Williams, C., & Preston, C. (2017). Genetic diversity of giant reed (*Arundo donax*) in Australia. *Weed Biology and Management*, 17(1), 17-28.
- Mandi, L., & Abissy, M. (2000). Utilization of *Arundo donax* and *Typha latifolia* for heavy metals removal from urban wastewater. Reuse of treated wastewaters for alfalfa irrigation. In 3rd international symposium on wastewater, reclamation, recycling and reuse (Paris, 3-7 July 2000) (pp. 158-165).
- Mann, J. J., Barney, J. N., Kyser, G. B., & Di Tomaso, J. M. (2013). *Miscanthus* × *giganteus* and



- Arundo donax* shoot and rhizome tolerance of extreme moisture stress. *Gcb Bioenergy*, 5(6), 693-700.
- Mariani, C., Cabrini, R., Danin, A., Piffanelli, P., Fricano, A., Gomarasca, S., Dicandilo, M., Grassi, F. and Soave, C. (2010). Origin, diffusion and reproduction of the giant reed (*Arundo donax* L.): a promising weedy energy crop. *Annals of Applied Biology*, 157(2), 191-202.
- Marques, A. C., Fuinhas, J. A., & Pereira, D. A. (2018). Have fossil fuels been substituted by renewables? An empirical assessment for 10 European countries. *Energy policy*, 116, 257-265.
- Martínez-Atienza, J., Jiang, X., Garcíadeblas, B., Mendoza, I., Zhu, J. K., Pardo, J. M., & Quintero, F. J. (2007). Conservation of the salt overly sensitive pathway in rice. *Plant physiology*, 143(2), 1001-1012.
- Mathy, S., Menanteau, P., & Criqui, P. (2018). After the Paris Agreement: measuring the global decarbonization wedges from national energy scenarios. *Ecological economics*, 150, 273-289.
- Matysik, J., Alia, Bhalu, B., & Mohanty, P. (2002). Molecular mechanisms of quenching of reactive oxygen species by proline under stress in plants. *Current Science*, 525-532.
- Mayak, S., Tirosh, T., & Glick, B. R. (2004). Plant growth-promoting bacteria confer resistance in tomato plants to salt stress. *Plant physiology and Biochemistry*, 42(6), 565-572.
- Mehmood, M. A., Ibrahim, M., Rashid, U., Nawaz, M., Ali, S., Hussain, A., & Gull, M. (2017). Biomass production for bioenergy using marginal lands. *Sustainable Production and Consumption*, 9, 3-21.
- Meloni, D. A., Gulotta, M. R., Martínez, C. A., & Oliva, M. A. (2004). The effects of salt stress on growth, nitrate reduction and proline and glycinebetaine accumulation in *Prosopis alba*. *Brazilian Journal of Plant Physiology*, 16, 39-46.
- Mendoza-Cózatl, D. G., Jobe, T. O., Hauser, F., & Schroeder, J. I. (2011). Long-distance transport, vacuolar sequestration, tolerance, and transcriptional responses induced by cadmium and arsenic. *Current opinion in plant biology*, 14(5), 554-562.
- Metzger, J. O., & Hüttermann, A. (2009). Sustainable global energy supply based on lignocellulosic biomass from afforestation of degraded areas. *Naturwissenschaften*, 96(2), 279-288.
- Metzker, M. L. (2010). Sequencing technologies—the next generation. *Nature reviews genetics*, 11(1), 31-46.
- Miller, G. A. D., Suzuki, N., Ciftci-Yilmaz, S. U. L. T. A. N., & Mittler, R. O. N. (2010). Reactive oxygen species homeostasis and signalling during drought and salinity stresses. *Plant, cell & environment*, 33(4), 453-467.
- Mimouni, H., Wasti, S., Manaa, A., Gharbi, E., Chalh, A., Vandoorne, B., Lutts, S. and Ahmed, H.B. (2016). Does salicylic acid (SA) improve tolerance to salt stress in plants? A study of SA effects

- on tomato plant growth, water dynamics, photosynthesis, and biochemical parameters. *Omics: a journal of integrative biology*, 20(3), 180-190.
- Mirza, N., Pervez, A., Mahmood, Q., Shah, M. M., & Shafqat, M. N. (2011). Ecological restoration of arsenic contaminated soil by *Arundo donax* L. *Ecological Engineering*, 37(12), 1949-1956.
- Mittler, R. (2002). Oxidative stress, antioxidants and stress tolerance. *Trends in plant science*, 7(9), 405-410.
- Møller, I.S., Gilliam, M., Jha, D., Mayo, G.M., Roy, S.J., Coates, J.C., Haseloff, J. and Tester, M. (2009). Shoot Na<sup>+</sup> exclusion and increased salinity tolerance engineered by cell type-specific alteration of Na<sup>+</sup> transport in *Arabidopsis*. *The Plant Cell*, 21(7), 2163-2178.
- Montero-Palmero, M. B., Martín-Barranco, A., Escobar, C., & Hernández, L. E. (2014). Early transcriptional responses to mercury: a role for ethylene in mercury-induced stress. *New Phytologist*, 201(1), 116-130.
- Monti, A., & Cosentino, S. L. (2015). Conclusive results of the European project OPTIMA: optimization of perennial grasses for biomass production in the mediterranean area. *BioEnergy Research*, 8(4), 1459-1460.
- Msanne, J., Lin, J., Stone, J. M., & Awada, T. (2011). Characterization of abiotic stress-responsive *Arabidopsis thaliana* RD29A and RD29B genes and evaluation of transgenes. *Planta*, 234(1), 97-107.
- Muench, S., & Guenther, E. (2013). A systematic review of bioenergy life cycle assessments. *Applied Energy*, 112, 257-273.
- Munns, R., & Termaat, A. (1986). Whole-plant responses to salinity. *Functional Plant Biology*, 13(1), 143-160.
- Munns, R., & Tester, M. (2008). Mechanisms of salinity tolerance. *Annu. Rev. Plant Biol.*, 59, 651-681.
- Nackley, L. L., & Kim, S. H. (2015). A salt on the bioenergy and biological invasions debate: salinity tolerance of the invasive biomass feedstock *Arundo donax*. *Gcb Bioenergy*, 7(4), 752-762.
- Nagajyoti, P. C., Lee, K. D., & Sreekanth, T. V. M. (2010). Heavy metals, occurrence and toxicity for plants: a review. *Environmental chemistry letters*, 8(3), 199-216.
- Nakano, T., Suzuki, K., Fujimura, T., & Shinshi, H. (2006). Genome-wide analysis of the ERF gene family in *Arabidopsis* and rice. *Plant physiology*, 140(2), 411-432.
- Negrão, S., Schmöckel, S. M., & Tester, M. (2017). Evaluating physiological responses of plants to salinity stress. *Annals of botany*, 119(1), 1-11.
- Nevo, Y., & Nelson, N. (2006). The NRAMP family of metal-ion transporters. *Biochimica et Biophysica Acta (BBA)-Molecular Cell Research*, 1763(7), 609-620.

- Nguyen, H.T., Silva, J.E., Podicheti, R., Macrander, J., Yang, W., Nazareus, T.J., Nam, J.W., Jaworski, J.G., Lu, C., Scheffler, B.E. and Mockaitis, K. (2013). Camelina seed transcriptome: a tool for meal and oil improvement and translational research. *Plant biotechnology journal*, 11(6), 759-769.
- Nixon, D. J., Stephens, W., Tyrrel, S. F., & Brierley, E. D. R. (2001). The potential for short rotation energy forestry on restored landfill caps. *Bioresource technology*, 77(3), 237-245.
- No, A. (2011). *Arundo donax Distribution and Impact Report*.
- Ohkubo, Y., Tanaka, M., Tabata, R., Ogawa-Ohnishi, M., & Matsubayashi, Y. (2017). Shoot-to-root mobile polypeptides involved in systemic regulation of nitrogen acquisition. *Nature plants*, 3(4), 1-6.
- Ohlrogge, J., Allen, D., Berguson, B., DellaPenna, D., Shachar-Hill, Y., & Stymne, S. (2009). Driving on biomass. *Science*, 324(5930), 1019-1020.
- ONU. *World population prospects 2019*.
- Oshlack, A., & Wakefield, M. J. (2009). Transcript length bias in RNA-seq data confounds systems biology. *Biology direct*, 4(1), 1-10.
- Østergaard, P. A., Duic, N., Noorollahi, Y., Mikulcic, H., & Kalogirou, S. (2020). Sustainable development using renewable energy technology. *Renewable Energy*, 146, 2430-2437.
- Pan, J., Plant, J. A., Voulvoulis, N., Oates, C. J., & Ihlenfeld, C. (2010). Cadmium levels in Europe: implications for human health. *Environmental geochemistry and health*, 32(1), 1-12.
- Panta, S., Flowers, T., Lane, P., Doyle, R., Haros, G., & Shabala, S. (2014). Halophyte agriculture: success stories. *Environmental and experimental botany*, 107, 71-83.
- Papazoglou, E. G. (2007). *Arundo donax* L. stress tolerance under irrigation with heavy metal aqueous solutions. *Desalination*, 211(1-3), 304-313.
- Papazoglou, E. G., Karantounias, G. A., Vemmos, S. N., & Bouranis, D. L. (2005). Photosynthesis and growth responses of giant reed (*Arundo donax* L.) to the heavy metals Cd and Ni. *Environment international*, 31(2), 243-249.
- Papazoglou, E. G., Serelis, K. G., & Bouranis, D. L. (2007). Impact of high cadmium and nickel soil concentration on selected physiological parameters of *Arundo donax* L. *European Journal of Soil Biology*, 43(4), 207-215.
- Parida, A. K., Das, A. B., & Mohanty, P. (2004). Defense potentials to NaCl in a mangrove, *Bruguiera parviflora*: differential changes of isoforms of some antioxidative enzymes. *Journal of plant physiology*, 161(5), 531-542.
- Park, J., Song, W.Y., Ko, D., Eom, Y., Hansen, T.H., Schiller, M., Lee, T.G., Martinoia, E. and Lee, Y. (2012). The phytochelatin transporters AtABCC1 and AtABCC2 mediate tolerance to

- cadmium and mercury. *The Plant Journal*, 69(2), 278-288.
- Parrotta, L., Guerriero, G., Sergeant, K., Cai, G., & Hausman, J. F. (2015). Target or barrier? The cell wall of early-and later-diverging plants vs cadmium toxicity: differences in the response mechanisms. *Frontiers in Plant Science*, 6, 133.
- Pauwels, L., Morreel, K., De Witte, E., Lammertyn, F., Van Montagu, M., Boerjan, W., Inzé, D. and Goossens, A. (2008). Mapping methyl jasmonate-mediated transcriptional reprogramming of metabolism and cell cycle progression in cultured *Arabidopsis* cells. *Proceedings of the National Academy of Sciences*, 105(4), 1380-1385.
- Pawlak-Sprada, S., Arasimowicz-Jelonek, M., Podgórska, M., & Deckert, J. (2011). Activation of phenylpropanoid pathway in legume plants exposed to heavy metals. Part I. Effects of cadmium and lead on phenylalanine ammonia-lyase gene expression, enzyme activity and lignin content. *Acta Biochimica Polonica*, 58(2).
- Peck, G. G. (1998, June). Hydroponic growth characteristics of *Arundo donax* L. under salt stress. In *Arundo and saltcedar: the deadly duo*, Proceedings of a workshop on combating the threat from *Arundo* and *Saltcedar*.
- Perdue, R. E. (1958). *Arundo donax*—source of musical reeds and industrial cellulose. *Economic Botany*, 12(4), 368-404.
- Pérez-Rodríguez, P., Riano-Pachon, D. M., Corrêa, L. G. G., Rensing, S. A., Kersten, B., & Mueller-Roeber, B. (2010). PInTFDB: updated content and new features of the plant transcription factor database. *Nucleic acids research*, 38(suppl\_1), D822-D827.
- Pilu, R., Cassani, E., Landoni, M., Badone, F.C., Passera, A., Cantaluppi, E., Corno, L. and Adani, F. (2014). Genetic characterization of an Italian Giant Reed (*Arundo donax* L.) clones collection: exploiting clonal selection. *Euphytica*, 196(2), 169-181.
- Pilu, R., Manca, A., & Landoni, M. (2013). *Arundo donax* as an energy crop: pros and cons of the utilization of this perennial plant. *Maydica*, 58(1), 54-59.
- Piotrowska-Niczyporuk, A., Bajguz, A., Zambrzycka, E., & Godlewska-Żyłkiewicz, B. (2012). Phytohormones as regulators of heavy metal biosorption and toxicity in green alga *Chlorella vulgaris* (Chlorophyceae). *Plant Physiology and Biochemistry*, 52, 52-65.
- Pires, J. C. M. (2019). Negative emissions technologies: a complementary solution for climate change mitigation. *Science of The Total Environment*, 672, 502-514.
- Pitelis, C. (2020). Mega Tech, Unicorns and the Sharing Economy: Can Penrose and Hymer Help Us Predict?. *Strategic Management Review*, forthcoming.
- Poli, M., Salvi, S., Li, M., & Varotto, C. (2017). Selection of reference genes suitable for normalization of qPCR data under abiotic stresses in bioenergy crop *Arundo donax* L. *Scientific*

reports, 7(1), 1-11.

- Pompeiano, A., Remorini, D., Vita, F., Guglielminetti, L., Miele, S., & Morini, S. (2017). Growth and physiological response of *Arundo donax* L. to controlled drought stress and recovery. *Plant Biosystems-An International Journal Dealing with all Aspects of Plant Biology*, 151(5), 906-914.
- Pompeiano, A., Vita, F., Alpi, A., & Guglielminetti, L. (2015). *Arundo donax* L. response to low oxygen stress. *Environmental and Experimental Botany*, 111, 147-154.
- Popp, M., Larher, F., & Weigel, P. (1985). Osmotic adaption in Australian mangroves. In *Ecology of coastal vegetation* (pp. 247-253). Springer, Dordrecht.
- Poustini, K., Siosemardeh, A., & Ranjbar, M. (2007). Proline accumulation as a response to salt stress in 30 wheat (*Triticum aestivum* L.) cultivars differing in salt tolerance. *Genetic Resources and Crop Evolution*, 54(5), 925-934.
- Priya, P., & Jain, M. (2013). RiceSRTFDB: a database of rice transcription factors containing comprehensive expression, cis-regulatory element and mutant information to facilitate gene function analysis. Database, 2013.
- Puglisi, I., Cicero, L. L., & Piero, A. R. L. (2013). The glutathione S-transferase gene superfamily: an in silico approach to study the post translational regulation. *Biodegradation*, 24(4), 471-485.
- Qin, Z., Zhuang, Q., Zhu, X., Cai, X., & Zhang, X. (2011). Carbon consequences and agricultural implications of growing biofuel crops on marginal agricultural lands in China. *Environmental Science & Technology*, 45(24), 10765-10772.
- Qiu, Q. S., Guo, Y., Dietrich, M. A., Schumaker, K. S., & Zhu, J. K. (2002). Regulation of SOS1, a plasma membrane Na<sup>+</sup>/H<sup>+</sup> exchanger in *Arabidopsis thaliana*, by SOS2 and SOS3. *Proceedings of the National Academy of Sciences*, 99(12), 8436-8441.
- Quinn, L.D., Straker, K.C., Guo, J., Kim, S., Thapa, S., Kling, G., Lee, D.K. and Voigt, T.B. (2015). Stress-tolerant feedstocks for sustainable bioenergy production on marginal land. *BioEnergy Research*, 8(3), 1081-1100.
- Ragauskas, A. J. (2016). Challenging/interesting lignin times. *Biofuels, Bioproducts & Biorefining*, 10(5).
- Rai, V. K. (2002). Role of amino acids in plant responses to stresses. *Biologia plantarum*, 45(4), 481-487.
- Rajendran, K., Tester, M., & Roy, S. J. (2009). Quantifying the three main components of salinity tolerance in cereals. *Plant, cell & environment*, 32(3), 237-249.
- Rajpal, C., & Tomar, P. C. (2020). CADAVERINE: A POTENT MODULATOR OF PLANTS AGAINST ABIOTIC STRESSES: CADAVERINE: A POTENT MODULATOR. *Journal of*

- microbiology, biotechnology and food sciences, 10(2), 205-210.
- Raturi, A. K. (2019). Renewables 2019 global status report.
- Redjala, T., Sterckeman, T., & Morel, J. L. (2009). Cadmium uptake by roots: contribution of apoplast and of high-and low-affinity membrane transport systems. *Environmental and Experimental Botany*, 67(1), 235-242.
- Rehl, T., Lansche, J., & Müller, J. (2012). Life cycle assessment of energy generation from biogas—Attributional vs. consequential approach. *Renewable and Sustainable Energy Reviews*, 16(6), 3766-3775.
- REN21. Renewables 2016 Global Status Report. 2016.
- Richards, L. A. (1947). Diagnosis and improvement of saline and alkaline soils. *Soil Science*, 64(5), 432.
- Ricke, K. L., Millar, R. J., & MacMartin, D. G. (2017). Constraints on global temperature target overshoot. *Scientific reports*, 7(1), 1-7.
- Rivera, A., Bravo, C., & Buob, G. (2017). Climate change and land Ice. *Int. Encyclopedia Geogr.: People, Earth, Environ. Technol*, 1-15.
- Roberts, A., Trapnell, C., Donaghey, J., Rinn, J. L., & Pachter, L. (2011). Improving RNA-Seq expression estimates by correcting for fragment bias. *Genome biology*, 12(3), 1-14.
- Robertson, G., Schein, J., Chiu, R., Corbett, R., Field, M., Jackman, S.D., Mungall, K., Lee, S., Okada, H.M., Qian, J.Q. and Griffith, M. (2010). De novo assembly and analysis of RNA-seq data. *Nature methods*, 7(11), 909-912.
- Robertson, G.P., Dale, V.H., Doering, O.C., Hamburg, S.P., Melillo, J.M., Wander, M.M., Parton, W.J., Adler, P.R., Barney, J.N., Cruse, R.M. and Duke, C.S. (2008). Sustainable biofuels redux. *Science*, 322(5898), 49-50.
- Röder, M., & Thornley, P. (2018). Waste wood as bioenergy feedstock. Climate change impacts and related emission uncertainties from waste wood based energy systems in the UK. *Waste Management*, 74, 241-252.
- Roos, A., & Ahlgren, S. (2018). Consequential life cycle assessment of bioenergy systems—a literature review. *Journal of Cleaner Production*, 189, 358-373.
- Roy, S. J., Negrão, S., & Tester, M. (2014). Salt resistant crop plants. *Current opinion in Biotechnology*, 26, 115-124.
- Ruangcharus, C., Kim, S. U., & Hong, C. O. (2020). Mechanism of cadmium immobilization in phosphate-amended arable soils. *Applied Biological Chemistry*, 63(1), 1-7.
- Rucińska-Sobkowiak, R. (2016). Water relations in plants subjected to heavy metal stresses. *Acta Physiologiae Plantarum*, 38(11), 1-13.

- Sabeen, M., Mahmood, Q., Irshad, M., Fareed, I., Khan, A., Ullah, F., Hussain, J., Hayat, Y. and Tabassum, S. (2013). Cadmium phytoremediation by *Arundo donax* L. from contaminated soil and water. *BioMed research international*, 2013.
- Sablok, G., Fu, Y., Bobbio, V., Laura, M., Rotino, G.L., Bagnaresi, P., Allavena, A., Velikova, V., Viola, R., Loreto, F. and Li, M. (2014). Fuelling genetic and metabolic exploration of C 3 bioenergy crops through the first reference transcriptome of *Arundo donax* L. *Plant Biotechnology Journal*, 12(5), 554-567.
- Saini, S., Kaur, N., & Pati, P. K. (2021). Phytohormones: Key players in the modulation of heavy metal stress tolerance in plants. *Ecotoxicology and Environmental Safety*, 223, 112578.
- Saini, S., Sharma, I., Kaur, N., & Pati, P. K. (2013). Auxin: a master regulator in plant root development. *Plant cell reports*, 32(6), 741-757.
- Sairam, R. K., & Tyagi, A. (2004). Physiology and molecular biology of salinity stress tolerance in plants. *Current science*, 407-421.
- Saito, S., Hirai, N., Matsumoto, C., Ohigashi, H., Ohta, D., Sakata, K., & Mizutani, M. (2004). *Arabidopsis* CYP707A s encode (+)-abscisic acid 8'-hydroxylase, a key enzyme in the oxidative catabolism of abscisic acid. *Plant physiology*, 134(4), 1439-1449.
- Sánchez, E., Scordia, D., Lino, G., Arias, C., Cosentino, S. L., & Nogués, S. (2015). Salinity and water stress effects on biomass production in different *Arundo donax* L. clones. *BioEnergy Research*, 8(4), 1461-1479.
- Sarsekeyeva, F., Zayadan, B. K., Usserbaeva, A., Bedbenov, V. S., Sinetova, M. A., & Los, D. A. (2015). Cyanofuels: biofuels from cyanobacteria. Reality and perspectives. *Photosynthesis research*, 125(1), 329-340.
- Sasaki, A., Yamaji, N., Yokosho, K., & Ma, J. F. (2012). Nramp5 is a major transporter responsible for manganese and cadmium uptake in rice. *The Plant Cell*, 24(5), 2155-2167.
- Saxena, S. C., Kaur, H., Verma, P., Petla, B. P., Andugula, V. R., & Majee, M. (2013). Osmoprotectants: potential for crop improvement under adverse conditions. In *Plant acclimation to environmental stress* (pp. 197-232). Springer, New York, NY.
- Scandalios, J. G. (2005). Oxidative stress: molecular perception and transduction of signals triggering antioxidant gene defenses. *Brazilian journal of medical and biological research*, 38(7), 995-1014.
- Scarlat, N., Dallemand, J. F., Monforti-Ferrario, F., & Nita, V. (2015). The role of biomass and bioenergy in a future bioeconomy: Policies and facts. *Environmental Development*, 15, 3-34.
- Schellingen, K., Van Der Straeten, D., Remans, T., Vangronsveld, J., Keunen, E., & Cuypers, A. (2015). Ethylene signalling is mediating the early cadmium-induced oxidative challenge in

- Arabidopsis thaliana*. *Plant Science*, 239, 137-146.
- Schellingen, K., Van Der Straeten, D., Vandenbussche, F., Prinsen, E., Remans, T., Vangronsveld, J., & Cuypers, A. (2014). Cadmium-induced ethylene production and responses in *Arabidopsis thaliana* rely on ACS2 and ACS6 gene expression. *BMC plant biology*, 14(1), 1-14.
- Schena, M., Shalon, D., Davis, R. W., & Brown, P. O. (1995). Quantitative monitoring of gene expression patterns with a complementary DNA microarray. *Science*, 270(5235), 467-470.
- Schulz, M. H., Zerbino, D. R., Vingron, M., & Birney, E. (2012). Oases: robust de novo RNA-seq assembly across the dynamic range of expression levels. *Bioinformatics*, 28(8), 1086-1092.
- Secretariat, R. (2018). Renewables 2018: Global Status Report (GSR). Renewable Energy Policy Network for the 21st Century (REN 21). Paris, France.[Online]. Available: [http://www.ren21.net/wpcontent/uploads/2018/06/17-8652\\_GSR2018\\_FullReport\\_web\\_-1.pdf](http://www.ren21.net/wpcontent/uploads/2018/06/17-8652_GSR2018_FullReport_web_-1.pdf).
- Serba, D. D., Uppalapati, S. R., Krom, N., Mukherjee, S., Tang, Y., Mysore, K. S., & Saha, M. C. (2016). Transcriptome analysis in switchgrass discloses ecotype difference in photosynthetic efficiency. *BMC genomics*, 17(1), 1-14.
- Shaheen, S., Ahmad, R., Mahmood, Q., Mubarak, H., Mirza, N., & Hayat, M. T. (2018). Physiology and selected genes expression under cadmium stress in *Arundo donax* L. *International journal of phytoremediation*, 20(11), 1162-1167.
- Shahid, S. A., & Al-Shankiti, A. (2013). Sustainable food production in marginal lands—Case of GDLA member countries. *International soil and water conservation research*, 1(1), 24-38.
- Sharma, S. S., & Dietz, K. J. (2006). The significance of amino acids and amino acid-derived molecules in plant responses and adaptation to heavy metal stress. *Journal of experimental botany*, 57(4), 711-726.
- Sharma, S. S., & Dietz, K. J. (2009). The relationship between metal toxicity and cellular redox imbalance. *Trends in plant science*, 14(1), 43-50.
- Shavrukov, Y. (2013). Salt stress or salt shock: which genes are we studying?. *Journal of Experimental Botany*, 64(1), 119-127.
- Shendure, J. (2008). The beginning of the end for microarrays?. *Nature methods*, 5(7), 585-587.
- Shim, D., Hwang, J.U., Lee, J., Lee, S., Choi, Y., An, G., Martinoia, E. and Lee, Y. (2009). Orthologs of the class A4 heat shock transcription factor HsfA4a confer cadmium tolerance in wheat and rice. *The Plant Cell*, 21(12), 4031-4043.
- Shivakumar, A., Dobbins, A., Fahl, U., & Singh, A. (2019). Drivers of renewable energy deployment in the EU: An analysis of past trends and projections. *Energy Strategy Reviews*, 26, 100402.
- Shrivastava, P., & Kumar, R. (2015). Soil salinity: A serious environmental issue and plant growth promoting bacteria as one of the tools for its alleviation. *Saudi journal of biological sciences*,



22(2), 123-131.

- Shu, S., Guo, S. R., & Yuan, L. Y. (2012). A review: polyamines and photosynthesis. *Advances in Photosynthesis-Fundamental Aspects InTech*, 439-464.
- Sicilia, A., Santoro, D. F., Testa, G., Cosentino, S. L., & Piero, A. R. L. (2020). Transcriptional response of giant reed (*Arundo donax* L.) low ecotype to long-term salt stress by unigene-based RNAseq. *Phytochemistry*, 177, 112436.
- Sicilia, A., Testa, G., Santoro, D. F., Cosentino, S. L., & Lo Piero, A. R. (2019). RNASeq analysis of giant cane reveals the leaf transcriptome dynamics under long-term salt stress. *BMC plant biology*, 19(1), 1-24.
- Sidhu, G. P. S., Bali, A. S., & Bhardwaj, R. (2019). Role of organic acids in mitigating cadmium toxicity in plants. In *Cadmium tolerance in plants* (pp. 255-279). Academic Press.
- Singh, P., Singh, I., & Shah, K. (2019). Reduced activity of nitrate reductase under heavy metal cadmium stress in rice: An in silico answer. *Frontiers in plant science*, 9, 1948.
- Singh, S., Parihar, P., Singh, R., Singh, V. P., & Prasad, S. M. (2016). Heavy metal tolerance in plants: role of transcriptomics, proteomics, metabolomics, and ionomics. *Frontiers in plant science*, 6, 1143.
- Singh, V. P., Singh, S., Kumar, J., & Prasad, S. M. (2015). Investigating the roles of ascorbate-glutathione cycle and thiol metabolism in arsenate tolerance in ridged *Luffa* seedlings. *Protoplasma*, 252(5), 1217-1229.
- Skevas, T., Swinton, S. M., & Hayden, N. J. (2014). What type of landowner would supply marginal land for energy crops?. *Biomass and Bioenergy*, 67, 252-259.
- Slavov, G.T., Nipper, R., Robson, P., Farrar, K., Allison, G.G., Bosch, M., Clifton-Brown, J.C., Donnison, I.S. and Jensen, E. (2014). Genome-wide association studies and prediction of 17 traits related to phenology, biomass and cell wall composition in the energy grass *Miscanthus sinensis*. *New phytologist*, 201(4), 1227-1239.
- Smeets, E. M., Faaij, A. P., Lewandowski, I. M., & Turkenburg, W. C. (2007). A bottom-up assessment and review of global bio-energy potentials to 2050. *Progress in Energy and combustion science*, 33(1), 56-106.
- Smeets, K., Opdenakker, K., Remans, T., Forzani, C., Hirt, H., Vangronsveld, J., & Cuypers, A. (2013). The role of the kinase OXI1 in cadmium-and copper-induced molecular responses in *Arabidopsis thaliana*. *Plant, cell & environment*, 36(6), 1228-1238.
- Smith, S. L., Thelen, K. D., & MacDonald, S. J. (2013). Yield and quality analyses of bioenergy crops grown on a regulatory brownfield. *Biomass and bioenergy*, 49, 123-130.
- Snapp, S. S., Shennan, C., & Van Bruggen, A. H. C. (1991). Effects of salinity on severity of infection

- by *Phytophthora parasitica* Dast., ion concentrations and growth of tomato, *Lycopersicon esculentum* Mill. *New Phytologist*, 119(2), 275-284.
- Sobkowiak, R., & Deckert, J. (2006). Proteins induced by cadmium in soybean cells. *Journal of plant physiology*, 163(11), 1203-1206.
- Soldatos, P. (2015). Economic aspects of bioenergy production from perennial grasses in marginal lands of South Europe. *Bioenergy Research*, 8(4), 1562-1573.
- SONG, W.Y., MENDOZA-CÓZATL, D.G., Lee, Y., Schroeder, J.I., AHN, S.N., LEE, H.S., Wicker, T. and Martinoia, E. (2014). Phytochelatin–metal (loid) transport into vacuoles shows different substrate preferences in barley and *A. rabidopsis*. *Plant, cell & environment*, 37(5), 1192-1201.
- Souza, G.M., Ballester, M.V.R., de Brito Cruz, C.H., Chum, H., Dale, B., Dale, V.H., Fernandes, E.C., Foust, T., Karp, A., Lynd, L. and Maciel Filho, R. (2017). The role of bioenergy in a climate-changing world. *Environmental development*, 23, 57-64.
- Srivastava, N., Srivastava, M., Manikanta, A., Singh, P., Ramteke, P. W., & Mishra, P. K. (2017). Nanomaterials for biofuel production using lignocellulosic waste. *Environmental Chemistry Letters*, 15(2), 179-184.
- Steffens, B. (2014). The role of ethylene and ROS in salinity, heavy metal, and flooding responses in rice. *Frontiers in plant science*, 5, 685.
- Stohs, S. J., & Bagchi, D. (1995). Oxidative mechanisms in the toxicity of metal ions. *Free radical biology and medicine*, 18(2), 321-336.
- Strabala, T.J., O'donnell, P.J., Smit, A.M., Ampomah-Dwamena, C., Martin, E.J., Netzler, N., Nieuwenhuizen, N.J., Quinn, B.D., Foote, H.C. and Hudson, K.R. (2006). Gain-of-function phenotypes of many *CLAVATA3/ESR* genes, including four new family members, correlate with tandem variations in the conserved *CLAVATA3/ESR* domain. *Plant Physiology*, 140(4), 1331-1344.
- Sudha, S., & Vasudevan, N. (2009). Constructed wetlands for treating wastewater from crocodile farm. *Journal of Ecotoxicology & Environmental Monitoring*, 19(3), 277-284.
- Sundaramoorthy, P., Chidambaram, A., Ganesh, K. S., Unnikannan, P., & Baskaran, L. (2010). Chromium stress in paddy:(i) nutrient status of paddy under chromium stress;(ii) phytoremediation of chromium by aquatic and terrestrial weeds. *Comptes rendus biologiques*, 333(8), 597-607.
- Szabados, L., & Savouré, A. (2010). Proline: a multifunctional amino acid. *Trends in plant science*, 15(2), 89-97.
- Székely G, Abrahám E, Csépló A, Rigó G, Zsigmond L, Csiszár J, Ayaydin F, Strizhov N, Jásik J, Schmelzer E, Koncz C, Szabados L. (2008). Duplicated *P5CS* genes of *Arabidopsis* play distinct

roles in stress regulation and developmental control of proline biosynthesis. *Plant Journal*; 53:11-28

- Taha, M., Foda, M., Shahsavari, E., Aburto-Medina, A., Adetutu, E., & Ball, A. (2016). Commercial feasibility of lignocellulose biodegradation: possibilities and challenges. *Current opinion in biotechnology*, 38, 190-197.
- Takahashi W, Takamizo T, Kobayashi M, Ebina M. Plant regeneration from calli in giant reed (*Arundo donax* L.). *Grassland Sci.* 2010;56:224–229
- Takahashi, T., & Kakehi, J. I. (2010). Polyamines: ubiquitous polycations with unique roles in growth and stress responses. *Annals of botany*, 105(1), 1-6.
- Tang, Y., Xie, J. S., & Geng, S. (2010). Marginal land-based biomass energy production in China. *Journal of Integrative Plant Biology*, 52(1), 112-121.
- Tchounwou, P. B., Yedjou, C. G., Patlolla, A. K., & Sutton, D. J. (2012). Heavy metal toxicity and the environment. *Molecular, clinical and environmental toxicology*, 133-164.
- Thompson, J., & Bannigan, J. (2008). Cadmium: toxic effects on the reproductive system and the embryo. *Reproductive toxicology*, 25(3), 304-315.
- Tilman, D., Hill, J., & Lehman, C. (2006). Carbon-negative biofuels from low-input high-diversity grassland biomass. *Science*, 314(5805), 1598-1600.
- Tóth, G., Hermann, T., Da Silva, M. R., & Montanarella, L. (2016). Heavy metals in agricultural soils of the European Union with implications for food safety. *Environment international*, 88, 299-309.
- Trapnell, C., Williams, B.A., Pertea, G., Mortazavi, A., Kwan, G., van Baren, M.J., Salzberg, S.L., Wold, B.J. and Pachter, L. (2010). Transcript assembly and abundance estimation from RNA-Seq reveals thousands of new transcripts and switching among isoforms. *Nature biotechnology*, 28(5), 511.
- Tsugane, K., Kobayashi, K., Niwa, Y., Ohba, Y., Wada, K., & Kobayashi, H. (1999). A recessive *Arabidopsis* mutant that grows photoautotrophically under salt stress shows enhanced active oxygen detoxification. *The Plant Cell*, 11(7), 1195-1206.
- Tsukagoshi, H., Suzuki, T., Nishikawa, K., Agarie, S., Ishiguro, S., & Higashiyama, T. (2015). RNA-seq analysis of the response of the halophyte, *Mesembryanthemum crystallinum* (ice plant) to high salinity. *PloS one*, 10(2), e0118339.
- UNFCCC, C. Adoption of the Paris Agreement (29 January 2016), Decision 1/CP. 21, referred in Report of the Conference of the Parties on its twenty-first session, held in Paris from 30 November to 13 December 2, UN Doc. FCCC/CP/2015/10/Add. 1, at preamble.
- Uraguchi, S., & Fujiwara, T. (2013). Rice breaks ground for cadmium-free cereals. *Current opinion*

in plant biology, 16(3), 328-334.

- Valdivia, E. R., Chevalier, D., Sampedro, J., Taylor, I., Niederhuth, C. E., & Walker, J. C. (2012). DVL genes play a role in the coordination of socket cell recruitment and differentiation. *Journal of experimental botany*, 63(3), 1405-1412.
- Valenzuela, C. E., Acevedo-Acevedo, O., Miranda, G. S., Vergara-Barros, P., Holuigue, L., Figueroa, C. R., & Figueroa, P. M. (2016). Salt stress response triggers activation of the jasmonate signaling pathway leading to inhibition of cell elongation in *Arabidopsis* primary root. *Journal of experimental botany*, 67(14), 4209-4220.
- Van de Mortel, J.E., Almar Villanueva, L., Schat, H., Kwekkeboom, J., Coughlan, S., Moerland, P.D., Ver Loren van Themaat, E., Koornneef, M. and Aarts, M.G. (2006). Large expression differences in genes for iron and zinc homeostasis, stress response, and lignin biosynthesis distinguish roots of *Arabidopsis thaliana* and the related metal hyperaccumulator *Thlaspi caerulescens*. *Plant physiology*, 142(3), 1127-1147.
- Van de Mortel, J.E., Schat, H., Moerland, P.D., Van Themaat, E.V.L., Van Der Ent, S.J.O.E.R.D., Blankestijn, H., Ghandilyan, A., Tsiatsiani, S. and Aarts, M.G. (2008). Expression differences for genes involved in lignin, glutathione and sulphate metabolism in response to cadmium in *Arabidopsis thaliana* and the related Zn/Cd-hyperaccumulator *Thlaspi caerulescens*. *Plant, Cell & Environment*, 31(3), 301-324.
- Vanhoudt, N., Vandenhove, H., Horemans, N., Wannijn, J., Bujanic, A., Vangronsveld, J., & Cuypers, A. (2010). Study of oxidative stress related responses induced in *Arabidopsis thaliana* following mixed exposure to uranium and cadmium. *Plant physiology and biochemistry*, 48(10-11), 879-886.
- Vanstraelen, M., & Benková, E. (2012). Hormonal interactions in the regulation of plant development. *Annual review of cell and developmental biology*, 28, 463-487.
- Verbruggen, N., Hermans, C., & Schat, H. (2009). Molecular mechanisms of metal hyperaccumulation in plants. *New phytologist*, 181(4), 759-776.
- Victor, N., Nichols, C., & Zelek, C. (2018). The US power sector decarbonization: Investigating technology options with MARKAL nine-region model. *Energy Economics*, 73, 410-425.
- Voss, I., Sunil, B., Scheibe, R., & Raghavendra, A. S. (2013). Emerging concept for the role of photorespiration as an important part of abiotic stress response. *Plant biology*, 15(4), 713-722.
- Wagner, M., Mangold, A., Lask, J., Petig, E., Kiesel, A., & Lewandowski, I. (2019). Economic and environmental performance of miscanthus cultivated on marginal land for biogas production. *Gcb Bioenergy*, 11(1), 34-49.
- Wakeel, A., Farooq, M., Qadir, M., & Schubert, S. (2011). Potassium substitution by sodium in

- plants. *Critical reviews in plant sciences*, 30(4), 401-413.
- Wang, L., Feng, Z., Wang, X., Wang, X., & Zhang, X. (2010). DEGseq: an R package for identifying differentially expressed genes from RNA-seq data. *Bioinformatics*, 26(1), 136-138.
- Wang, T., Park, Y. B., Caporini, M. A., Rosay, M., Zhong, L., Cosgrove, D. J., & Hong, M. (2013). Sensitivity-enhanced solid-state NMR detection of expansin's target in plant cell walls. *Proceedings of the National Academy of Sciences*, 110(41), 16444-16449.
- Wang, W., Vinocur, B., & Altman, A. (2003). Plant responses to drought, salinity and extreme temperatures: towards genetic engineering for stress tolerance. *Planta*, 218(1), 1-14.
- Wang, Y., & Nii, N. (2000). Changes in chlorophyll, ribulose biphosphate carboxylase-oxygenase, glycine betaine content, photosynthesis and transpiration in *Amaranthus tricolor* leaves during salt stress. *The Journal of Horticultural Science and Biotechnology*, 75(6), 623-627.
- Wang, Z., Gerstein, M., & Snyder, M. (2009). RNA-Seq: a revolutionary tool for transcriptomics. *Nature reviews genetics*, 10(1), 57-63.
- Wani, P. A., Khan, M. S., & Zaidi, A. (2012). Toxic effects of heavy metals on germination and physiological processes of plants. In *Toxicity of heavy metals to legumes and bioremediation* (pp. 45-66). Springer, Vienna.
- Wani, S. H., Kumar, V., Shriram, V., & Sah, S. K. (2016). Phytohormones and their metabolic engineering for abiotic stress tolerance in crop plants. *The Crop Journal*, 4(3), 162-176.
- Watanabe, M., Ohnishi, J. I., & Kanai, R. (1984). Intracellular localization of phosphoenolpyruvate carboxykinase in bundle sheath cells of C4 plants. *Plant and cell physiology*, 25(1), 69-76.
- Webster, R.J., Driever, S.M., Kromdijk, J., McGrath, J., Leakey, A.D., Siebke, K., Demetriades-Shah, T., Bonnage, S., Peloe, T., Lawson, T. and Long, S.P. (2016). High C3 photosynthetic capacity and high intrinsic water use efficiency underlies the high productivity of the bioenergy grass *Arundo donax*. *Scientific reports*, 6(1), 1-10.
- Weiland, P. (2010). Biogas production: current state and perspectives. *Applied microbiology and biotechnology*, 85(4), 849-860.
- Weng, H., Yoo, C. Y., Gosney, M. J., Hasegawa, P. M., & Mickelbart, M. V. (2012). Poplar GTL1 is a Ca<sup>2+</sup>/calmodulin-binding transcription factor that functions in plant water use efficiency and drought tolerance. *PLoS One*, 7(3), e32925.
- Williams, C. M. J., Biswas, T. K., Schrale, G., Virtue, J. G., & Heading, S. (2008, May). Use of saline land and wastewater for growing a potential biofuel crop (*Arundo donax* L.). In *Irrigation Australia 2008 Conference*, Melbourne, Australia.
- Williams, C.M.J., Biswas, T.K., Black, I.D., Marton, L., Czako, M., Harris, P.L., Pollock, R., Heading, S. and Virtue, J.G. (2008, March). Use of poor quality water to produce high biomass

yields of giant reed (*Arundo donax* L.) on marginal lands for biofuel or pulp/paper. In International Symposium on Underutilized Plants for Food Security, Nutrition, Income and Sustainable Development 806 (pp. 595-602).

- Woodward, A. W., & Bartel, B. (2005). Auxin: regulation, action, and interaction. *Annals of botany*, 95(5), 707-735.
- Wormit, A., & Usadel, B. (2018). The multifaceted role of pectin methylesterase inhibitors (PMEIs). *International journal of molecular sciences*, 19(10), 2878.
- Wu, D., Cai, S., Chen, M., Ye, L., Chen, Z., Zhang, H., Dai, F., Wu, F. and Zhang, G. (2013). Tissue metabolic responses to salt stress in wild and cultivated barley. *PLoS one*, 8(1), e55431.
- Wu, H., Chen, C., Du, J., Liu, H., Cui, Y., Zhang, Y., He, Y., Wang, Y., Chu, C., Feng, Z. and Li, J. (2012). Co-overexpression FIT with AtbHLH38 or AtbHLH39 in *Arabidopsis*-enhanced cadmium tolerance via increased cadmium sequestration in roots and improved iron homeostasis of shoots. *Plant Physiology*, 158(2), 790-800.
- Xie, M., Zhang, J., Tschaplinski, T. J., Tuskan, G. A., Chen, J. G., & Muchero, W. (2018). Regulation of lignin biosynthesis and its role in growth-defense tradeoffs. *Frontiers in plant science*, 9, 1427.
- Xiong, L., Ishitani, M., Lee, H., & Zhu, J. K. (2001). The *Arabidopsis* LOS5/ABA3 locus encodes a molybdenum cofactor sulfurase and modulates cold stress–and osmotic stress–responsive gene expression. *The Plant Cell*, 13(9), 2063-2083.
- Yadav, S. K. (2010). Heavy metals toxicity in plants: an overview on the role of glutathione and phytochelatin in heavy metal stress tolerance of plants. *South African journal of botany*, 76(2), 167-179.
- Yang, J., Zhang, J., Liu, K., Wang, Z., & Liu, L. (2007). Involvement of polyamines in the drought resistance of rice. *Journal of Experimental Botany*, 58(6), 1545-1555.
- Yang, Q., Chen, Z.Z., Zhou, X.F., Yin, H.B., Li, X., Xin, X.F., Hong, X.H., Zhu, J.K. and Gong, Z. (2009). Overexpression of SOS (Salt Overly Sensitive) genes increases salt tolerance in transgenic *Arabidopsis*. *Molecular Plant*, 2(1), 22-31.
- Yang, T., & Poovaiah, B. W. (2003). Calcium/calmodulin-mediated signal network in plants. *Trends in plant science*, 8(10), 505-512.
- Yang, X., Duan, J., Wang, L., Li, W., Guan, J., Beecham, S., & Mulcahy, D. (2015). Heavy metal pollution and health risk assessment in the Wei River in China. *Environmental monitoring and assessment*, 187(3), 1-11.
- Yoo, C. Y., Pence, H. E., Jin, J. B., Miura, K., Gosney, M. J., Hasegawa, P. M., & Mickelbart, M. V. (2010). The *Arabidopsis* GTL1 transcription factor regulates water use efficiency and drought tolerance by modulating stomatal density via transrepression of SDD1. *The Plant Cell*, 22(12),

4128-4141.

- Young, M. D., Wakefield, M. J., Smyth, G. K., & Oshlack, A. (2010). Gene ontology analysis for RNA-seq: accounting for selection bias. *Genome biology*, 11(2), 1-12.
- Yusuf, N. N. A. N., Kamarudin, S. K., & Yaakub, Z. (2011). Overview on the current trends in biodiesel production. *Energy conversion and management*, 52(7), 2741-2751.
- Zapata, P. J., Serrano, M., Pretel, M. T., & Botella, M. A. (2008). Changes in free polyamine concentration induced by salt stress in seedlings of different species. *Plant growth regulation*, 56(2), 167-177.
- Zeeman, S.C., Thorneycroft, D., Schupp, N., Chapple, A., Weck, M., Dunstan, H., Haldimann, P., Bechtold, N., Smith, A.M. and Smith, S.M. (2004). Plastidial  $\alpha$ -glucan phosphorylase is not required for starch degradation in *Arabidopsis* leaves but has a role in the tolerance of abiotic stress. *Plant Physiology*, 135(2), 849-858.
- Zegada-Lizarazu, W., Salvi, S., & Monti, A. (2020). Assessment of mutagenized giant reed clones for yield, drought resistance and biomass quality. *Biomass and Bioenergy*, 134, 105501.
- Zhang, D.W., Yuan, S., Xu, F., Zhu, F., Yuan, M., Ye, H.X., Guo, H.Q., Lv, X., Yin, Y. and Lin, H.H. (2016c). Light intensity affects chlorophyll synthesis during greening process by metabolite signal from mitochondrial alternative oxidase in *Arabidopsis*. *Plant, cell & environment*, 39(1), 12-25.
- Zhang, H., Cui, F., Wu, Y., Lou, L., Liu, L., Tian, M., Ning, Y., Shu, K., Tang, S. and Xie, Q. (2015). The RING finger ubiquitin E3 ligase SDIR1 targets SDIR1-INTERACTING PROTEIN1 for degradation to modulate the salt stress response and ABA signaling in *Arabidopsis*. *The Plant Cell*, 27(1), 214-227.
- Zhang, H., Du, C., Wang, Y., Wang, J., Zheng, L., & Wang, Y. (2016a). The *Reaumuria trigyna* leucoanthocyanidin dioxygenase (RtLDOX) gene complements anthocyanidin synthesis and increases the salt tolerance potential of a transgenic *Arabidopsis* LDOX mutant. *Plant Physiology and Biochemistry*, 106, 278-287.
- Zhang, J. J., Lu, Y. C., Zhang, S. H., Lu, F. F., & Yang, H. (2016). Identification of transcriptome involved in atrazine detoxification and degradation in alfalfa (*Medicago sativa*) exposed to realistic environmental contamination. *Ecotoxicology and environmental safety*, 130, 103-112.
- Zhang, J., Li, Y., Zhang, C., & Jing, Y. (2008). Adsorption of malachite green from aqueous solution onto carbon prepared from *Arundo donax* root. *Journal of hazardous materials*, 150(3), 774-782.
- Zhang, P., Wang, R., Ju, Q., Li, W., Tran, L. S. P., & Xu, J. (2019). The R2R3-MYB transcription factor MYB49 regulates cadmium accumulation. *Plant physiology*, 180(1), 529-542.
- Zhang, Y., Xiao, W., Luo, L., Pang, J., Rong, W., & He, C. (2012). Downregulation of OsPK1, a

- cytosolic pyruvate kinase, by T-DNA insertion causes dwarfism and panicle enclosure in rice. *Planta*, 235(1), 25-38.
- Zhao, D., Li, T., Wang, J., & Zhao, Z. (2015). Diverse strategies conferring extreme cadmium (Cd) tolerance in the dark septate endophyte (DSE), *Exophiala pisciphila*: evidence from RNA-seq data. *Microbiological Research*, 170, 27-35.
- Zhong, M., Yuan, Y., Shu, S., Sun, J., Guo, S., Yuan, R., & Tang, Y. (2016). Effects of exogenous putrescine on glycolysis and Krebs cycle metabolism in cucumber leaves subjected to salt stress. *Plant Growth Regulation*, 79(3), 319-330.
- Zhou, J., Rocklin, A. M., Lipscomb, J. D., Que, L., & Solomon, E. I. (2002). Spectroscopic studies of 1-aminocyclopropane-1-carboxylic acid oxidase: molecular mechanism and CO<sub>2</sub> activation in the biosynthesis of ethylene. *Journal of the American Chemical Society*, 124(17), 4602-4609.
- Zhu, J. K. (2002). Salt and drought stress signal transduction in plants. *Annual review of plant biology*, 53(1), 247-273.
- Zhu, J. K. (2016). Abiotic stress signaling and responses in plants. *Cell*, 167(2), 313-324.
- Zörb, C., Geilfus, C. M., & Dietz, K. J. (2019). Salinity and crop yield. *Plant biology*, 21, 31-38.
- Zörb, C., Senbayram, M., & Peiter, E. (2014). Potassium in agriculture—status and perspectives. *Journal of plant physiology*, 171(9), 656-669.
- Zou, J., Qi, Q., Katavic, V., Marillia, E. F., & Taylor, D. C. (1999). Effects of antisense repression of an *Arabidopsis thaliana* pyruvate dehydrogenase kinase cDNA on plant development\*. *Plant molecular biology*, 41(6), 837-849.



## List of publications

- Sicilia, A., Santoro, D. F., Testa, G., Cosentino, S. L., & Piero, A. R. L. (2020). Transcriptional response of giant reed (*Arundo donax* L.) low ecotype to long-term salt stress by unigene-based RNAseq. *Phytochemistry*, 177, 112436.
- Sicilia, A., Testa, G., Santoro, D. F., Cosentino, S. L., & Lo Piero, A. R. (2019). RNASeq analysis of giant cane reveals the leaf transcriptome dynamics under long-term salt stress. *BMC plant biology*, 19(1), 1-24.

## List of participations to congress

- Erasmus + Programme (KA103) Traineeship for a period of 6 months, from 1st June 2021 to 1st December 2021 at the Instituto de Biología Molecular y Celular de Plantas (IBMCP) belonging to the Consejo Superior de Investigaciones Científicas (CSIC) and Universitat Politècnica de València (UPV), Spain
- LXIV SIGA Annual Congress "Plant genetic innovation for food security in a climate change scenario", 14 - 16/09/2021
- Course "CRISPR: Revolutionising genome editing advanced", organized by CRISPR Biotech Engineering, 07/05/2021
- Course "Salute e sicurezza nei luoghi di lavoro", 20 – 22/04/2021 (12 hours)
- Event organized by SIGA "Genetica Agraria: percorsi al femminile", 08/03/2021
- Course "Bioinformatic Method I", organized by Coursera, University of Toronto, 15/02/2021
- Course "Plant Bioinformatics", organized by Coursera, University of Toronto, 17/02/2021
- Course "R programming", organised by Coursera, John Hopkins University, 26/12/2020
- Web event "Symposium on Plant Health with a Young Scientist Web Workshop", 16/12/2020
- SIGA Young Web Meeting, 07/07//2020
- Postgraduate master's qualification in Biology, 30/11/2020, Catania
- Summer School "Stress resilience in plants: from molecules to field", organized by Professor A. Shubert and P. Perata. Web seminar, September 8th – 10th, 2020
- Basic statistic course with implementation of R software, held by Professor C. Dimauro and A. Cesarini. The course was held in November, 2020 (45 hours)
- Course "Gestione ed interpretazione dei dati biologici complessi: basi teoriche e utilizzo dei software di analisi Excel e R". held by Dott. Mario Di Guardo, 31/10/2019 – 11/02/019
- LXIII SIGA Annual Congress "Science and innovation for sustainable agriculture intensification: the contribution of plant genetics and breeding", Napoli, 10 – 13/09/2019
- Summer School 'Epigenetic and RNA-mediated regulation in plant development and stress response', Conegliano (TV), 17-20/07/2019

## Acknowledgments

All the pages in this work wouldn't have been achieved without the contribution of several people whose effort to this research was essential. This pathway was not just a scientific and educational investment, but it also gave me an emotional and human growth.

My supervisor Prof. Angela Roberta Lo Piero gave me the great opportunity to overcome any wall during my doctorate research. I want to express my sincere gratitude to her, because she believed in me since the first moment, and helping me in all possible ways to overtake any trouble, even when I was upset for my results, leaving me the freedom to undertake every experience encounter during these Ph.D. years. I also need to thank Angelo Sicilia, who helped me through my first steps in this research field. Angelo is not just a colleague, he is a close friend and it has been a honour to work with him. Furthermore, I'd like to mention Emanuele Scialo', a person that I had the good fortune to meet just recently, whose knowledge and skills have significantly improved my know-how in science. Angelo and Emanuele have been load-bearing walls in these years, without them I would have never been able to reach any goals. Special thanks to all people working at the Department of Agricultural, Food and Environmental (Di3A) of the University of Catania, in particular to Prof. Giorgio Testa who helped has been very precious for me. The contribution of Prof. Testa and his research team in each step of the experimental trial allowed me to learn and obtain a deep knowledge, especially in crop species. In addition, I'd like to jump a bit on the other side of my land, precisely on the shining Valencia. Special gratitude to the Dr. Diego Orzáez Calatayud, who accepted the responsibility to receive me as a training student in his IBMCP laboratory at the UPV (Universidad Politécnica de Valencia) for a couple of months. Moreover, I'd like to say thanks to all of researches working at IBMCP laboratory for giving me the honour to work with during my staying at Valencia. Lastly but not the least, I thank all my family for always supporting my choice and providing me love and shining ideas that have allowed me to become what I am today.